Final Report

# DALLAS/FORT WORTH CAMx MODELING: IMPROVED MODEL PERFORMANCE AND TRANSPORT ASSESSMENT

**HARC Project H35, Phase 2**

Prepared for

The Houston Advanced Research Center
4800 Research Forest Dr.
The Woodlands, TX 77381

Prepared by

Edward Tai
Chris Emery
Yiqin Jia
Greg Yarwood

ENVIRON International Corporation
101 Rowland Way, Suite 220
Novato, CA 94945

August 2, 2005

# TABLE OF CONTENTS

**Page**

**EXECUTIVE SUMMARY ..... ES-1**

**1. INTRODUCTION ..... 1-1**

Report Organization ..... 1-3

**2. ANALYSIS OF TWO ALTERNATIVE MM5 SIMULATIONS ..... 2-1**

Hourly Performance ..... 2-1
Daily Average Performance ..... 2-2
Modeled Mixing Depths ..... 2-2
Comparison of Modeled and Observed Vertical Profiles ..... 2-3
Intercomparison of Precipitation Patterns ..... 2-4

**3. BASE CASE UPDATE "RUN 20" ..... 3-1**

Model Performance Evaluation ..... 3-2

**4. OZONE SENSITIVITY TO CHANGES IN THE DOMAIN SIZE ..... 4-1**

CAMx Domain from "RUN 20" ..... 4-1
Expanded Domain Modeling ..... 4-3
Run 21: High Top ..... 4-5
Run 22: Expanded Grid ..... 4-6
Run 23: High Top and Expanded Grid ..... 4-6

**5. OZONE SENSITIVITY TO METEOROLOGY ..... 5-1**

Run 28: CMAQ Kv Profile ..... 5-2
Run 24: Eta/Noah PBL Scheme ..... 5-3
Run 25: Grell Convection Scheme ..... 5-3

**6. OZONE SENSITIVITY TO CHANGES IN EMISSIONS ..... 6-1**

Run 26: Decreased Mobile Source NOx ..... 6-2
Run 27: Increased Biogenic VOC and NOx ..... 6-2
Run 29: Increased Point Source VOC ..... 6-3

**7. OZONE SENSITIVITY TO CHEMISTRY CHANGES ..... 7-1**

CB2002 Mechanism ..... 7-1
NOx Recycling Reactions: CB4xi ..... 7-2
Results ..... 7-3
Run 30: CB4x*i* ..... 7-3
Run 31: CB2002 ..... 7-4
Summary ..... 7-4

**8. PROCESS ANALYSIS ..... 8-1**

Updates to the CAMx Chemical Process Analysis ..... 8-2
Scenarios Selected for Process Analysis ..... 8-4
Model Performance Evaluation ..... 8-5
Analysis of CPA Results ..... 8-17
Sensitivity to pH2O2/pHNO3 Cut Point ..... 8-29
Summary ..... 8-30

**9. CAMx 2010 FUTURE YEAR OZONE MODELING ..... 9-1**

Modeling Inputs ..... 9-1
2010 Emissions ..... 9-5
Modeling Results ..... 9-12

**10. SUMMARY AND CONCLUSIONS ..... 10-1**

Improving Model Performance ..... 10-1
Revised Base Case: Run34 ..... 10-3
Chemical Process Analysis ..... 10-3
Updated Transport Assessment ..... 10-5
Impact of CAIR on 2010 Emissions ..... 10-5
Impact of CAIR on 2010 Ozone Levels ..... 10-6
Impact of CAIR on Ozone Transport ..... 10-7
Impact of Alternate Meteorology ..... 10-9
Impact of Updated Source Apportionment Method: APCA2 ..... 10-10

**11. REFERENCES ..... 11-1**

## APPENDIX

Appendix A: Model Performance Products for Run34
Appendix B: APCA Tables for Each Run on Each Day

## TABLES

Table 1-1. TCEQ ozone monitors operating in the DFW 4-km grid during August 1999 ..... 1-2
Table 3-1. Concentrations (ppb) used to define CAMx initial and boundary conditions. ..... 3-1
Table 3-2. Comparison of the 1-hour and 8-hour coefficient of determination from each scatter plot of the predicted and observed daily maximum ozone in Runs 17b and 20. ..... 3-2
Table 4-1. MM5 and CAMx vertical grid structures based on 28 sigma-p levels. Heights (m) are above ground level according to a standard atmosphere; pressure is in millibars ..... 4-1
Table 4-2. Domain definitions of Runs 20 to 23. ..... 4-3
Table 4-3. Comparison of the 1-hour and 8-hour coefficient of determination from each scatter plot of the predicted and observed daily maximum ozone in Runs 20, 21, 22, and 23. ..... 4-6
Table 5-1. List of meteorology used for each CAMx sensitivity run ..... 5-1
Table 5-2. Comparison of the 1-hour and 8-hour coefficient of determination from each scatter plot of the predicted and observed daily maximum ozone from four CAMx simulations using different meteorological inputs. ..... 5-3
Table 6-1. Daily emissions inside the expanded 36-km domain on August 17, 1999. ..... 6-1
Table 6-2. Comparison of the 1-hour and 8-hour coefficient of determination from each scatter plot of the predicted and observed daily maximum ozone from four CAMx simulations with different emissions. ..... 6-2
Table 7-1. Comparison of OH + $NO_2$ reaction rate constants ..... 7-1
Table 7-2. Reactions added in the CB4xi mechanism and whether they are included in other condensed chemical mechanisms ..... 7-2
Table 7-3. Comparison of the 1-hour and 8-hour coefficient of determination from each scatter plot of the predicted and observed daily maximum ozone using different chemistry ..... 7-3
Table 8-1. Chemical process analysis (CPA) variables calculated in CAMx for the CB4 and SAPRC99 mechanisms ..... 8-2
Table 8-2. CAMx scenarios selected for process analysis using CPA ..... 8-4
Table 8-3. Key to CPA figure legends ..... 8-17
Table 9-1. Concentrations [ppb] used to define initial and boundary conditions ..... 9-5
Table 9-2. CAIR area source emission scaling factors from 2001 to 2010 for each state inside the expanded DFW domain, but outside the original DFW domain ..... 9-6
Table 9-3. CAIR off-road source emission scaling factors from 2001 to 2010 for each state inside the expanded DFW domain, but outside

the original DFW domain ..... 9-7

Table 9-4. CAIR mobile source emission scaling factors from 2001 to 2010 for each state inside the expanded DFW domain, but outside the original DFW domain ..... 9-8
Table 9-5. CAIR point source (EGU + non-EGU) emission scaling factors from 2001 to 2010 for each state inside the expanded DFW domain, but outside the original DFW domain..... 9-9
Table 9-6. 2010 weekday NOx emissions for the DFW episode by source apportionment region..... 9-10
Table 9-7. 2010 weekday VOC emissions for the DFW episode by source apportionment region..... 9-11
Table 9-8. List of the four source apportionment runs for the 2010 future year ..... 9-12
Table 9-9. Episode average contributions from all source regions and emission groups to the Dallas/Fort Worth NAA in CAMx Run 34 for the 2010 future year..... 9-14
Table 9-10. Episode average contributions from all source regions and emission groups to the Dallas/Fort Worth 4-County Core in CAMx Run 34 for the 2010 future year..... 9-15
Table 9-11. A comparison of point source emissions between the 2010 base case and 2010 CAIR EGU control case ..... 9-18
Table 9-12. A comparison of 2010 episode average ozone contributions (ppb) from point sources with and without EGU controls in relation to each state's change in NOx controls from EGUs in the DFW NAA..... 9-22
Table 9-13. A comparison of 2010 episode average ozone contributions (ppb) from point sources with and without EGU controls in relation to each state's change in NOx controls from EGUs in the DFW 4-county core..... 9-23
Table 9-14. A comparison of 2010 peak ozone contributions (ppb) from point sources to the DFW NAA with and without EGU controls..... 9-25
Table 9-15. A comparison of 2010 peak ozone contributions (ppb) from anthropogenic sources to the DFW NAA with and without EGU controls. ..... 9-26
Table 9-16. Episode average contributions (ppb) from all source regions and emission groups to the DFW 9-county NAA in CAMx Run 38 (APCA2) for 2010, and difference in contributions between APCA2 and APCA ..... 9-28
Table 9-17. Episode average contributions (ppb) from all source regions and emission groups to the DFW 4-County Core in CAMx Run 38 (APCA2) for 2010; and difference in contributions between APCA2 and APCA ..... 9-29
Table 9-18. A comparison of APCA and APCA2 2010 peak 8-hour ozone contributions (ppb) from anthropogenic sources to the DFW NAA..... 9-31
Table 9-19. Episode average contributions (ppb) from all source regions and emission groups to the DFW NAA in CAMx Run 37 for 2010, and the difference in contributions between Runs 36 and 37 for 2010. ..... 9-35
Table 9-20. Episode average contributions (ppb) from all source regions and emission groups to the DFW 4-county core in CAMx Run 37 for

2010, and the difference in contributions between Runs 36 and 37 for 2010 ..... 9-36
Table 9-21. A comparison of peak anthropogenic contributions (ppb) to 8-hour ozone between CAMx Run 36 and Run 37 in the DFW 9-county NAA ..... 9-38

## FIGURES

Figure 1-1. Dallas/Fort Worth 4-km grid for the August 1999 episode ..... 1-3
Figure 2-1(a). Hourly site-averaged MM5 wind performance for Runs 5, 6, and 7 in the DFW 4-km modeling domain. ..... 2-5
Figure 2-1(b). Hourly site-averaged MM5 temperature performance for Runs 5, 6, and 7 in the DFW 4-km modeling domain. ..... 2-6
Figure 2-1(c). Hourly site-averaged MM5 humidity performance for Runs 5, 6, and 7 in the DFW 4-km modeling domain. ..... 2-7
Figure 2-2(a). Daily site-averaged MM5 wind performance for Runs 5, 6, and 7 in the DFW 4-km modeling domain. ..... 2-8
Figure 2-2(b). Daily site-averaged MM5 temperature performance for Runs 5, 6, and 7 in the DFW 4-km modeling domain. ..... 2-9
Figure 2-2(c). Daily site-averaged MM5 humidity performance for Runs 5, 6, and 7 in the DFW 4-km modeling domain. ..... 2-10
Figure 2-3. MM5-derived effective PBL depth for Runs 5, 6, and 7 in the DFW 4-km modeling domain, August 17, 1999 at 1500 LST ..... 2-11
Figure 2-4(a). Comparison of wind, temperature, and humidity profiles from MM5 Runs 5, 6, and 7 at the DFW rawinsonde site, August 17, 1999 at 1800 LST. ..... 2-12
Figure 2-4(b). Comparison of wind profiles from MM5 Runs 5, 6, and 7 at the NOAA Palestine profiler site, August 17, 1999 at 1800 LST. ..... 2-13
Figure 2-4(c). Comparison of wind profiles from MM5 Runs 5, 6, and 7 at the DFW AVAS profiler site, August 17, 1999 at 1800 LST ..... 2-13
Figure 2-5. Total predicted accumulated rainfall between 12Z August 15 to 12Z August 22 in the MM5 12-km domain for Runs 5, 6, and 7. ..... 2-14
Figure 3-1. Time series of 1-hour ozone at sites inside the DFW 4-km domain from CAMx Runs 17b and 20. ..... 3-3
Figure 3-2. Daily statistics of the 1999 DFW 1-hour ozone in the 4-km domain from CAMx Runs 17b and 20. ..... 3-6
Figure 3-3. Daily statistics of the 1999 DFW 8-hour ozone in the 4-km domain from CAMx Runs 17b and 20. ..... 3-7
Figure 3-4. Scatter and quantile-quantile plots of the largest predicted daily maximum 1-hour ozone near each monitor (within 9x9 cell area) and the observed daily maximum 1-hour ozone for Runs 17b and 20 in the 1999 DFW Episode. ..... 3-8
Figure 3-5. Scatter and quantile-quantile plots of the largest predicted daily maximum 8-hour ozone near each monitor (within 9x9 cell area) and the observed daily maximum 8-hour ozone for Runs 17b and 20 in the 1999 DFW Episode. ..... 3-8
Figure 3-6. Spatial plots of the daily maximum 1-hour ozone in the DFW 4-km domain on August 17, 1999 from Runs 17b and 20. ..... 3-9
Figure 3-7. Spatial plots of the daily maximum 8-hour ozone in the

DFW 4-km domain on August 17, 1999 from Runs 17b and 20. ..... 3-9

Figure 4-1. CAMx DFW modeling domain with the standard and expanded 36-km domains..... 4-2
Figure 4-2. MM5 and CAMx modeling domains for DFW with the expanded domain. ..... 4-4
Figure 4-3. Assignment of boundary conditions in the mixed layer for the standard and expanded domains for DFW. ..... 4-5
Figure 4-4. Time series of 1-hour ozone at sites inside the DFW 4-km domain from CAMx runs using different domain configurations (see Table 4-2) ..... 4-7
Figure 4-5. Daily statistics of the 1999 DFW 1-hour ozone in the 4-km domain from CAMx runs using different domain configurations (see Table 4-2) ..... 4-10
Figure 4-6. Daily statistics of the 1999 DFW 8-hour ozone in the 4-km domain from CAMx runs using different domain configurations (see Table 4-2) ..... 4-11
Figure 4-7. Scatter plots of the daily maximum observed and largest predicted 1-hour ozone near each monitor (within 9x9 cell area) from four CAMx runs using different domain configurations of the August 1999 DFW episode..... 4-12
Figure 4-8. Scatter plots of the daily maximum observed and largest predicted 8-hour ozone near each monitor (within 9x9 cell area) from four CAMx runs using different domain configurations of the August 1999 DFW episode..... 4-13
Figure 4-9. Spatial plots of the daily maximum 1-hour ozone in the 12-km domain on August 17, 1999 from four CAMx runs with different domain configurations. ..... 4-14
Figure 4-10. Spatial plots of the daily maximum 1-hour ozone in the DFW 4-km domain on August 17, 1999 from four CAMx runs with different domain configurations..... 4-15
Figure 4-11. Spatial plots of the daily maximum 8-hour ozone in the DFW 4-km domain on August 17, 1999 from four CAMx runs with different domain configurations..... 4-16
Figure 5-1. Vertical profiles of the vertical diffusivity over a grid cell in Dallas from four sets of meteorology. ..... 5-2
Figure 5-2. Time series of 1-hour ozone at sites inside the DFW 4-km domain from four CAMx runs using different meteorology inputs..... 5-5
Figure 5-3. Daily statistics of the 1999 DFW 1-hour ozone in the 4-km domain from four CAMx runs with different meteorology inputs. ..... 5-8
Figure 5-4. Daily statistics of the 1999 DFW 8-hour ozone in the 4-km domain from four CAMx runs with different meteorology inputs. ..... 5-9
Figure 5-5. Scatter and quantile-quantile plots of the largest predicted daily maximum 1-hour ozone near each monitor (within 9x9 cell area) and the observed daily maximum 1-hour ozone for four CAMx runs using different meteorology inputs in the 1999 DFW Episode. ..... 5-10
Figure 5-6. Scatter and quantile-quantile plots of the largest predicted daily maximum 8-hour ozone near each monitor (within 9x9 cell area) and the observed daily maximum 8-hour ozone for four CAMx runs

using different meteorology inputs in the 1999 DFW Episode. ..... 5-11

Figure 5-7. Spatial plots of the daily maximum 1-hour ozone in the 12-km domain on August 17, 1999 from four CAMx simulations using different meteorology inputs..... 5-12
Figure 5-8. Spatial plots of the daily maximum 1-hour ozone in the DFW 4-km domain on August 17, 1999 from four CAMx simulations using different meteorology inputs..... 5-13
Figure 5-9. Spatial plots of the daily maximum 8-hour ozone in the DFW 4-km domain on August 17, 1999 from four CAMx simulations using different meteorology inputs..... 5-14
Figure 6-1. Time series of 1-hour ozone at sites inside the DFW 4-km domain from four CAMx runs with differences in the emissions. ..... 6-4
Figure 6-2. Daily statistics of the 1999 DFW 1-hour ozone in the 4-km domain from four CAMx runs with differences in the emissions. ..... 6-7
Figure 6-3. Daily statistics of the 1999 DFW 8-hour ozone in the 4-km domain from four CAMx runs with differences in the emissions. ..... 6-8
Figure 6-4. Scatter and quantile-quantile plots of the largest predicted daily maximum 1-hour ozone near each monitor (within 9x9 cell area) and the observed daily maximum 1-hour ozone for four CAMx runs with different emissions in the 1999 DFW Episode. ..... 6-9
Figure 6-5. Scatter and quantile-quantile plots of the largest predicted daily maximum 8-hour ozone near each monitor (within 9x9 cell area) and the observed daily maximum 8-hour ozone for four CAMx runs with different emissions in the 1999 DFW Episode. ..... 6-10
Figure 6-6. Spatial plots of the daily maximum 1-hour ozone in the 12-km domain on August 17, 1999 from four CAMx simulations with differences in the emissions..... 6-11
Figure 6-7. Spatial plots of the daily maximum 1-hour ozone in the DFW 4-km domain on August 17, 1999 from four CAMx simulations with differences in the emissions. ..... 6-12
Figure 6-8. Spatial plots of the daily maximum 8-hour ozone in the DFW 4-km domain on August 17, 1999 from four CAMx simulations with differences in the emissions. ..... 6-13
Figure 7-1. Time series of 1-hour ozone at sites inside the DFW 4-km domain from three CAMx runs using different chemistry..... 7-5
Figure 7-2. Daily statistics of the 1999 DFW 1-hour ozone in the 4-km domain from three CAMx runs using different chemistry..... 7-8
Figure 7-3. Daily statistics of the 1999 DFW 8-hour ozone in the 4-km domain from three CAMx runs using different chemistry..... 7-9
Figure 7-4. Scatter and quantile-quantile plots of the largest predicted daily maximum 1-hour ozone near each monitor (within 9x9 cell area) and the observed daily maximum 1-hour ozone for three CAMx runs using different chemistry in the 1999 DFW Episode..... 7-10
Figure 7-5. Scatter and quantile-quantile plots of the largest predicted daily maximum 8-hour ozone near each monitor (within 9x9 cell area) and the observed daily maximum 8-hour ozone for three CAMx runs using different chemistry in the 1999 DFW Episode..... 7-11
Figure 7-6. Spatial plots of the daily maximum 1-hour ozone in

the 12-km domain on August 17, 1999 from three CAMx simulations using different chemistry. ..... 7-12
Figure 7-7. Spatial plots of the daily maximum 1-hour ozone in the DFW 4-km domain on August 17, 1999 from three CAMx simulations using different chemistry. ..... 7-13
Figure 7-8. Spatial plots of the daily maximum 8-hour ozone in the DFW 4-km domain on August 17, 1999 from three CAMx simulations using different chemistry ..... 7-14
Figure 8-1. Time series of 1-hour ozone at sites inside the DFW 4-km domain for Runs 33, 34 and 35. ..... 8-7
Figure 8-2. Daily statistics of the 1999 DFW 1-hour ozone in the 4-km domain for CAMx runs 23, 33, 34 and 35. ..... 8-10
Figure 8-3. Daily statistics of the 1999 DFW 8-hour ozone in the 4-km domain for CAMx runs 23, 33, 34 and 35 ..... 8-11
Figure 8-4. Scatter and quantile-quantile plots of the largest predicted daily maximum 1-hour ozone near each monitor (within 9x9 cell area) and the observed daily maximum 1-hour ozone for Runs 23, 33, 34 and 35 .... 8-12
Figure 8-5. Scatter and quantile-quantile plots of the largest predicted daily maximum 8-hour ozone near each monitor (within 9x9 cell area) and the observed daily maximum 8-hour ozone for Runs 23, 33, 34 and 35 .... 8-13
Figure 8-6. Spatial plots of the daily maximum 1-hour ozone in the 12-km domain on August 17, 1999 from Runs 23, 33, 34 and 35 ..... 8-14
Figure 8-7. Spatial plots of the daily maximum 1-hour ozone in the DFW 4-km domain on August 17, 1999 from Runs 23, 33, 34 and 35. ..... 8-15
Figure 8-8. Spatial plots of the daily maximum 8-hour ozone in the DFW 4-km domain on August 17, 1999 from Runs 23, 33, 34 and 35 ..... 8-16
Figure 8-9. CAMx chemical process analysis results averaged over the PBL depth for Run 33 at 13:00 on August 17, 1999 ..... 8-20
Figure 8-10. CAMx chemical process analysis results averaged over the PBL depth for the DFW 4-km grid in Run 33 at 13:00 on August 19, 1999..... 8-21
Figure 8-11. CAMx chemical process analysis results averaged over the PBL depth for the DFW 4-km grid in Run 33 at 13:00 on August 21, 1999..... 8-22
Figure 8-12. CAMx chemical process analysis results averaged over the PBL depth for the DFW 4-km grid in Run 34 at 13:00 on August 17, 1999..... 8-23
Figure 8-13. CAMx chemical process analysis results averaged over the PBL depth for the DFW 4-km grid in Run 34 at 13:00 on August 19, 1999..... 8-24
Figure 8-14. CAMx chemical process analysis results averaged over the PBL depth for the DFW 4-km grid in Run 34 at 13:00 on August 21, 1999..... 8-25
Figure 8-15. CAMx chemical process analysis results averaged over the PBL depth for the DFW 4-km grid in Run 35 at 13:00 on August 17, 1999..... 8-26
Figure 8-16. CAMx chemical process analysis results averaged over the PBL depth for the DFW 4-km grid in Run 35 at 13:00 on August 19, 1999..... 8-27
Figure 8-17. CAMx chemical process analysis results averaged over the PBL depth for the DFW 4-km grid in Run 35 at 13:00 on August 21, 1999..... 8-28
Figure 8-18. Comparison of Ox production from VOC-limited (left) and NOx-limited (right) conditions when the pH2O2/pHNO3 cut point set to 0.15 (top) and 0.35 (bottom) for Run 34 on August 17, 1999 at 13:00. ..... 8-29
Figure 8-19. Comparison of Ox production from VOC-limited (left) and NOx-limited (right) conditions when the pH2O2/pHNO3 cut point set

to 0.15 (top) and 0.35 (bottom) for Run 34 on August 21, 1999 at 13:00. ..... 8-30

Figure 9-1. Source area map for source apportionment modeling in the DFW 36-km expanded domain. ..... 9-2
Figure 9-2. Source area map for source apportionment modeling in the 12-km domain ..... 9-3
Figure 9-3. Source area map for source apportionment modeling in the 4-km domain. ..... 9-4
Figure 9-4. Spatial plots of the episode maximum 8-hour base case ozone for 1999 and 2010 in the DFW 4-km and 12-km domains using the Run 34 configuration ..... 9-13
Figure 9-5. Bar charts of the episode average contribution to 8-hour ozone from all source regions and emission groups for Dallas/Fort Worth NAA (top) and 4-county core (bottom) using CAMx Run 34 for the 2010 future year ..... 9-16
Figure 9-6. Bar charts of the episode average contribution to 8-hour ozone from all source regions and emission groups for Dallas/Fort Worth NAA (top) and 4-county core (bottom) using CAMx Run 34 for the 2010 future year ..... 9-16
Figure 9-7. NOx control factors applied to EGUs for each state in future year 2010 ..... 9-17
Figure 9-8. Spatial maps of the episode maximum 8-hour ozone in 2010 for the base case (run 34) and for the EGU controls (run 36) in the DFW 4-km and 12-km domains ..... 9-20
Figure 9-9. Episode average 2010 contributions to high 8-hour ozone from each source area and emission group to the DFW NAA (top) and 4-county core (bottom) in CAMx Runs 34 and 36. ..... 9-21
Figure 9-10. Episode average 2010 contributions to high 8-hour ozone from each source area and emission group to the DFW NAA (top) and 4-county core (bottom) in CAMx Runs 34 and 36. ..... 9-21
Figure 9-11. Change in episode average EGU contributions to high 8-hour ozone against change in emissions, by state, fir the DFW NAA and 4-county core area. ..... 9-24
Figure 9-12. Episode average 2010 contributions to high 8-hour ozone in the DFW NAA for Run 36 (APCA) and Run 38 (APCA2). ..... 9-30
Figure 9-13. Episode average 2010 contributions to high 8-hour ozone in the DFW 4-county core for Run 36 (APCA) and Run 38 (APCA2). ..... 9-30
Figure 9-14. Spatial maps of the episode maximum 8-hour ozone in 2010 for CAMx Runs 36 and 37 in the DFW 4-km and 12-km domains ..... 9-34
Figure 9-15. Episode average 2010 contributions to high 8-hour ozone in the DFW NAA receptor from CAMx Runs 36 and 37.. ..... 9-37
Figure 9-16. Episode average 2010 contributions to high 8-hour ozone in the DFW 4-county core from CAMx Runs 36 and 37 ..... 9-37
Figure 10-1. Assignment of oxidant production as VOC and NOx-limited for the DFW 4-km grid in Run 34 at 13:00 on August 17, 1999 ..... 10-5
Figure 10-2. Percentage NOx reductions due to CAIR applied to EGUs for each State in future year 2010. ..... 10-6
Figure 10-3. The impacts of CAIR EGU NOx reductions on 2010 episode maximum 8-hour ozone for the 12-km and DFW 4-km grids ..... 10-7
Figure 10-4. Episode average 2010 contributions (ppb) to high 8-hour ozone in the DFW 9-county NAA by source region and emissions group with and without CAIR controls ..... 10-8

Figure 10-5. Change in episode average EGU contributions to high 8-hour ozone in DFW against change in emissions, by State ..... 10-8
Figure 10-6. Episode average 2010 contributions (ppb) to high 8-hour ozone in the DFW 9-county NAA by source region and emissions group with two different meteorological inputs..... 10-9
Figure 10-7. Episode average 2010 contributions (ppb) to high 8-hour ozone in the DFW 9-county NAA by source region and emissions group with two different APCA methods ..... 10-10

# EXECUTIVE SUMMARY

The Texas Commission on Environmental Quality (TCEQ) is developing an 8-hour ozone State Implementation Plan (SIP) for the Dallas/Fort Worth (DFW) region using the Comprehensive Air Quality model with extensions. The Texas Environmental Research Consortium (TERC) sponsored Phase 1 of Project H35 to examine the role of ozone transport in causing high 8-hour ozone in eastern Texas, including the DFW region.

Phase 2 of Project H35 improved ozone model performance for the August 13-22, 1999 DFW SIP episode and investigated how updated modeling assumptions impact ozone transport assessments. There were three components to the work:

- CAMx sensitivity runs were completed to investigate how changes in modeling inputs and assumptions affect ozone model performance. Two MM5 runs were completed to support the CAMx sensitivity analysis.
- Chemical Process Analysis was used to investigate the revised 1999 base case and two related model scenarios.
- APCA ozone source apportionment was used to investigate the impact of several modeling assumptions on ozone transport for 2010 future year scenarios.

## Improved 1999 Model Performance: Run 34

Sensitivity tests showed the expansion of the modeling domain eastward, northward, and higher produced slightly improved model performance with less reliance on boundary conditions. Using the larger domain, additional sensitivity tests evaluated ozone sensitivity to changes in the emissions, meteorology, and chemistry to show that reducing NOx in the DFW core counties, adding more biogenic emissions, and implementing the NOx recycling reactions in CB4 consistently produced higher ozone. These runs generally improved the normalized bias and average paired peak accuracy, but hurt the unpaired peak accuracy. The use of the CMAQ-based vertical diffusivity profiles and the CB2002 chemical mechanism lowered ozone. All other tests either led to mixed results or very little change.

A new 1999 base case for the DFW SIP modeling called “Run 34” was developed in Phase 2 of Project H35. Changes in Run 34 from the previous Run 17b base case are:

- Expanded modeling domain extending to the Atlantic Ocean and Canada.
- Higher model top at about 14-km.
- Meteorology from MM5 “Run 6” using the Noah/Eta PBL scheme.
- Enhanced near surface mixing from the “Kv100” adjustment.
- Extended inorganic chemistry (CB4xi) with “NOx recycling” reactions.

Run 34 shows improved ozone model performance compared to Run 17b. A tendency toward ozone under-prediction (negative bias) was improved by the updated meteorology “MM5 Run 6” and the chemistry updates (NOx recycling). The “Kv100” vertical mixing adjustment, which sets the largest diffusivity in the lowest 100m of each column to all layers in the first 100m, improved ozone predictions in areas with intense surface NO emissions in the DFW core area. Expanding the modeling domain, both vertically and horizontally, reduced uncertainties in

specifying boundary conditions at some cost of increased computer resources to model a larger domain.

**Process Analysis of 1999 Model Results**

Chemical Process Analysis (CPA) was used to investigate several aspects of atmospheric chemistry that are important to understanding DFW model performance and control strategy development. New modeling tools were developed to analyze CPA results through the entire boundary layer rather than just near the surface. CPA analysis of results for the DFW area from "Run 34" and two related scenarios revealed many common features across modeled days and scenarios:

- Ozone production showed hot spots over urban areas and major NOx point sources in rural areas consistently across days.
- The areas of most intense oxidant production tend to be VOC-limited on all days but there are differences in the extent of VOC and NOx-limited areas between days
- August 17$^{th}$ is the most extensively VOC-limited day during the episode: Other days examined were less strongly VOC-limited than August 17$^{th}$.
- When NOx emissions were reduced in the DFW core as a sensitivity test, the VOC-limited area almost completely disappeared on days other than August 17$^{th}$.
- The regions that tend to be VOC-limited are the Dallas and Fort Worth urban cores.
- The fraction of OH radicals reacting with isoprene (relative to all hydrocarbons) revealed areas outside of the DFW urban/suburban area where biogenic emissions have high importance.
- An area of low fraction of OH reacting with isoprene runs from south to north (Waco to DFW) near IH-35. The relatively low importance of isoprene in these areas is due to differences in land cover (i.e., agricultural and urban areas) leading to low biogenic emission levels. This land cover difference likely contributes to the DFW urban area tending to be VOC-limited.

The CPA analysis confirmed results of earlier emission reduction sensitivity tests in showing that the DFW area has regions of both VOC and NOx sensitivity. The biogenic emission inventory plays a critical role in defining which parts of DFW are VOC vs. NOx sensitive.

**Updates to 2010 Ozone Transport Assessment**

Ozone source apportionment modeling was completed for 2010 to evaluate how several factors influence results already developed in Phase 1 of Project H35, specifically:

- Expected reductions in 2010 EGU NOx emission levels expected to result from EPA's Clean Air Interstate Rule (CAIR).
- Modeling uncertainties related to meteorology, as represented by the difference between alternate MM5 runs completed in this study.
- Modeling uncertainties related to improvements in the APCA source apportionment technique to better represent chemical destruction of ozone as it is transported.

## Impacts of CAIR on 2010 Emissions

The impacts of EPA's Clean Air Interstate Rule (CAIR) on EGU emissions were modeled based on information provided in the CAIR Technical Support Documents. Texas' NOx emissions from EGUs were to be reduced by 1%. Louisiana's EGU NOx was reduced by 26 %. The EGU controls reduced NOx emissions in both Kentucky and Florida by over 300 tons/day. Georgia, Tennessee, Alabama, Mississippi, and Louisiana all reduced NOx emissions by over 100 tons per day.

## Impacts of CAIR on 2010 Ozone Transport

Ozone modeling for 2010 showed that ozone reductions due to CAIR were greatest in the vicinity of large reductions. Within the 12-km grid used for DFW modeling, Mississippi showed the largest decrease in episode maximum 8-hour ozone, dropping up to 15 ppb near the Mississippi River, and EGUs in this state were reduced 55 %. The states that experienced the largest EGU NOx reductions due to CAIR generally had the largest corresponding reductions in ozone transport into the DFW area. The DFW area showed little decrease to the episode average and episode peak (both reduced 0.3 ppb) high 8-hour ozone due to CAIR reductions because of the strong impact of local emissions on high ozone levels in DFW. CAIR might provide greater benefit in the DFW area with greater reductions in local emissions in place.

## Impact of Alternate Meteorology on 2010 Ozone Transport

We evaluated the sensitivity of DFW ozone transport assessments to using alternate meteorological data from the MM5 model (MM5 Run 7 with the "Grell" convection scheme). Local sources and source regions north and east of DFW contributed more to DFW high ozone when the Grell convection scheme was used in MM5. These source regions include the 16-county DFW region, northeast Texas, Louisiana, Arkansas, and Oklahoma. Contributions from source regions south of DFW – central Texas, southern Texas, and Mexico/Gulf of Mexico – contributed less with Grell. Houston was an exception in contributing more with Grell by up to 2 ppb because the Grell scheme increased ozone levels in the Houston area by up to 30 ppb. Ozone transport contributions from States more distant than Oklahoma, Louisiana, Arkansas changed by less than 0.1 ppb due to the change in meteorological data. When Grell was used in MM5, contributions were less reliant on boundary conditions by an average of 2 ppb, as contributions from initial conditions and anthropogenic sources were higher.

## Impact of Updated Source Apportionment Models on 2010 Ozone Transport

We evaluated the sensitivity of DFW ozone transport assessments to changing the CAMx source apportionment methodology. The updated Anthropogenic Precursor Culpability Assessment method, called APCA2, better distinguishes between chemical processes that create and destroy ozone. The updated APCA2 methodology allocates less ozone to distant sources, more ozone to local sources, and about the same ozone to sources at intermediate distances. Ozone contributions from far distant sources, such as boundary conditions (BCs) and the Northern Plains, decrease with APCA2 because they are subject to chemical destruction during multi-day transport. The contribution of BCs to high 8-hour ozone in DFW decreased by 5.5 ppb (16 %)

whereas the contribution of local DFW sources increased by 3.5 ppb (8%) using APCA2. The contributions of sources at an upwind distance of about two States were about equal between APCA and APCA2. These changes are sufficiently small that they aren't expected to alter existing conclusions from Phase 1 of Project H35. We recommend that the APCA2 method be used for future ozone transport assessment modeling.

# 1. INTRODUCTION

The Texas Commission on Environmental Quality (TCEQ) is developing an 8-hour ozone State Implementation Plan (SIP) for the Dallas/Fort Worth (DFW) region using the Comprehensive Air Quality model with extensions (CAMx; ENVIRON, 2004a). The TCEQ performed an episode selection analysis and identified the period of August 13-22, 1999 as a suitable episode for representing conditions conducive to high 8-hour (and 1-hour) ozone levels (UT/ENVIRON, 2002). Developing base year (1999) ozone model inputs for the August 13-22 episode was described by Mansell et al. (2003) and Emery et al. (2004). Future year modeling for this episode period in 2010 was described by ENVIRON (2004b) and Mansell et al. (2004).

The Texas Environmental Research Consortium (TERC) sponsored Phase 1 of Project H35 to examine the role of ozone transport in causing high 8-hour ozone in eastern Texas, including the DFW region. TERC Project H35 complemented an earlier transport assessment for the DFW area completed for TERC Project H27 (Stoeckenius and Yarwood, 2004). TERC Project H36 (ENVIRON, 2005) was a companion to H35 Phase 1 and evaluated potential emission controls for major point sources in upwind states that were identified as potentially significant sources of ozone transport in Phase 1of Project H35.

The goals of Project H35 Phase 2 were to improve ozone model performance for the August 13-22, 1999 DFW episode and then investigate how updated modeling assumptions impact ozone transport assessments. There were three components to this work:

1. Performing CAMx sensitivity runs to investigate how changes in modeling inputs and assumptions impact ozone model performance. Two MM5 runs ten CAMx runs were completed for this purpose. These sensitivity tests resulted in a revised 1999 base case with improved model. Factors considered in sensitivity tests were:

    - Extension of the vertical modeling domain.
    - Extension of the horizontal modeling domain.
    - Adoption of vertical diffusivity fields based on the approach of CMAQ.
    - Implementation of the Eta/Noah PBL/LSM scheme in MM5.
    - Implementation of the Grell convection scheme in MM5.
    - A 30% NOx decrease in on-road and off-road mobile NOx emissions in the 4 DFW core counties.
    - A 100% VOC increase from all non-EGU point sources.
    - A 30% increase in domain-wide biogenics.
    - Adoption of NOx recycling reactions for the CB4 chemical mechanism (CB4xi).
    - Adoption of the CB2002 chemical mechanism.

2. Using Chemical Process Analysis (CPA) to investigate specific aspects of CAMx model performance for the revised 1999 base case and two related scenarios. CPA was used for:

    - Determining geographic areas of high ozone productivity.
    - Classifying geographic areas as being “VOC-limited” or “NOx-limited” with respect to ozone formation chemistry.

- Investigating the efficiency of ozone formation chemistry as measured by the "OH chain length."
- Determining the contribution of biogenic (isoprene) emissions to VOC reactivity and ozone production.

Improvements were made to the CAMx Process Analysis algorithms in the course of this work.

3. Performing ozone source apportionment modeling to evaluate how model improvements developed for the 1999 base case impact transport assessments completed with 2010 emissions. The sensitivity of 2010 ozone concentrations and transport assessments to several factors were investigated:

- Expected reductions in 2010 EGU NOx emission levels expected to result from EPA's Clean Air Interstate Rule (CAIR).
- Modeling uncertainties related to meteorology, as represented by the difference between two MM5 runs.
- Modeling uncertainties related to improvements in the APCA ozone source apportionment technique.

The CAMx 4-km grid covering the DFW area is shown in Figure 1-1. CAMx model performance in the 4-km grid was evaluated against data from continuous air monitoring stations (CAMS) operated in the DFW area in 1999 that are listed in Table 1-1.

**Table 1-1.** TCEQ ozone monitors operating in the DFW 4-km grid during August 1999.

| Site ID | Easting | Northing | Description | Street | City | County |
|---|---|---|---|---|---|---|
| CAMS_31 | 295.47 | -740.74 | airs480850005 | Hillcrest Rd. | Frisco | Collin |
| CAMS_63 | 294.36 | -764.24 | airs481130075 | Nuestra Dr. | Dallas North | Dallas |
| CAMS_56 | 257.81 | -735.32 | airs481210034 | Denton Airport | Denton | Denton |
| CAMS_94 | 276.41 | -818.04 | airs481390015 | Midlothian Tower | Midlothian | Ellis |
| CAMS_86 | 426.77 | -819.60 | airs484230007 | County Road | Tyler | Smith |
| CAMS_57 | 268.91 | -788.56 | airs484390057 | E Arkansas Ln. | Arlington | Tarrant |
| CAMS_13 | 244.22 | -778.53 | airs484391002 | Ross Ave. | Forth Worth NW | Tarrant |
| CAMS_17 | 250.69 | -765.49 | airs484392003 | Alta Vista Rd. | Keller | Tarrant |
| CAMS401 | 290.03 | -775.32 | airs481130069 | Hinton Dr. | Dallas | Dallas |
| CAMS402 | 289.59 | -791.02 | airs481130087 | W Redbird Ln. | Dallas | Dallas |
| CAMS___ | 288.82 | -747.66 | airs481210054 | Colony | Denton | Denton |

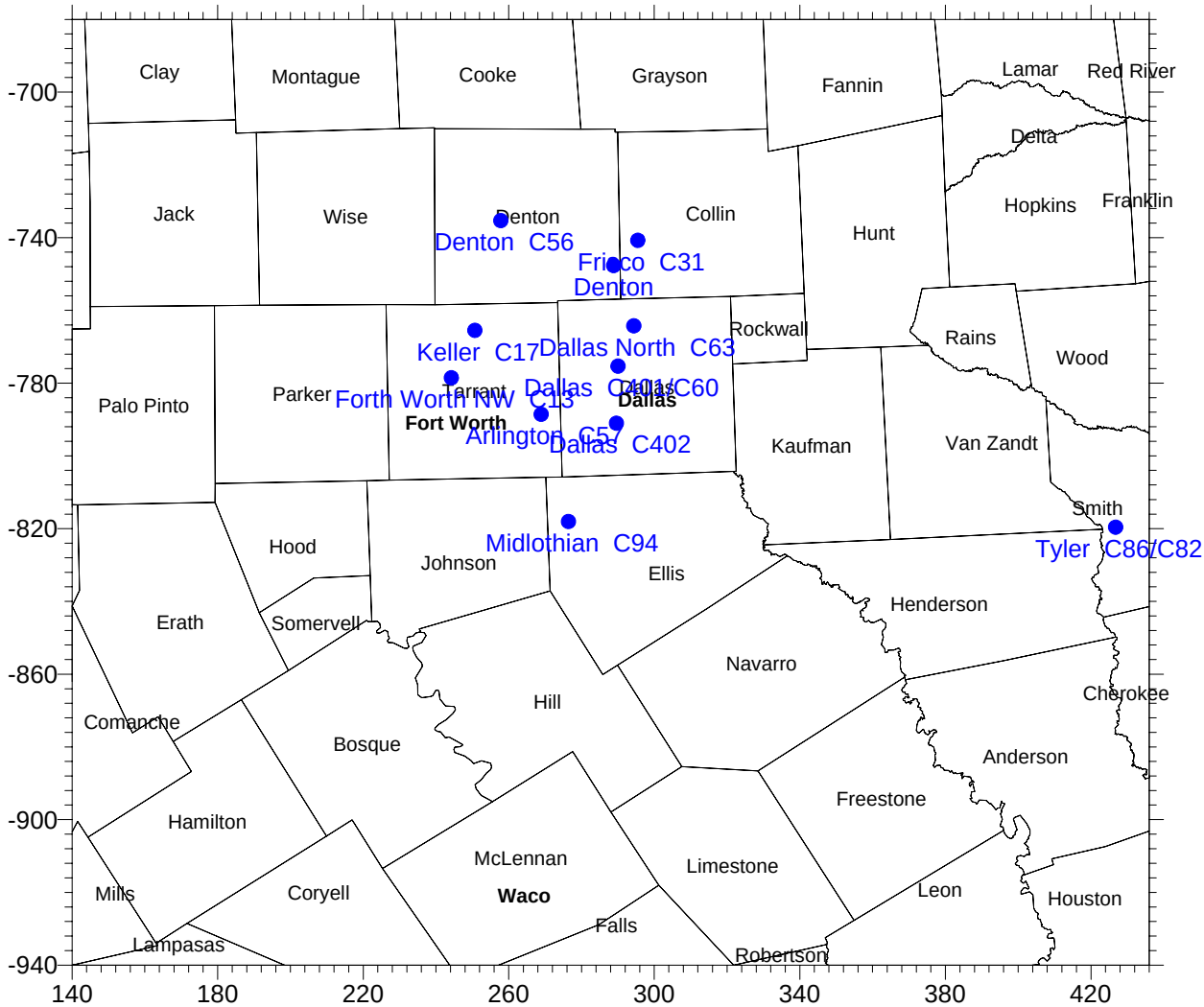


**CAMx Grid Dimensions**
**LCP Grid with reference origin at (40 N, 100 W)**
**True Latitudes at 30 N and 60 N**

**4 km Grid (with buffers): 74 x 65 from (140, -940) to (436, -680)**

**Figure 1-1.** Dallas/Fort Worth 4-km grid for the August 1999 episode.

## REPORT ORGANIZATION

Section 2 documents the MM5 meteorological model performance of the two alternative MM5 simulations relative to the original MM5 run.

Section 3 first compares the base case prior to this study, Run 17b (Emery et al., 2004) to a new run called Run 20 that included updated mobile source emissions provided by the TCEQ.

Section 4 compares the impacts of using larger horizontal and vertical model domains starting from Run 20.

Section 5 evaluates ozone sensitivity to different meteorological inputs developed from several alternate MM5 runs.

Section 6 shows the model performance impacts of several across-the-board changes in the emissions that should be considered sensitivity tests.

Section 7 examines the sensitivity of model performance to changes in the chemical mechanism used in CAMx.

Section 8 describes the development of a new base case, called Run 34, that combines changes developed in Sections 2-7 that were considered justifiable model improvements. Section 8 also presents Process Analysis of Run 34 and two related CAMx runs using CPA.

Section 9 examines the impact of model updates developed for Run 34 on 2010 ozone levels and transport contributions determined using APCA ozone source apportionment. Section 9 also investigates the sensitivity of APCA transport assessments to several factors.

A summary and conclusions are presented in Section 10.

# 2. ANALYSIS OF TWO ALTERNATIVE MM5 SIMULATIONS

A key component of the H-35 Phase 2 sensitivity tests is to develop two alternative MM5 simulations and investigate their impacts on CAMx performance:

1) Replace the Pleim-Xiu LSM/PBL schemes with the Eta + Noah schemes;
2) Replace the Kain-Fritsch sub-grid cumulus convection scheme with the Grell scheme.

This section documents the meteorological model performance of these two alternative MM5 simulations relative to the original run.

Several years ago, ENVIRON selected the Pleim-Xiu (P-X) LSM/PBL scheme for Texas MM5 modeling efforts in East Texas, south-central Texas, and DFW due to its improved performance for winds, temperature, and PBL depth over the original configuration (i.e., the simple 5-layer soil model with Gayno-Seaman and MRF PBL schemes). Recent MM5 modeling for DFW has indicated that PBL depths remain much too high using P-X, as indicated by several measures. The Eta PBL scheme is a widely used alternative approach that is known to generally lead to lower mixing depths. It was also necessary to choose an alternative soil model as well since Eta does not couple to the P-X LSM; we selected the Noah LSM, which is the only other approach available that has technical capabilities on par with the P-X methodology. HARC also suggested a separate MM5 simulation using an alternative cumulus parameterization scheme. The second MM5 test simply replaces the original Kain-Fritsch approach with the Grell scheme (all other model options remain consistent with the original P-X configuration).

## HOURLY PERFORMANCE

Statistical model performance was determined for the two alternative MM5 runs similarly to that reported by ENVIRON for the original MM5 configuration (Emery et al., 2004). For the purposes of this report, we maintain the label of the original run ("Run 5"), and assign the labels "Run 6" to the Eta/Noah simulation, and "Run 7" to the Grell simulation. Hourly statistical results for winds, temperature, and humidity from all valid MM5-observation pairings within the 4-km DFW domain are shown in Figure 2-1.

As expected, results from Run 5 and Run 7 are comparable for wind, temperature and moisture. This was expected because invoking a different sub-grid cumulus parameterization should not have significant impacts during periods where convection is absent (such as the bulk of days during the August 13-22, 1999 period), and because convective schemes are not invoked for high-resolution grids such as the 4-km DFW domain. Both runs show slight over estimation of wind speed during most of episode days, a relatively high warm bias for the daytime temperature, and a low humidity bias on the 12-km and 4-km domains.

In Run 6, however, the over prediction of wind speed is reduced, and a low wind speed bias becomes relatively dominant. The moisture under estimation in Run 5 and 7 is improved in Run 6 – this is most obvious on the 12-km domain (not shown). But the warm daytime temperature bias is made worse in Run 6. Reasons for this will become more clear as we discuss the impacts that Run 6 has on PBL heights below. With a reduced daytime mixing depth resulting from the use of the Eta/Noah schemes, water vapor and heat are concentrated within the boundary layer,

which increases surface humidity (better performance) and temperature (worse performance). The impact on wind performance is harder to explain, except to say that the approach used in Eta is based upon a turbulent kinetic energy model, which can lead to a significant difference in the momentum profile compared to a bulk approach such as P-X.

## DAILY AVERAGE PERFORMANCE

Daily statistical results for winds, temperature, and humidity from all valid MM5-observation pairings within the 4-km DFW domain are shown in Figure 2-2. Performance for winds is rather good for all three runs. The statistics for wind speed and direction are all within the benchmarks for acceptable performance on both 12- and 4-km domains, with the possible exception of wind direction gross error for Run 7 on the 4-km domain. Notice how Run 6 significantly differs from the other runs with a net negative bias and generally improved gross error and IOA. However, Run 6 is not necessarily the best in terms of wind direction.

Temperature bias and gross error from Run 5 and 7 on the 4-km domain are within the benchmark. Temperature bias and gross error from Run 6 on the 4-km domain are relatively high due to the warmer daytime bias. The low humidity bias persists, but the humidity bias and gross error of Run 6 on the 4-km domain are much lower than the other two runs. Run 6 clearly gives the best performance for the moisture simulation.

## MODELED MIXING DEPTHS

Figure 2-3 presents the diagnosed mixing depths from MM5 Runs 5, 6, and 7 at 1500 LST on August 17, 1999. These were not taken directly from MM5 output of PBL heights, but rather diagnosed from the CAMx-ready vertical diffusivity (Kv) files, which were in turn calculated from the MM5 output PBL depths (and TKE in the case of Run 6). Therefore, the heights indicated in the figure show the “effective” mixing depth in CAMx as represented by the air quality model’s vertical grid structure. The difference in the features between the three fields in Figure 2-3 are common to all days in the episode. Throughout this report, we will show modeling results for August 17 in particular because it is the day when observed ozone levels were the highest over the episode yet CAMx exhibits some of the largest under prediction problems.

Notice that Runs 5 and 7 are nearly identical, which makes sense given that the same PBL option is used in both (P-X). Notice that the PBL “holes” seen in Run 7 are associated with the location of lakes, and these appear in the same location day after day. It is unclear why the Run 5 fields do not show the influence of these lakes in the same way. These holes are caused by the relatively cool water temperatures that lead to a stabilization of the PBL in those columns. The effects of the lakes are also indicated to some extent in the Run 6 PBL fields.

Notice that Run 6 is significantly different from Runs 5 and 7 in several aspects. First and foremost, the Eta PBL scheme, possibly in combination with differences arising from the use of Noah LSM, results in much lower mixing depths. Over the several days investigated, Eta consistently leads to maximum PBL depths of 1000-1800 m, compared to the relatively consistent maxima of 2000-2600 m diagnosed by P-X. Second, the Eta/Noah combination results in much more spatial variation in the mixing depth than P-X, and this variation changes

hour-to-hour and day-to-day. A potentially significant impact on CAMx performance would be expected from the Eta-derived Kv fields.

## COMPARISON OF MODELED AND OBSERVED VERTICAL PROFILES

Vertical profile measurement data are available from four sites located within or near the DFW area:

1. The DFW rawinsonde (WBAN #72249), which records wind, temperature, and humidity throughout the troposphere by balloon ascent twice daily at 0600 and 1800 LST each day;
2. The DFW AVAS, which was operated during an MIT airport field study in 1999, and consists of a blend of data from several sensors, providing hourly winds up to a few km;
3. The TCEQ Hinton SODAR, which provides some limited hourly winds up to ~1-km;
4. The NOAA Palestine Profiler, which provides hourly winds up to a few km.

Data from these sites were plotted together with modeled profiles of wind, temperature, and humidity (where applicable) to gauge model performance within the lowest few km. Examples are shown in Figure 2-4 for the afternoon of August 17 (additional plots are provided on an accompanying CD). The findings on this day are generally applicable to other days of the episode.

At the rawinsonde site (shown at 1800 LST), the wind speed/direction profiles were replicated fairly well in all three MM5 runs. Temperatures tended to be over predicted in the P-X runs (5 and 7), but very well modeled in the Eta run (Run 6). Recall that the daily maximum temperatures near the surface tended to be highly over predicted in the Eta run, but at this particular hour the entire temperature profile is simulated rather well. Run 6 also results in a better replication of the humidity profile. Note the break in the Run 6 profile at about 1.5-km, which agrees with a change in temperature lapse rate at the same altitude. This is the modeled PBL top, and it agrees much better with the measured profiles than either Run 5 or 7, which both suggest a much deeper mixing depth. However, model performance for the humidity profile is generally poor for all three runs.

The wind speed and directions profiles at the NOAA Palestine profiler site were also simulated rather well, with Run 6 indicating slightly better performance. However, the profiler does not resolve winds below 500-1000 m, so near-surface performance is impossible to gauge. Since the observed wind profiles at AVAS and Hinton are limited by very sparse data in the low elevation (most below 1-km), especially at Hinton, model performance is difficult to interpret at those sites. The simulated wind profiles from the three MM5 runs all have relatively large errors compared to the AVAS and Hinton observed profiles. We are particularly skeptical of the data quality from the Hinton site. While these profile data were provided to MM5 for observation nudging via the FDDA input file, we believe that the model is not sufficiently influenced by them because of the sparseness of their data.

Overall, Run 6 results in relatively better wind speed, temperature, and humidity profiles with lower bias for most of the time periods plotted. The simulated wind speed profiles of Run 5 are also acceptable and comparable to those of Run 6 in most of cases. Run 7 often results in slightly stronger low-level wind speeds; the cause of this is not clear, but it may be associated

with stronger convective outflows cause by the Grell scheme from simulated systems upstream of DFW.

## INTERCOMPARISON OF PRECIPITATION PATTERNS

Run 7 indicated a surprising degree of difference in the wind profiles relative to Run 5. Given that the only change in these two MM5 runs was the substitution of the sub-grid cumulus convection from Kain-Fritsch to Grell, it is difficult to diagnose the cause of this, especially since there was no significant convective activity anywhere near the 4-km DFW domain during the core days of the modeling episode. To investigate the changes in rainfall patterns brought about by use of the Grell scheme, the total accumulated surface precipitation (resolved + sub-grid convective) predicted by Runs 5, 6, and 7 were plotted. Figure 2-5 shows the results of summing hourly precipitation from the three runs over the August 15-22, 1999 period.

As expected, similar patterns are seen with Run 5 and 6, which use the same Kain-Fristch scheme. Minor differences in the patterns are attributed to the different boundary layer and soil models used. Run 7, however, shows a dirth of precipitation over land; note the lack of precipitation in the sea-breeze convergence zone along most of the coastline. This result was not expected, given our (and other's) past experience that the Grell scheme generally produces much more widespread, and often more intense, rainfall in the southern U.S. While it is not outside the realm of possibility that this reduction in coastal precipitation can have an influence on low-level wind profiles as far away as DFW, it is not clear why the wind profiles would be so different on certain days such as August 17.

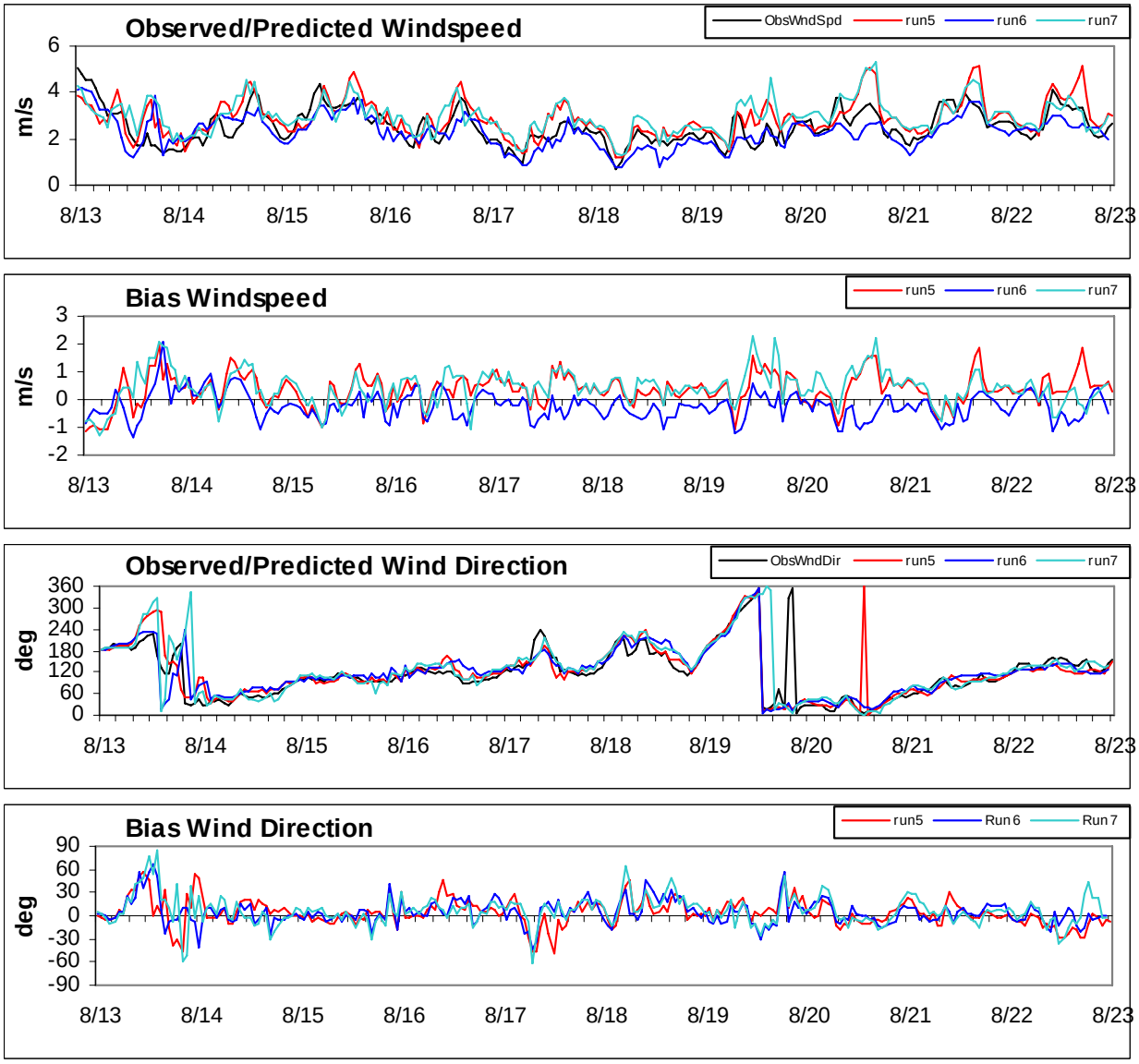


**Figure 2-1(a).** Hourly site-averaged MM5 wind performance for Runs 5, 6, and 7 in the DFW 4-km modeling domain.

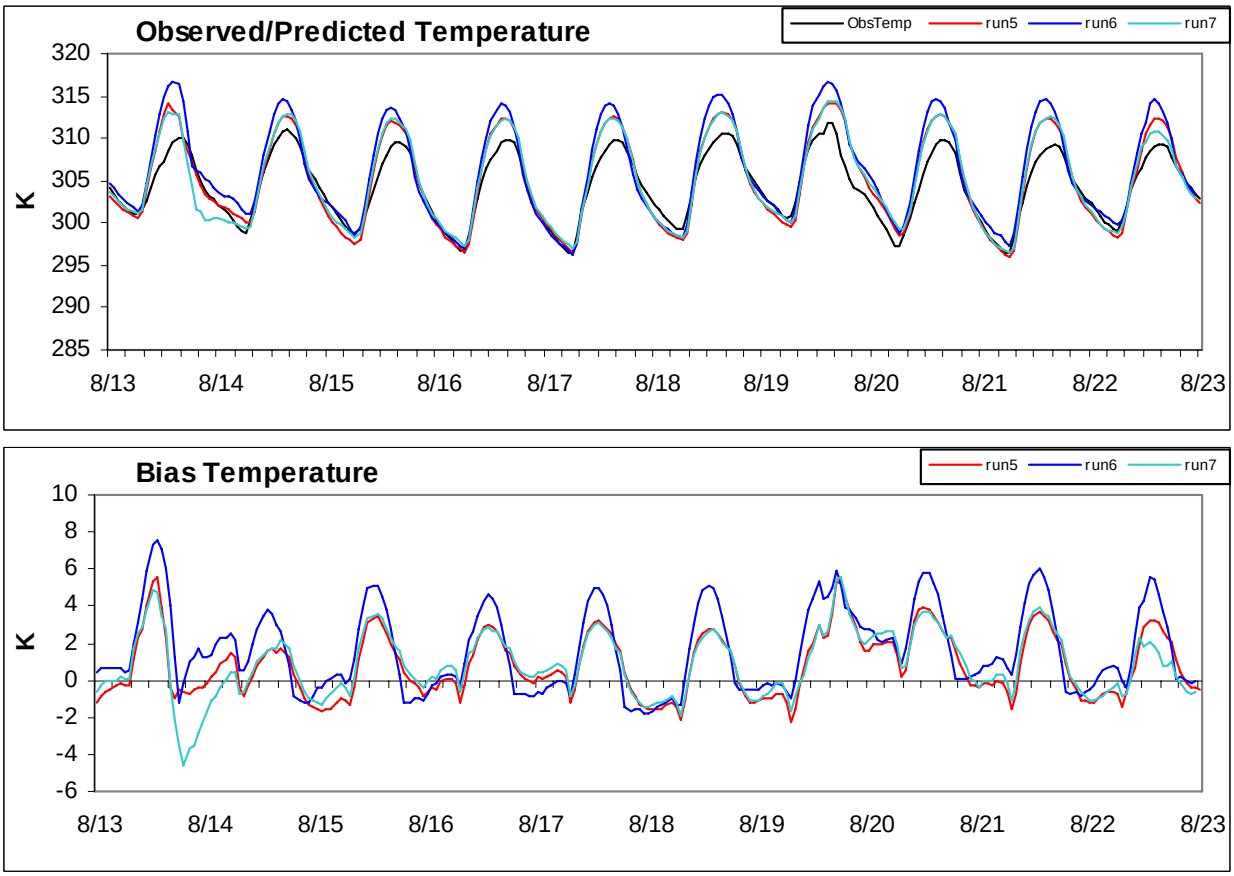


**Figure 2-1(b).** Hourly site-averaged MM5 temperature performance for Runs 5, 6, and 7 in the DFW 4-km modeling domain.

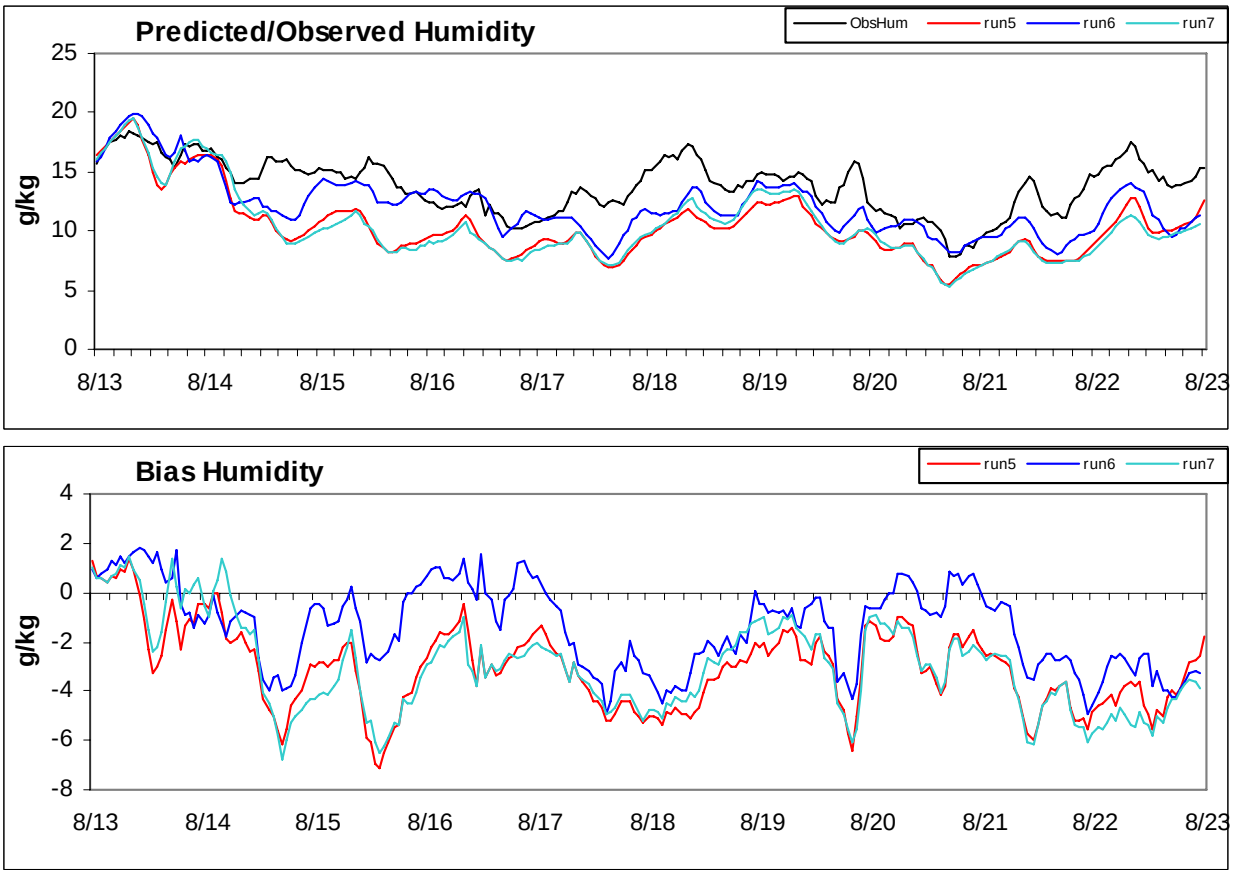


**Figure 2-1(c).** Hourly site-averaged MM5 humidity performance for Runs 5, 6, and 7 in the DFW 4-km modeling domain.

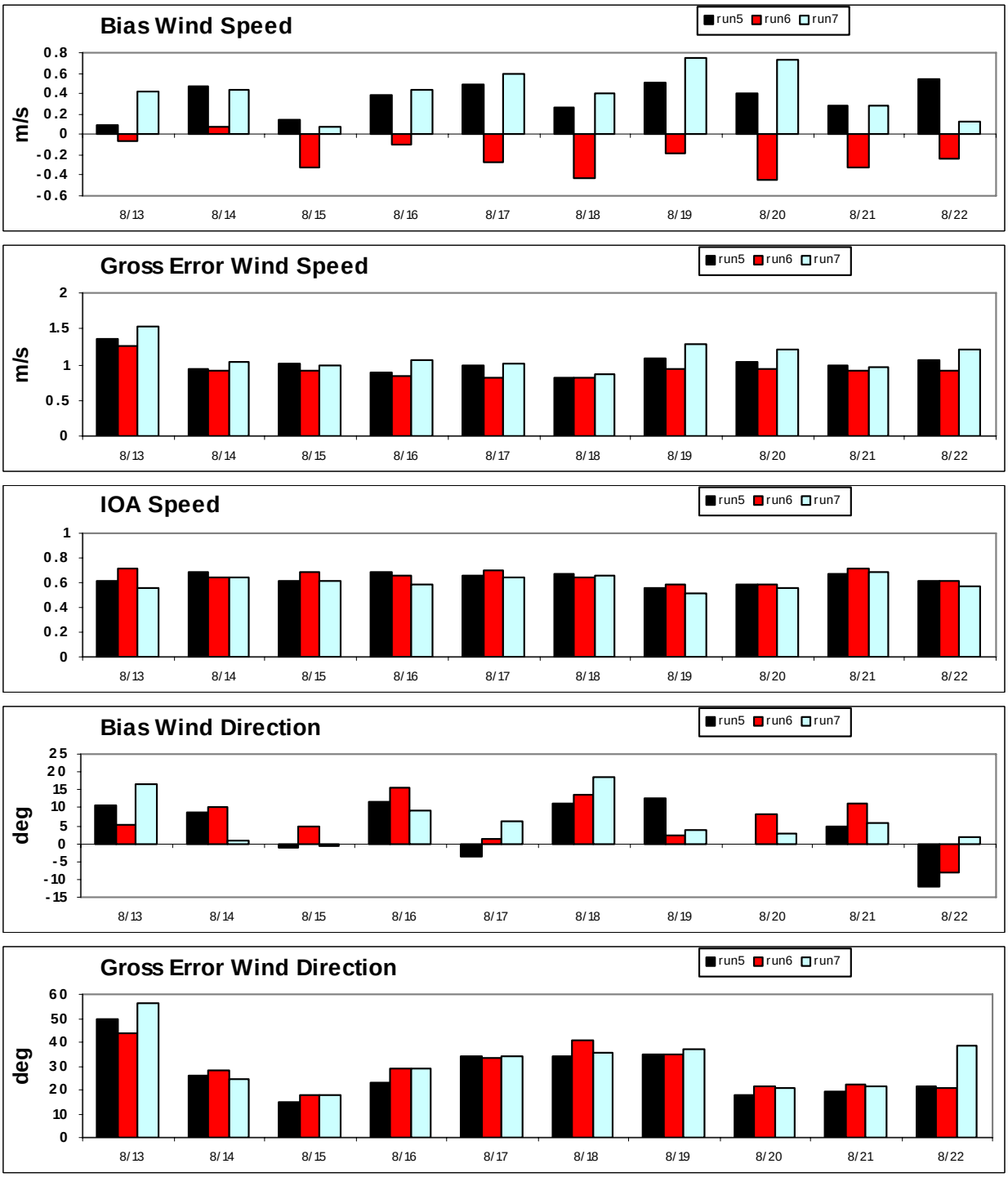


**Figure 2-2(a).** Daily site-averaged MM5 wind performance for Runs 5, 6, and 7 in the DFW 4-km modeling domain.

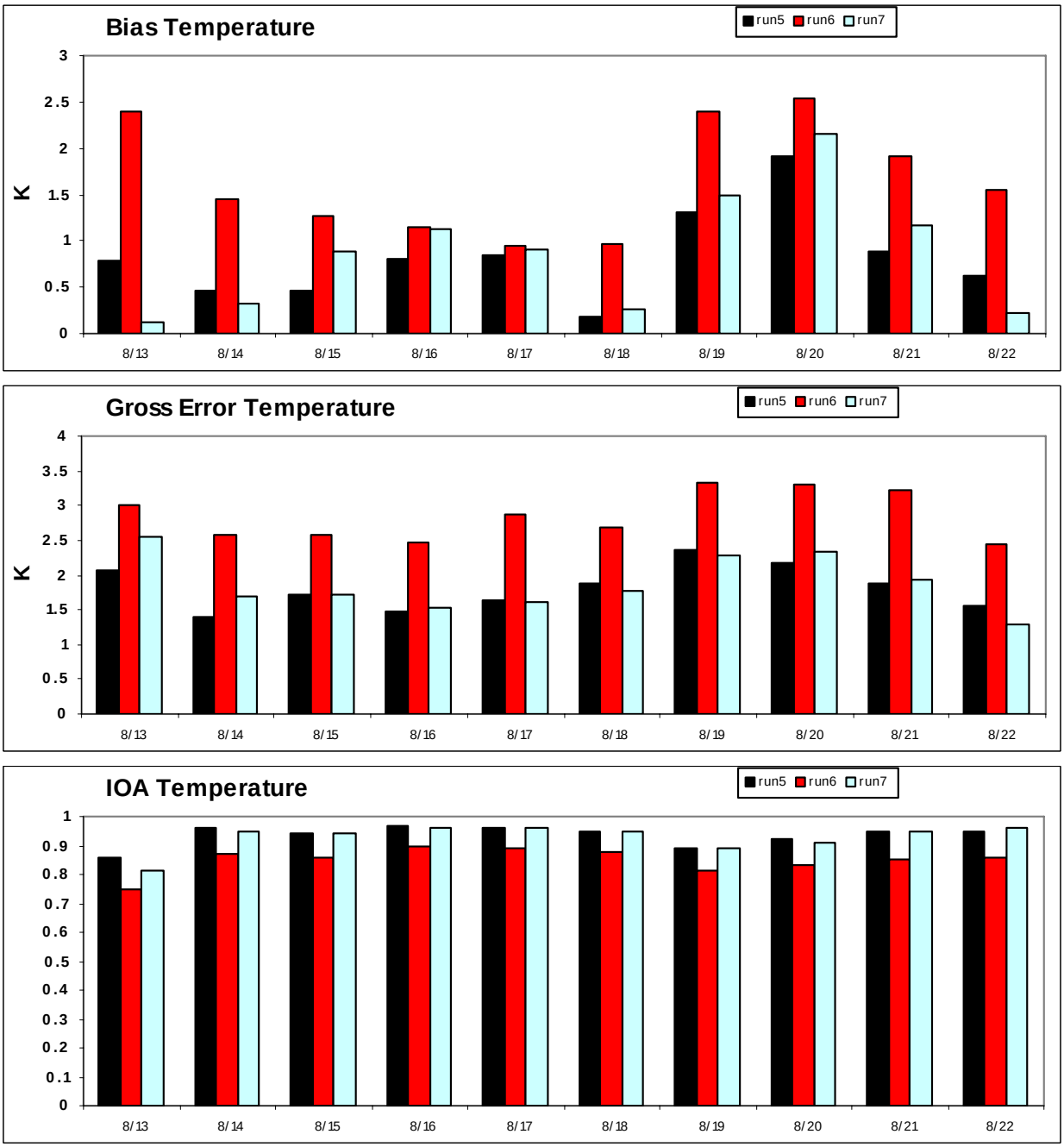


**Figure 2-2(b).** Daily site-averaged MM5 temperature performance for Runs 5, 6, and 7 in the DFW 4-km modeling domain.

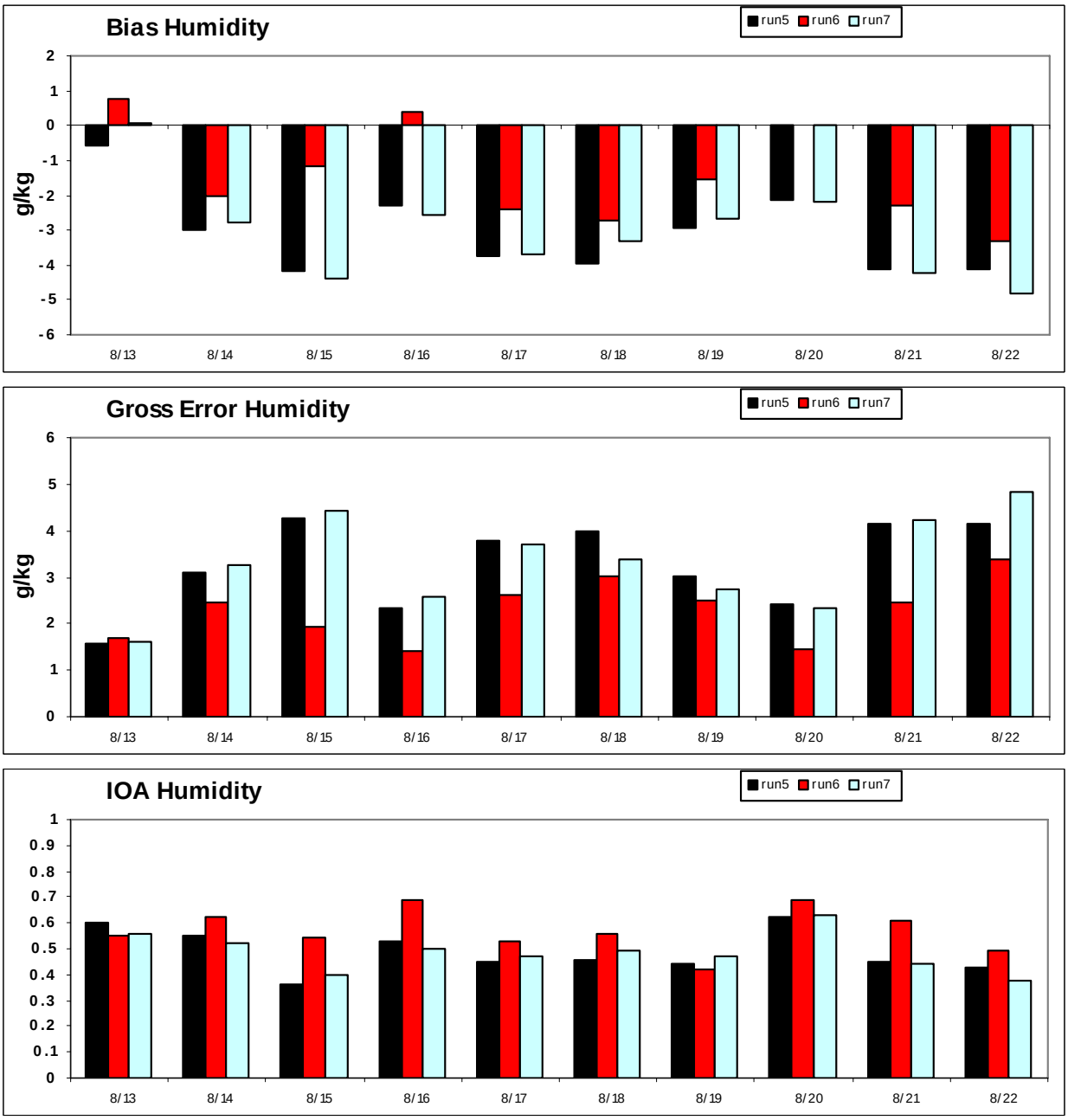


**Figure 2-2(c).** Daily site-averaged MM5 humidity performance for Runs 5, 6, and 7 in the DFW 4-km modeling domain.

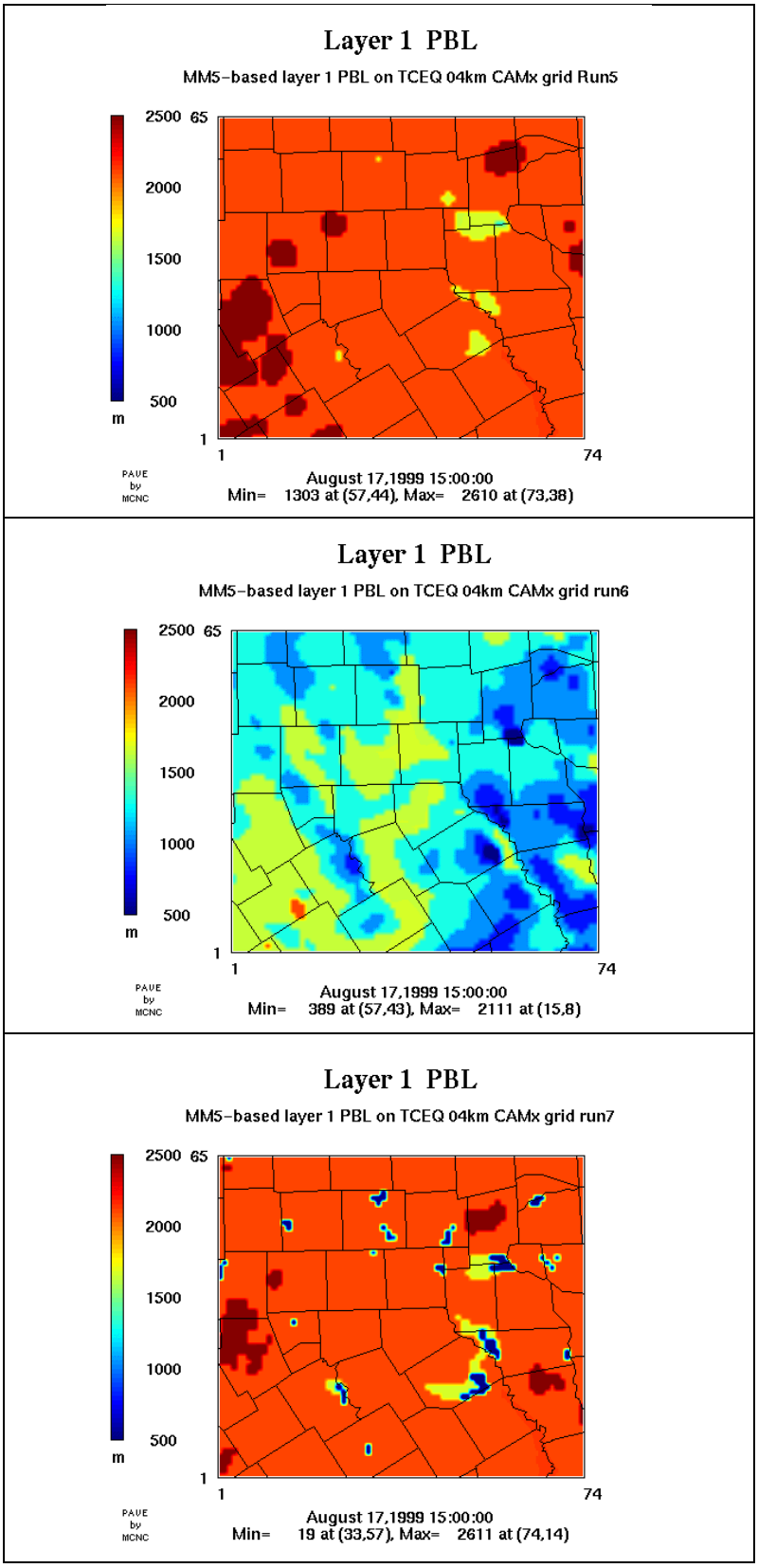


**Figure 2-3.** MM5-derived effective PBL depth for Runs 5, 6, and 7 in the DFW 4-km modeling domain, August 17, 1999 at 1500 LST.

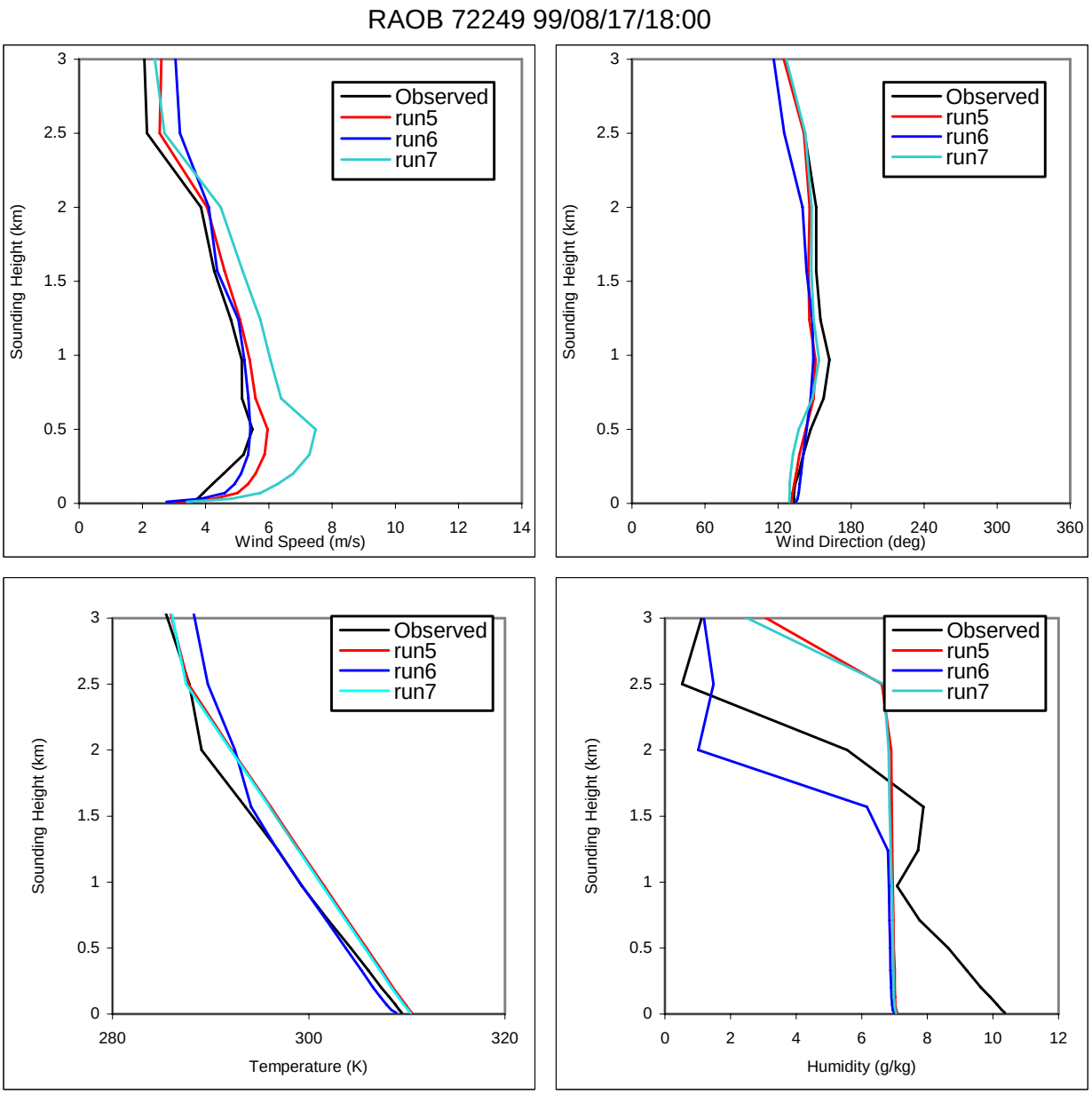


**Figure 2-4(a).** Comparison of wind, temperature, and humidity profiles from MM5 Runs 5, 6, and 7 at the DFW rawinsonde site, August 17, 1999 at 1800 LST.

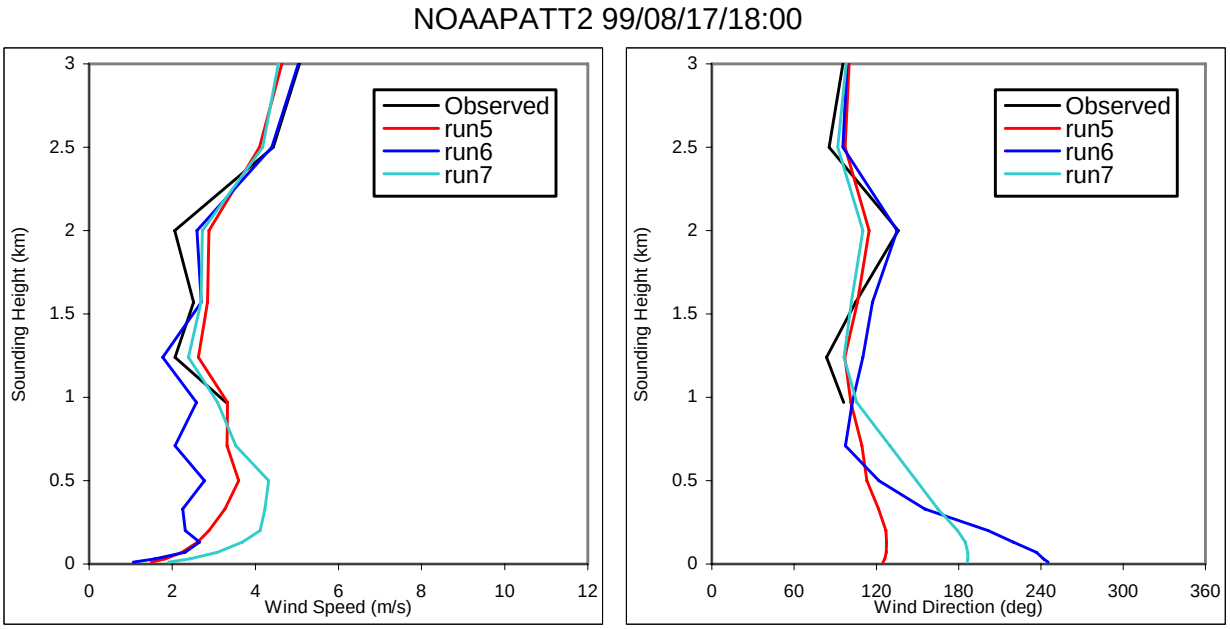


**Figure 2-4(b).** Comparison of wind profiles from MM5 Runs 5, 6, and 7 at the NOAA Palestine profiler site, August 17, 1999 at 1800 LST.

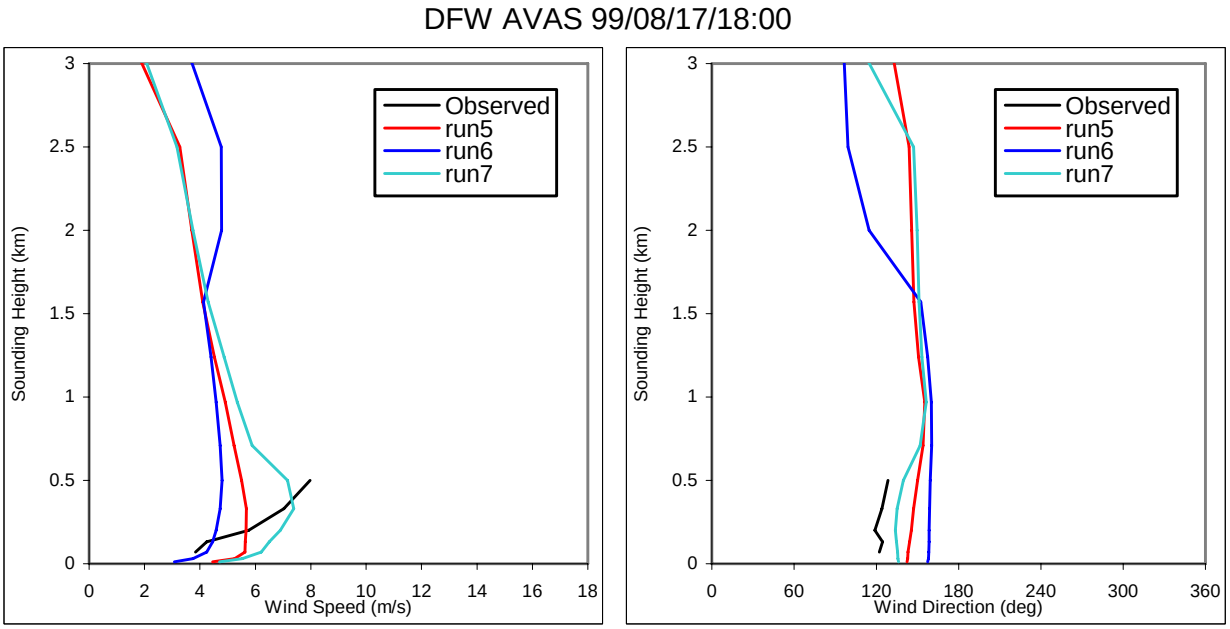


**Figure 2-4(c).** Comparison of wind profiles from MM5 Runs 5, 6, and 7 at the DFW AVAS profiler site, August 17, 1999 at 1800 LST.

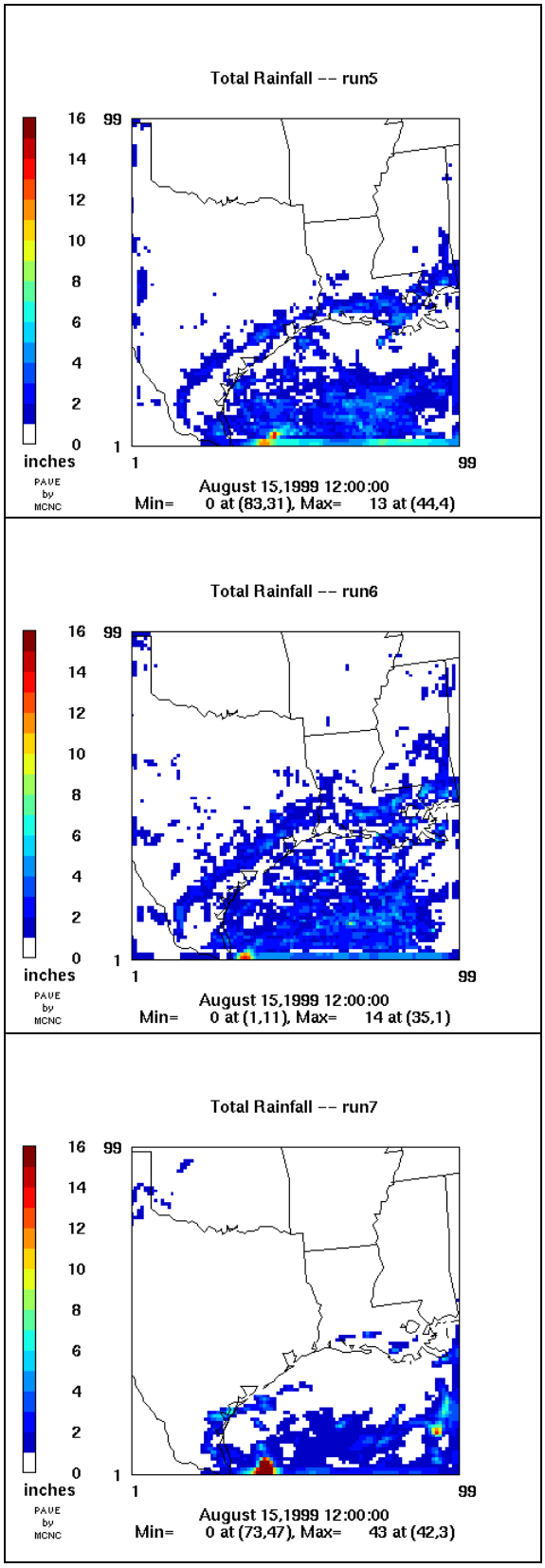


**Figure 2-5.** Total predicted accumulated rainfall between 12Z August 15 to 12Z August 22 in the MM5 12-km domain for Runs 5, 6, and 7.

# 3. BASE CASE UPDATE "RUN20"

Prior to this project, the latest CAMx base case developed by ENVIRON for Dallas/Fort Worth was referred to as "Run 17b" (Emery et al., 2004). This run used meteorology extracted from MM5 "Run 5" and emissions from TCEQ, both of which were generated in July 2004. The vertical domain extended to approximately 4-km. The 36-km domain spanned 1620-km in the west-east direction and 1656-km in the north-south direction, covering Texas to the Florida panhandle in the south, and southern Nebraska to southern Ohio in the north.

Boundary conditions were classified into three categories: clean, moderate, and dirty. Table 3-1 lists boundary concentrations associated with each group. Boundaries over the Gulf of Mexico were assigned clean conditions. The western boundary, the southern boundary over Mexico, and the northern boundary over Nebraska were set to the moderate group up to 1700 m and clean farther aloft. The remaining sections of the north and east boundaries were set to dirty conditions below 1700 m, and clean above this level. Initial conditions were clean everywhere.

**Table 3-1**. Concentrations (ppb) used to define CAMx initial and boundary conditions.

| Species | Dirty | Moderate | Clean |
|---|---|---|---|
| O3 | 40 | 40 | 40 |
| CO | 200 | 200 | 100 |
| NO | 0.1 | 0.1 | 0.1 |
| NO2 | 1 | 1 | 1 |
| HNO3 | 3 | 3 | 1 |
| HNO2 | 0.001 | 0.001 | 0.001 |
| ALD2 | 0.555 | 0.555 | 0.05 |
| ETH | 0.51 | 0.51 | 0.15 |
| HCHO | 2.1 | 2.1 | 0.05 |
| OLE | 0.3 | 0.3 | 0.05 |
| PAR | 14.9 | 14.9 | 7.6 |
| TOL | 0.18 | 0.18 | 0.0786 |
| XYL | 0.0975 | 0.0975 | 0.0688 |
| ISOP | 3.6 | 0.1 | 0.001 |
| PAN | 0.1 | 0.1 | 0.1 |
| H2O2 | 3 | 3 | 1 |
| MEOH | 8.5 | 0.001 | 0.001 |
| ETOH | 1.1 | 0.001 | 0.001 |

CAMx Run 20 duplicated Run 17b with a few changes. TCEQ provided a new set of mobile emissions in August 2004, replacing the older mobile emissions used in Run 17b. Initial conditions were set to the moderate group (see Table 3-1) below 1700 m, instead of clean. A minor format correction was made to the boundary condition file that had no impact on model results.

## MODEL PERFORMANCE EVALUATION

All runs were evaluated by examining time series plots, daily statistics, scatter plots and spatial plots of the daily peak ozone. Figure 3-1 displays the time series of 1-hour predicted and observed ozone at each monitoring station in the DFW 4-km modeling domain. Except for the two spin-up days, Run 17b and Run 20 were nearly identical, suggesting that all the changes in Run 20 were due to the changes in the initial conditions.

Figures 3-2 and 3-3 show CAMx model performance statistics for 1-hour and 8-hour ozone, respectively, for each date. The red horizontal lines represent the 1-hour performance goals set by the EPA. Peak accuracy, normalized bias, and normalized error from Runs 17b and Run 20 were the same on all but the spin-up dates.

Figure 3-4 compares each date's highest observed 1-hour ozone to the highest predicted 1-hour ozone in the 9 cell by 9 cell grid surrounding the corresponding observation site for all sites in the 4-km DFW domain. Each blue cross represents a predicted and observed pairing for each site and date from August 15 to 22. The pink circles represent quantile plots at every $5^{th}$ percentile. The short red dashes represent the ±20% goal set by the EPA. The coefficient of determination ($R^2$) is nearly unchanged between Run 17b and Run 20. Blocks of 9 by 9 cells were used in accordance with EPA draft modeling guidance which recommends using a block of cells that is the same size as a single 36-km grid cell.

Figure 3-5 shows scatter plot and quantile plots of the predicted and observed daily maximum 8-hour ozone from all sites in Runs 17b and 20. Like Figure 2-4, the predicted values represent the highest ozone in the 9 cell by 9 cell block surrounding each observation site. The $R^2$ was the same in Run 20 as in Run 17b.

Table 3-2 summarizes the $R^2$ from each scatter plot of 1-hour and 8-hour ozone using the three methods defined by the EPA for computing the predicted peak. The first extracts the highest daily maximum ozone in the 9 by 9 block of cells surrounding the observation site, as previously discussed. The second method selects from the 9 by 9 grid cells to find the closest value to the observed ozone. The third uses bilinear interpolation to calculate the predicted daily maximum at the site location. Scatter plots of the latter two metrics are not shown. All $R^2$ values are identical between Run 17b and Run 20.

**Table 3-2**. Comparison of the 1-hour and 8-hour coefficient of determination from each scatter plot of the predicted and observed daily maximum ozone in Runs 17b and 20.

| | 1-hour $R^2$ | | | 8-hour $R^2$ | | |
|---|---|---|---|---|---|---|
| | max 9x9 | closest | interpolated | max 9x9 | closest | Interpolated |
| Run 17b | 0.40 | 0.84 | 0.35 | 0.38 | 0.74 | 0.26 |
| Run 20 | 0.40 | 0.84 | 0.35 | 0.38 | 0.74 | 0.26 |

Figure 3-6 shows spatial plots of the daily maximum 1-hour ozone in the 4-km domain from both Run 17b and Run 20 on August 17, 1999 – the date with the highest observed ozone. Figure 3-7 shows the daily maximum 8-hour ozone. No significant differences were detected.

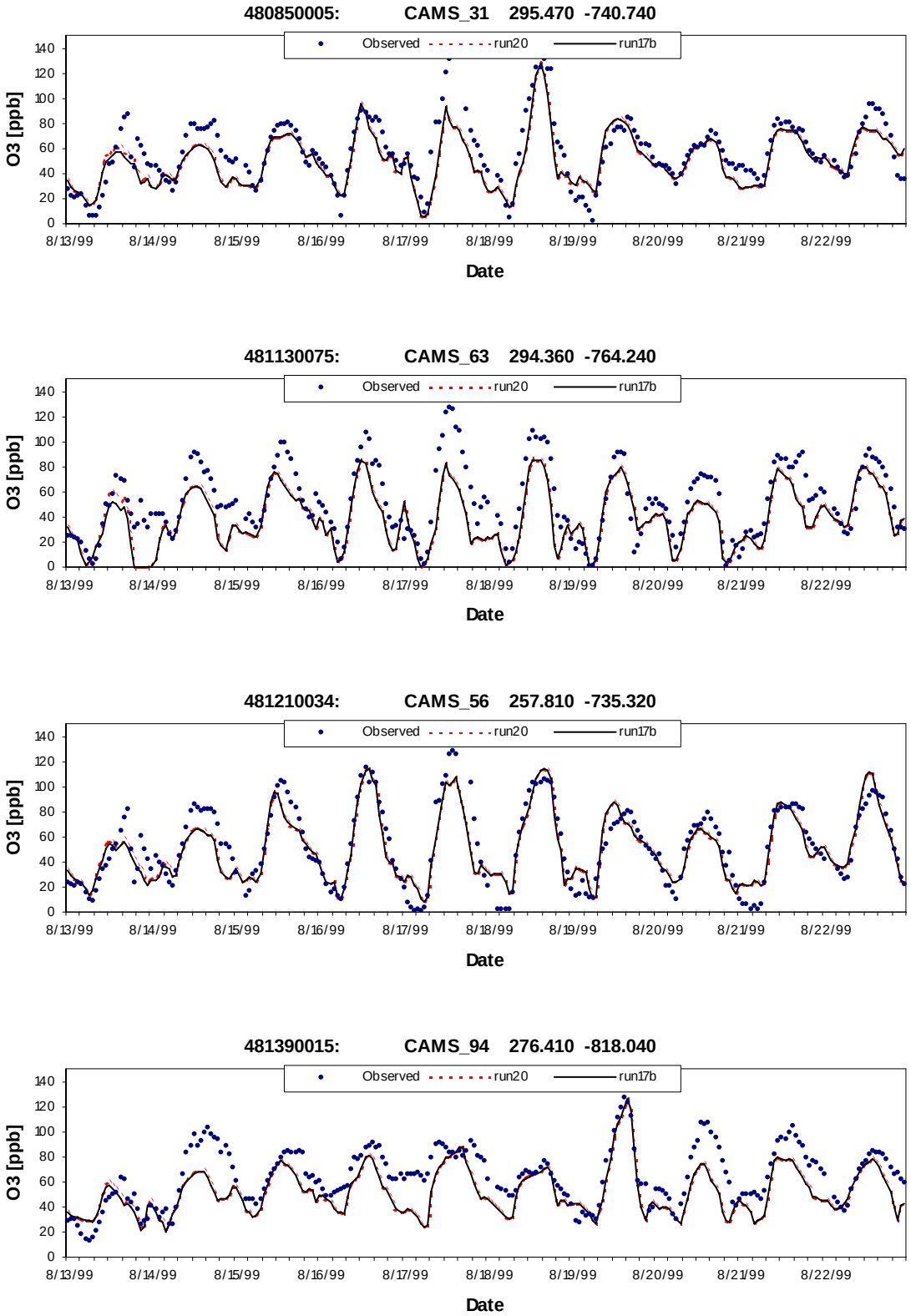


**Figure 3-1**. Time series of 1-hour ozone at sites inside the DFW 4-km domain from CAMx Runs 17b and 20.

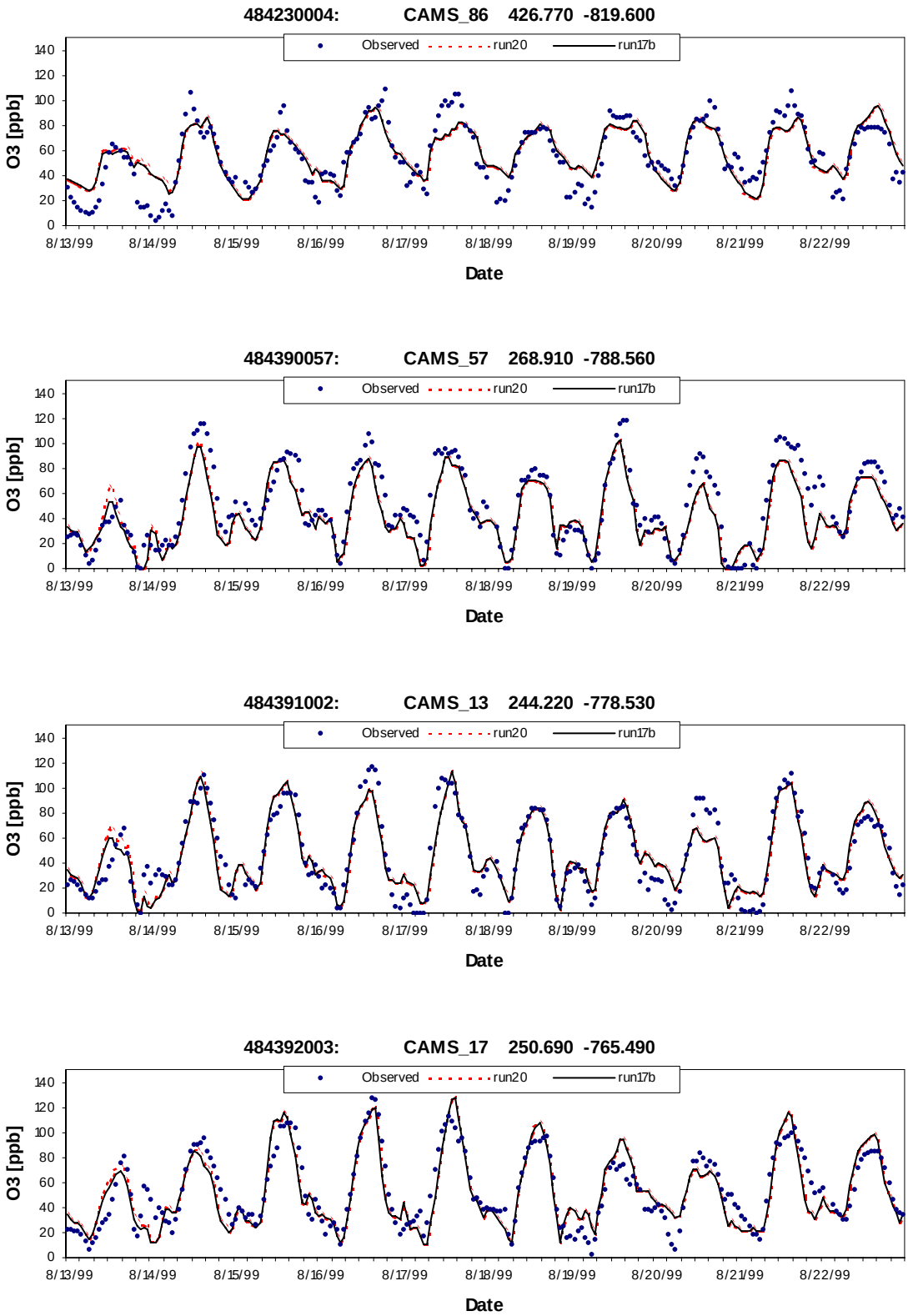


**Figure 3-1**. (Cont.) Time series of 1-hour ozone at sites inside the DFW 4-km domain from CAMx Runs 17b and 20.

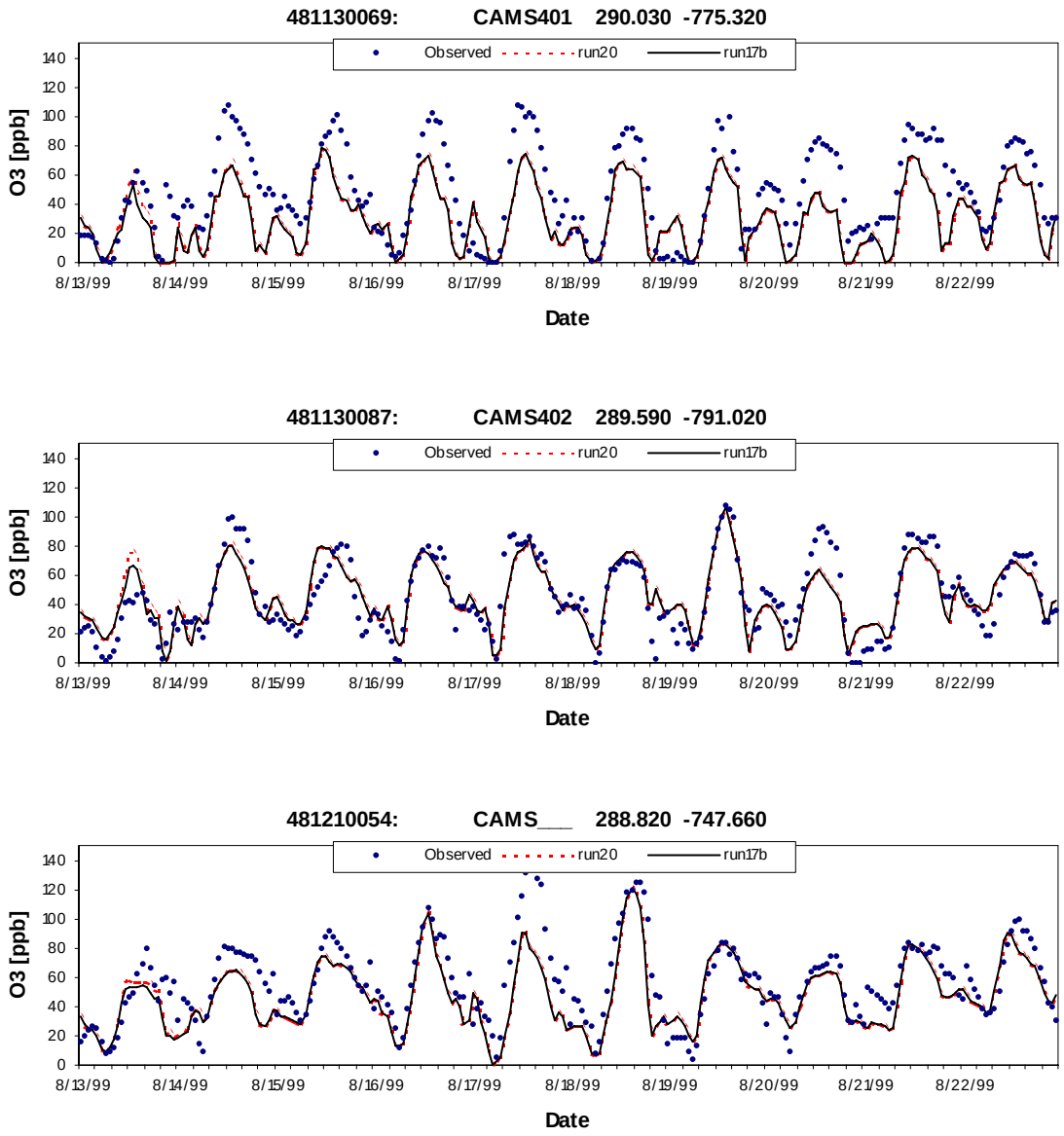


**Figure 3-1**. (Concl.) Time series of 1-hour ozone at sites inside the DFW 4-km domain from CAMx Runs 17b and 20.

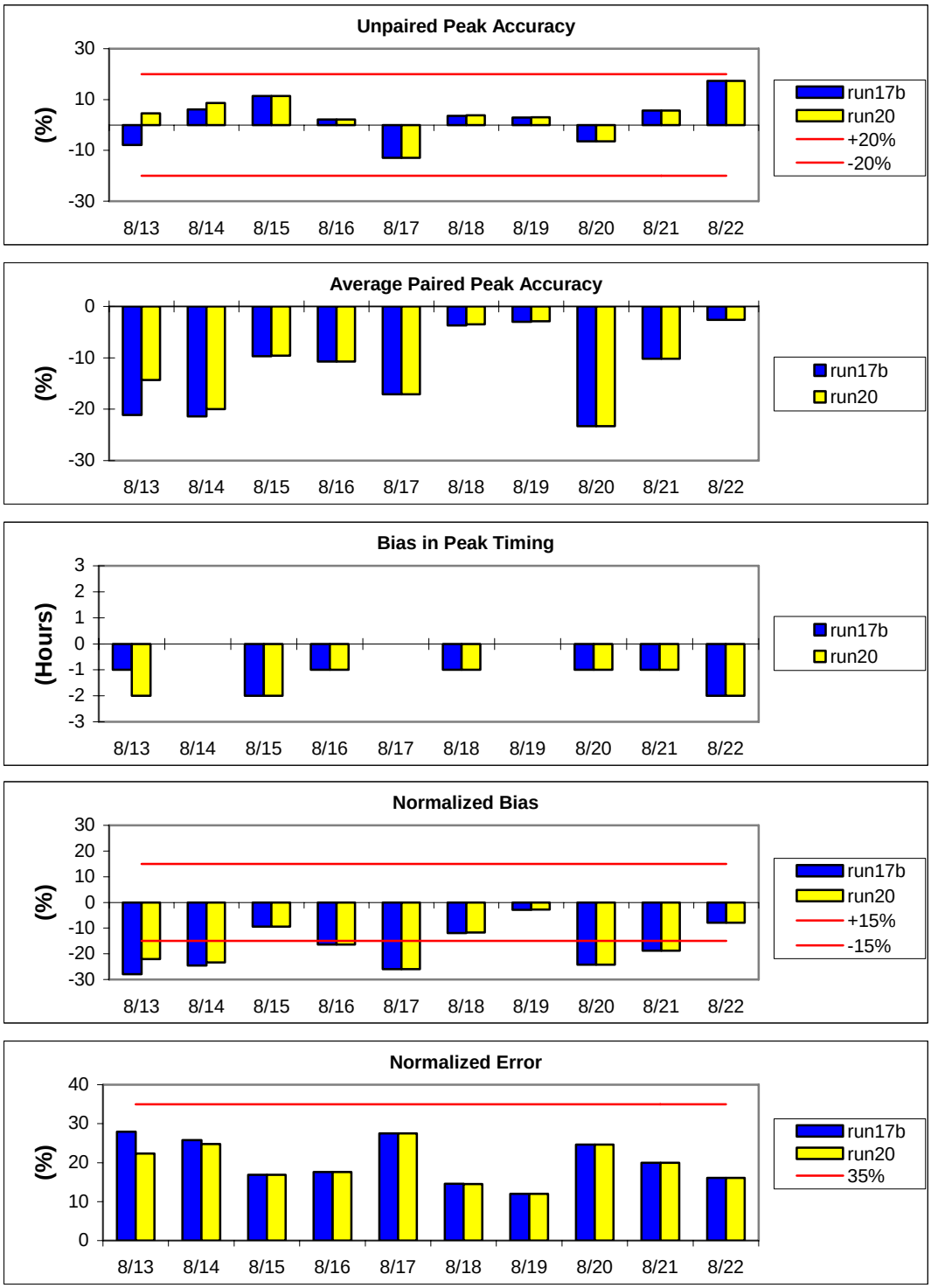


**Figure 3-2**. Daily statistics of the 1999 DFW 1-hour ozone in the 4-km domain from CAMx Runs 17b and 20.

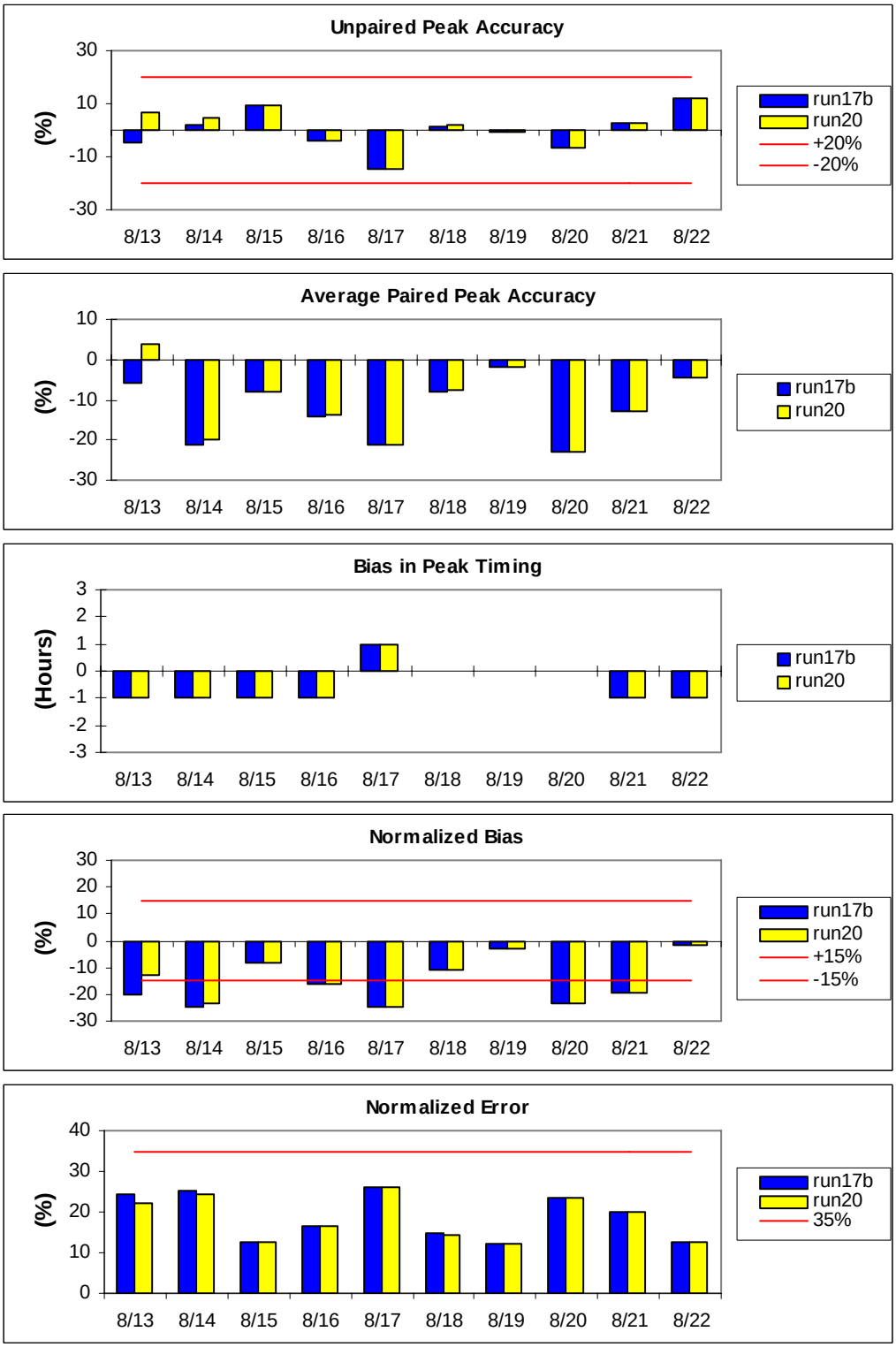


**Figure 3-3.** Daily statistics of the 1999 DFW 8-hour ozone in the 4-km domain from CAMx Runs 17b and 20.

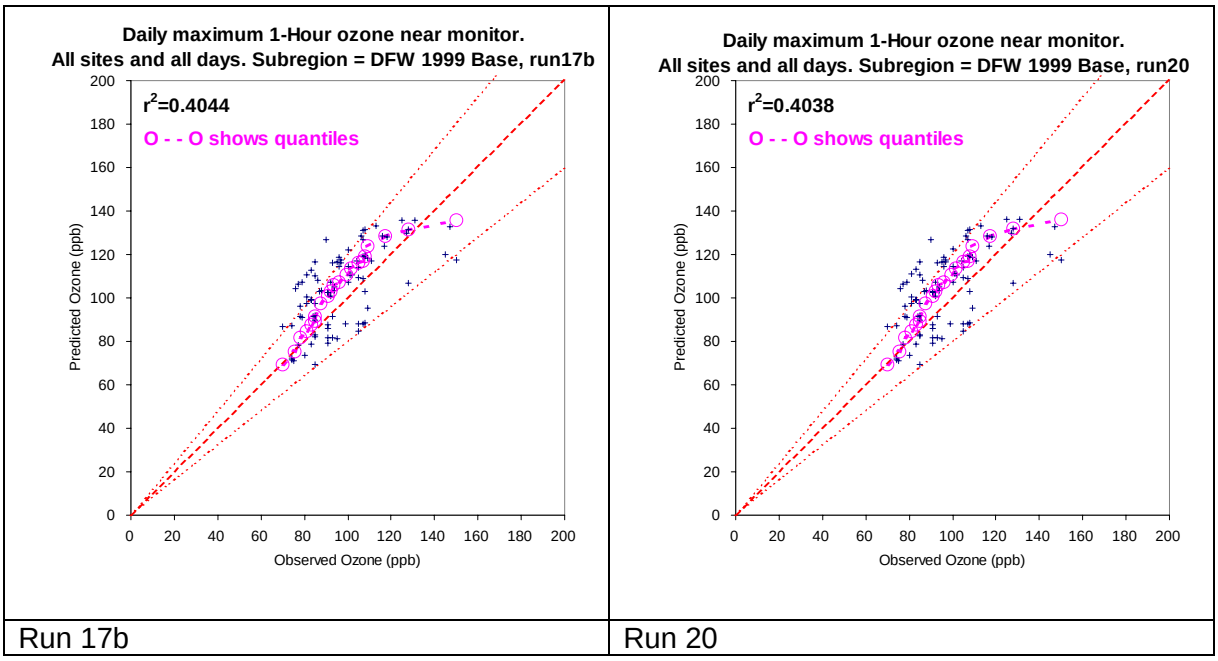


**Figure 3-4**. Scatter and quantile-quantile plots of the largest predicted daily maximum 1-hour ozone near each monitor (within 9x9 cell area) and the observed daily maximum 1-hour ozone for Runs 17b and 20 in the 1999 DFW Episode.

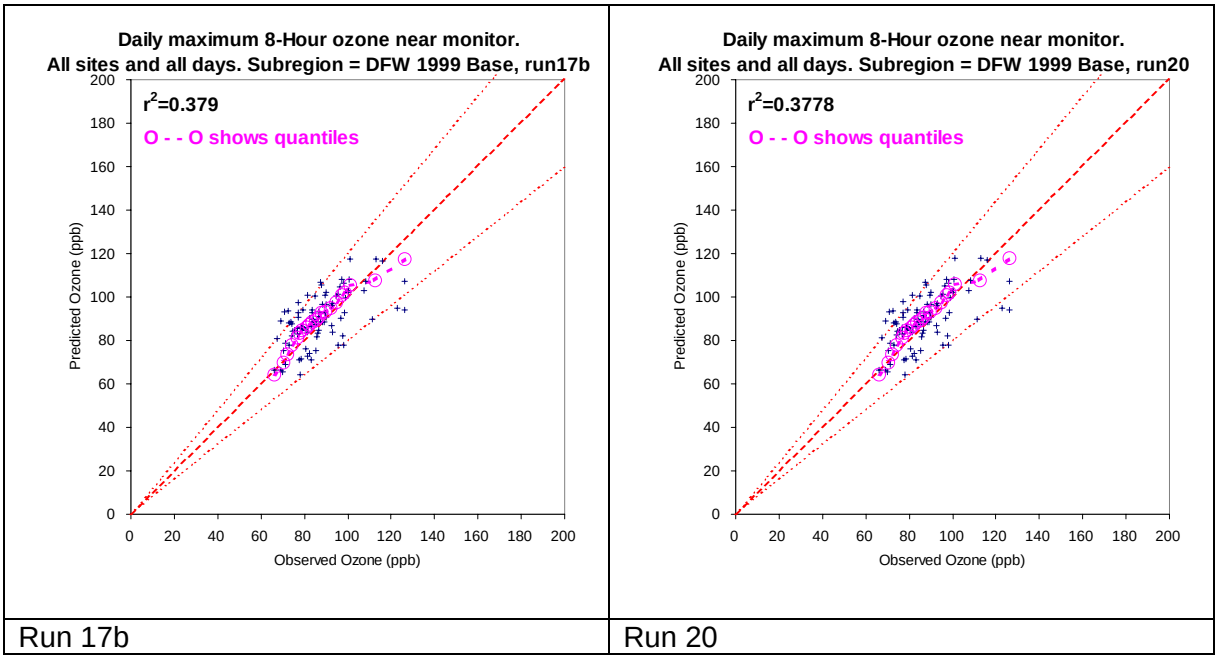


**Figure 3-5**. Scatter and quantile-quantile plots of the largest predicted daily maximum 8-hour ozone near each monitor (within 9x9 cell area) and the observed daily maximum 8-hour ozone for Runs 17b and 20 in the 1999 DFW Episode.

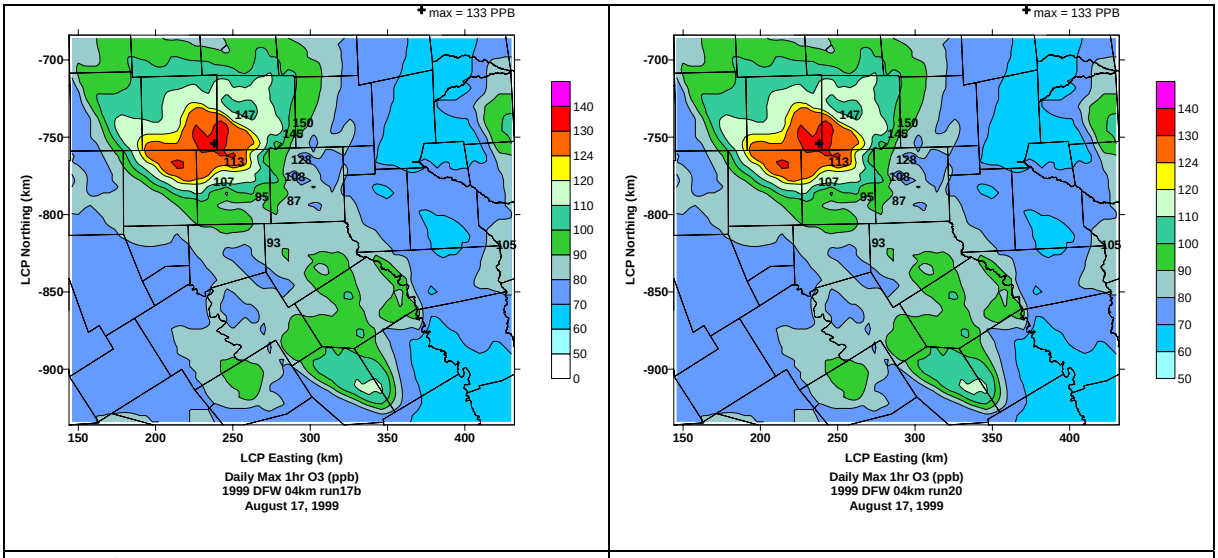


| Run 17b | Run 20 |
|---|---|

**Figure 3-6**. Spatial plots of the daily maximum 1-hour ozone in the DFW 4-km domain on August 17, 1999 from Runs 17b and 20.

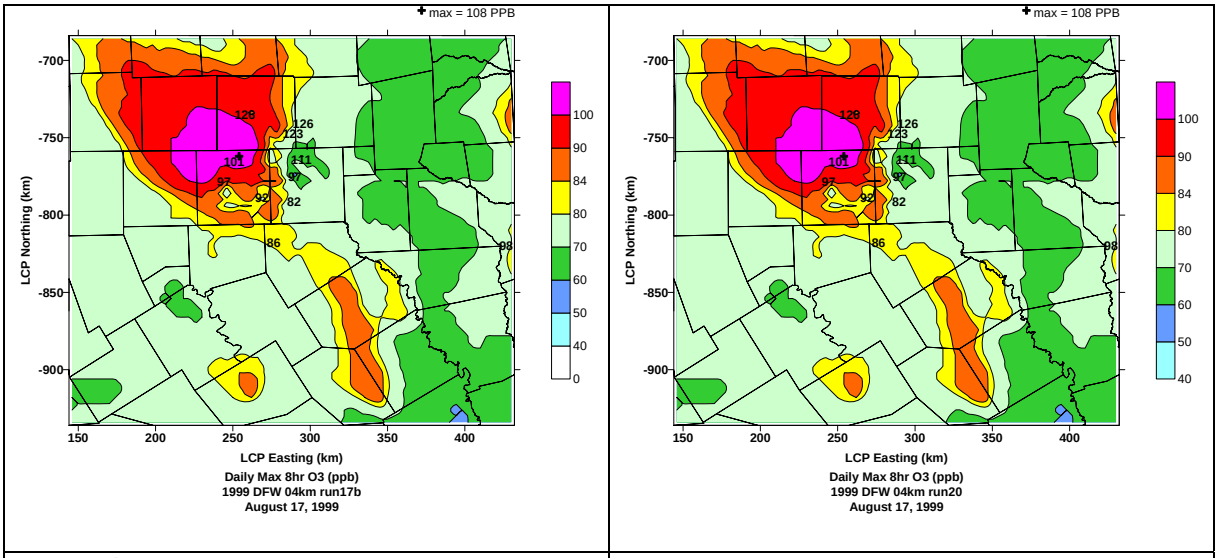


| Run 17b | Run 20 |
|---|---|

**Figure 3-7**. Spatial plots of the daily maximum 8-hour ozone in the DFW 4-km domain on August 17, 1999 from Runs 17b and 20.

# 4. OZONE SENSITIVITY TO CHANGES IN THE DOMAIN SIZE

This section evaluates model performance of the 1999 DFW episode when the domain is expanded vertically and horizontally toward the north and east.

## CAMx DOMAIN FROM "RUN 20"

In Run 20, the 36-km grid spanned 1620-km by 1656-km, extending as far north as southern Nebraska and southern Ohio, and as far east as the Florida panhandle. The expanded domain spans 2484-km in the east-west direction and 2412-km in the north-south direction. The larger domain still covers most of Texas, but now extends into southeastern North Dakota, southern Maine, and across all of Florida. Figure 4-1 displays a map comparing the original and expanded domains.

In the past, CAMx coincided with the first 15 vertical layers from MM5, which topped out at an altitude of just below 4-km. To extend the top to over 15-km, five additional layers were added, each spaced roughly 2 to 3-km apart. The vertical layering structure from MM5 and CAMx are listed in Table 4-1.

**Table 4-1.** MM5 and CAMx vertical grid structures based on 28 sigma-p levels. Heights (m) are above ground level according to a standard atmosphere; pressure is in millibars.

| Layer | sigma | pressure | height | thickness | CAMx Layers | IC/BC |
|---|---|---|---|---|---|---|
| 28 | 0.0000 | 50.00 | 18874.41 | 1706.76 | | |
| 27 | 0.0250 | 73.75 | 17167.65 | 1362.47 | | |
| ---------- Extended CAMx Top ---------- | | | | | | |
| 26 | 0.0500 | 97.50 | **15805.17** | 2133.42 | --20--- | ^ |
| 25 | 0.1000 | 145.00 | **13671.75** | 1664.35 | --19--- | \| |
| 24 | 0.1500 | 192.50 | 12007.40 | 1376.75 | | \| |
| 23 | 0.2000 | 240.00 | **10630.65** | 1180.35 | --18--- | \| |
| 22 | 0.2500 | 287.50 | 9450.30 | 1036.79 | | \| |
| 21 | 0.3000 | 335.00 | **8413.52** | 926.80 | --17--- | \| |
| 20 | 0.3500 | 382.50 | 7486.72 | 839.57 | | \| |
| 19 | 0.4000 | 430.00 | 6647.15 | 768.53 | | Clean IC/BC |
| 18 | 0.4500 | 477.50 | **5878.62** | 709.45 | --16--- | \| |
| 17 | 0.5000 | 525.00 | 5169.17 | 659.47 | | \| |
| 16 | 0.5500 | 572.50 | 4509.70 | 616.58 | | \| |
| ---------- Original CAMx Top ---------- | | | | | | \| |
| 15 | 0.6000 | 620.00 | **3893.12** | 579.34 | --15--- | \| |
| 14 | 0.6500 | 667.50 | **3313.78** | 546.67 | --14--- | \| |
| 13 | 0.7000 | 715.00 | **2767.11** | 517.77 | --13--- | \| |
| 12 | 0.7500 | 762.50 | **2249.35** | 491.99 | --12--- | v |
| 11 | 0.8000 | 810.00 | **1757.36** | 376.81 | --11--- | ---------- |
| 10 | 0.8400 | 848.00 | **1380.55** | 273.60 | --10--- | ^ |
| 9 | 0.8700 | 876.50 | **1106.95** | 266.37 | ---9--- | \| |
| 8 | 0.9000 | 905.00 | **840.58** | 259.54 | ---8--- | \| |
| 7 | 0.9300 | 933.50 | **581.04** | 169.41 | ---7--- | \| |
| 6 | 0.9500 | 952.50 | **411.63** | 166.65 | ---6--- | \| |
| 5 | 0.9700 | 971.50 | **244.98** | 82.31 | ---5--- | Moderate IC/BC |
| 4 | 0.9800 | 981.00 | **162.67** | 65.38 | ---4--- | \| |
| 3 | 0.9880 | 988.60 | **97.29** | 56.87 | ---3--- | \| |
| 2 | 0.9950 | 995.25 | **40.43** | 20.23 | ---2--- | \| |
| 1 | 0.9975 | 997.62 | **20.19** | 20.19 | ---1--- | v |
| 0 | 1.0000 | 1000.00 | **0.00** | ========= Surface ====== | | |

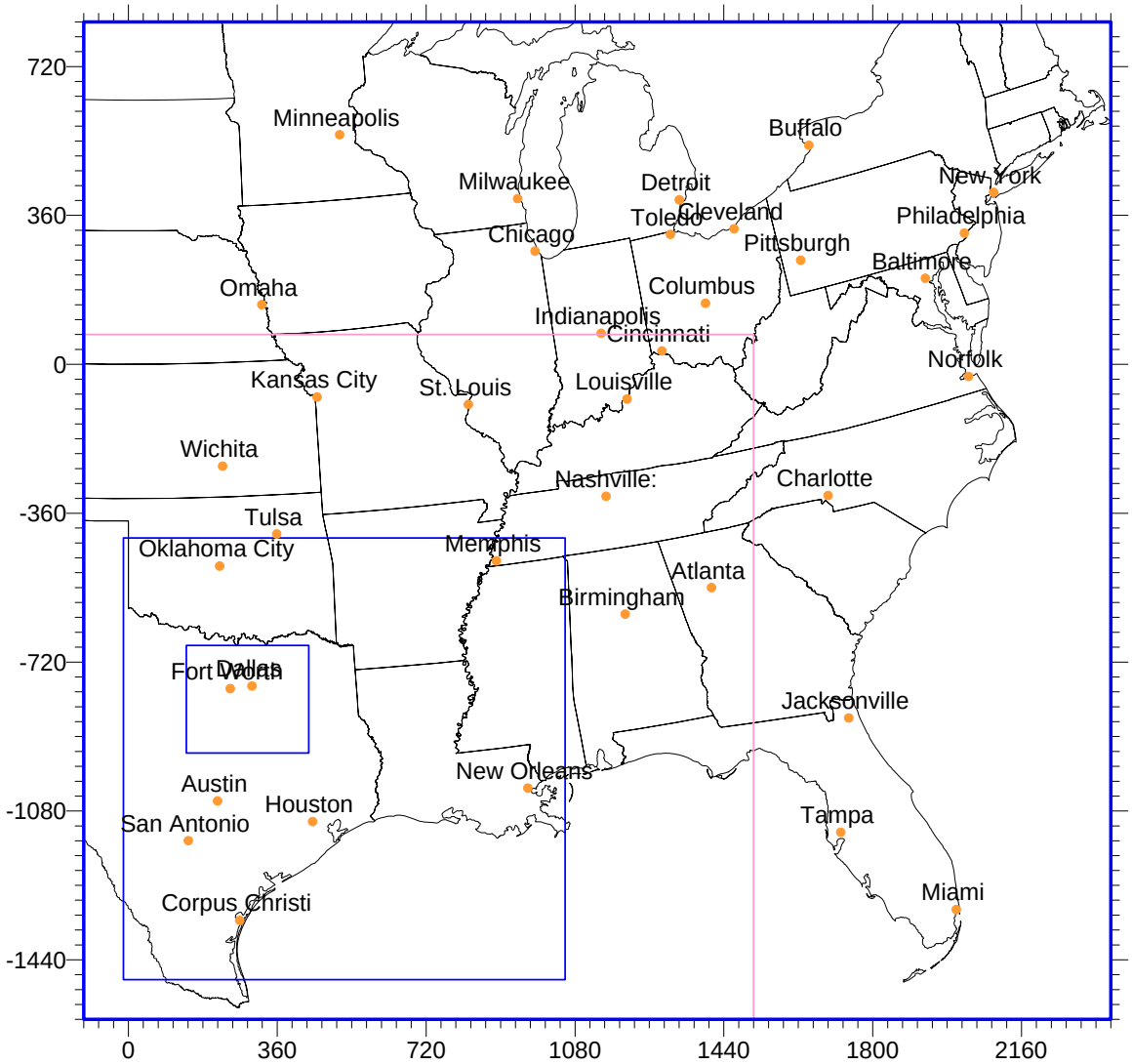


CAMx Grid Definitions for DFW

| | nx x ny | SW to NE Corners |
|---|---|---|
| CAMx 36km (standard) | 45 x 46 | (-108, -1584) to (1512, 72) |
| CAMx 36km expanded | 69 x 67 | (-108, -1584) to (2376, 828) |
| CAMx 12km | 89 x 89* | ( -12, -1488) to (1056, -420) |
| CAMx 04km | 74 x 65* | ( 140, -940) to ( 436, -680) |

* includes buffer cells

**Figure 4-1**. CAMx DFW modeling domain with the standard and expanded 36-km domains.

## EXPANDED DOMAIN MODELING

Four runs were exercised, all using different combinations of horizontal and vertical domains as listed in Table 4-2. All runs will be compared to Run 20.

**Table 4-2**. Domain definitions of Runs 20 to 23.

| | Horizontal domain | Vertical top | nx* x ny* x nz |
|---|---|---|---|
| Run 20 (base) | Standard | 4-km | 45 x 46 x 15 |
| Run 21 | Standard | 14-km | 45 x 45 x 20 |
| Run 22 | Expanded | 4-km | 69 x 67 x 15 |
| Run 23 | Expanded | 14-km | 69 x 67 x 20 |

* 36-km coarse grid

All runs used meteorology from MM5 Run 5. The expanded CAMx 36-km domain went beyond the eastern edge of the MM5 36-km domain, as shown in Figure 4-2. Meteorology from the MM5 108-km domain was interpolated to 36-km resolution to fill in everything east of the 2160-km LCP easting.

Vertical diffusivity fields were generated from MM5 Run 5 using the O'Brien-based vertical diffusivity profile methodology. Additionally, a "patch" was applied to the diffusivity field using an approach recently tested by the TCEQ. In each vertical column, the maximum diffusivity encountered in the lowest 100 m was applied to all layers below 100 m. This was tested by TCEQ in their own modeling with this episode and meteorological dataset to reduce over predictions in surface precursor NOx and VOC concentrations. This patch is called "Kv100".

Emissions for the expanded domain incorporated all of the emissions from TCEQ in the standard 36-km domain, as used in Run 20. Outside the standard 36-km domain, emissions were obtained from modeling work conducted for the Oklahoma Department of Environmental Quality (ODEQ). Initial conditions were identical in all runs. Below 1700 m, the model was initialized with moderate concentrations, as described in Table 3-1; aloft, conditions were assumed to be clean.

Figure 4-3 shows the categories assigned to all lateral boundaries in the standard and expanded domains. See Table 3-1 for concentrations associated with each category. In the expanded domain, the eastern boundary was assigned clean conditions since it was entirely over the ocean. The northern boundary was set to moderate because most of the major urban centers were inside the expanded domain. Both domains were clean above 1700 m.

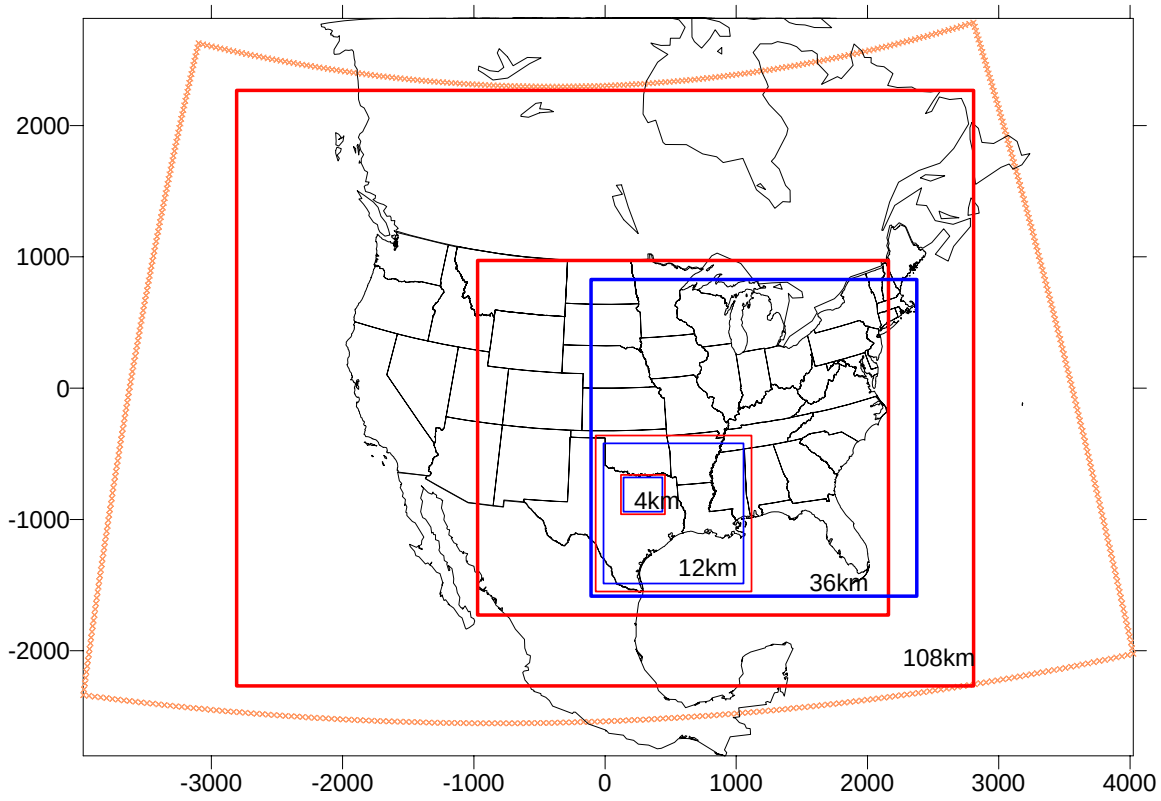


**MM5 and CAMx Grid Definitions for DFW**

× EDAS Boundary

| | Dot points | SW and NE corners |
|---|---|---|
| MM5 108km | 53 x 43 | (-2808,-2268) to (2808,2268) |
| MM5 36km | 88 x 76 | ( -972,-1728) to (2160, 972) |
| MM5 12km | 100 x 100 | ( -72,-1548) to (1116, -360) |
| MM5 04km | 85 x 76 | ( 120, -960) to ( 456, -660) |
| CAMx 36km | 69 x 67 | (-108, -1584) to (2376, 828) |
| CAMx 12km | 89 x 89* | ( -12, -1488) to (1056, -420) |
| CAMx 04km | 74 x 65* | ( 140, -940) to ( 436, -680) |

* includes buffer cells

**Figure 4-2**. MM5 and CAMx modeling domains for DFW with the expanded domain.

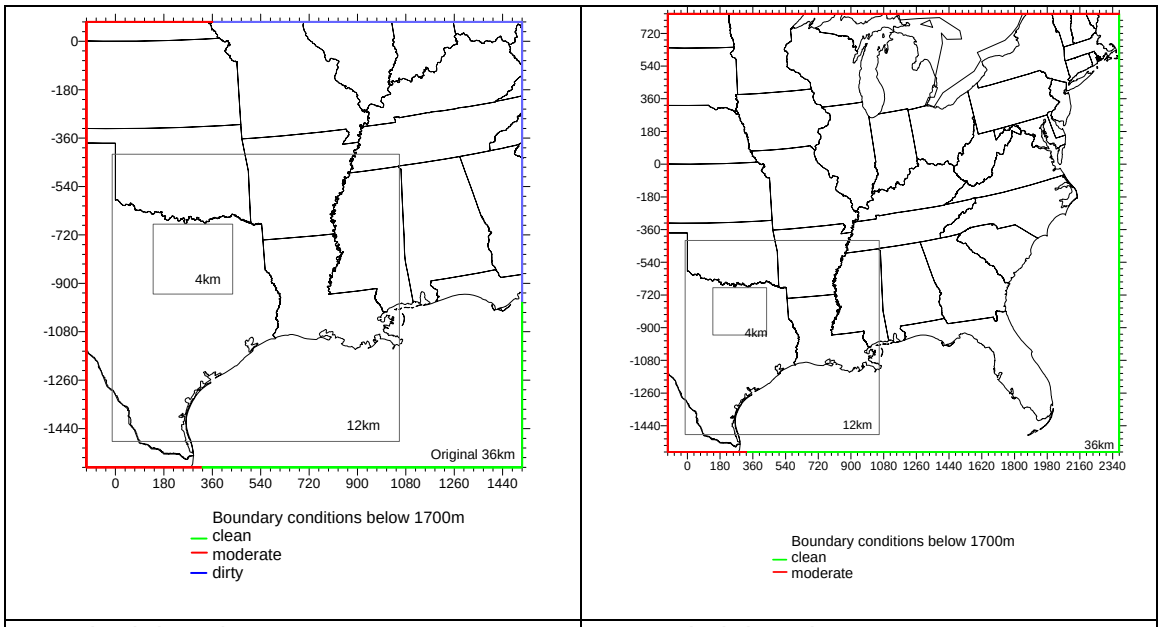


| Standard domain | Expanded domain |
|---|---|

**Figure 4-3**. Assignment of boundary conditions in the mixed layer for the standard and expanded domains for DFW.

Figures 4-4 to 4-11 show a package of model performance plots for Runs 20 to 23 similar to the plots shown in Figures 3-1 to 3-7. The time series plots in Figure 4-4 reveal subtle differences among the four runs. Throughout this report, we will show modeling results for August 17 in particular because it is the day when observed ozone levels were the highest over the episode yet CAMx exhibits some of the largest under prediction problems.

## RUN 21: HIGH TOP

Run 21, which had a higher model top compared to Run 20, generated slightly worse 1-hour and 8-hour daily performance statistics on numerous dates compared to Run 20, as can be seen in Figures 4-5 and 4-6, respectively. Table 4-3 summarizes the $R^2$ from the scatter plots for each of the three EPA computation methods in each of the four runs for 1-hour and 8-hour ozone. Run 21 has the same $R^2$ as Run 20 in all cases except the scatter plot of the closest 1-hour peak to the observed ozone in the 9 by 9 cell block, where $R^2$ was slightly worse. Spatial plots of the daily maximum ozone on August 17 show similar features between Runs 20 and 21 in the 12-km domain (Figure 4-9), and a peak 1 ppb higher over the DFW region in Run 21 for both 1-hour and 8-hour ozone (Figures 4-10 and 4-11, respectively).

**Table 4-3**. Comparison of the 1-hour and 8-hour coefficient of determination from each scatter plot of the predicted and observed daily maximum ozone in Runs 20, 21, 22, and 23.

| | 1-hour $R^2$ | | | 8-hour $R^2$ | | |
|---|---|---|---|---|---|---|
| | **max 9x9** | **closest** | **interpolated** | **max 9x9** | **closest** | **interpolated** |
| Run 20: Base | 0.40 | 0.84 | 0.35 | 0.38 | 0.74 | 0.26 |
| Run 21: Extended Top | 0.40 | 0.83 | 0.35 | 0.38 | 0.74 | 0.26 |
| Run 22: Expanded Domain | 0.41 | 0.85 | 0.37 | 0.39 | 0.76 | 0.27 |
| Run 23: Both | 0.42 | 0.86 | 0.38 | 0.41 | 0.78 | 0.28 |

## RUN 22: EXPANDED GRID

Statistics for Run 22, which used the larger horizontal domain compared to Run 20, were slightly better than Run 20 on the last three dates of the simulation. On the other dates, they were mixed. The coefficient of determination in the daily maximum scatter plots for Run 22 was slightly higher than Run 20 using all three methods for computing the maximum 1-hour and 8-hour ozone. Spatial plots in Figure 4-9 show a 5 ppb drop in 1-hour ozone in East Texas from Run 22 to Run 20. The 1-hour peak in the 4-km DFW domain was 1 ppb higher.

## RUN 23: HIGH TOP AND EXPANDED GRID

Run 23, which used the expanded horizontal domain and 15-km modeling top, generated slightly better performance in the DFW 4-km domain than the other three runs, as can be seen in Figures 4-5 and 4-6 for 1-hour and 8-hour statistics, respectively. Table 4-3 shows that Run 23 always had the highest coefficient of determination among the four runs. The 12-km spatial plots of the daily maximum ozone on August 17 show a decrease in the 1-hour ozone peak in East Texas similar to Run 22. In the 4-km domain, Run 23 generated more 1-hour and 8-hour ozone over DFW than the other three runs.

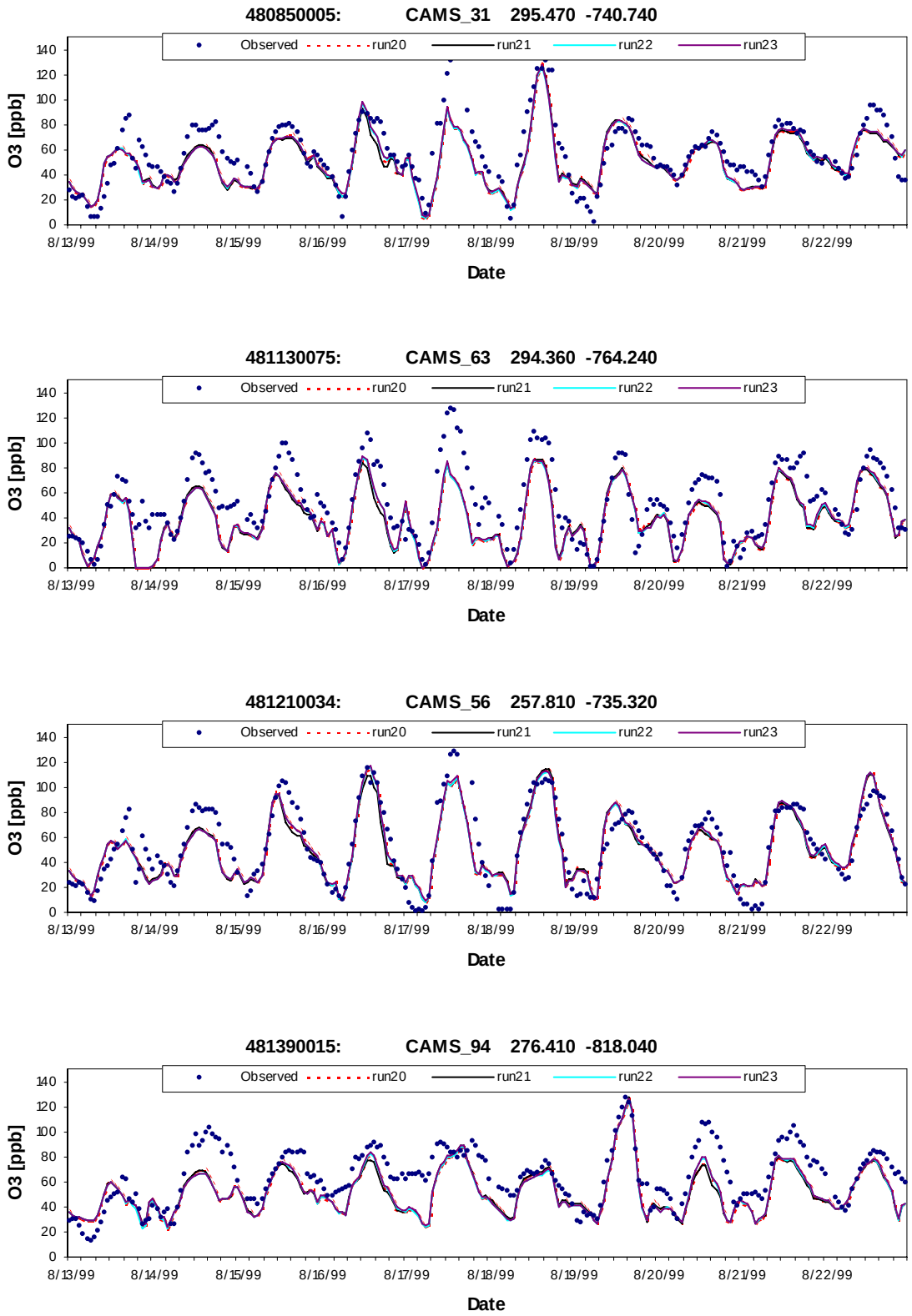


**Figure 4-4**. Time series of 1-hour ozone at sites inside the DFW 4-km domain from CAMx runs using different domain configurations (see Table 4-2).

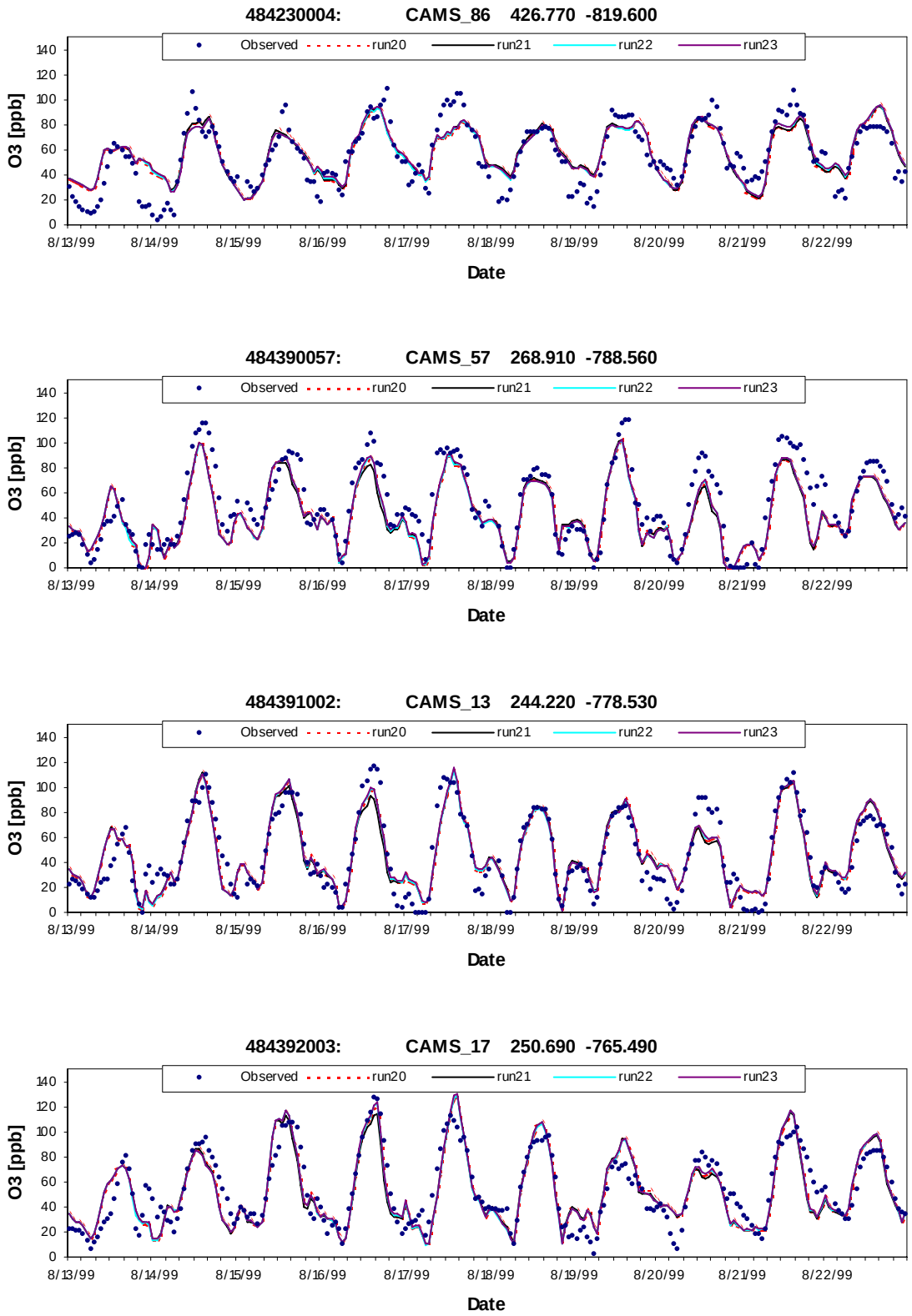


**Figure 4-4**. (Cont.) Time series of 1-hour ozone at sites inside the DFW 4-km domain from CAMx runs using different domain configurations (see Table 4-2).

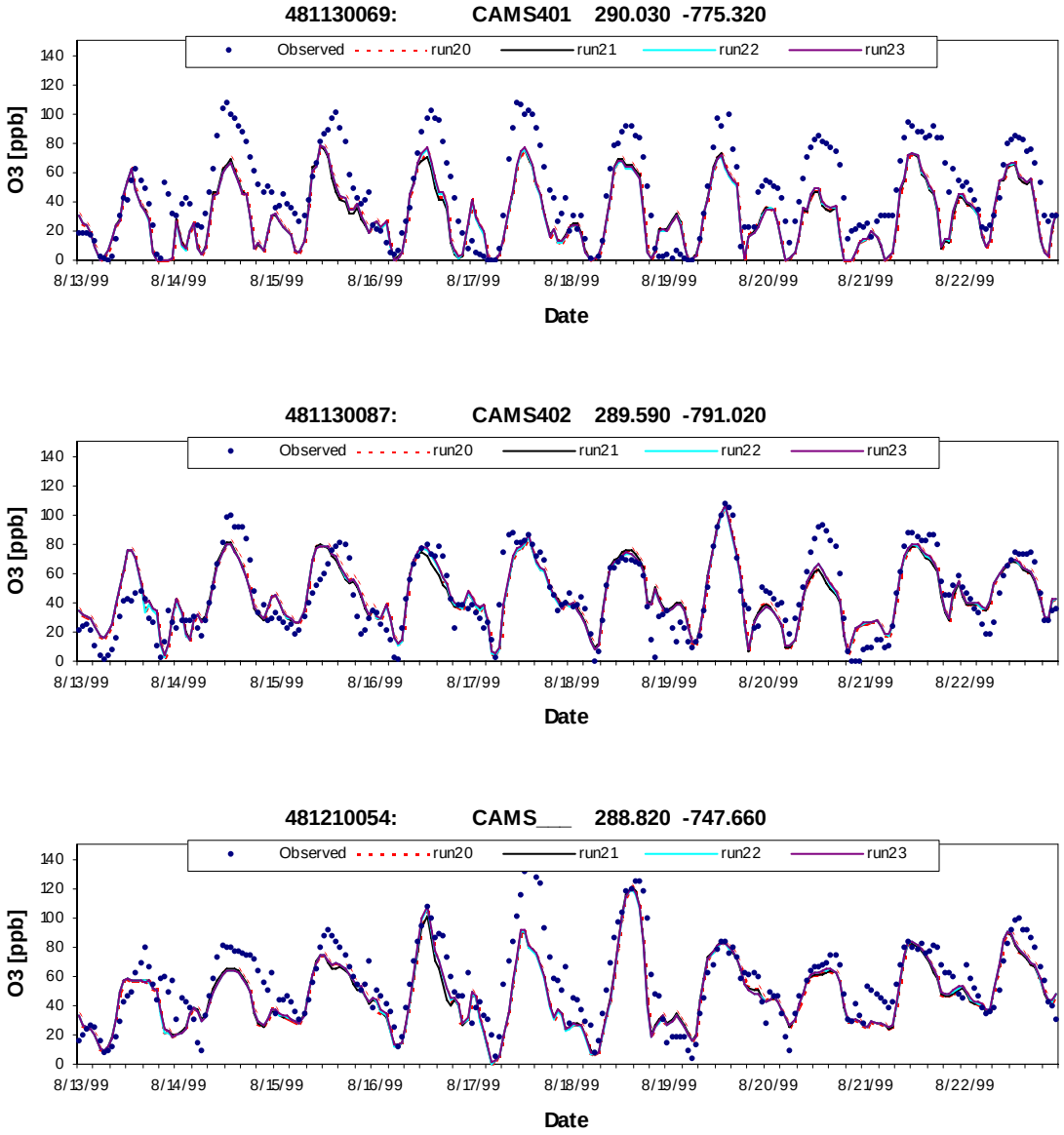


**Figure 4-4**. (Concl.) Time series of 1-hour ozone at sites inside the DFW 4-km domain from CAMx runs using different domain configurations (see Table 4-2).

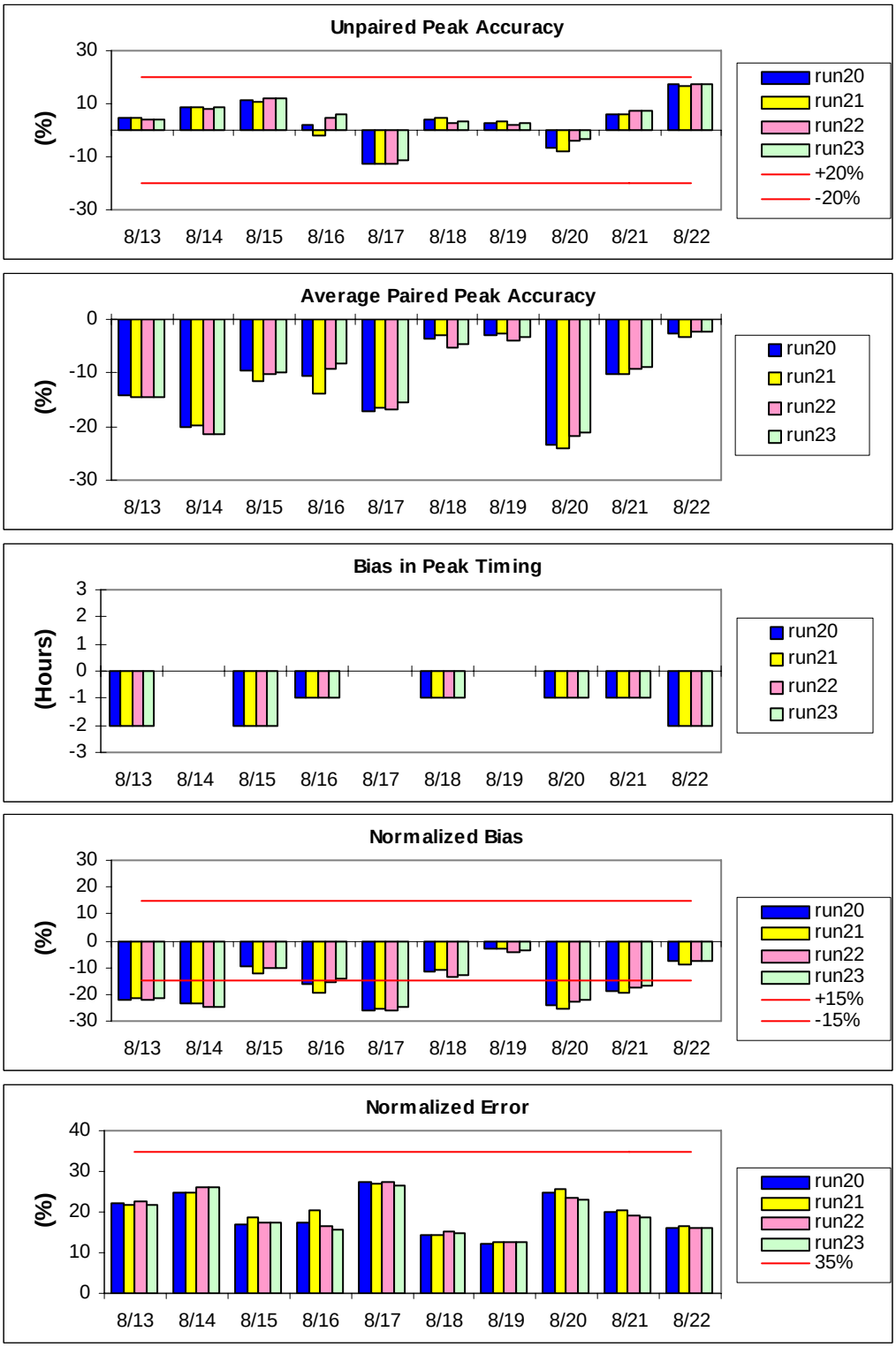


**Figure 4-5**. Daily statistics of the 1999 DFW 1-hour ozone in the 4-km domain from CAMx runs using different domain configurations (see Table 4-2).

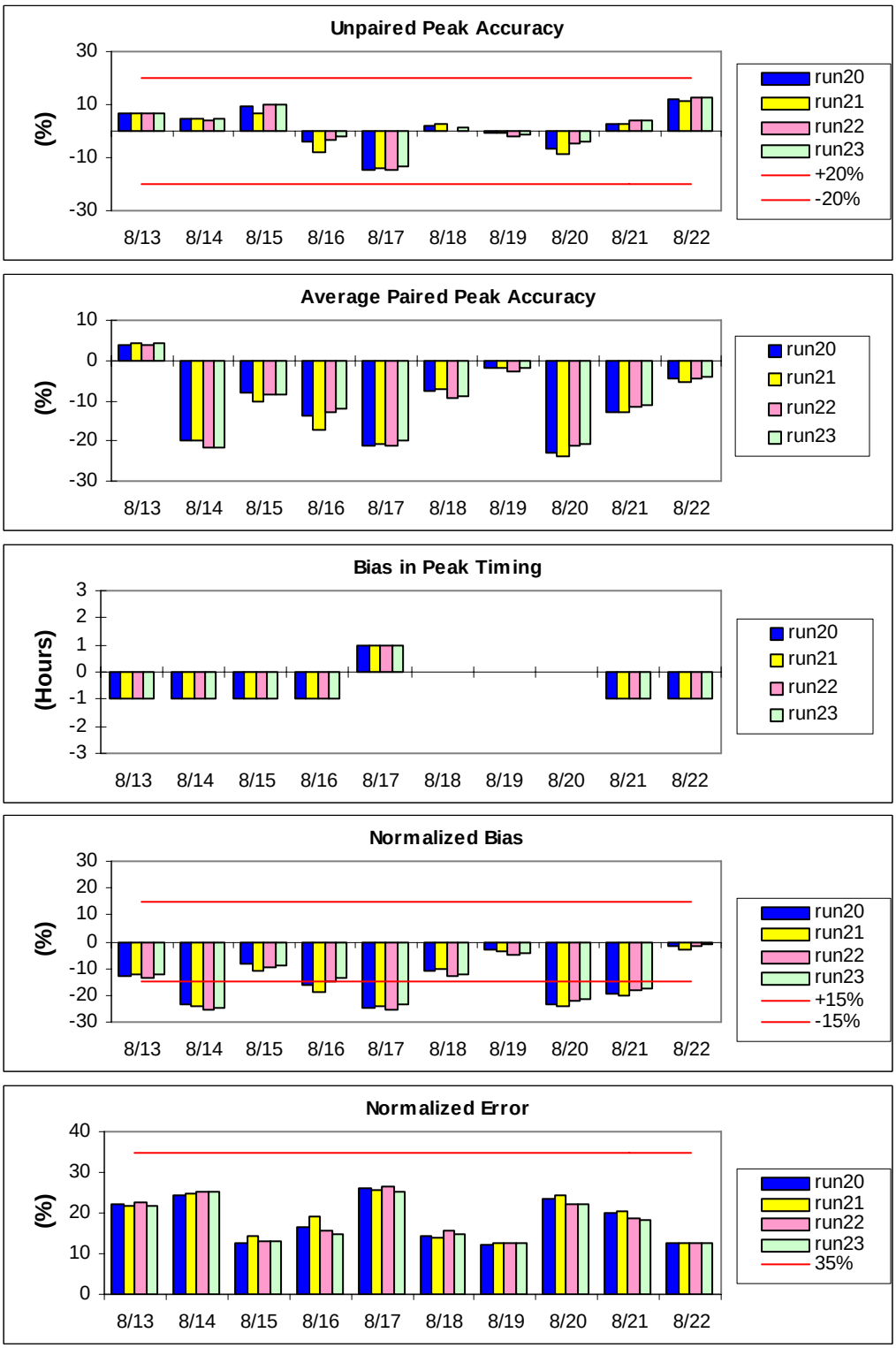


**Figure 4-6.** Daily statistics of the 1999 DFW 8-hour ozone in the 4-km domain from CAMx runs using different domain configurations (see Table 4-2).

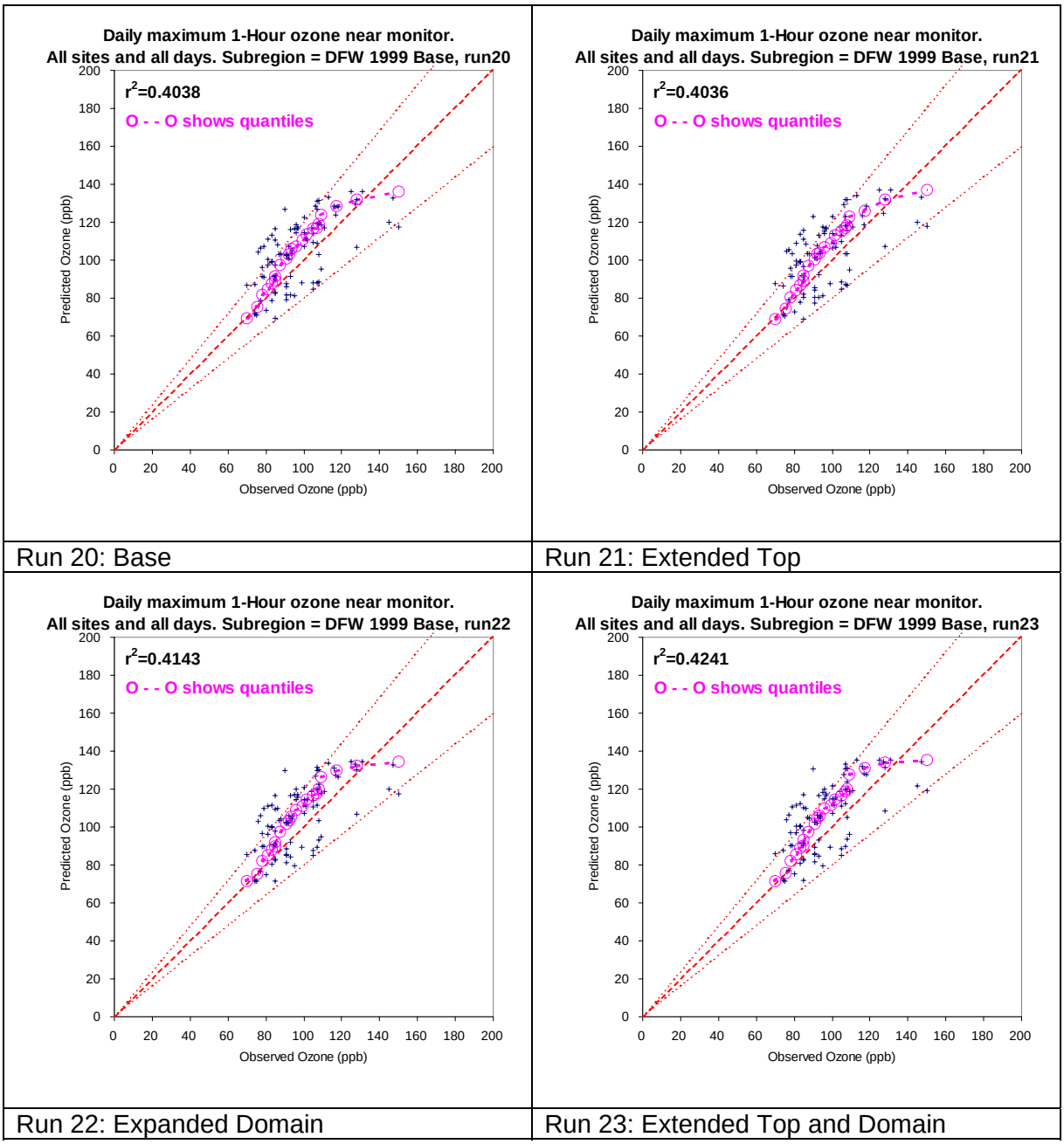


**Figure 4-7.** Scatter plots of the daily maximum observed and largest predicted 1-hour ozone near each monitor (within 9x9 cell area) from four CAMx runs using different domain configurations of the August 1999 DFW episode.

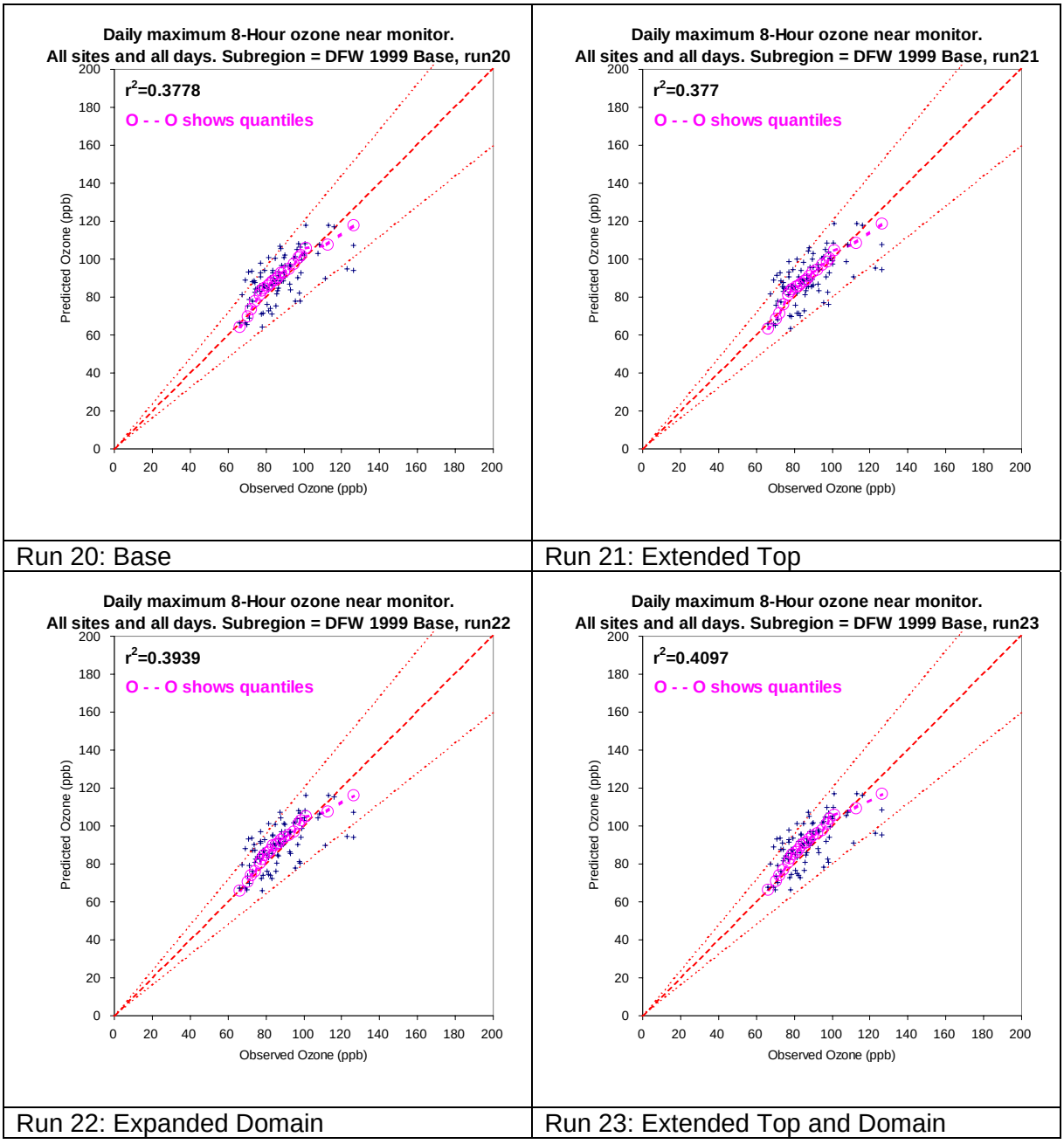


**Figure 4-8**. Scatter plots of the daily maximum observed and largest predicted 8-hour ozone near each monitor (within 9x9 cell area) from four CAMx runs using different domain configurations of the August 1999 DFW episode.

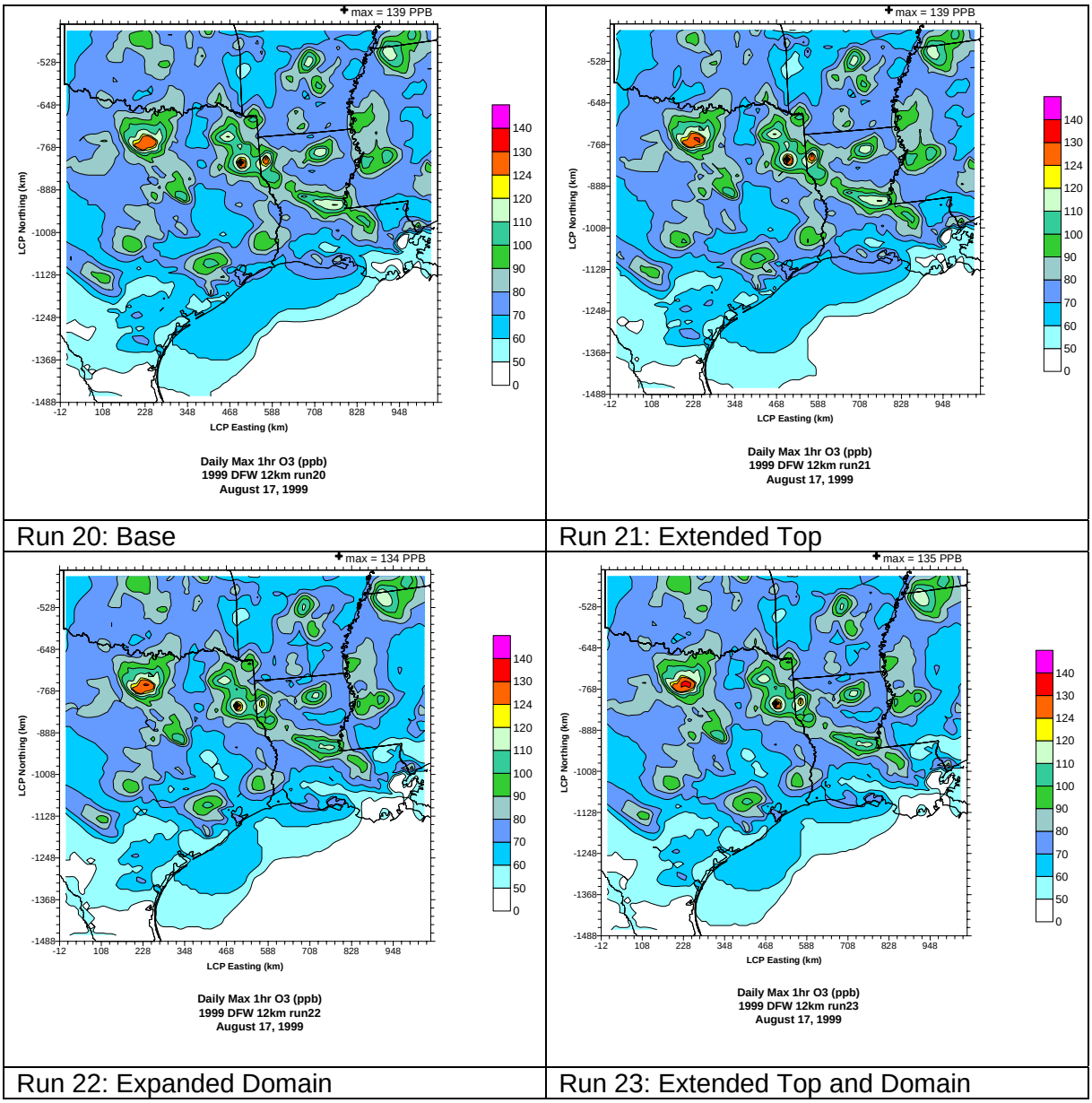


**Figure 4-9.** Spatial plots of the daily maximum 1-hour ozone in the 12-km domain on August 17, 1999 from four CAMx runs with different domain configurations.

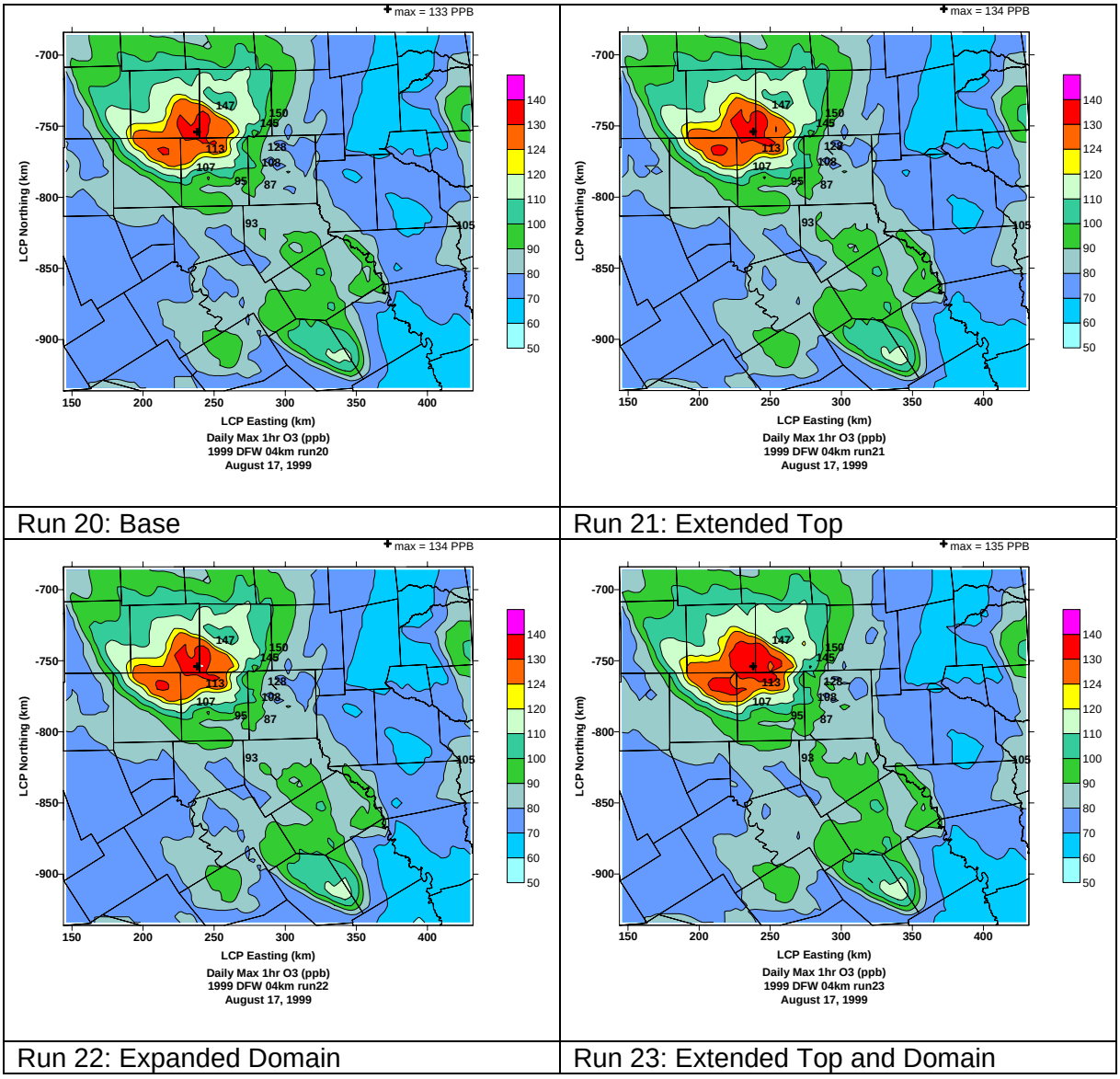


**Figure 4-10**. Spatial plots of the daily maximum 1-hour ozone in the DFW 4-km domain on August 17, 1999 from four CAMx runs with different domain configurations.

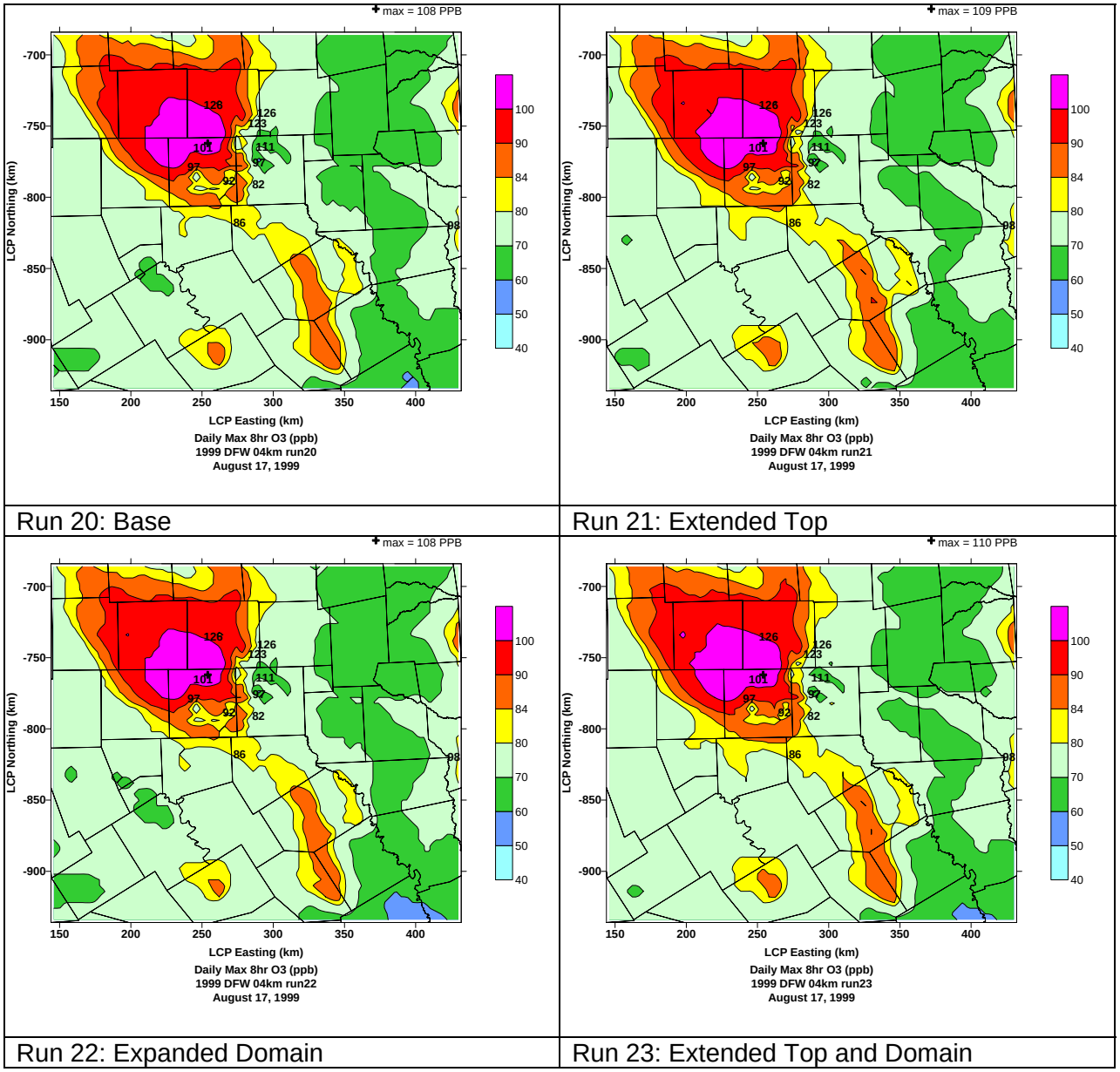


**Figure 4-11**. Spatial plots of the daily maximum 8-hour ozone in the DFW 4-km domain on August 17, 1999 from four CAMx runs with different domain configurations.

# 5. OZONE SENSITIVITY TO METEOROLOGY

This section evaluates ozone performance in the Dallas/Fort Worth 4-km domain using four sets of meteorology. Section 4 showed that model performance improved with the expanded horizontal domain and 15-km model top in Run 23; therefore, all runs in this section used the larger domain and higher top to evaluate sensitivity to meteorology. All runs used the same set of emissions as in Run 23. Boundary conditions were moderate over the north, west, and part of the southern boundary up to 1700 m; conditions were clean everywhere else. All runs were initialized with moderate conditions below 1700 m and clean conditions aloft.

CAMx used meteorology inputs from three MM5 simulations. MM5 Run 5 used the Pleim-Xiu PBL and land surface model with the Kain-Fritsch cumulus scheme. MM5 Run 6 replaced the Pleim-Xiu system with the Eta PBL scheme with the Noah land surface model. MM5 Run 7 was similar to Run 5, except that the Grell cumulus scheme was implemented in place of the Kain-Fritsch scheme. Table 5-1 summarizes the meteorology and vertical diffusivity method extracted for each CAMx run.

**Table 5-1.** List of meteorology used for each CAMx sensitivity run.

| CAMx Run | MM5 Run | | | Kv profile Methodology |
|---|---|---|---|---|
| | Run ID | PBL/LSM | Cumulus | |
| Run 23 | Run 5 | Pleim-Xiu | Kain-Fritsch | O'Brien |
| Run 28 | Run 5 | Pleim-Xiu | Kain-Fritsch | CMAQ |
| Run 24 | Run 6 | Eta/Noah | Kain-Fritsch | TKE |
| Run 25 | Run 7 | Pleim-Xiu | Grell | O'Brien |

Figure 5-1 shows profiles of the vertical diffusivity extracted from MM5 on the afternoons of August 17 and 18 in a column over Dallas. The Kv's from MM5 Run 6 and Run 5 based upon the CMAQ methodology were significantly larger than the extractions using the O'Brien Kv method. As was done in Runs 20-23, all vertical diffusivity fields for these runs were "patched" such that in each column, the largest diffusivity value in the lowest 100 m was used for every layer below 100 m. This patch is called "Kv100". Figure 5-1 shows Kv profiles before the Kv100 patch was applied.

Figures 5-2 to 5-9 show daily statistics, time series, scatter plots, and spatial plots similar to Figures 4-4 to 4-11, but for the four runs using different meteorological inputs. All runs were compared to the base Run 23.

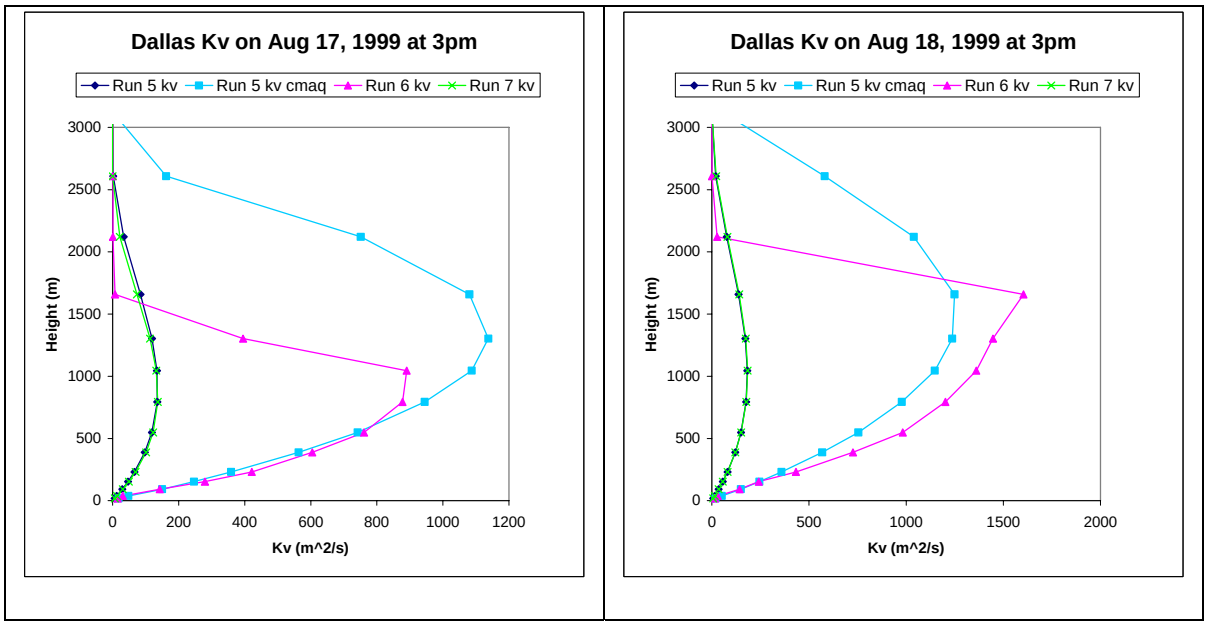


**Figure 5-1.** Vertical profiles of the vertical diffusivity over a grid cell in Dallas from four sets of meteorology.

## RUN 28: CMAQ Kv PROFILE

Run 28, which used the high Kv's based upon the CMAQ calculation methodology, generally predicted lower daytime peaks and higher night-time ozone than Run 23, as can be seen in the time series plots in Figure 5-2. Spatial plots of the daily maximum ozone on August 17 show significantly lower 1-hour ozone through much of the 12-km domain; in the 4-km domain, the peak in Run 28 was 10 ppb lower and farther to the west of the higher observed peaks when compared to Run 23. The 8-hour ozone peak in the 4-km domain was 7 ppb lower in Run 28.

The 1-hour unpaired peak accuracy was more negative on most dates in Run 28, improving the accuracy on 5 dates, but worsening accuracy on August 28 beyond the EPA –20 % goal. The average paired peak accuracy, which was negative on all days in the base run, was more negative in Run 28. The normalized error was better in Run 28 on all days except August 21. The 8-hour statistics were mixed.

Table 5-2 shows the coefficient of determination of the scatter plots comparing the daily peak observed to each of the three different methods of calculating the peak predicted ozone. The use of the CMAQ Kv's improved $R^2$ only when the predicted values were bi-linearly interpolated to each observation site.

**Table 5-2**. Comparison of the 1-hour and 8-hour coefficient of determination from each scatter plot of the predicted and observed daily maximum ozone from four CAMx simulations using different meteorological inputs.

| | 1-hour $R^2$ | | | 8-hour $R^2$ | | |
|---|---|---|---|---|---|---|
| | max 9x9 | closest | interpolated | max 9x9 | closest | interpolated |
| Run 23: Base | 0.42 | 0.86 | 0.38 | 0.41 | 0.78 | 0.28 |
| Run 28: CMAQ Kv | 0.44 | 0.71 | 0.48 | 0.39 | 0.67 | 0.42 |
| Run 24: Eta/Noah | 0.44 | 0.90 | 0.51 | 0.35 | 0.83 | 0.42 |
| Run 25: Grell | 0.35 | 0.91 | 0.41 | 0.42 | 0.87 | 0.36 |

## RUN 24: ETA/NOAH PBL SCHEME

Run 24, which used meteorology from the MM5 Eta/Noah configuration, predicted 1-hour ozone that greatly differed from Run 23. Time series shown in Figure 5-2 show occasional daytime peaks that were much higher compared to the other three runs. In some cases, like CAMS 63, the higher ozone matched the observed better; in other cases, such as on August 16 and August 21 at CAMS 56, the other three runs performed better as Run 24 significantly over predicted the ozone.

The daily statistics shown in Figure 5-3 show that Run 24 had the best normalized bias on most days. On August 20 and 21, Run 24 was within the ±15% EPA performance goal for 1-hour bias; the other three runs all exceeded this criterion on both dates. Normalized error for 1-hour ozone was lower than Run 23 on all dates except August 17; for 8-hour ozone, Run 24 was similar or better on all dates. Run 24 had the best of the four average paired peak accuracy on numerous dates for both 1-hour and 8-hour ozone, as shown in Figure 5-4, but its performance was mixed for unpaired peaks.

The scatter plots of the daily-observed and predicted peaks had higher coefficient of determinations for all three methods of computing the predicted daily maximum 1-hour ozone. For 8-hour ozone, the peak obtained by using the largest value in the 9 by 9 cell surrounding each observation site resulted in a lower $R^2$ in Run 24 compared to Run 23; the $R^2$ using the other two methods were higher. Scatter plots using the largest predicted ozone near each observation site are shown in Figure 5-5 and 5-6 for 1-hour and 8-hour ozone.

The 12-km spatial plot of the 1-hour peak predicted ozone on August 17 in Figure 5-7 show that Run 24 produced significantly higher peaks over East Texas and Houston, but a lower peak over Dallas/Fort Worth. In the 4-km domain, the DFW peaks for 1-hour and 8-hour ozone are shifted eastward in Run 24 compared to Run 23, but lower in concentration.

## RUN 25: GRELL CONVECTION SCHEME

The use of the Grell cumulus scheme in the MM5 simulation for CAMx Run 25 yielded mixed results in the 1-hour time series plots (Figure 5-2). At numerous stations, including CAMS 31, 63, and 56, Run 25 predicted less ozone than Run 23 on August 16 and 18, which worsened model performance, and more ozone on August 17, which improved performance.

The daily statistics for both 1-hour and 8-hour ozone in Figures 5-3 and 5-4 show no definitive improvement over Run 23. Yet, the coefficient of determination improved on five of the six scatter plots that compared the daily observed peaks to each of the three methods for examining the peak predicted 1-hour and 8-hour ozone. The metric using the closest predicted ozone in the 9 cell by 9 cell grid surrounding each observation site had the second highest value of all the runs evaluated.

In the 12-km spatial plots of the daily maximum on August 17, Run 25 generated a 1-hour peak over Houston that was significantly higher than in Run 23. In the DFW 4-km domain, both the 1-hour and 8-hour plots increase the domain peak by 2 ppb *and* shift the peak eastward, where higher ozone was observed.

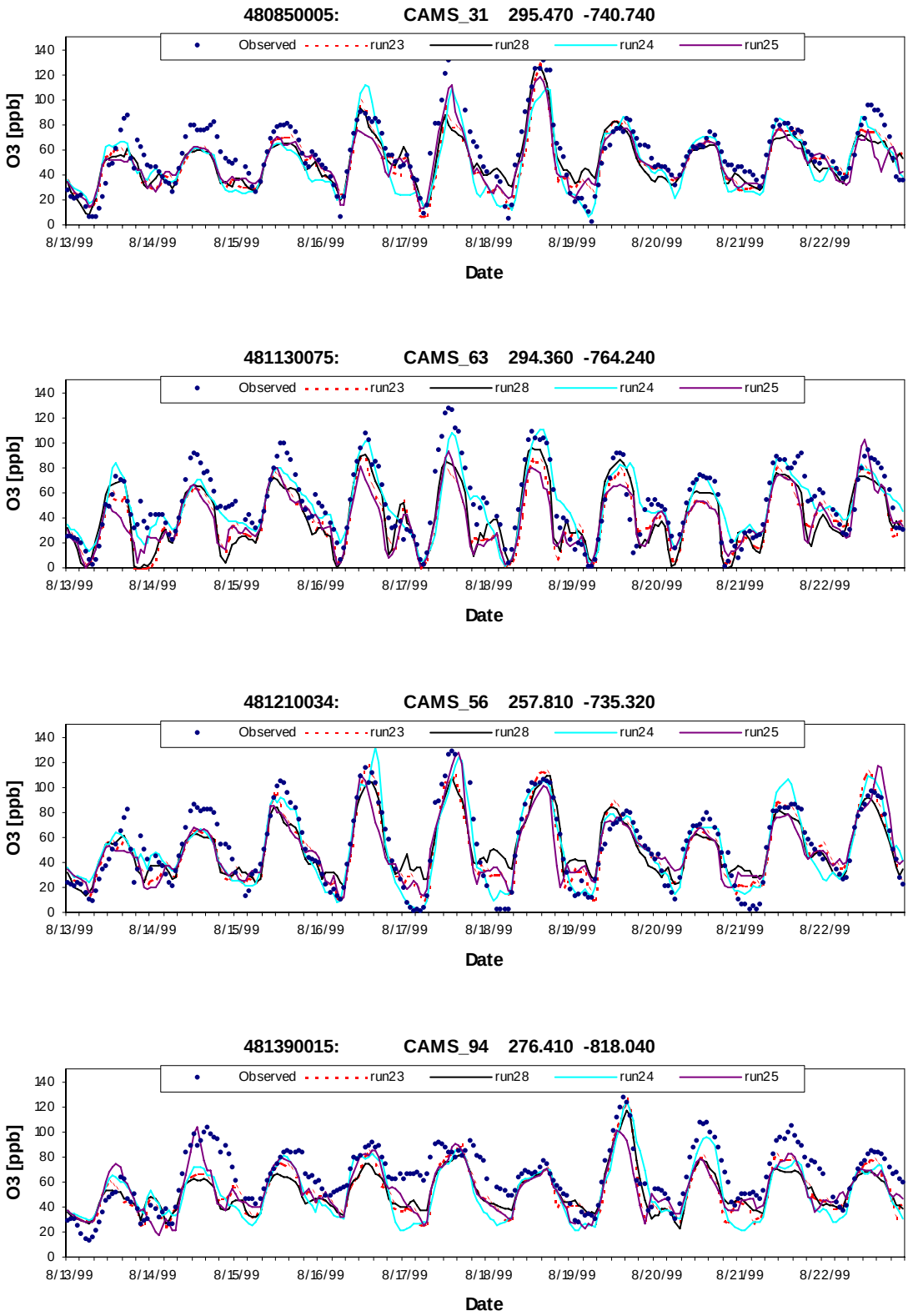


**Figure 5-2**. Time series of 1-hour ozone at sites inside the DFW 4-km domain from four CAMx runs using different meteorology inputs.

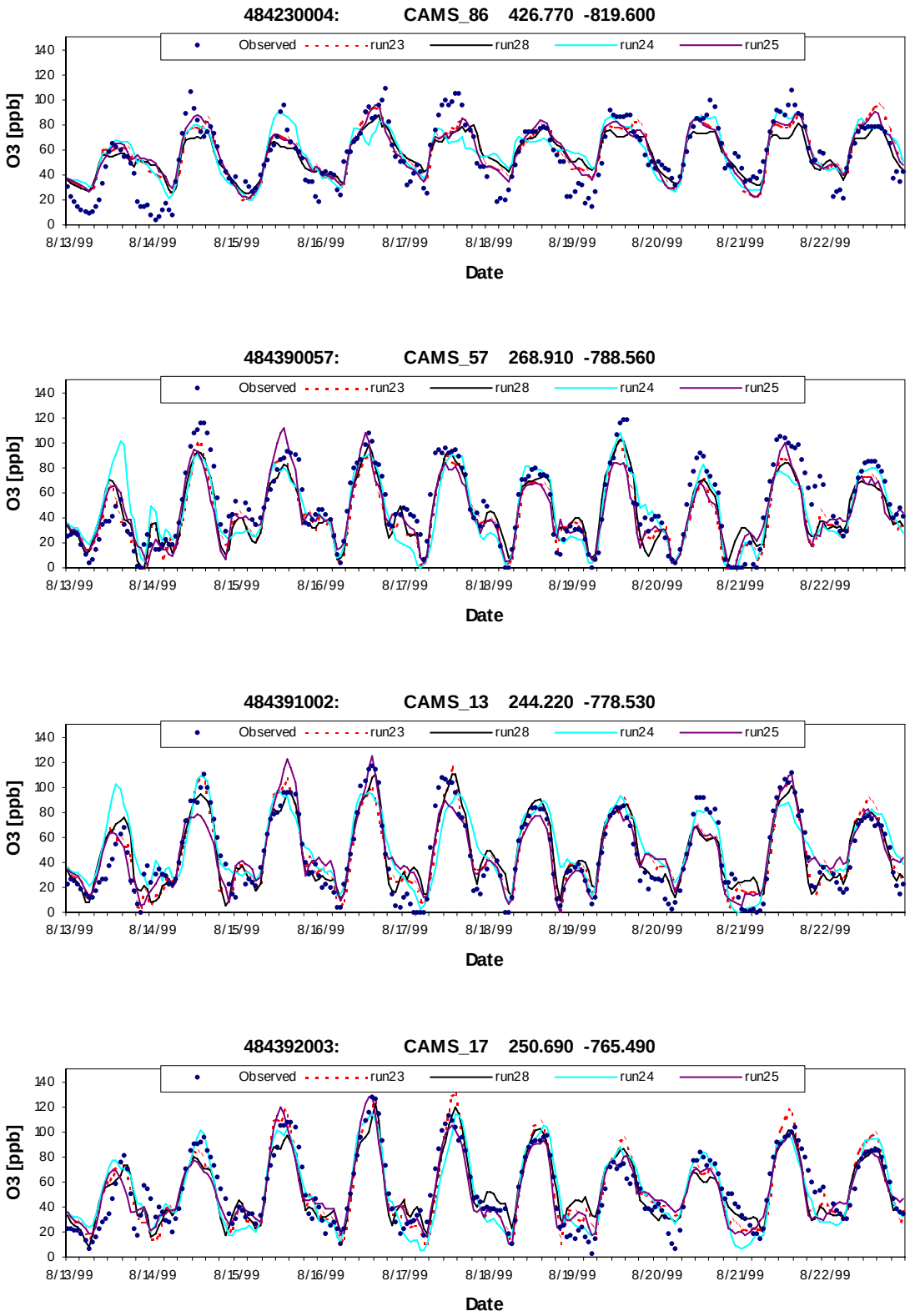


**Figure 5-2**. (Cont.) Time series of 1-hour ozone at sites inside the DFW 4-km domain from four CAMx runs using different meteorology inputs.

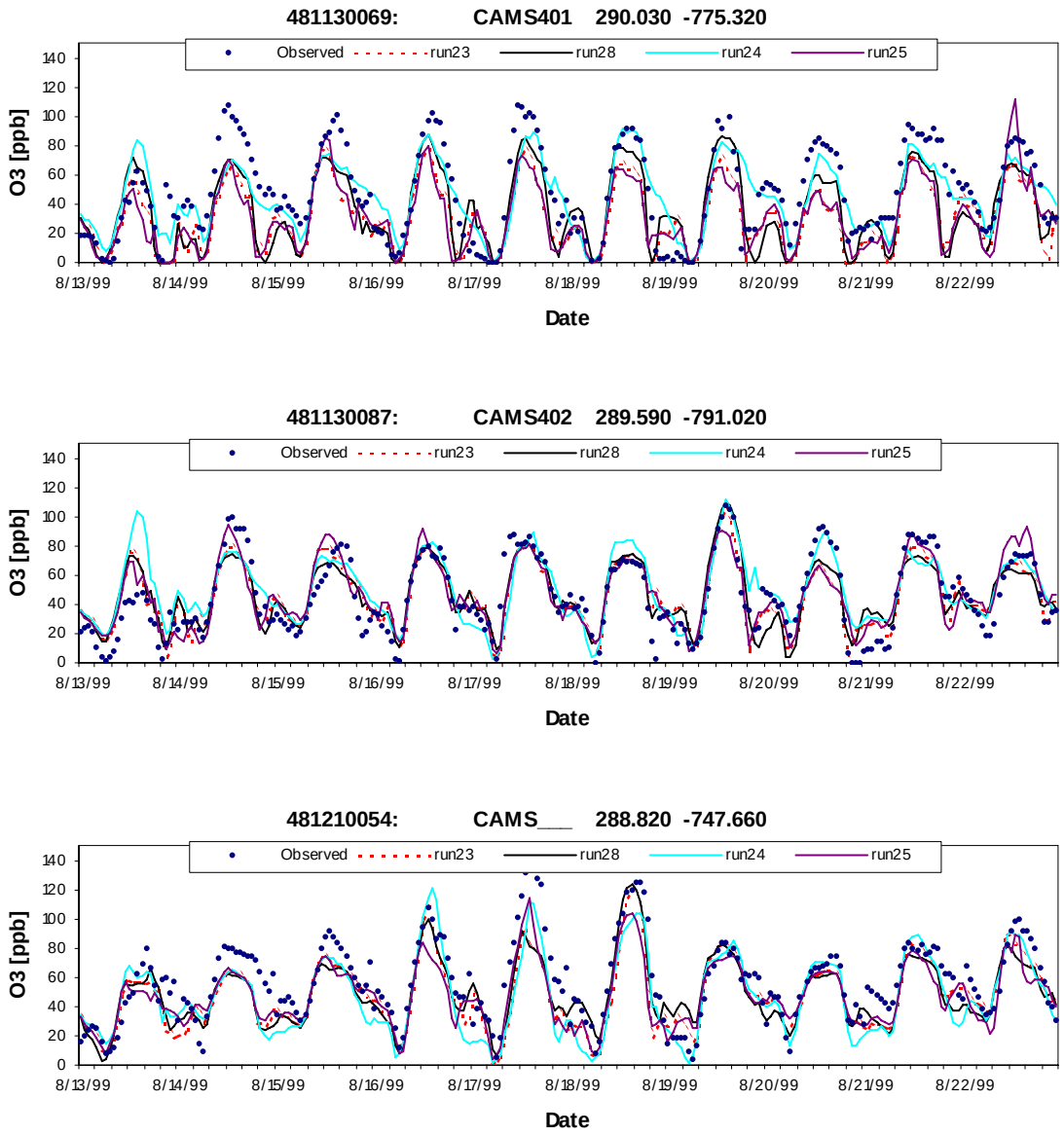


**Figure 5-2**. (Concl.) Time series of 1-hour ozone at sites inside the DFW 4-km domain from four CAMx runs using different meteorology inputs.

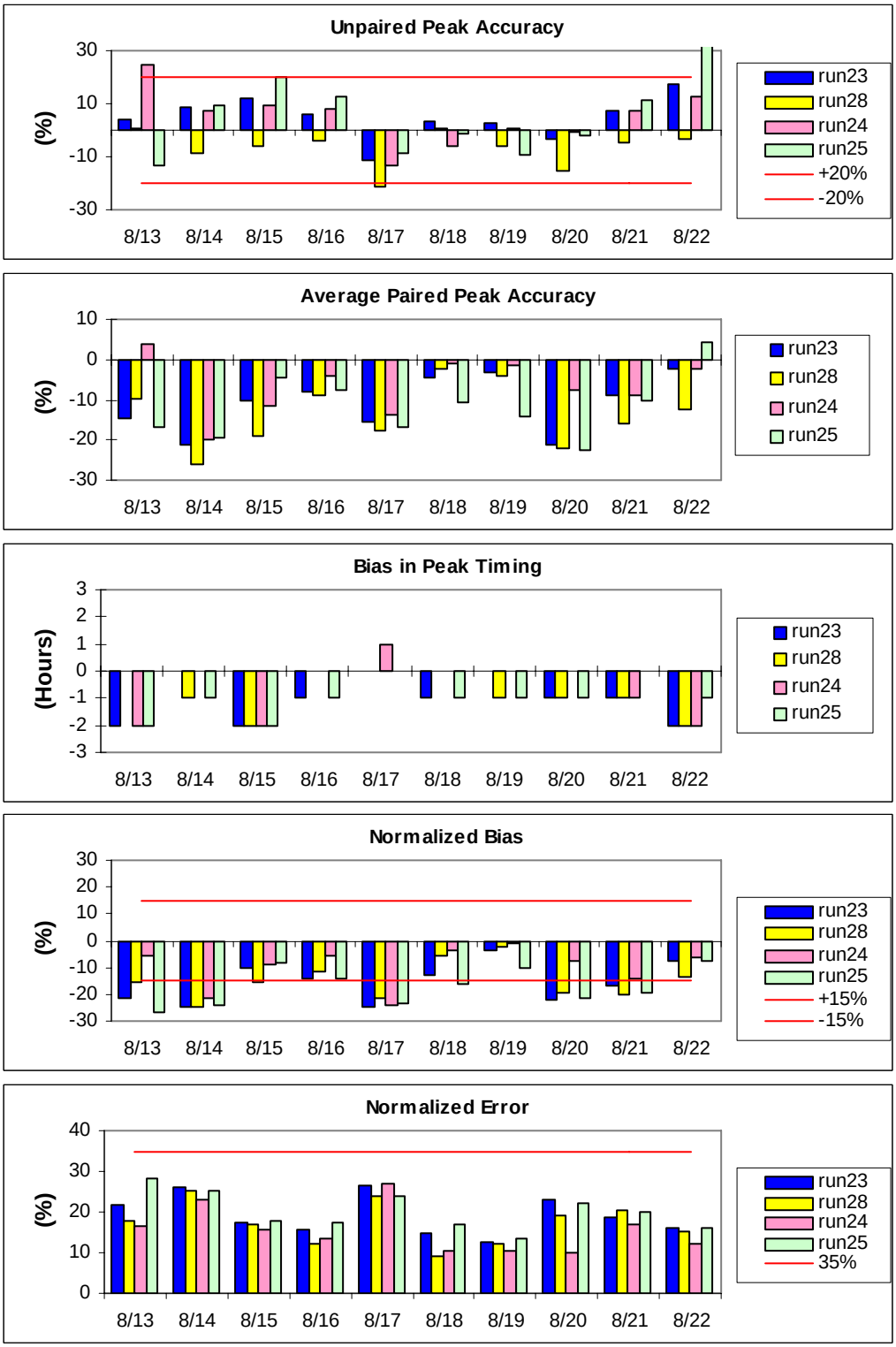


**Figure 5-3.** Daily statistics of the 1999 DFW 1-hour ozone in the 4-km domain from four CAMx runs with different meteorology inputs.

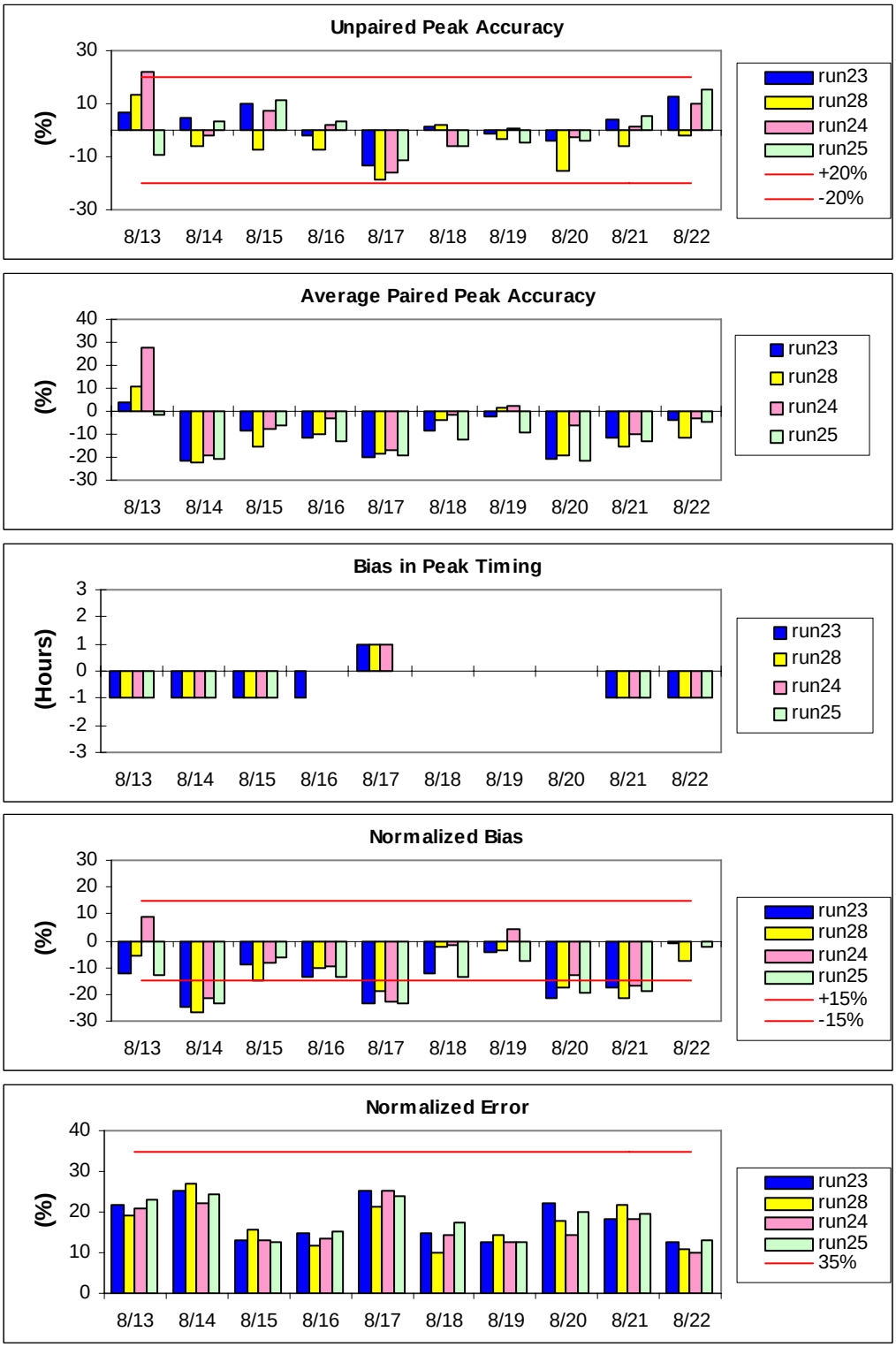


**Figure 5-4**. Daily statistics of the 1999 DFW 8-hour ozone in the 4-km domain from four CAMx runs with different meteorology inputs.

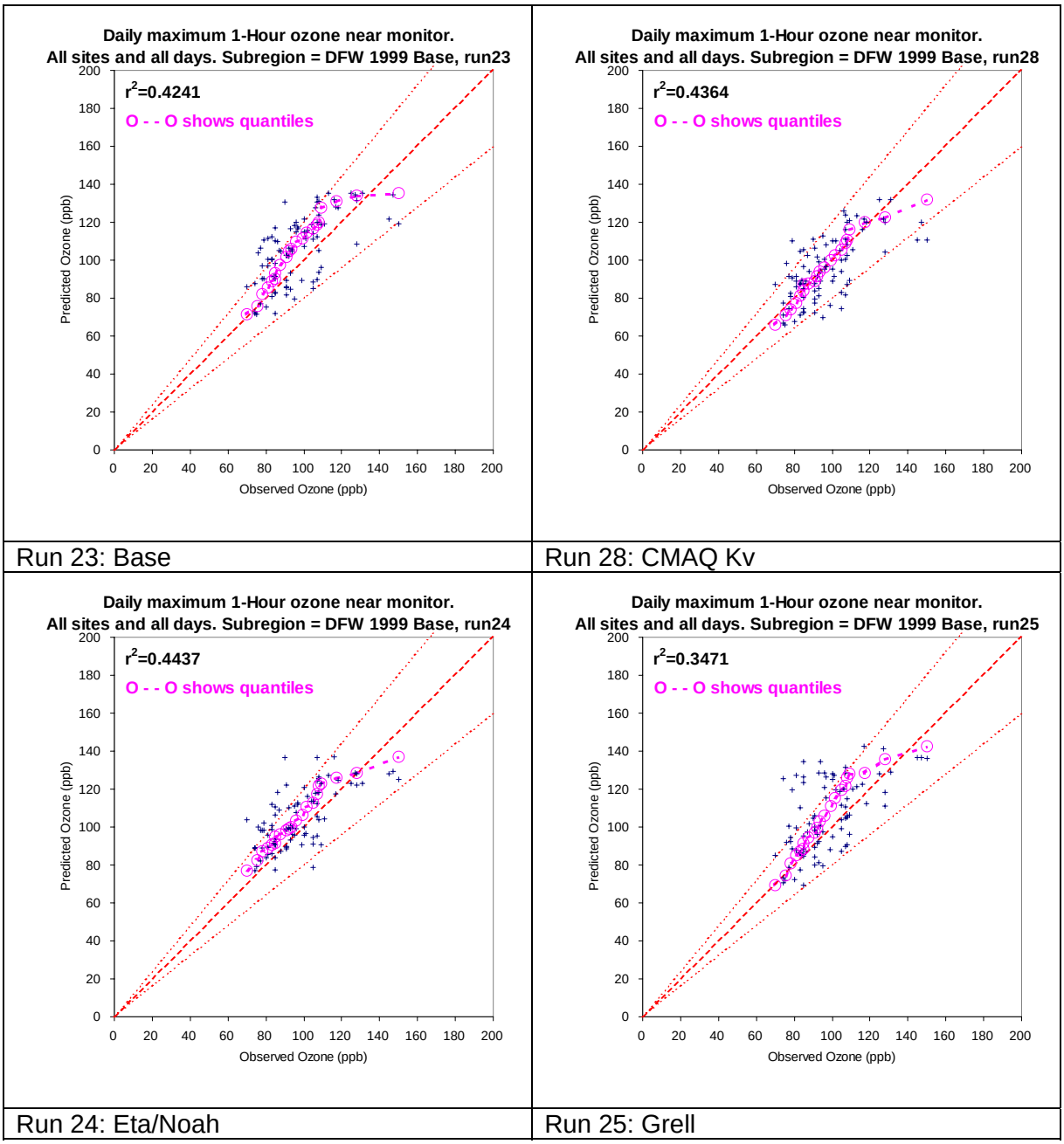


**Figure 5-5.** Scatter and quantile-quantile plots of the largest predicted daily maximum 1-hour ozone near each monitor (within 9x9 cell area) and the observed daily maximum 1-hour ozone for four CAMx runs using different meteorology inputs in the 1999 DFW Episode.

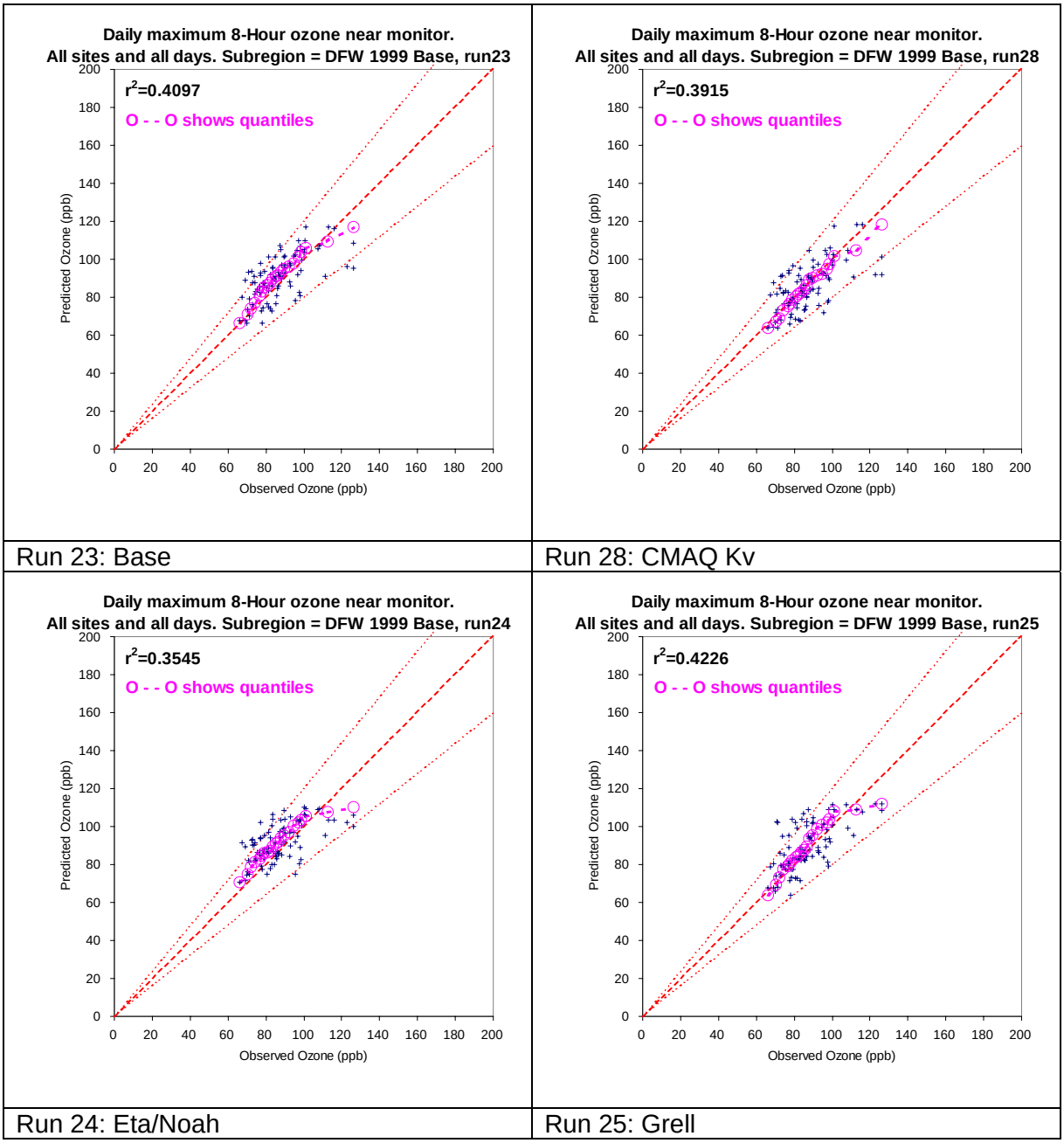


**Figure 5-6**. Scatter and quantile-quantile plots of the largest predicted daily maximum 8-hour ozone near each monitor (within 9x9 cell area) and the observed daily maximum 8-hour ozone for four CAMx runs using different meteorology inputs in the 1999 DFW Episode.

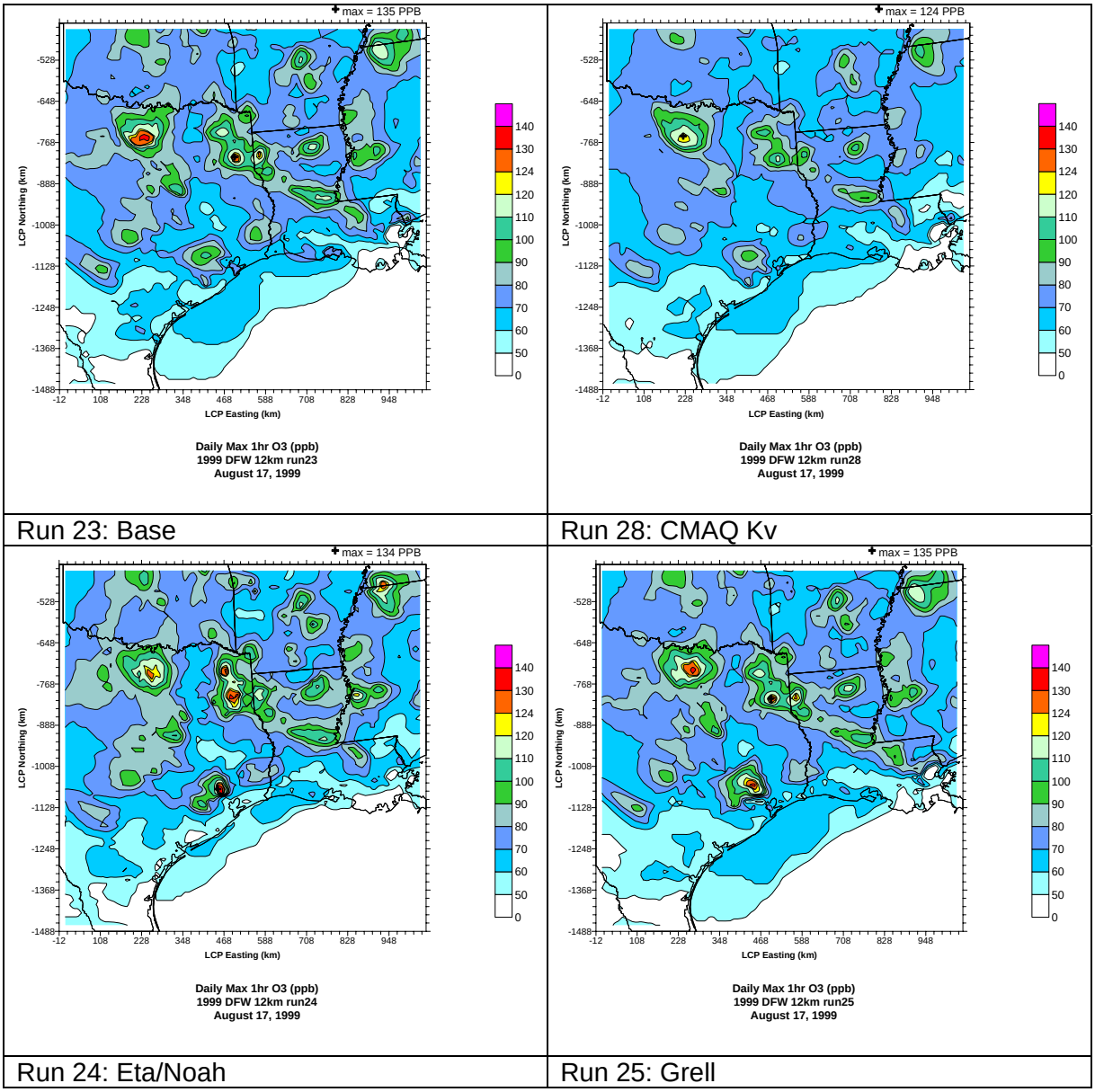


**Figure 5-7.** Spatial plots of the daily maximum 1-hour ozone in the 12-km domain on August 17, 1999 from four CAMx simulations using different meteorology inputs.

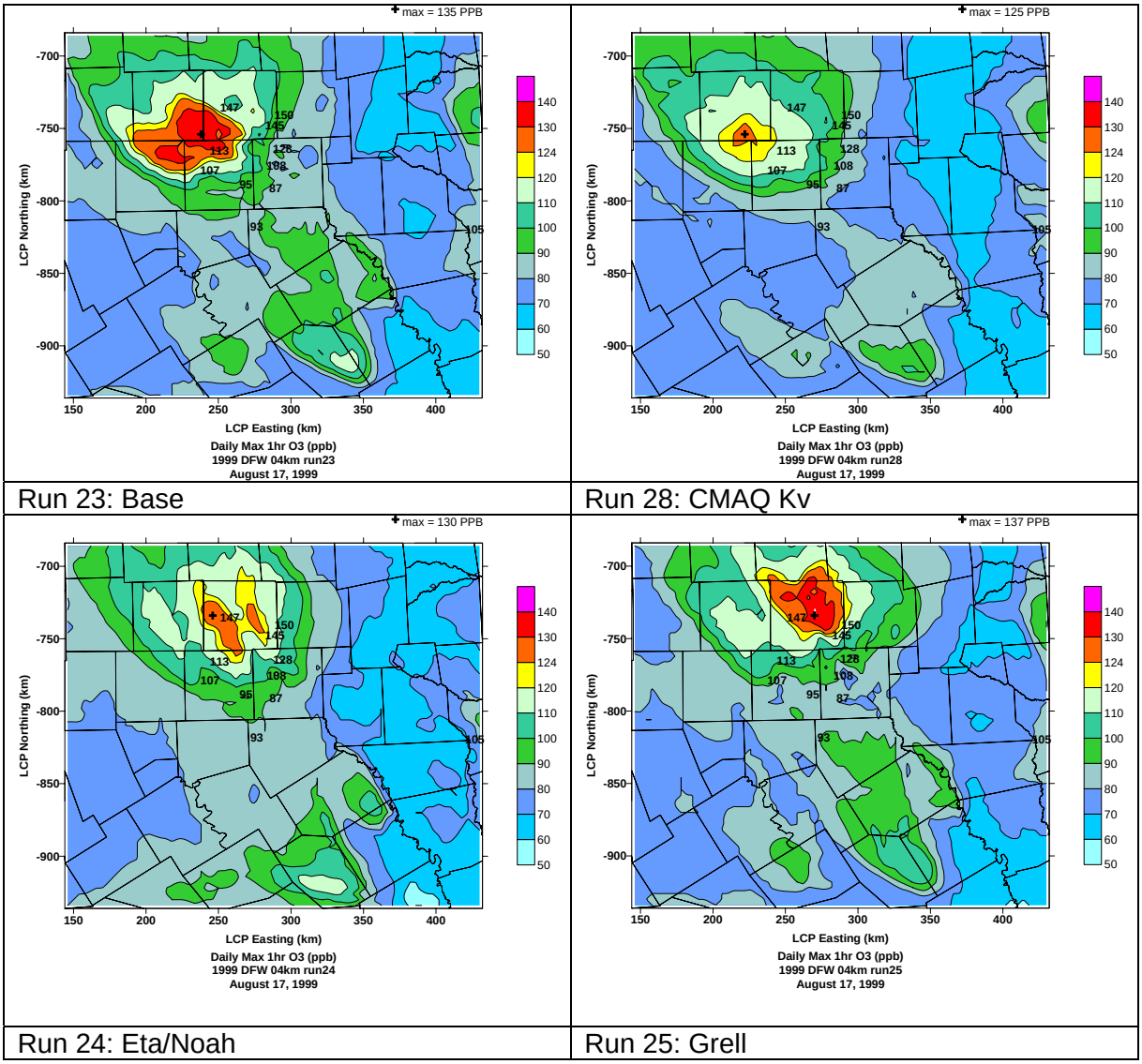


**Figure 5-8**. Spatial plots of the daily maximum 1-hour ozone in the DFW 4-km domain on August 17, 1999 from four CAMx simulations using different meteorology inputs.

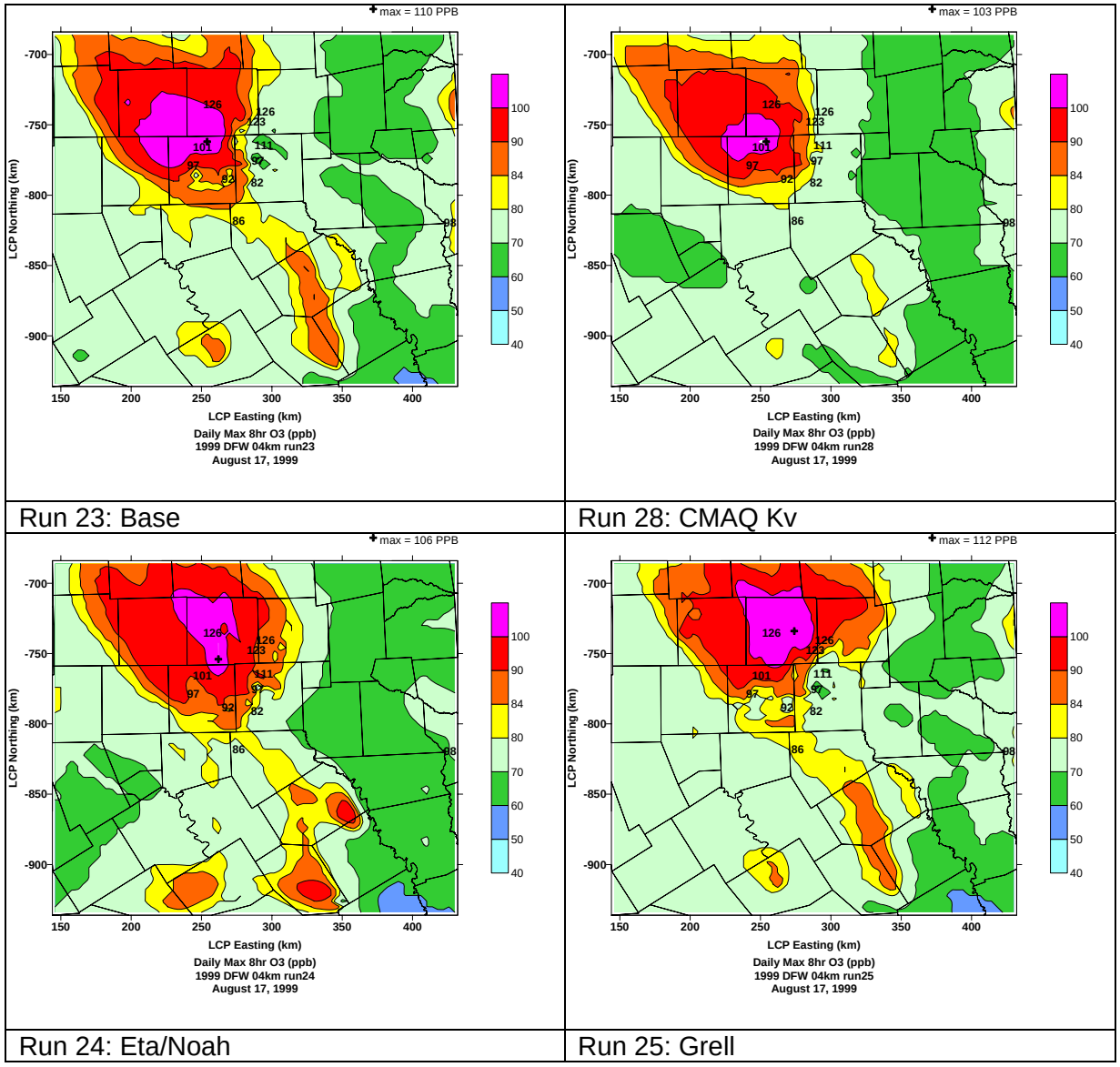


**Figure 5-9.** Spatial plots of the daily maximum 8-hour ozone in the DFW 4-km domain on August 17, 1999 from four CAMx simulations using different meteorology inputs.

# 6. OZONE SENSITIVITY TO CHANGES IN EMISSIONS

This section evaluates ozone sensitivity to changes in emissions for 1999. Note that these are just base-year sensitivity tests, not future year control strategies. The purpose of these tests is to evaluate how the model responds and if there is reason to believe that changes to the emission inventory are warranted. All emission changes were applied to the baseline emissions used in Run 23. In Run 26, on-road and off-road mobile NOx emissions were reduced 30 % in the four DFW core counties (Collin, Dallas, Denton, and Tarrant Counties). In Run 27, biogenic emissions were increased 30 % domain-wide. In Run 29, VOC emissions from non-EGU point sources were doubled. Table 6-1 summarizes the total emissions released in the expanded 36-km domain on August 17, 1999.

All runs were compared to the Run 23 base case. Each run used the expanded horizontal domain and 15-km top. Meteorology was extracted from MM5 Run 5 with the O'Brien Kv profile, which was shown to have limited vertical mixing within the boundary layer in Section 5, and will be explored more in Section 8. Initial conditions were moderate below 1700 m and clean aloft. Boundary conditions were moderate in the north, west, and southwest in the boundary layer and clean aloft.

**Table 6-1**. Daily emissions inside the expanded 36-km domain on August 17, 1999.

| 36-km expanded domain | Run 23: Base Case | Run 26: Mobile NOx decreased 30% | | Run 27: Biogenics increased 30% | | Run 29: NEGU VOC increased 100% | |
|---|---|---|---|---|---|---|---|
| | TPD | TPD | % change | TPD | % change | TPD | % change |
| Low-level | | | | | | | |
| NOx | 47245 | 47086 | -0.3 | 49732 | 5.3 | 47245 | 0.0 |
| VOC | 244373 | 244373 | 0.0 | 306174 | 25.3 | 247939 | 1.5 |
| CO | 252174 | 252174 | 0.0 | 258105 | 2.4 | 252174 | 0.0 |
| SO2 | 8456 | 8456 | 0.0 | 8456 | 0.0 | 8456 | 0.0 |
| | | | | | | | |
| Elevated | | | | | | | |
| NOx | 25682 | 25682 | 0.0 | 25682 | 0.0 | 25682 | 0.0 |
| VOC | 1361 | 1361 | 0.0 | 1361 | 0.0 | 2583 | 89.7 |
| CO | 8357 | 8357 | 0.0 | 8357 | 0.0 | 8357 | 0.0 |
| SO2 | 47032 | 47032 | 0.0 | 47032 | 0.0 | 47032 | 0.0 |

A set of model performance plots compares each run to Run 23 in Figures 6-1 to 6-8. Time series of 1-hour ozone from the four runs are in Figure 6-1. Daily statistics for the 4-km domain are shown in Figures 6-2 and 6-3 for 1-hour and 8-hour ozone, respectively. Scatter plots of the highest daily maxima 1-hour and 8-hour ozone near each monitor are displayed in Figure 6-4 and 6-5, respectively. Spatial plots of the daily maximum 1-hour ozone on August 17, 1999 for the 12-km and 4-km domains are displayed in Figure 6-6 and 6-7, respectively. Spatial plots of the daily maximum 8-hour ozone are displayed in Figure 6-8 for the 4-km domain.

## RUN 26: DECREASED MOBILE SOURCE NOx

In Run 26, the mobile NOx emissions were reduced 30 % inside the four core DFW counties, amounting to a 0.3% reduction in the total NOx emitted in the 36-km expanded domain. The time series plots showed improvements over Run 23. Statistics for 1-hour and 8-hour unpaired peak accuracy, normalized bias, and normalized error were better than Run 23 on most dates. Run 26 showed the best normalized error among the four runs.

The scatter plots showed higher coefficient of determination in Run 26 compared to Run 23 in all three methods of evaluating the predicted daily maximum 1-hour and 8-hour ozone. More ozone was generated when the NOx emissions were reduced, due to fewer scavengers in the lower layers. Table 6-2 lists the $R^2$ from these four runs. The spatial plots on August 17 show that the NOx reduction shifted the 1-hour peak eastward and higher by 4 ppb.

**Table 6-2**. Comparison of the 1-hour and 8-hour coefficient of determination from each scatter plot of the predicted and observed daily maximum ozone from four CAMx simulations with different emissions.

| | 1-hour $R^2$ | | | 8-hour $R^2$ | | |
|---|---|---|---|---|---|---|
| | max 9x9 | closest | interpolated | max 9x9 | closest | interpolated |
| Run 23: Base | 0.42 | 0.86 | 0.38 | 0.41 | 0.78 | 0.28 |
| Run 26: MV NOx –30% | 0.51 | 0.90 | 0.48 | 0.47 | 0.83 | 0.40 |
| Run 27: Bio +30% | 0.44 | 0.94 | 0.43 | 0.42 | 0.89 | 0.34 |
| Run 29: NEGU VOC +100% | 0.43 | 0.87 | 0.38 | 0.42 | 0.79 | 0.29 |

## RUN 27: INCREASED BIOGENIC VOC AND NOx

Run 27 added a 30% increase in biogenics, raising the total VOC and NOx emitted into the domain on August 17 by 25 % and 5 %, respectively. The daily statistics, 1-hour time series plots, and the spatial plots of daily maximum ozone on August 17 all showed higher ozone in Run 27 compared to Run 23.

The average paired peak accuracy and normalized bias in Run 27 for 1-hour ozone were the best of the four runs as the dominantly negative statistics in Run 23 became less negative in Run 27 due to the higher ozone. The unpaired peak accuracy was the worst of the four runs, as the peaks were too high; Run 27 failed to meet the 20% EPA performance goal on August 22. This statistic can be misleading because the observed peak is determined from a limited number of monitoring stations. To compensate for gaps in the observation network, it is better for the model to over predict the unpaired peak than to under predict. The increased biogenic emissions reduced the normalized error, but not as significantly as in Run 26. The 8-hour statistics revealed similar features except that the unpaired peak accuracy remained within acceptable EPA guidelines on all days.

All $R^2$ from Run 27 were higher than in Run 23, as shown in Table 6-2. The closest predicted peak in the 9 by 9 grid to the observed peak showed the greatest improvement, as the 1-hour $R^2$ was 0.94 – the highest coefficient of determination of all runs.

Spatial plots of the 1-hour ozone maximum in the 4-km domain on August 17 showed the peak increasing from 135 ppb in Run 23 to 151 ppb in Run 27 with a slight eastward progression. The 8-hour ozone peak near DFW was 11 ppb higher in Run 27.

**RUN 29: INCREASED POINT SOURCE VOC**

Run 29, which doubled the VOC emissions from all non-EGU point sources, showed minor improvements from Run 23. The spatial plot of the daily maximum 1-hour ozone on August 17 in the 4-km domain increased 2 ppb compared to Run 23; the 8-hour ozone plot was 1 ppb higher. All coefficients of determination of the scatter plots of the predicted and observed daily peak ozone improved by no more than 0.01.

The mobile NOx reductions inside the DFW core made the most improvements to the model performance for ozone, but by no means justify changing the emission inventory. Model performance was shown to be equally sensitive to changes in the meteorology, as discussed in Section 5, and to changes in the chemistry, which will be discussed in Section 7. Further evaluation of the DFW NOx emission inventory would be useful to reduce uncertainty.

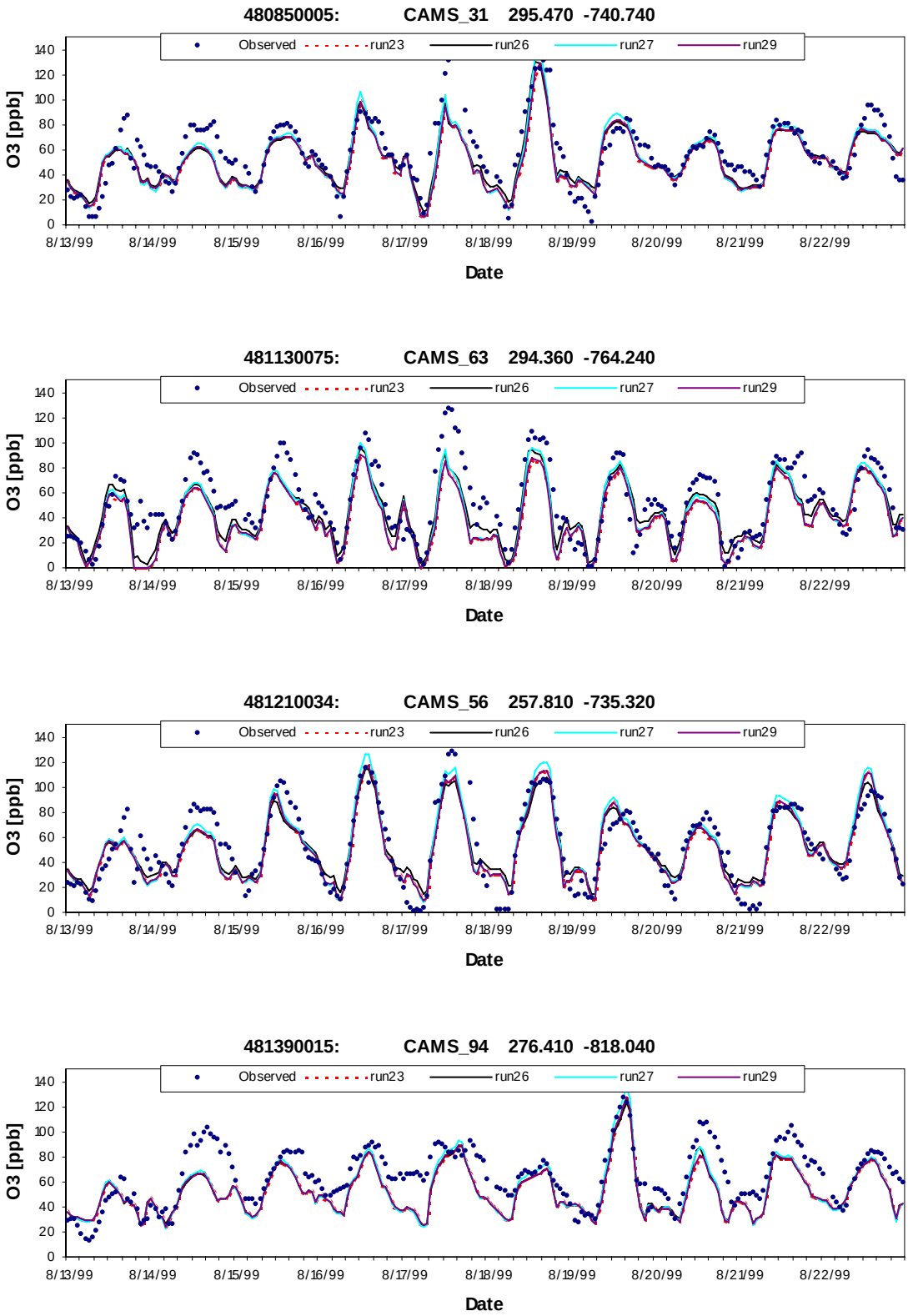


**Figure 6-1**. Time series of 1-hour ozone at sites inside the DFW 4-km domain from four CAMx runs with differences in the emissions.

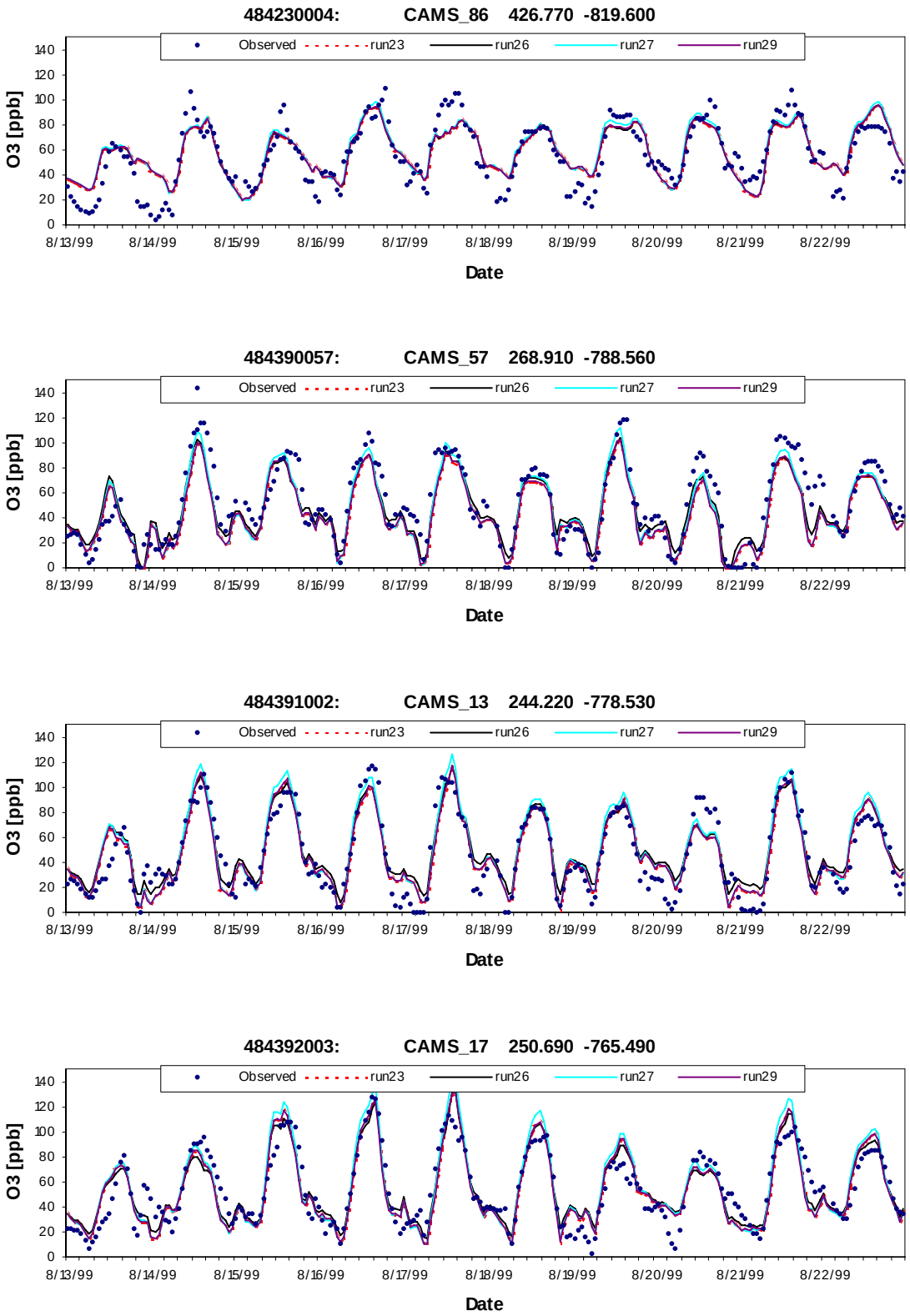


**Figure 6-1**. (Cont.) Time series of 1-hour ozone at sites inside the DFW 4-km domain from four CAMx runs with differences in the emissions.

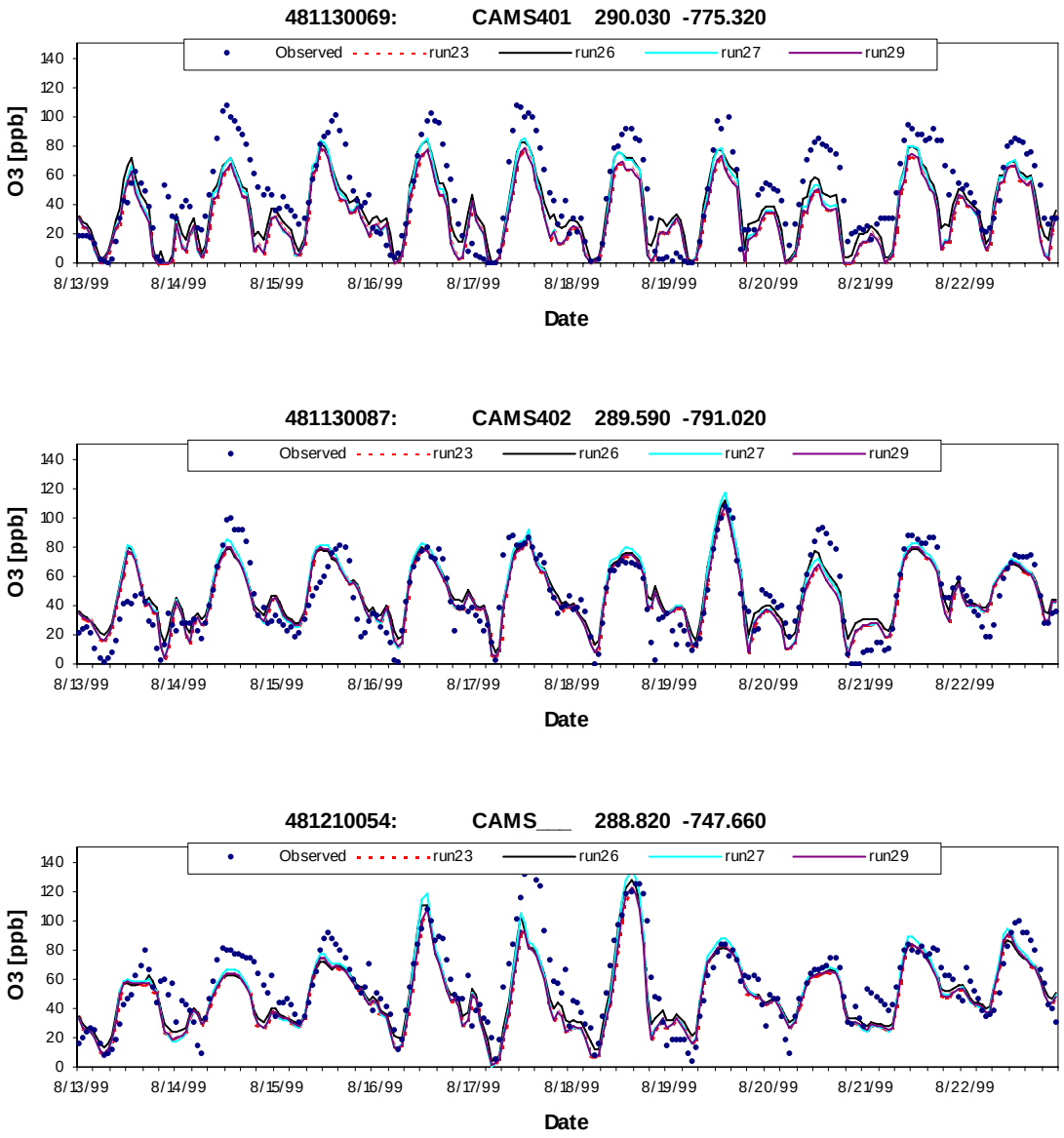


**Figure 6-1**. (Concl.) Time series of 1-hour ozone at sites inside the DFW 4-km domain from four CAMx runs with differences in the emissions.

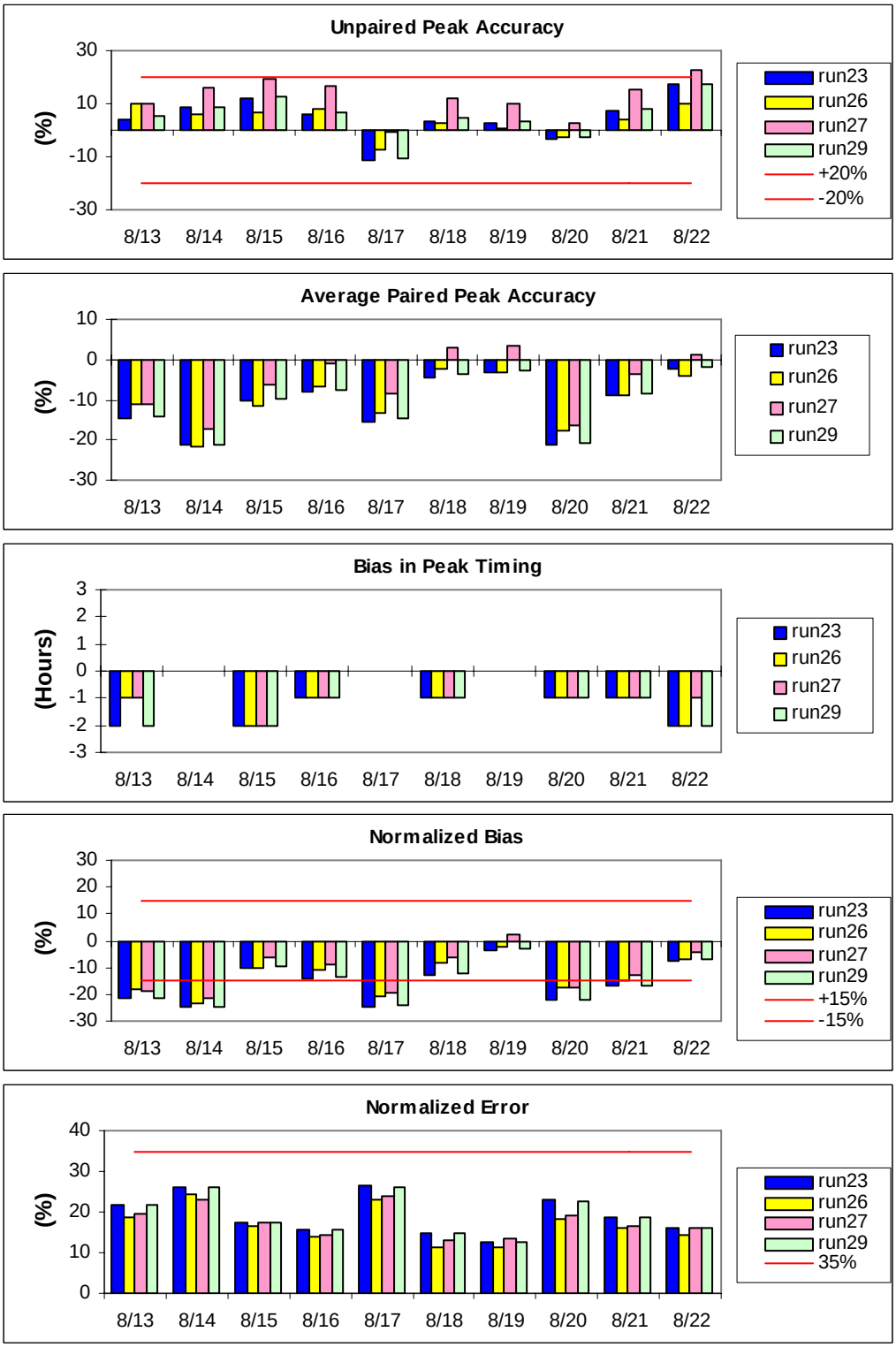


**Figure 6-2.** Daily statistics of the 1999 DFW 1-hour ozone in the 4-km domain from four CAMx runs with differences in the emissions.

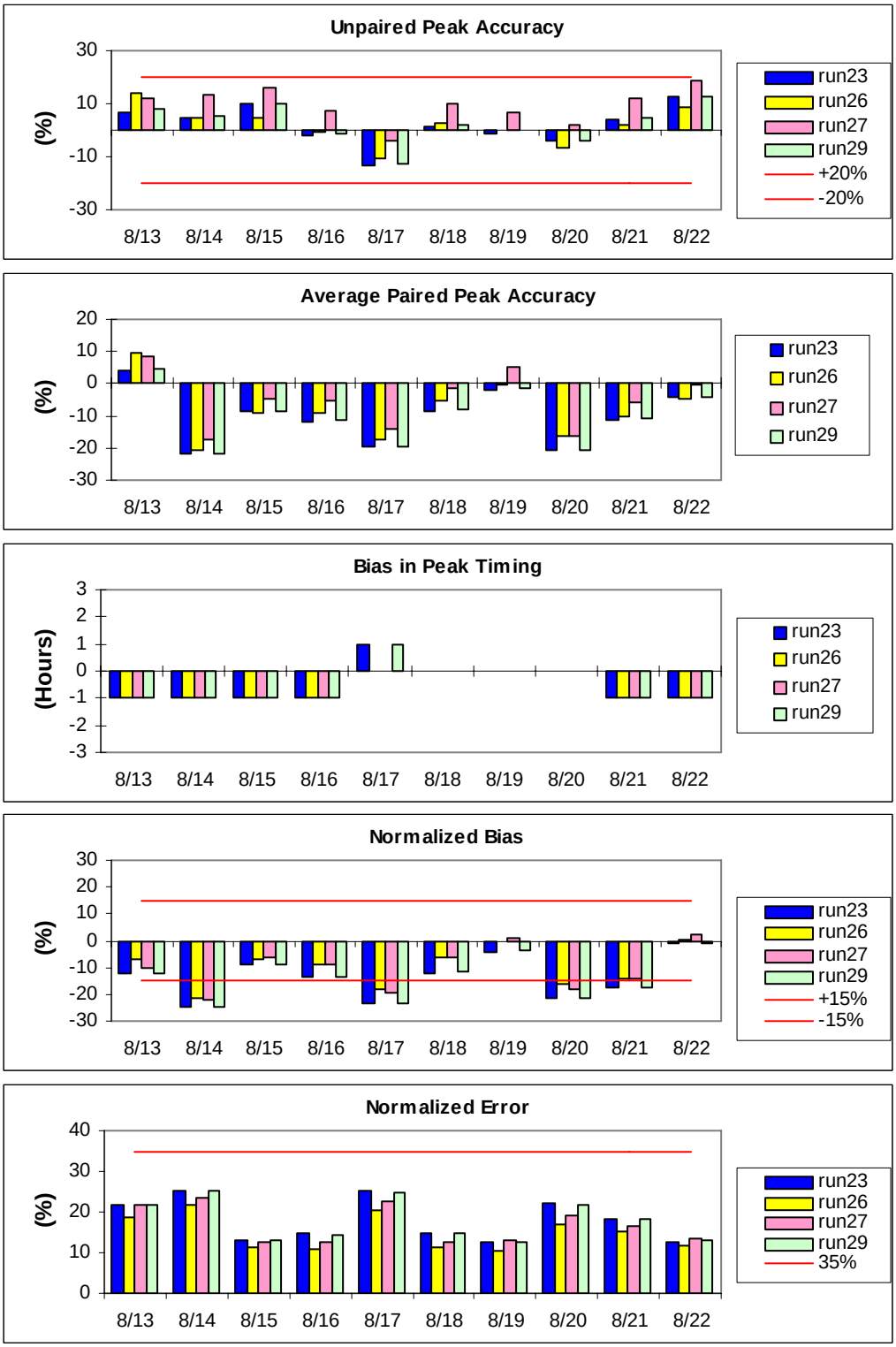


**Figure 6-3**. Daily statistics of the 1999 DFW 8-hour ozone in the 4-km domain from four CAMx runs with differences in the emissions.

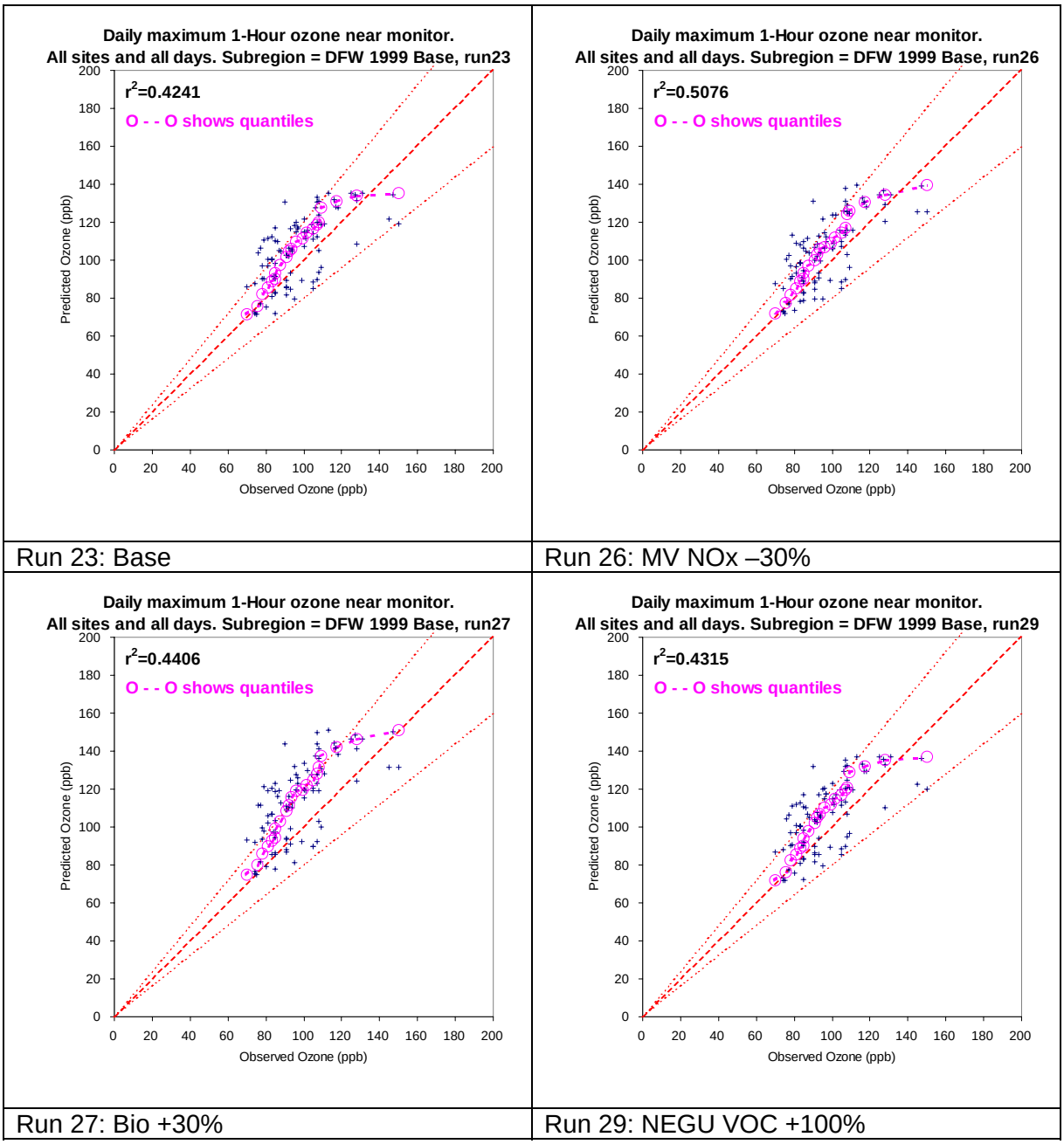


**Figure 6-4**. Scatter and quantile-quantile plots of the largest predicted daily maximum 1-hour ozone near each monitor (within 9x9 cell area) and the observed daily maximum 1-hour ozone for four CAMx runs with different emissions in the 1999 DFW Episode.

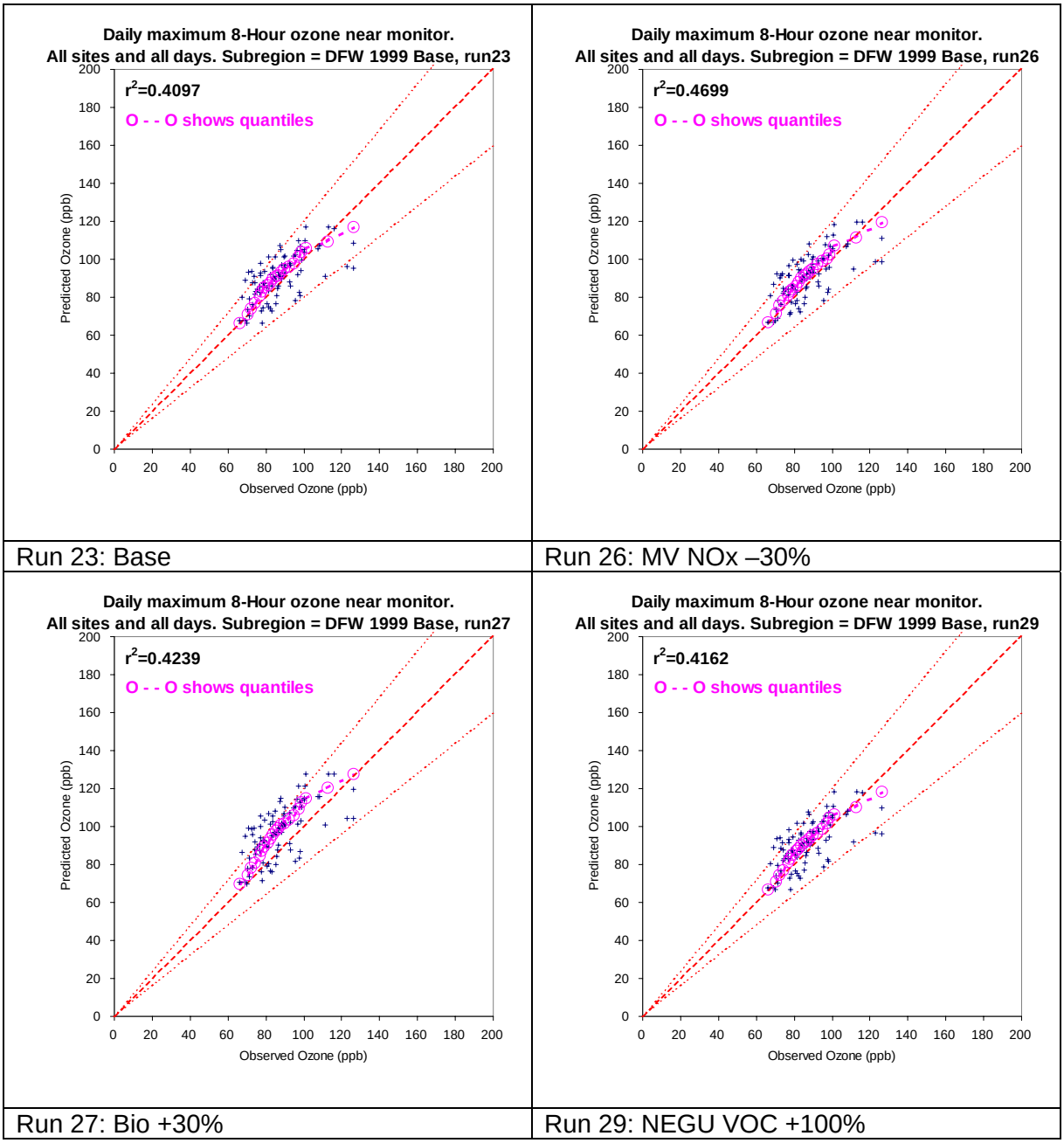


**Figure 6-5**. Scatter and quantile-quantile plots of the largest predicted daily maximum 8-hour ozone near each monitor (within 9x9 cell area) and the observed daily maximum 8-hour ozone for four CAMx runs with different emissions in the 1999 DFW Episode.

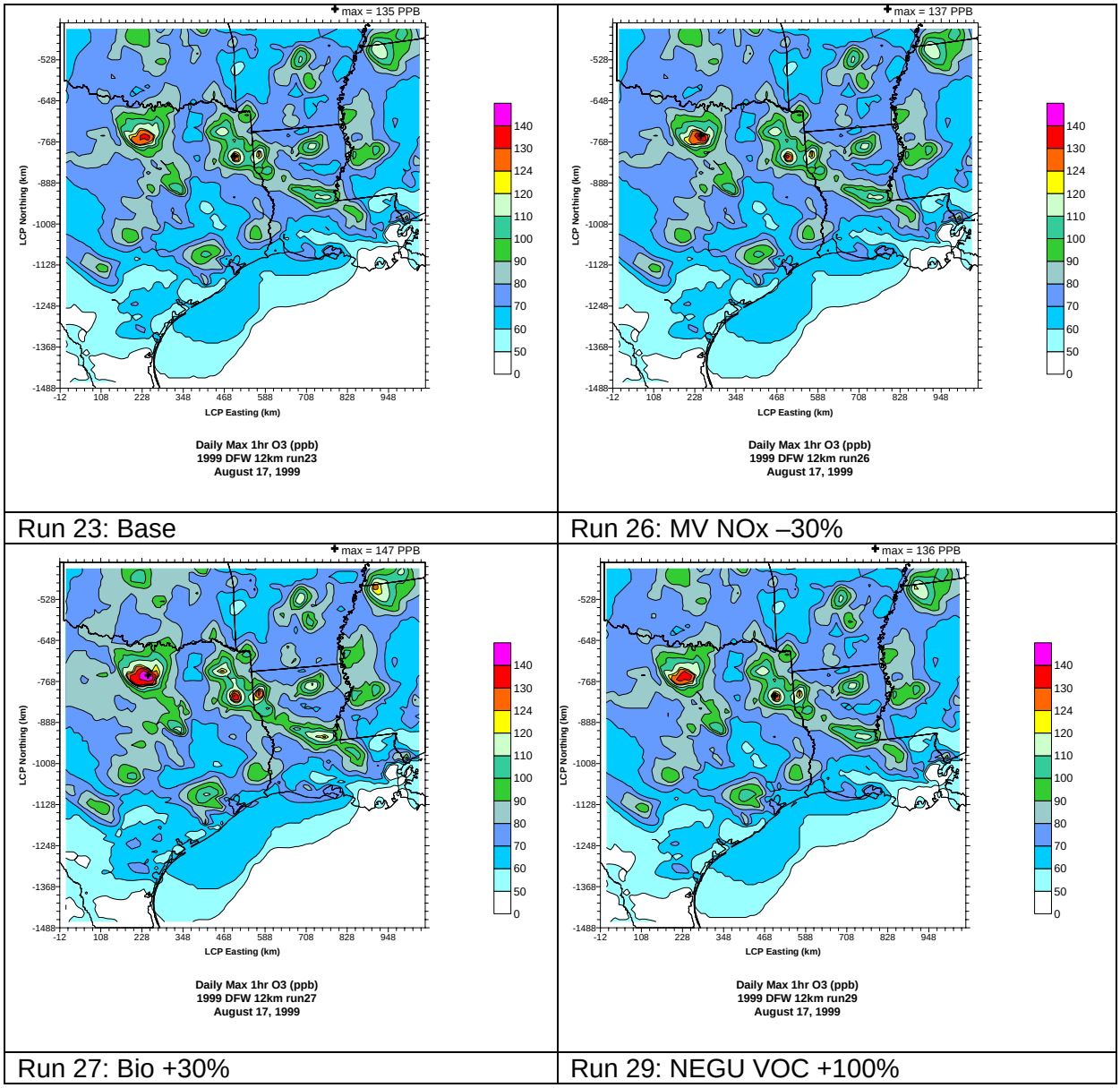


**Figure 6-6.** Spatial plots of the daily maximum 1-hour ozone in the 12-km domain on August 17, 1999 from four CAMx simulations with differences in the emissions.

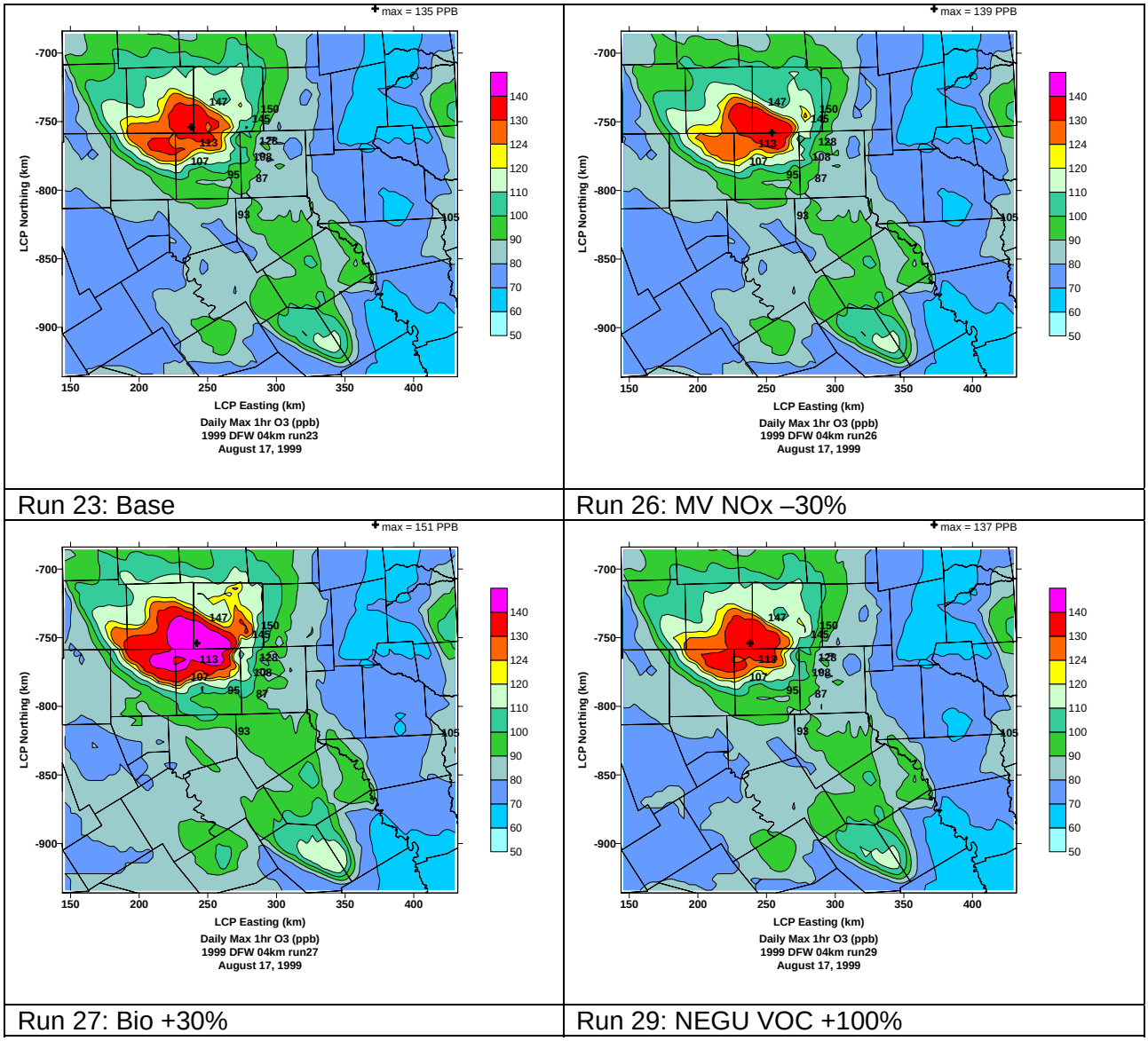


**Figure 6-7**. Spatial plots of the daily maximum 1-hour ozone in the DFW 4-km domain on August 17, 1999 from four CAMx simulations with differences in the emissions.

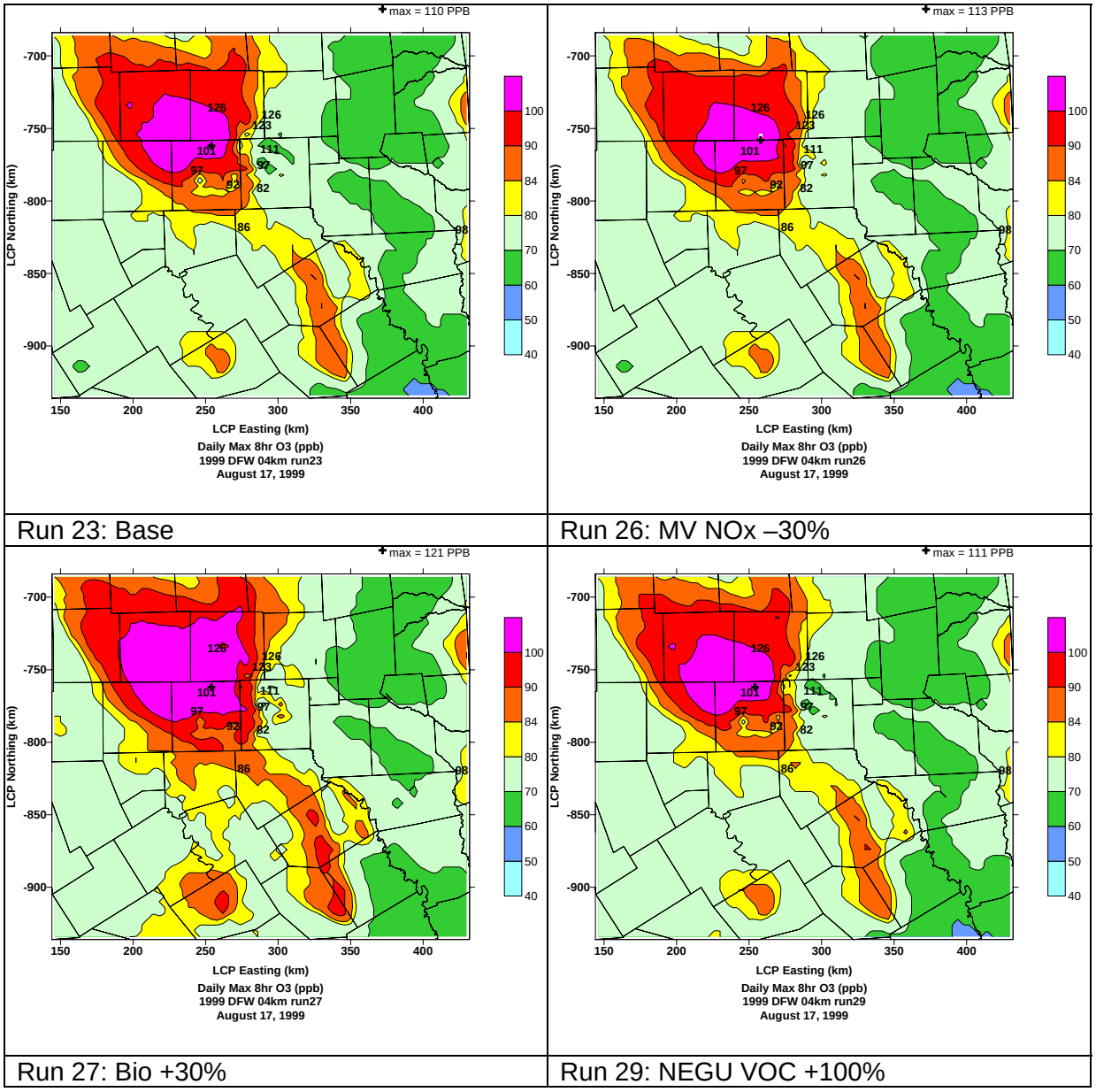


**Figure 6-8**. Spatial plots of the daily maximum 8-hour ozone in the DFW 4-km domain on August 17, 1999 from four CAMx simulations with differences in the emissions.

# 7. OZONE SENSITIVITY TO CHEMISTRY CHANGES

This section evaluates ozone sensitivity in the Dallas/Fort Worth region when CAMx is implemented with different chemistry. The base case (Run 23) used the standard CB4 chemical mechanism. Run 30 used a version of CB4 with added extra inorganic reactions (CB4xi) including several NOx recycling reactions. Run 31 used the CB2002 chemical mechanism.

All three runs were configured with the expanded horizontal domain and 15-km top. All runs used meteorology extracted from MM5 Run 5 with the O'Brien Kv profile. Emissions of the expanded domain included TCEQ emissions from the standard 36-km domain, and were identical in the three runs. Initial conditions were moderate below 1700 m and clean aloft. Boundary conditions were moderate over the west, north, and southwest in the mixed layer, and clean elsewhere.

## CB2002 MECHANISM

The CB2002 chemical mechanism (Jeffries et al. 2002) is a reformulation of the CB4 mechanism that includes updated reaction rate constants and has been evaluated against chamber data. The CB2002 reaction set is detailed in Appendix C. One of the motivations for developing CB2002 was that the OH + $NO_2$ reaction rate constant has been revised since CB4 was developed. The OH + $NO_2$ reaction is a major sink for both radicals and NOx under urban conditions and is so important that a chemical mechanism such as CB4 must be re-calibrated against SMOG chamber data if this rate constant is changed.

The OH + $NO_2$ reaction rates for CB4 and SAPRC99 are compared to CB2002 in Table 7-1. Both the NASA (JPL, 2003) and IUPAC (IUPAC, 2004) kinetic data review panels recommend values that are essentially identical to CB2002 shown in Table 7-1. The comparison for 298 K and 1013 mbar is most relevant to smog chamber data and urban ozone formation. For this condition, the OH + $NO_2$ reaction rate is about 15% low in SAPRC99 and 7% high in CB4.

**Table 7-1**. Comparison of OH + $NO_2$ reaction rate constants.

| **Temperature (K)** | **298** | **273** | **298** | **Difference from CB2002** |
|---|---|---|---|---|
| **Pressure (mbar)** | **1013** | **1013** | **491** | |
| CB2002 | 1.57E+04 | 1.96E+04 | 5.19E+03 | |
| CB4 | 1.68E+04 | 2.29E+04 | 8.15E+03 | +7% to +36% |
| SAPRC99 | 1.33E+04 | 1.80E+04 | 4.77E+03 | -9% to -18% |

Notes:
CB2002 has currently accepted values for the OH + $NO_2$ reaction rate constant.
The 298 K and 1013 mbar case is most relevant to smog chamber conditions.

CB2002 was used as an alternative to CB4 to test the sensitivity of CAMx ozone concentrations to mechanism changes. No recommendation is made regarding which mechanism is "better".

## NOx RECYCLING REACTIONS: CB4xi

Yarwood, Whitten and Rao (2005) reviewed the inorganic reaction set in the CB4 and several other mechanisms to identify reactions that should be added to CB4 for regional/annual modeling conditions. Seventeen reactions were added to CAMx mechanism 4 as shown in Table 7-2. Since these reactions mostly involve the inorganic reaction set this modification is referred to as extended inorganic chemistry (CB4xi).

**Table 7-2**. Reactions added in the CB4xi mechanism and whether they are included in other condensed chemical mechanisms.

| Number | Reaction | Included in CB2002 | Included in SAPRC99 |
|---|---|---|---|
| 101 | O1D + H2 = OH + HO2 | | |
| 102 | OH + H2 = HO2 | | Yes |
| 103 | OH + O = HO2 | | |
| 104 | OH + OH = O | | |
| 105 | OH + OH = H2O2 | | |
| 106 | HO2 + O = OH | | |
| 107 | H2O2 + O = OH + HO2 | | |
| 108 | NO3 + O = NO2 | | |
| 109 | NO3 + OH = HO2 + NO2 | Yes | Yes |
| 110 | NO3 + HO2 = HNO3 | Yes | Yes |
| 111 | NO3 + O3 = NO2 | | |
| 112 | NO3 + NO3 = 2 NO2 | Yes | Yes |
| 113 | PAN = C2O3 + NO2 | | |
| 114 | HNO3 = OH + NO2 | | Yes |
| 115 | N2O5 = NO2 + NO3 | | |
| 116 | NTR = NO2 + XO2 | | Yes |
| 117 | PNA = 0.61 HO2 + 0.61 NO + 0.39 OH + 0.39 NO2 | | Yes |

CB2002 from Jeffries, Voicu and Sexton (2002)
SAPRC99 from Carter (2000)
PAN = peroxyacetyl nitrate
PNA = peroxynitric acid
NTR = organic nitrates

The extended inorganic reactions are summarized as follows:

- Reactions of molecular hydrogen (101 and 102). Hydrogen is somewhat important to odd-hydrogen (OH and $HO_2$) for very dry conditions in the upper troposphere. Including hydrogen allows the air quality impacts of hydrogen as an alternative fuel to be evaluated. Currently, hydrogen is included in CAMx with a constant atmospheric concentration of 0.6 ppm (Novelli et al, 1999).
- Odd-oxygen reactions (103 to 107) that may be important for pristine conditions such as the upper troposphere. Including these reactions provides a more complete description of hydroxyl radical (OH) chemistry in the upper troposphere to improve modeling for persistent air toxics and mercury.
- Additional $NO_3$ radical reactions (108 to 112) to improve nighttime chemistry. The $NO_3$ radical is the main driver for atmospheric chemistry at night and including additional $NO_3$ removal reactions improves the calculation of nighttime destruction rates for several

types of reactive hydrocarbons (e.g., aldehydes, olefins) and for NOx (via $NO_3$ and $N_2O_5$ reactions).

- NOx recycling reactions (113 to 117) to improve the representation of the fate of NOx over multi-day timescales. These are all photolysis reactions that occur quite slowly in the troposphere. Reactions 113, 115 and 117 are only important for very cold conditions such as the upper troposphere where corresponding thermal decomposition reactions are slow. Reactions 114 and 116, photolysis of nitric acid and organic nitrates, are important to regional ozone and oxidant chemistry in the lower troposphere (Zaveri and Peters, 1999). These "NOx recycling reactions" slowly recycle nitrogen from an inactive form (NOz) to an active form (NOx).

## RESULTS

Figures 7-1 to 7-8 display a package of time series, statistics, scatter plots, and spatial plots for the three runs using different chemistry, similar to the plots in Figures 4-4 to 4-11. Figure 7-1 shows the time series of 1-hour ozone from Runs 23, 30, and 31 for each site inside the DFW 4-km domain. Figures 7-2 and 7-3 show model performance statistics for each date for 1-hour and 8-hour ozone, respectively. Figures 7-4 and 7-5 show the 1-hour and 8-hour scatter plots of the observed and largest daily maximum near each site. Figure 7-6 shows the spatial plot of the daily maximum ozone on August 17 for the 12-km domain from all three runs; Figures 7-7 and 7-8 show the daily maximum 1-hour and 8-hour ozone inside the 4-km domain.

## RUN 30: CB4xi

The adoption of the NOx recycling reactions for CB4 in Run 30 generated more ozone in both the daytime and nighttime when compared to Run 23, as shown in the time series plots. On most days, the higher ozone in Run 30 improved the mostly-negative normalized bias and average paired peak accuracy from Run 23 for both 1-hour and 8-hour ozone. Run 30 brought the normalized bias within EPA performance goals on August 21 for both 1-hour and 8-hour ozone. The 1-hour unpaired peak accuracy, which was positive on most days in Run 23, became too high in Run 30, pushing the accuracy on August 22 beyond the 20% goal set by the EPA. Positive unpaired peak accuracy is still more desirable than negative, since this statistic is one-sided as the observed peak is based on a limited number of monitoring stations . Normalized error was better on most days.

The coefficient of determination from the scatter plots for daily maximum ozone improved in Run 30 only when using the closest predicted value to the observed in the 9 by 9 cells for both 1-hour and 8-hour ozone. The other two metrics used to define the daily peak yielded similar or worse $R^2$ values, as shown in Table 7-3.

**Table 7-3.** Comparison of the 1-hour and 8-hour coefficient of determination from each scatter plot of the predicted and observed daily maximum ozone using different chemistry.

| | 1-hour $R^2$ | | | 8-hour $R^2$ | | |
|---|---|---|---|---|---|---|
| | Max 9x9 | Closest | Interpolated | Max 9x9 | Closest | Interpolated |
| Run 23: Base | 0.42 | 0.86 | 0.38 | 0.41 | 0.78 | 0.28 |
| Run 30: NOx recycling | 0.42 | 0.90 | 0.36 | 0.39 | 0.84 | 0.27 |
| Run 31: CB2002 | 0.46 | 0.78 | 0.38 | 0.45 | 0.68 | 0.28 |

Spatial plots of the daily maximum ozone inside the 4-km domain on August 17 showed a peak that was 4 ppb higher for 1-hour ozone in Run 30 compared to Run 23. The 8-hour peak was 3 ppb higher. There was no change in the location of the peak.

The higher regional ozone with CB4xi than CB4 is due to the NOx recycling reactions included in CB4xi. These reactions are the photolysis if organic nitrates and nitric acid that are included in other mechanisms such as SAPRC99 (Carter, 2000) and CBM-Z (Zaveri and Peters, 1999). The effect of these NOx recycling reactions partially explains why SAPRC99 tends to predict higher regional ozone than CB4.

**RUN 31: CB2002**

Run 31, in which the CB2002 chemical mechanism was used instead of CB4, produced less ozone than Run 23. On August 17, the daily peak in the 4-km domain was reduced 6 ppb in both 1-hour and 8-hour ozone.

Statistics did the opposite of Run 30. The 1-hour unpaired peak accuracy improved while the average paired peak accuracy and normalized bias worsened. Two dates that met the ±15 % EPA normalized bias goal in Run 23 failed to meet the goal in Run 31 for both 1-hour and 8-hour ozone. Of the three runs, Run 31 had the worst normalized error on almost every date.

The coefficient of determination for Run 31 was better than Run 23 only when using the metric that selected the largest predicted value in the 9 by 9 cells. The $R^2$ was significantly worse when using the value closest to the predicted in the 9 by 9 cells. Bilinear interpolation to the observation site yielded no change in the $R^2$.

**SUMMARY**

The CB4xi chemical mechanism, which includes the NOx recycling reactions, yielded higher ozone in the daytime and at night compared to CB4, and led to improved model performance. The CB2002 chemical mechanism lowered ozone compared to CB4. Further study using advanced techniques such as sensitivity analysis (DDM) and process analysis would be needed to further investigate why CB2002 performs more poorly than CB4. Based on these findings, all subsequent runs in Section 8 and 9 adopted the CB4xi chemical mechanism.

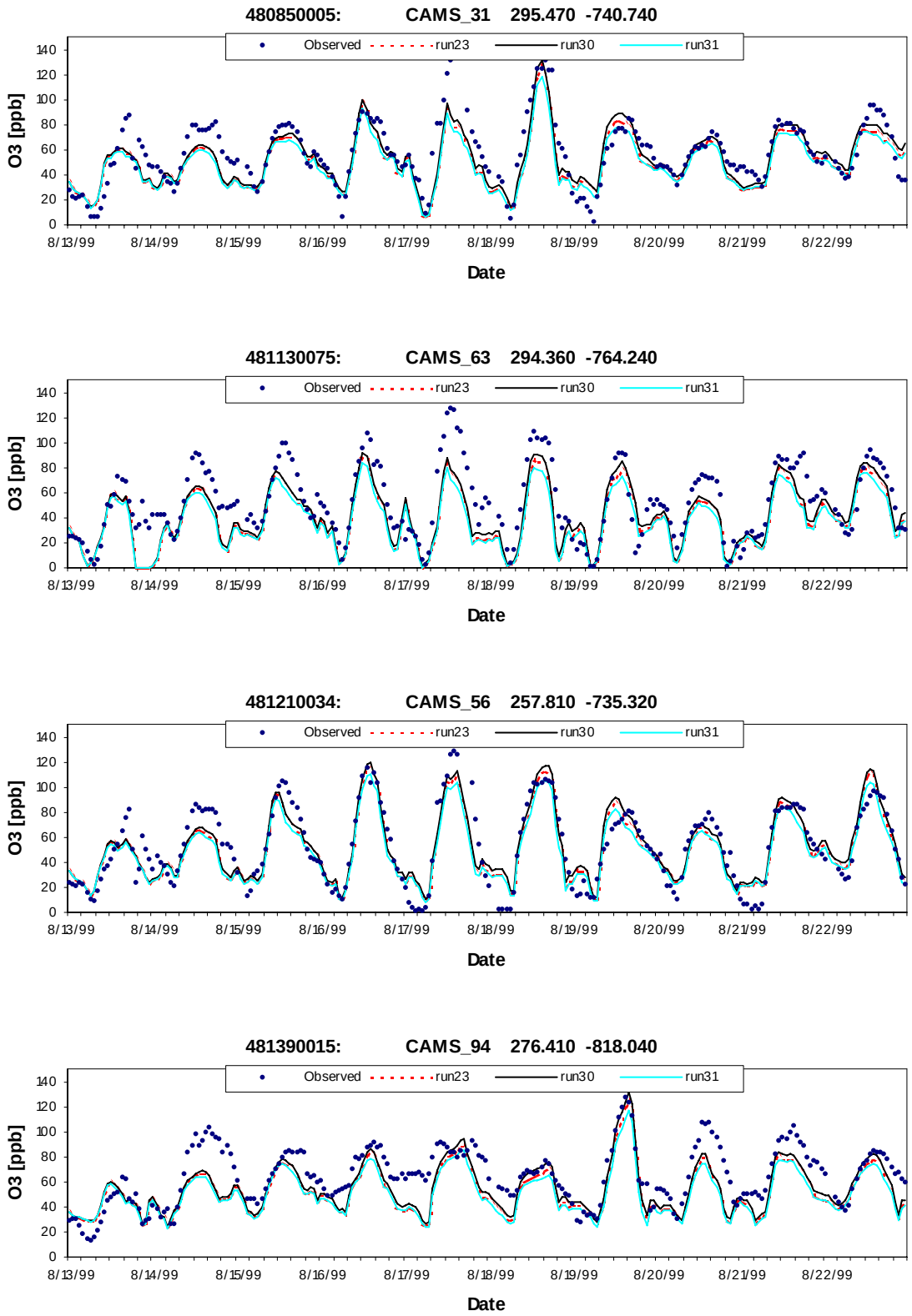


**Figure 7-1**. Time series of 1-hour ozone at sites inside the DFW 4-km domain from three CAMx runs using different chemistry.

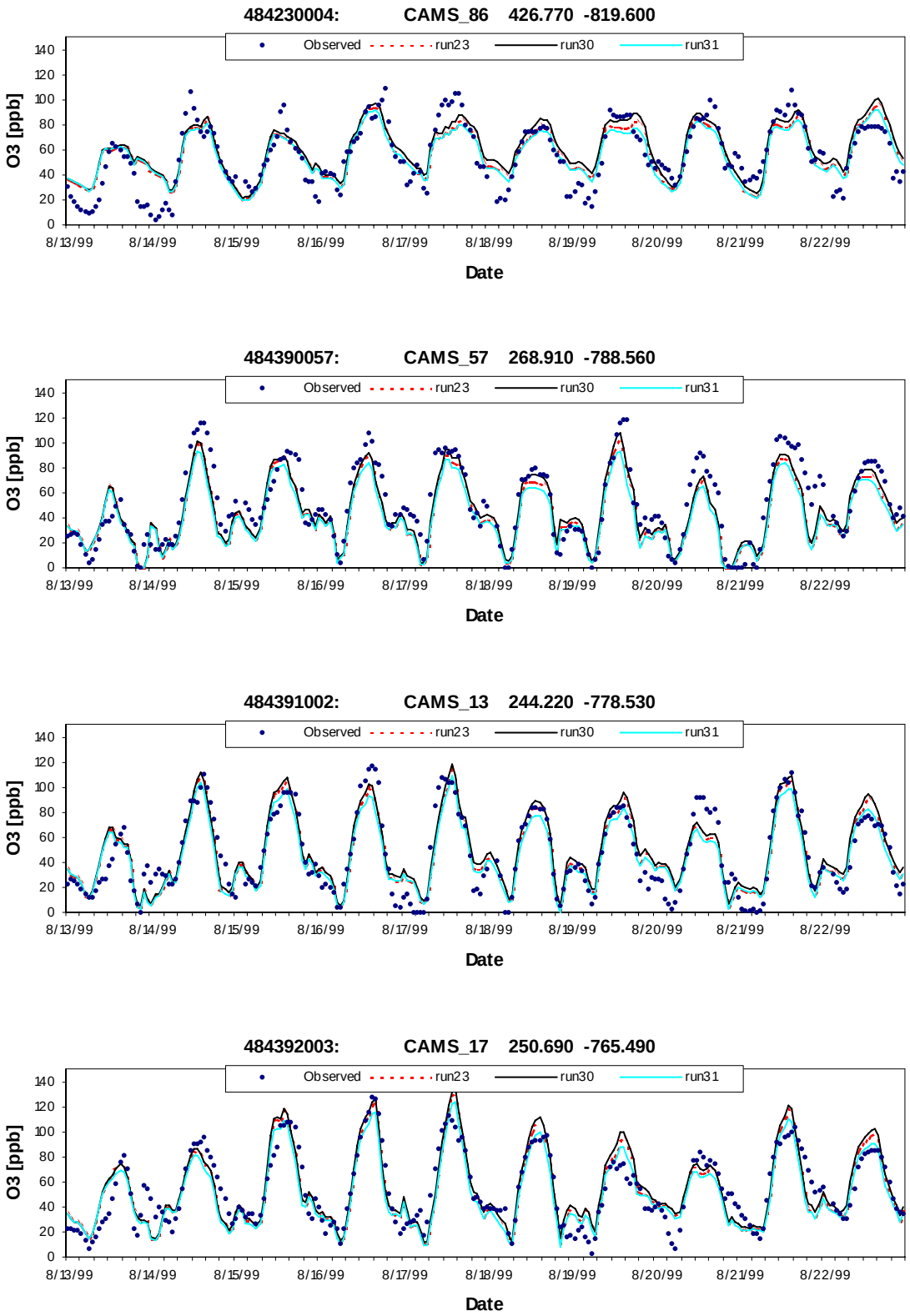


**Figure 7-1**. (Cont.) Time series of 1-hour ozone at sites inside the DFW 4-km domain from three CAMx runs using different chemistry.

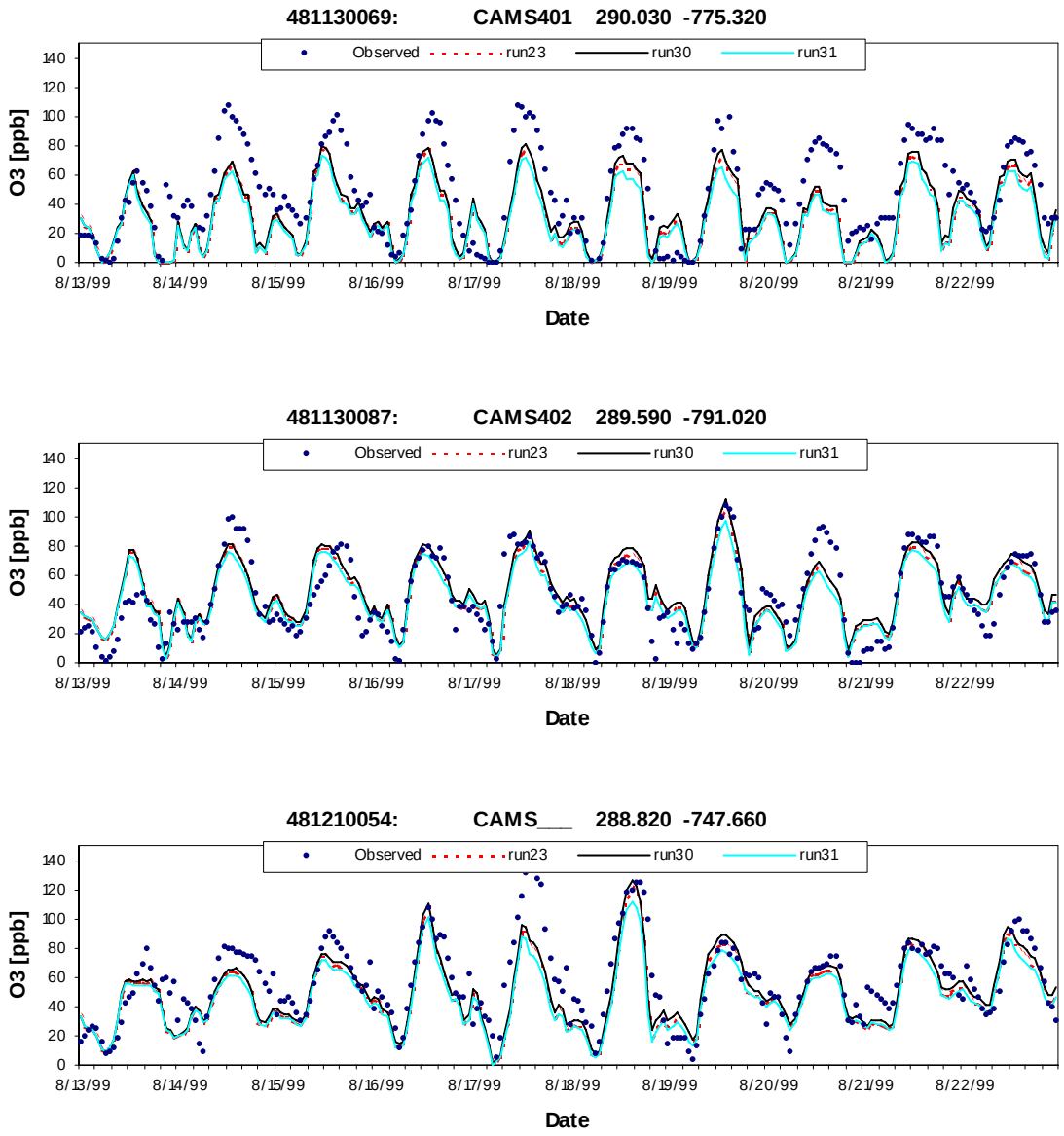


**Figure 7-1**. (Concl.) Time series of 1-hour ozone at sites inside the DFW 4-km domain from three CAMx runs using different chemistry.

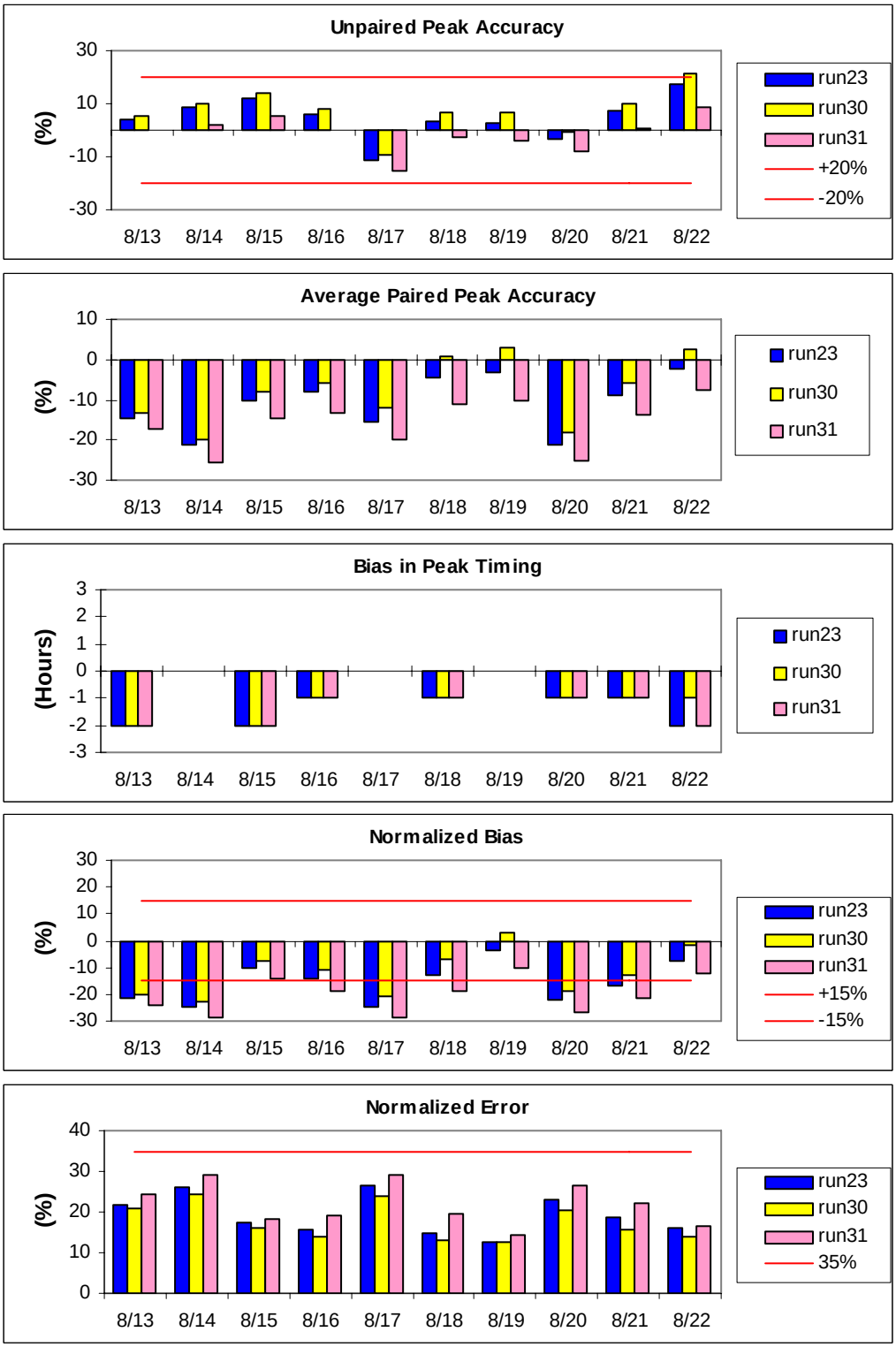


**Figure 7-2**. Daily statistics of the 1999 DFW 1-hour ozone in the 4-km domain from three CAMx runs using different chemistry.

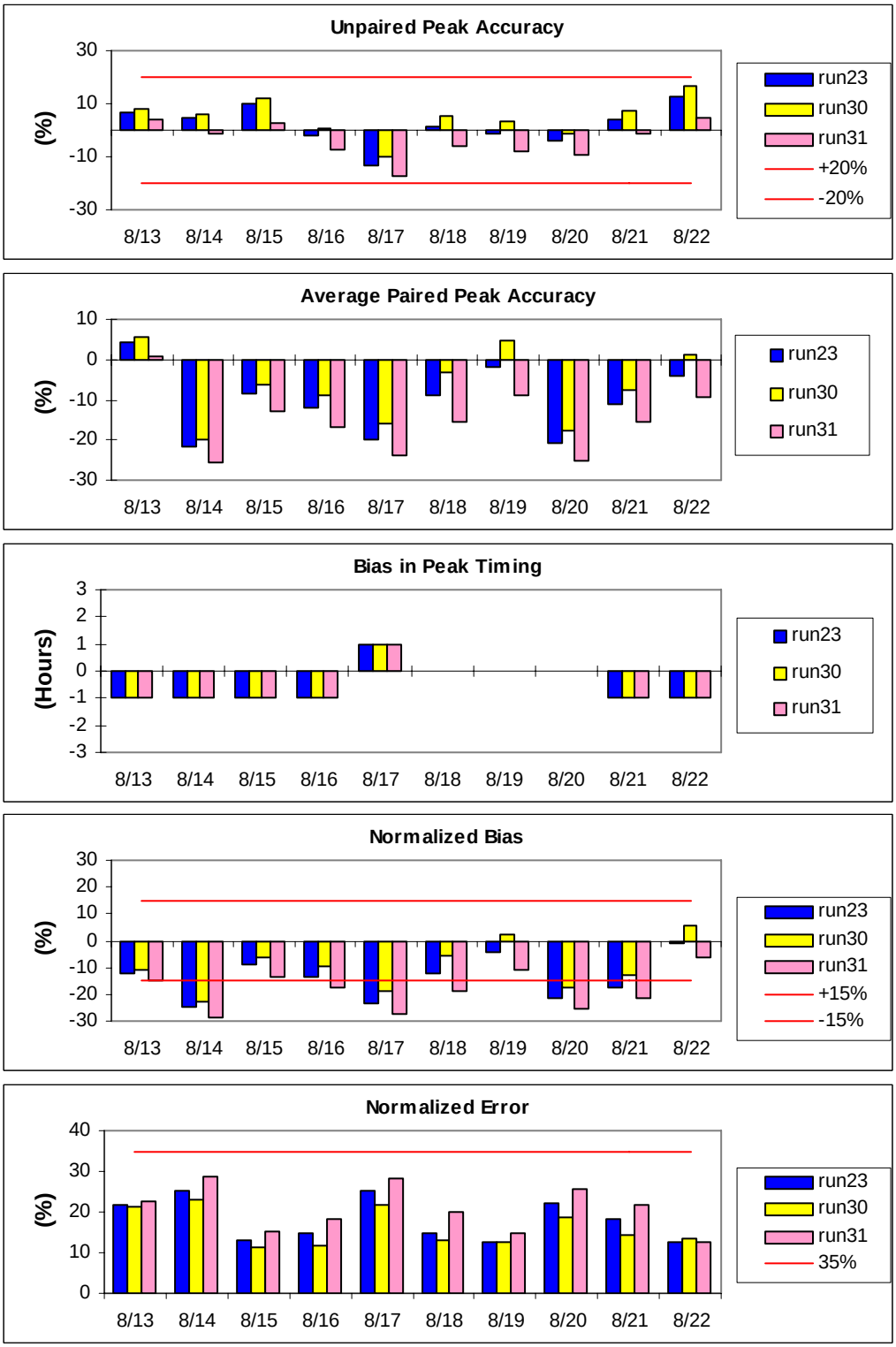


**Figure 7-3.** Daily statistics of the 1999 DFW 8-hour ozone in the 4-km domain from three CAMx runs using different chemistry.

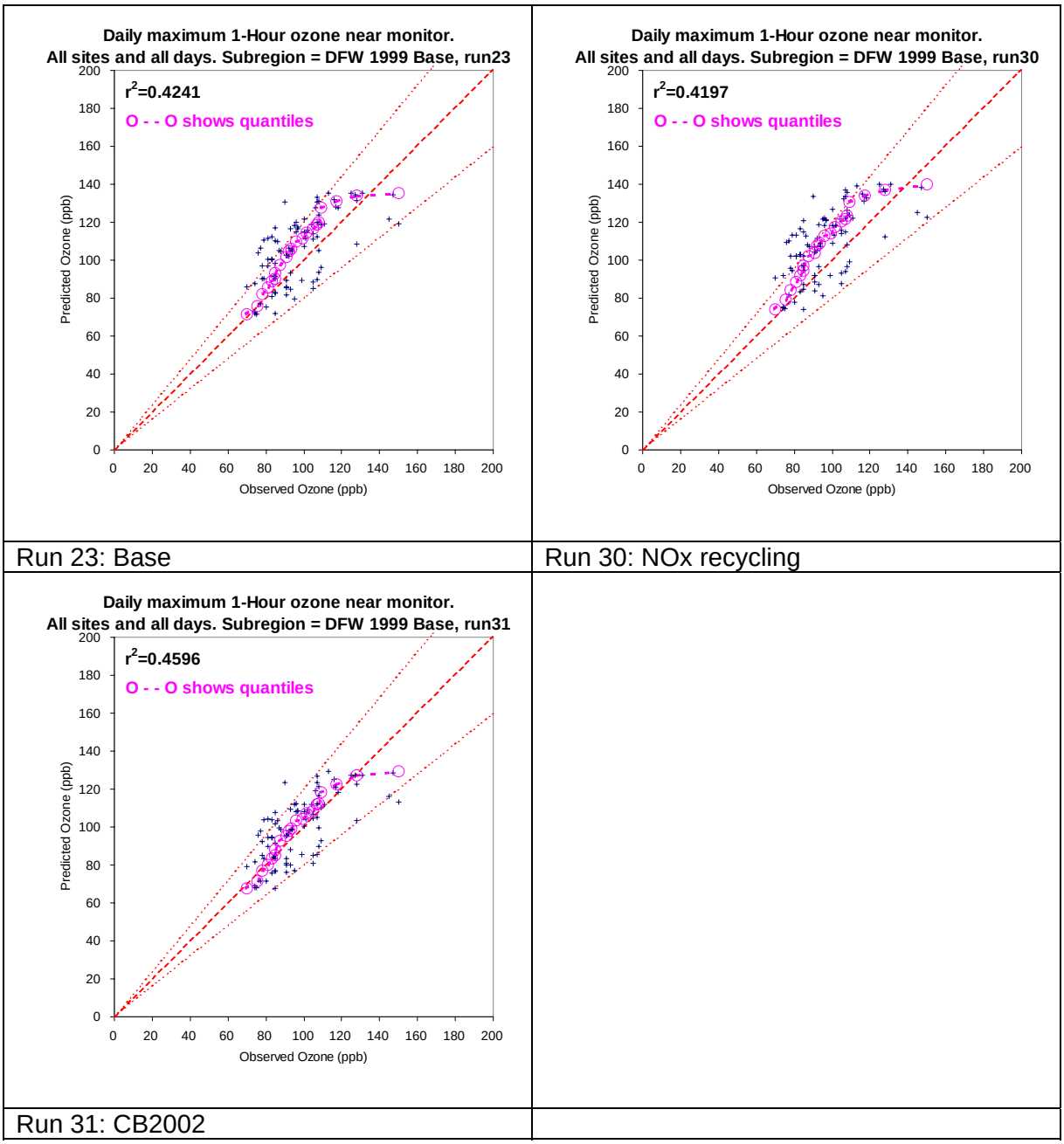


**Figure 7-4**. Scatter and quantile-quantile plots of the largest predicted daily maximum 1-hour ozone near each monitor (within 9x9 cell area) and the observed daily maximum 1-hour ozone for three CAMx runs using different chemistry in the 1999 DFW Episode.

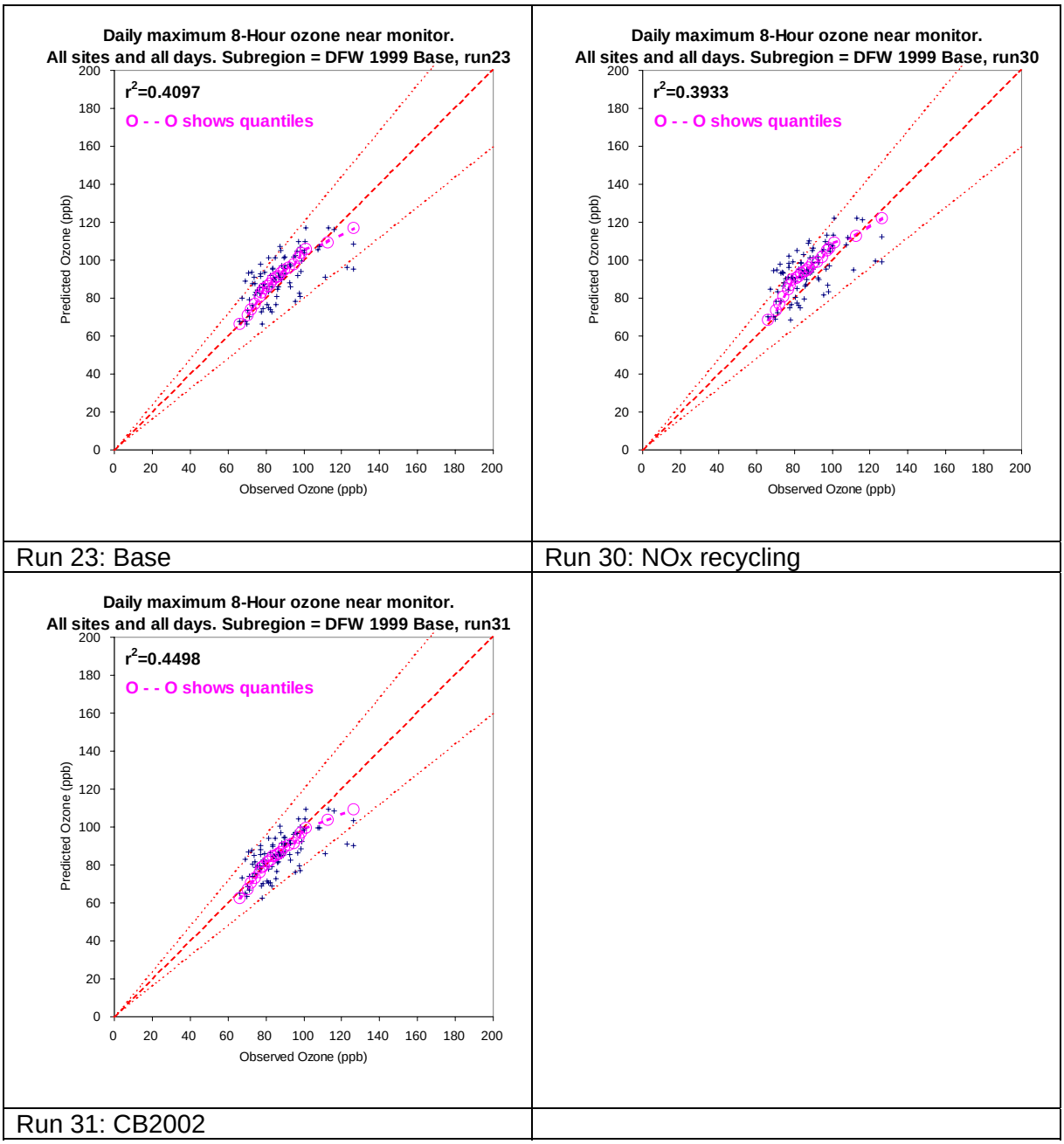


**Figure 7-5**. Scatter and quantile-quantile plots of the largest predicted daily maximum 8-hour ozone near each monitor (within 9x9 cell area) and the observed daily maximum 8-hour ozone for three CAMx runs using different chemistry in the 1999 DFW Episode.

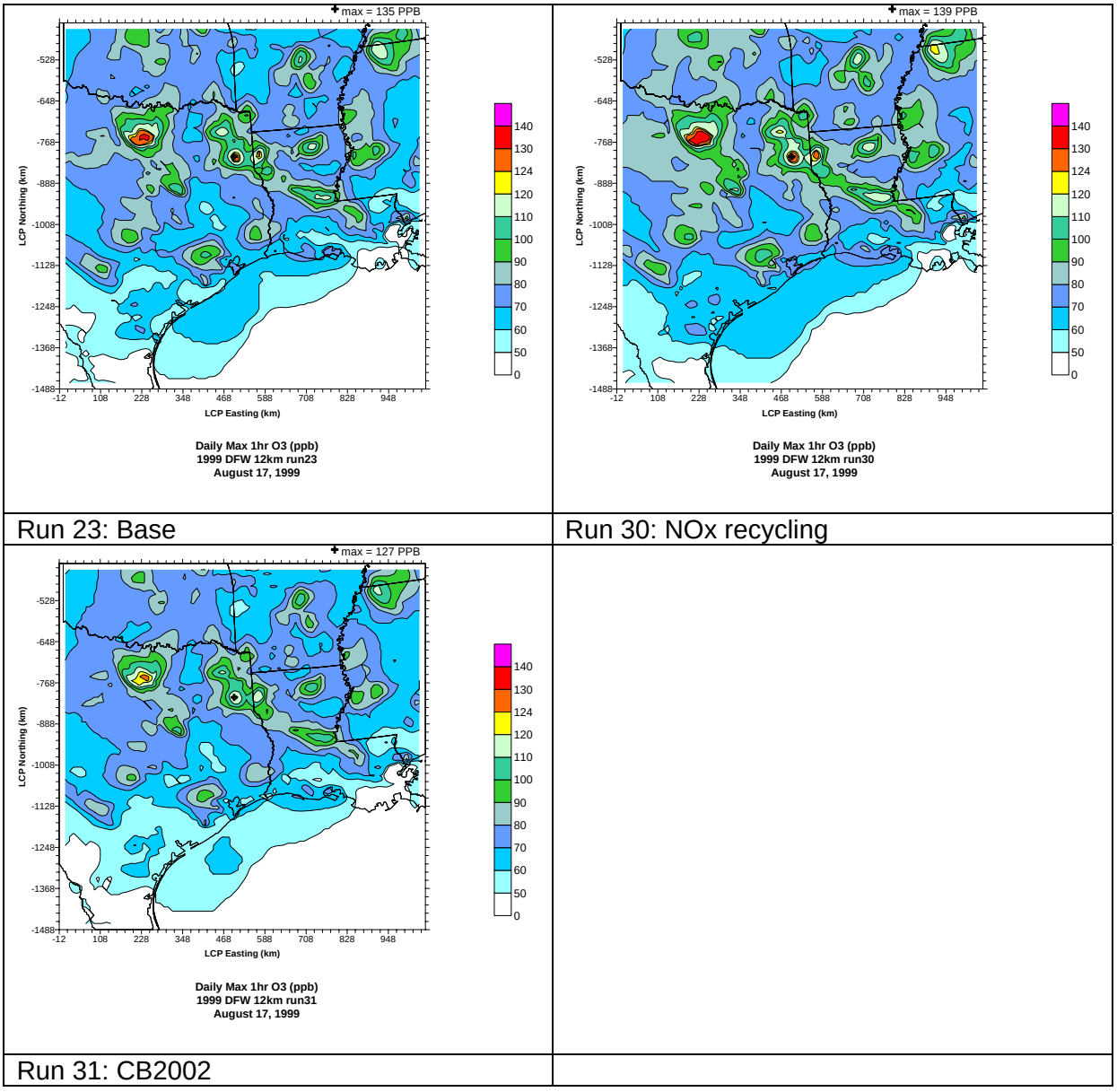


Run 23: Base

Run 30: NOx recycling

Run 31: CB2002

**Figure 7-6.** Spatial plots of the daily maximum 1-hour ozone in the 12-km domain on August 17, 1999 from three CAMx simulations using different chemistry.

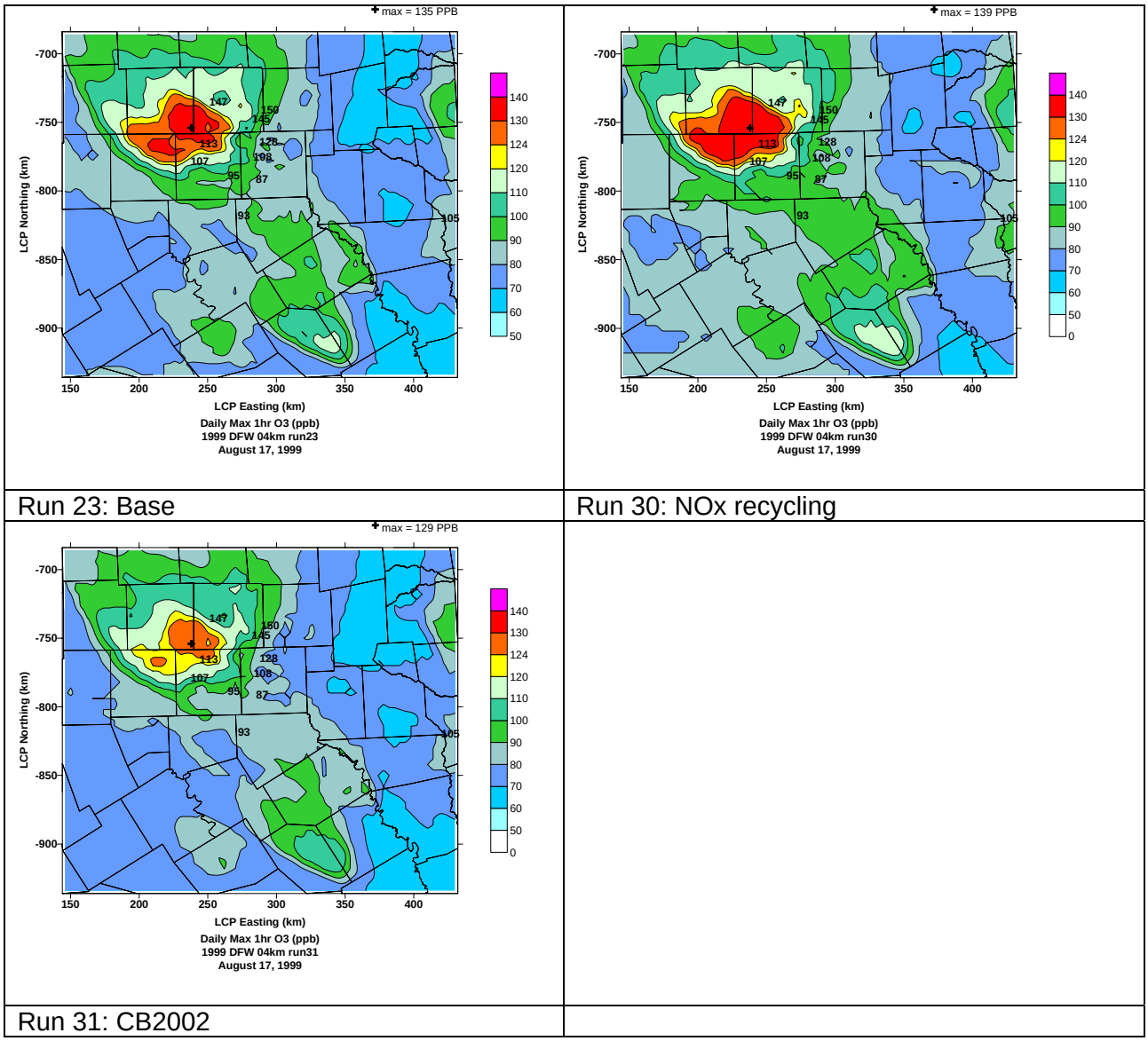


**Figure 7-7.** Spatial plots of the daily maximum 1-hour ozone in the DFW 4-km domain on August 17, 1999 from three CAMx simulations using different chemistry.

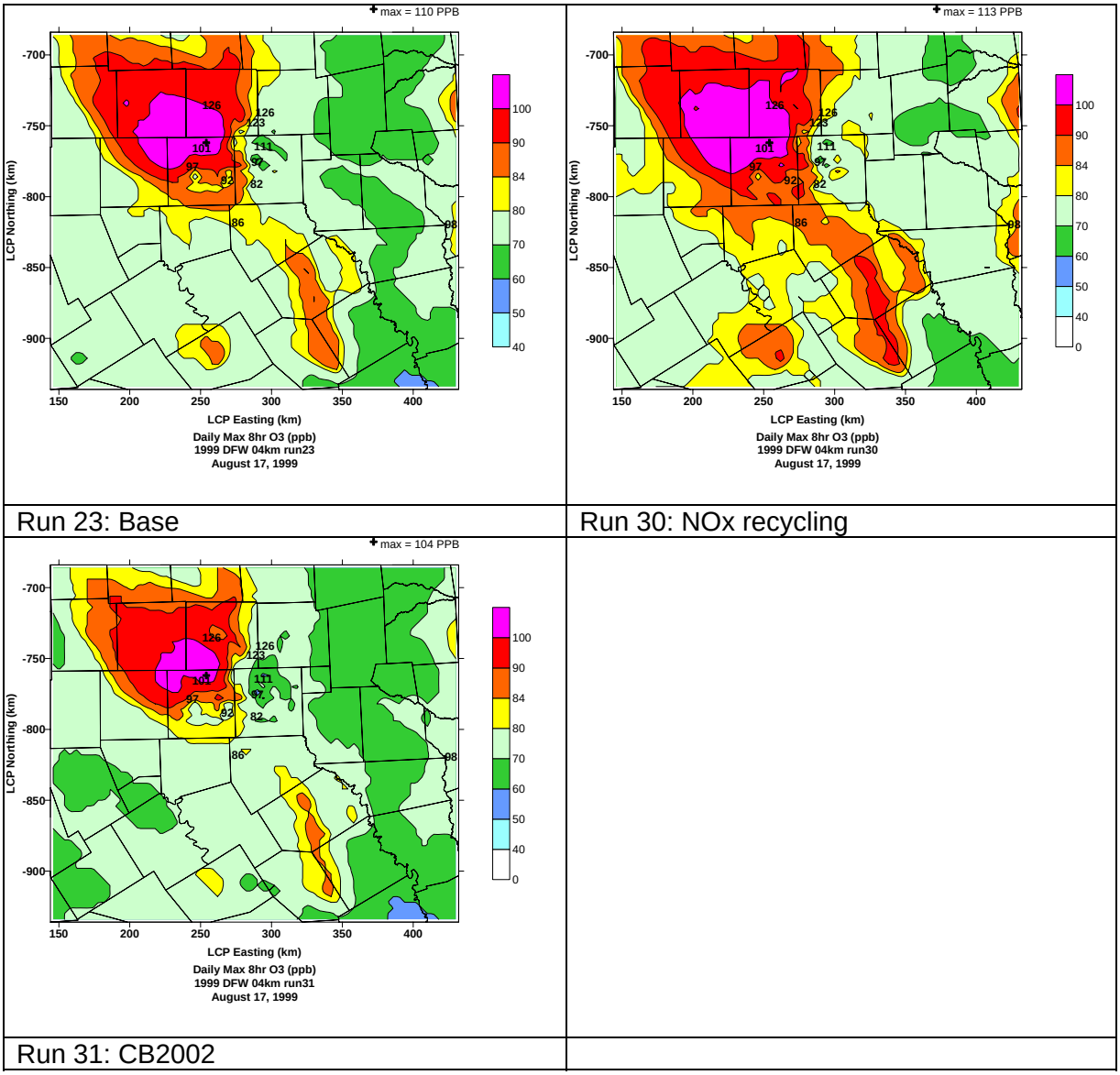


**Figure 7-8.** Spatial plots of the daily maximum 8-hour ozone in the DFW 4-km domain on August 17, 1999 from three CAMx simulations using different chemistry.

# 8. PROCESS ANALYSIS

Process Analysis (PA) can provide in-depth analyses of photochemical model performance by revealing the contributions individual physical and chemical processes within the air quality model (Jeffries and Tonnesen, 1994; ENVIRON, 2004a). Conventional model performance evaluation looks at how well model results agree with observed data – or, "how good are the model results." In contrast, PA provides information on "how the model obtained the answer it got" that can be interpreted to improve model performance and/or inform control strategy decisions.

There are several different types of PA implemented in CAMx (ENVIRON, 2004a), as discussed below. This project made use of the Chemical Process Analysis (CPA) option. CPA was used to investigate several aspects of atmospheric chemistry that are important to understanding DFW model performance and control strategy development:

- Determining geographic areas of high ozone productivity.
- Classifying geographic areas as being "VOC-limited" or "NOx-limited" with respect to ozone formation chemistry.
- Investigating the efficiency of ozone formation chemistry as measured by the "OH chain length."
- Determining the contribution of biogenic (isoprene) emissions to VOC reactivity and ozone production.

## Integrated Processes Rate (IPR) Analysis

The IPR method provides detailed process rate information for each physical process in CAMx (i.e., advection, diffusion, deposition, emissions, chemistry, etc.) for selected grid cells and selected species. The IPR outputs can be analyzed to determine what processes governed the model-predicted concentrations at any time and place. IPR information has often been plotted as a time series of process contributions for specific cells or groups of cells. IPR outputs have also been used to check the mass balance in the host model, i.e., to determine whether model concentrations are fully explained by the diagnosed process information or whether unexpected artifacts are occurring. The IPR data are relatively easy to interpret and can be analyzed using simple tools such as spreadsheets.

## Integrated Reaction Rate (IRR) Analysis

The IRR method provides detailed reaction rate information for all reactions in the chemical mechanism for selected grid cells. The IRR data can be analyzed to determine how the chemical changes occurring in the model are related to the chemical mechanism. For example, by analyzing rate information over groups of reactions it is possible to quantify chemically meaningful attributes such as radical initiation rates, radical propagation efficiencies, chain lengths, etc. Since these analyses tend to be complex, IRR data generally require post-processing to be useful.

### Chemical Process Analysis (CPA)

CPA is closely related to the IRR method but is designed to be more user friendly and accessible. As mentioned above, IRR data are generally only useful after the data have been post-processed into chemically meaningful parameters. With CPA, a selection of useful parameters is calculated within CAMx and then output to gridded files. The gridded CPA files use the same format as the gridded concentration outputs, so the same post-processing tools can be used for CPA data as for concentration data

## UPDATES TO THE CAMx CHEMICAL PROCESS ANALYSIS

This study started with an updated version of PA in CAMx version 4.03 as developed for the TCEQ by Tonnesen (2004). Tonnesen updated the CPA calculations to provide information on VOC vs. NOx sensitive ozone formation chemistry, reaction of OH radicals with different types of VOCs, radical production from olefin (alkene) reactions and the OH chain length. The list of CPA variables provided by Tonnesen's (2004) updated CAMx version is shown in Table 8-1.

**Table 8-1**. Chemical process analysis (CPA) variables calculated in CAMx for the CB4 and SAPRC99 mechanisms.

| Chemical Process Analysis (CPA) Parameters in CAMx | | Chemical Mechanism | |
|---|---|---|---|
| **Category and Description** | **Name** | **CB4** | **SAPRC99** |
| **Ox Budget** | | | |
| Ox Chemical Production | OxProd | X | X |
| Ox Chemical Destruction | OxLoss | X | X |
| VOC Sensitive Ox Prod | POx_VOC | X | |
| NOx Sensitive Ox Prod | POx_NOx | X | |
| Net O3 Production | PO3_net | X | |
| **Radical Initiation** | | | |
| New OH from O1D+H2O | newOH_O1D | X | X |
| New OH from H2O2 & HONO | newOH_radres | X | |
| New OH from O3+HC | newOH_OXwVOC | X | |
| New OH from isoprene | newOH_isop | X | |
| New OH from other sources | newOHother | | X |
| New HO2 from HCHO | nwHO2_HCHO | X | X |
| New HO2 from OLE & ETH | newHO2_OLE_ETH | X | |
| New HO2 Production (Total) | newHO2tot | X | X |
| New RO2 Production (Total) | newRO2tot | X | X |
| Total New HOx from isoprene | nHOx_isop | X | |
| **Radical Propagation** | | | |
| sum of OH+CO and OH+CH4 reactions | OHwCO_CH4 | X | X |
| OH reacted with ISOP | ISOPwOH | X | X |
| isoprene reactions with O3, NO3 and O3P | ISOPwOx | X | X |
| OH reacted with OLE | OHw_OLE | X | |
| OH reacted with ETH | OHw_ETH | X | |
| OH reacted with PAR | OHw_PAR | X | |
| OH reacted with TOL | OHw_TOL | X | |
| OH reacted with XYL | OHw_XYL | X | |
| OH reacted with total VOC | OHw_all_HC | X | X |

| Chemical Process Analysis (CPA) Parameters in CAMx | | Chemical Mechanism | |
|---|---|---|---|
| **Category and Description** | **Name** | **CB4** | **SAPRC99** |
| other OH propagation reactions | OHpropmisc | X | X |
| Total HO2 Production | HO2TotProd | X | X |
| Total RO2 Production | RO2TotProd | X | X |
| NO2 produced from reactions of HO2 | HO2_to_NO2 | X | |
| OH produced from reactions of HO2 | HO2_to_OH | X | |
| Yield of OH per HO2 | Y_OHperHO2 | X | |
| NO2 produced from reactions of RO2 | RO2_to_NO2 | X | |
| Total OH production | OH_reacted | X | X |
| OH Chain length | HOx_CL | X | |
| HOx Chain length | OH_CL | X | |
| HCHO production from isoprene | HCHOp_isop | X | X |
| HCHO production total | HCHOp_Tot | X | X |
| **Radical Termination** | | | |
| OH termination | OHterm | X | X |
| HO2 termination | HO2term | X | X |
| RO2 termination | RO2term | X | X |
| **NOx Termination (or Production)** | | | |
| OH+NO2 → HNO3 | HNO3_OHNO2 | X | X |
| NO3+HC → HNO3 | HNO3_NO3HC | X | X |
| N2O5+H2O → 2 HNO3 | HNO3_N2O5 | X | X |
| HNO3 reacted (to produce NOx) | HNO3reacte | X | |
| net PAN Prod | PANprodNet | X | X |
| net PAN Loss (source of NOx and a radical) | PANlossNet | X | X |
| HNO3 and RNO3 reacted to NO2 | NOzreact | | X |
| production of organic nitrates | RNO3_prod | X | |
| production of organic nitrates & XN | RNO3XNprod | | X |
| Radical Concentrations | | | |
| OH radical concentration | OH | X | X |
| HO2 radical concentration | HO2 | X | X |
| NO3 radical concentration | NO3 | X | X |
| N2O5 concentration | N2O5 | X | X |
| **Total Number of CPA Variables** | | **49** | **31** |

Two further updates were implemented for CPA in this study:

1. The calculation of CPA variables for the CB4 mechanism was reviewed and the calculations were updated to account for the 17 new inorganic reactions added to the CB4xi mechanism (referred to as the "NOx recycling" reactions).

2. A post-processor (VERTAVG) was developed to average CPA variables over multiple layers contained within the depth of the planetary boundary layer (PBL).

The second modification (vertical averaging) was implemented to provide CPA information that represents the full depth of the PBL. The PBL depth varies in space and time according to the strength and vertical extent of turbulent mixing. Turbulent mixing is specified for CAMx by Kv fields calculated from MM5 output data. The VERTAVG processor reads CAMx input files for

Kv, layer height, temperature and pressure and then calculates the PBL depth for each grid column at each hour. VERTAVG also reads the CAMx 3-D output file of CPA (or concentration) variables and calculates PBL average CPA variables for each grid column at each hour.

## SCENARIOS SELECTED FOR PROCESS ANALYSIS

CAMx sensitivity simulations Runs 20 – 31were reviewed by ENVIRON, TCEQ and HARC and three scenarios were selected for investigation using CPA. A TCEQ sensitivity test that investigated sensitivity to alternate vertical mixing (Kv) assumptions also was considered. The three scenarios selected for CPA analysis are listed in Table 8-2. The runs were designed as follows:

- The expanded modeling domain with 14-km model top was used in all cases to minimize the impacts of boundary condition assumptions.
- The CB4xi chemical mechanism with NOx recycling reactions was used in all cases.
- Initial conditions were moderate below 1700 m and clean aloft in all cases.
- Boundary conditions were moderate in the north, west, and southwest below 1700 m and clean aloft in all cases.
- The TCEQ's Kv3 vertical mixing assumption with MM5 Run 5 (Pleim-Xiu PBL scheme) was evaluated in Run 33.
- The Noah/Eta PBL scheme (MM5 Run 6) with Kv100 vertical mixing assumption was evaluated in Run 34.
- A reduction in NOx emission levels in the DFW core area obtained by reducing onroad and offroad mobile source NOx in the 4 core DFW counties by 30% was evaluated in Run 35.

**Table 8-2**. CAMx scenarios selected for process analysis using CPA.

| Scenario | Domain | Chemistry | MM5/Kv | Emissions |
|---|---|---|---|---|
| Run 33 | Expanded domain with 14-km top | CB4xi (NOx recycling) | Run 5 (P-X PBL)/ Kv3 | TCEQ base |
| Run 34 | Expanded domain with 14-km top | CB4xi (NOx recycling) | Run 6 (Eta PBL)/ Kv100 | TCEQ base |
| Run 35 | Expanded domain with 14-km top | CB4xi (NOx recycling) | Run 6 (Eta PBL)/ Kv100 | 30% less mobile NOx in DFW |

The "Kv100" vertical mixing assumption sets the Kv at each layer interface below 100 m to the maximum Kv below 100 m, in each grid column at each hour. This assumption creates stronger vertical mixing near the surface during convective periods and makes vertical mixing more competitive against chemical reaction for highly reactive species emitted at the surface (e.g., NO and isoprene). The Kv100 vertical mixing assumption is expected to reduce the magnitude of "ozone holes" of the Dallas urban core caused by intense surface NO emissions titrating ozone transported into the urban core. The Kv100 assumption is expected to have less impact on

suppressed ozone formation immediately downwind of the Dallas urban core resulting from intense NO emissions in the Dallas core.

The "Kv3" assumption tested by TCEQ combined the Kv100 assumption with a cap on PBL depth derived from Dallas profiler data. The PBL cap varied by day and was applied across the entire DFW 4-km grid. The PBL cap tended to reduce maximum PBL depths, especially on August 17$^{th}$.

## MODEL PERFORMANCE EVALUATION

Model performance for Runs 33-35 was compared to Run 23 to provide a link to the earlier sensitivity tests. A set of model performance plots is shown in Figures 8-1 to 8-8. Time series of 1-hour ozone from the four runs are in Figure 8-1. Daily statistics for the 4-km domain are shown in Figures 8-2 and 8-3 for 1-hour and 8-hour ozone, respectively. Scatter plots of the highest daily maximum 1-hour and 8-hour ozone near each monitor are displayed in Figure 8-4 and 8-5, respectively. Spatial plots of the daily maximum 1-hour ozone on August 17, 1999 for the 12-km and 4-km domains are displayed in Figure 8-6 and 8-7, respectively. Spatial plots of the daily maximum 8-hour ozone are displayed in Figure 8-8 for the 4-km domain.

### Run 33: P-X PBL, Kv3

Run 33 was based on the same meteorological input data as Run 23 (MM5 Run 5) but differed in having the TCEQ Kv3 vertical mixing assumption in the 4-km grid and using the CB4xi chemical mechanism with "NOx recycling" reactions. Statistics for 1-hour and 8-hour ozone normalized bias, and normalized errors were improved in Run 33 compared to Run 23 on almost all days (Figures 8-2 and 8-3). However, the unpaired peak accuracy was worse for Run 33 than 23 on many days because Run 33 had a tendency to over predict the maximum observed ozone levels. Positive unpaired peak accuracy is still more desirable than negative, since this statistic is one-sided as the observed peak is based on a limited number of monitoring stations. Scatter plots showed lower coefficients of determination ($R^2$) for Run 33 compared to Run 23 for both daily maximum 1-hour and 8-hour ozone (Figures 8-4 and 8-5). The $R^2$ was degraded because ozone levels were over predicted in Run 33.

Comparing the 4-km grid daily maximum ozone plots for August 17$^{th}$ (Figures 8-7 and 8-8) shows that Run 33 had higher ozone levels in the DFW area than Run 23. Comparing the 12-km grid daily maximum ozone plots for August 17$^{th}$ (Figure 8-6) shows that ozone increases were greater in the DFW area than elsewhere. The moderate increase in maximum ozone levels outside the DFW area are due to the NOx recycling reactions whereas the larger ozone increases in the DFW area are due to the Kv3 mixing assumption, added to the NOx recycling reactions.

### Run 34: Noah/Eta PBL, Kv100

Run 34 was based on different meteorological data than Runs 33 and 23. The meteorological data was extracted from MM5 Run 6, which used the Eta PBL scheme with the Noah land surface model. Section 2 showed that MM5 Run 6 yielded better performance statistics compared to MM5 Run 5, which was based on Pleim-Xiu PBL. Statistics for 1-hour and 8-hour

ozone normalized bias, and normalized errors were similar between Run 33 and 34 (Figures 8-2 and 8-3) but the unpaired peak accuracy was better for Run 34 than 33 because Run 34 avoided the tendency to over predict maximum ozone levels exhibited by Run 33. Scatter plots showed higher coefficients of determination ($R^2$) for Run 34 than Runs 23 and 33 for daily maximum 1-hour ozone (Figures 8-4). Run 23 had a better $R^2$ for daily maximum 8-hour ozone (Figures 8-5). Overall, Run 34 model performance is superior to both Runs 33 and 23.

Comparing the 12-km grid daily maximum ozone plots for August 17$^{th}$ (Figure 8-6) shows that Run 34 produced higher maximum ozone levels than Run 33 in areas of high ozone outside of DFW. This did not appear to cause higher ozone transport into the DFW area on August 17$^{th}$ judging from the 4-km grid daily maximum ozone plots shown in Figures 8-7 and 8-8. These figures also placed the modeled peak more eastward in Run 34 compared to Run 33, which is more in line with the ozone observations. It appears that the differences in DFW model performance between Runs 34 and 33 are mainly attributable to differences in the meteorological fields for the DFW area.

**Run 35: Less NOx in DFW**

Run 35 was the same as Run 34 except that mobile source NOx emissions were decreased by 30% in the four core DFW counties. This run was performed to better understand ozone sensitivity to changes in emissions, and by no means suggests that adjustments should be made to the mobile source inventory. Comparing the 12-km grid daily maximum 1-hour ozone for August 17$^{th}$ (Figure 8-6) shows that Runs 35 and 34 were essentially identical outside of the DFW area, as expected. In the DFW area, reducing surface NOx emissions in Run 35 increased the maximum 1-hr ozone levels immediately downwind of the DFW area on August 17$^{th}$ (Figure 8-7) because, on this day, DFW ozone formation was VOC-limited in Run 34. Under these conditions, the NOx reductions in Run 35 resulted in fewer scavengers, and more ozone. The time series plots (Figure 8-1) show only small differences between Runs 35 and 34. Decreasing DFW mobile NOx emissions either raised or lowered maximum ozone levels depending upon monitor location and day. Statistics for 1-hour and 8-hour unpaired peak accuracy, normalized bias, and normalized errors were somewhat improved in Run 35 compared to Run 34, but there wasn't consistent improvement on all days (Figures 8-2 and 8-3). Reducing DFW NOx emissions helped model performance less in Run 34 than it did in Run 23 (discussed in Section 6) due to differences in the meteorological input data.

Scatter plots showed higher coefficients of determination ($R^2$) for Run 35 compared to Run 34 for both daily maximum 1-hour and 8-hour ozone (Figures 8-4 and 8-5). The $R^2$ improved because high ozone levels were better predicted with reduced DFW NOx emission levels. This results from the tendency for high surface NOx emissions in the DFW core to suppress modeled ozone formation immediately downwind of the urban area in areas where high ozone levels were monitored during this episode. Similar differences were seen when DFW NOx emissions were reduced between Runs 23 and 26, as discussed in Section 6.

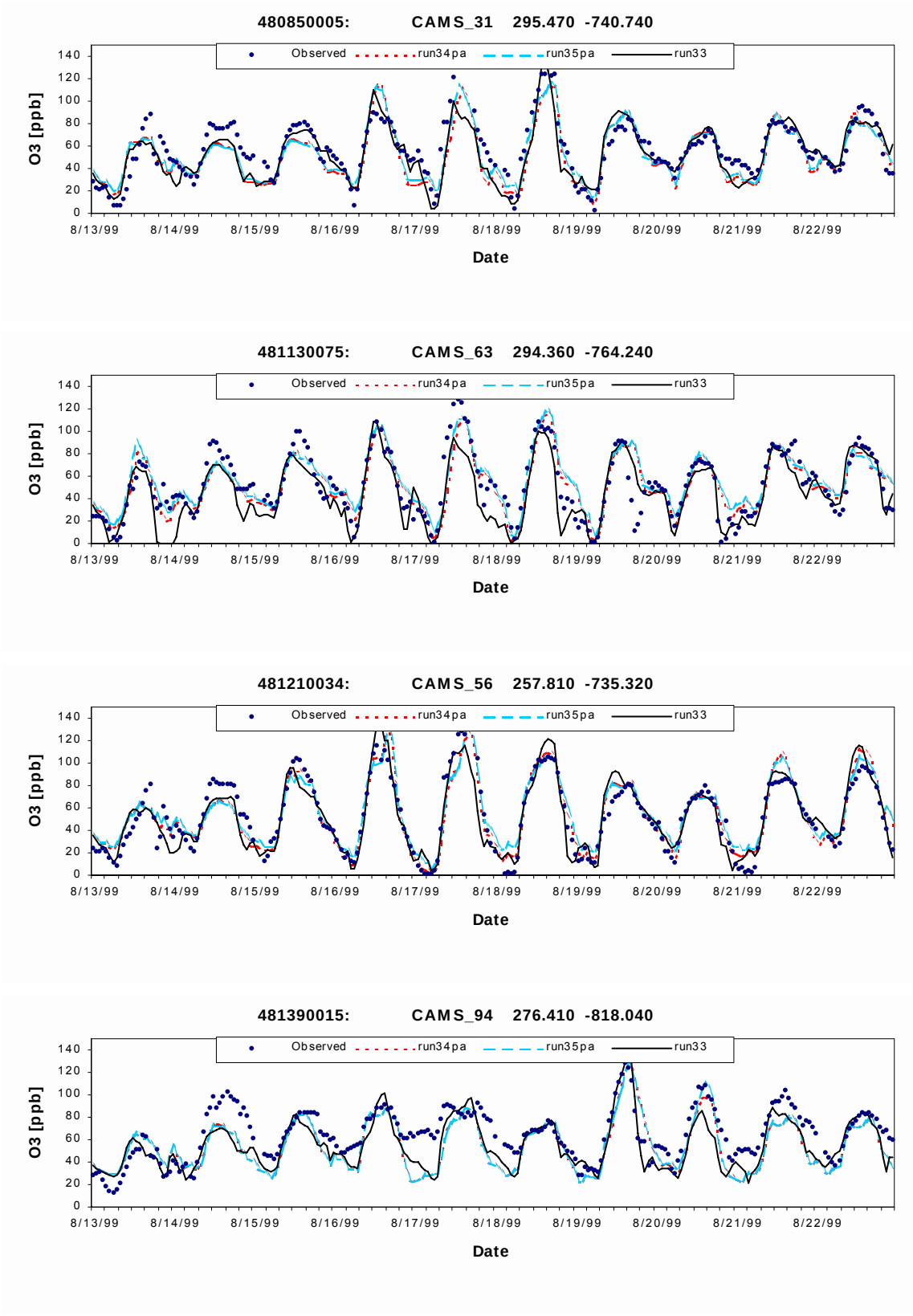


**Figure 8-1**. Time series of 1-hour ozone at sites inside the DFW 4-km domain for Runs 33, 34 and 35.

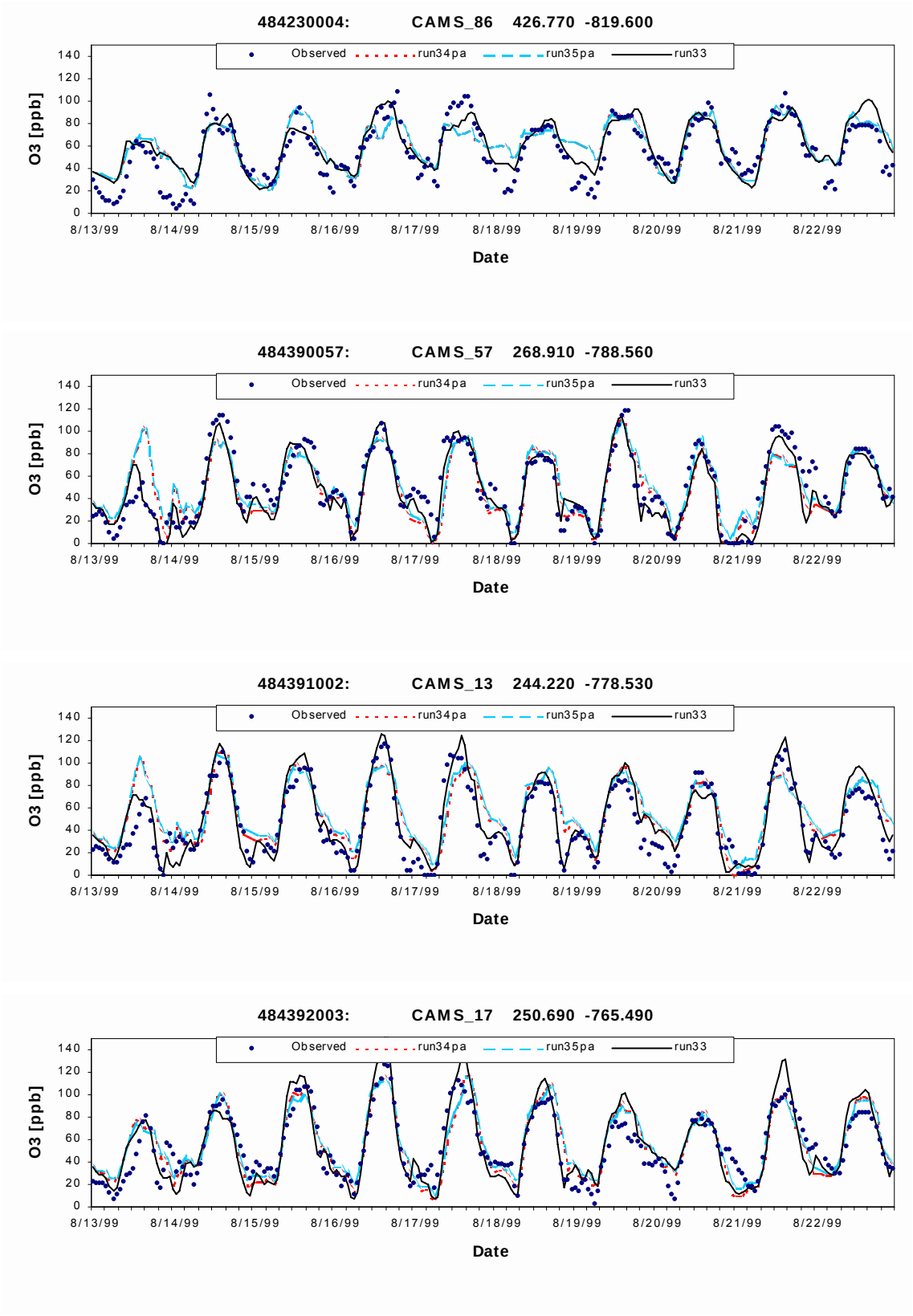


**Figure 8-1**. (Cont.) Time series of 1-hour ozone at sites inside the DFW 4-km domain for Runs 33, 34 and 35.

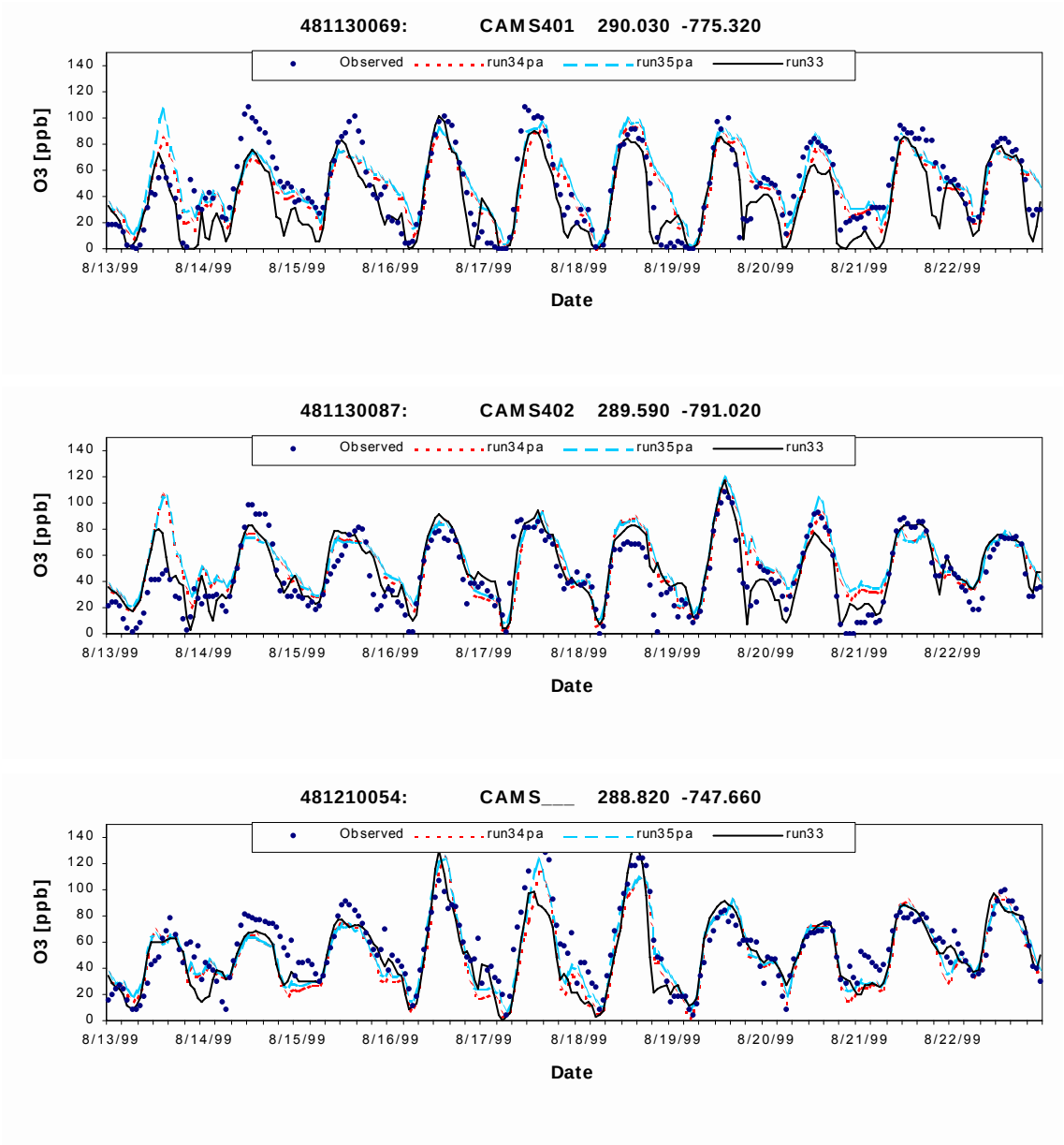


**Figure 8-1**. (Concl.) Time series of 1-hour ozone at sites inside the DFW 4-km domain for Runs 33, 34 and 35.

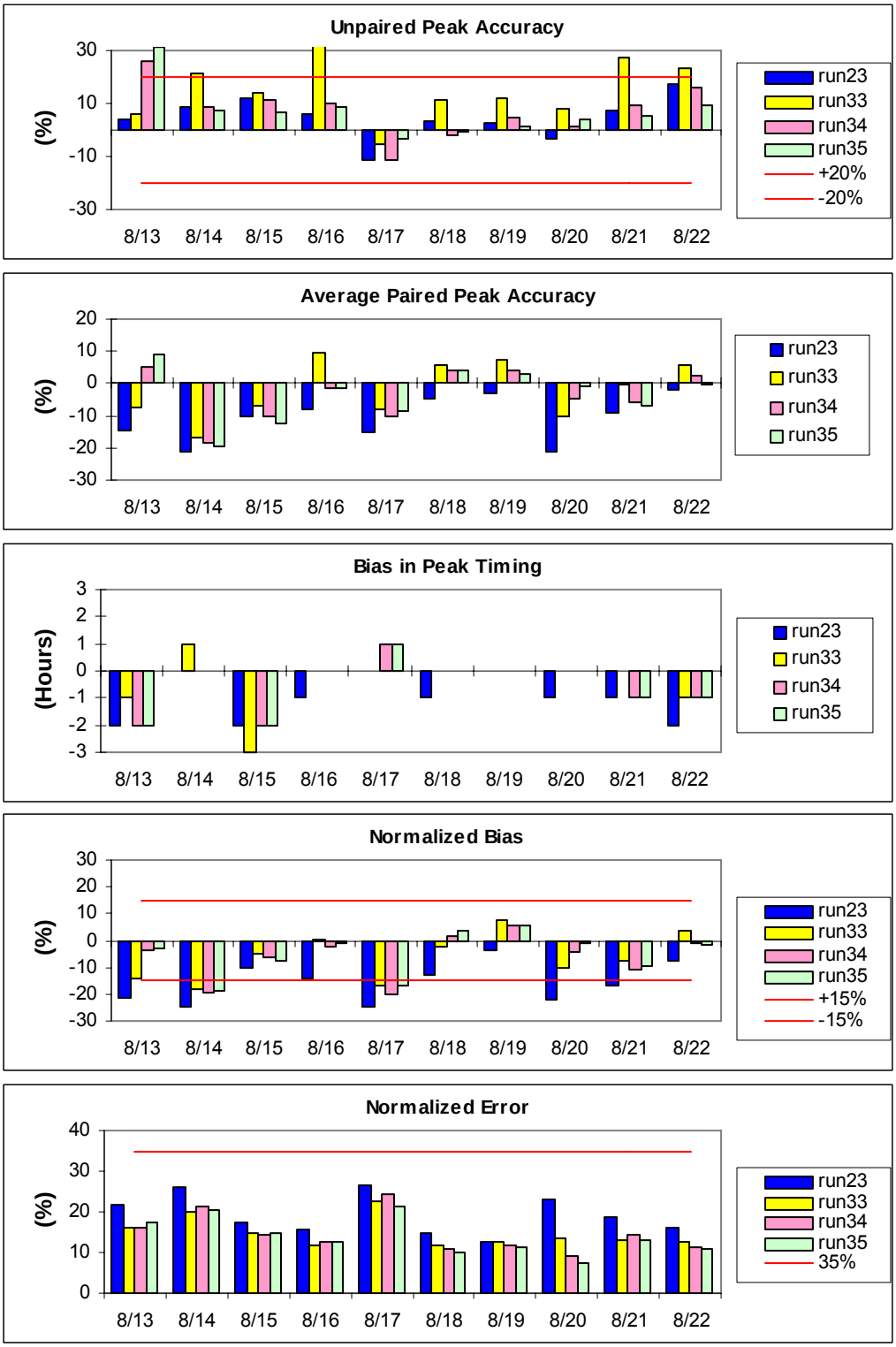


**Figure 8-2.** Daily statistics of the 1999 DFW 1-hour ozone in the 4-km domain for CAMx runs 23, 33, 34 and 35.

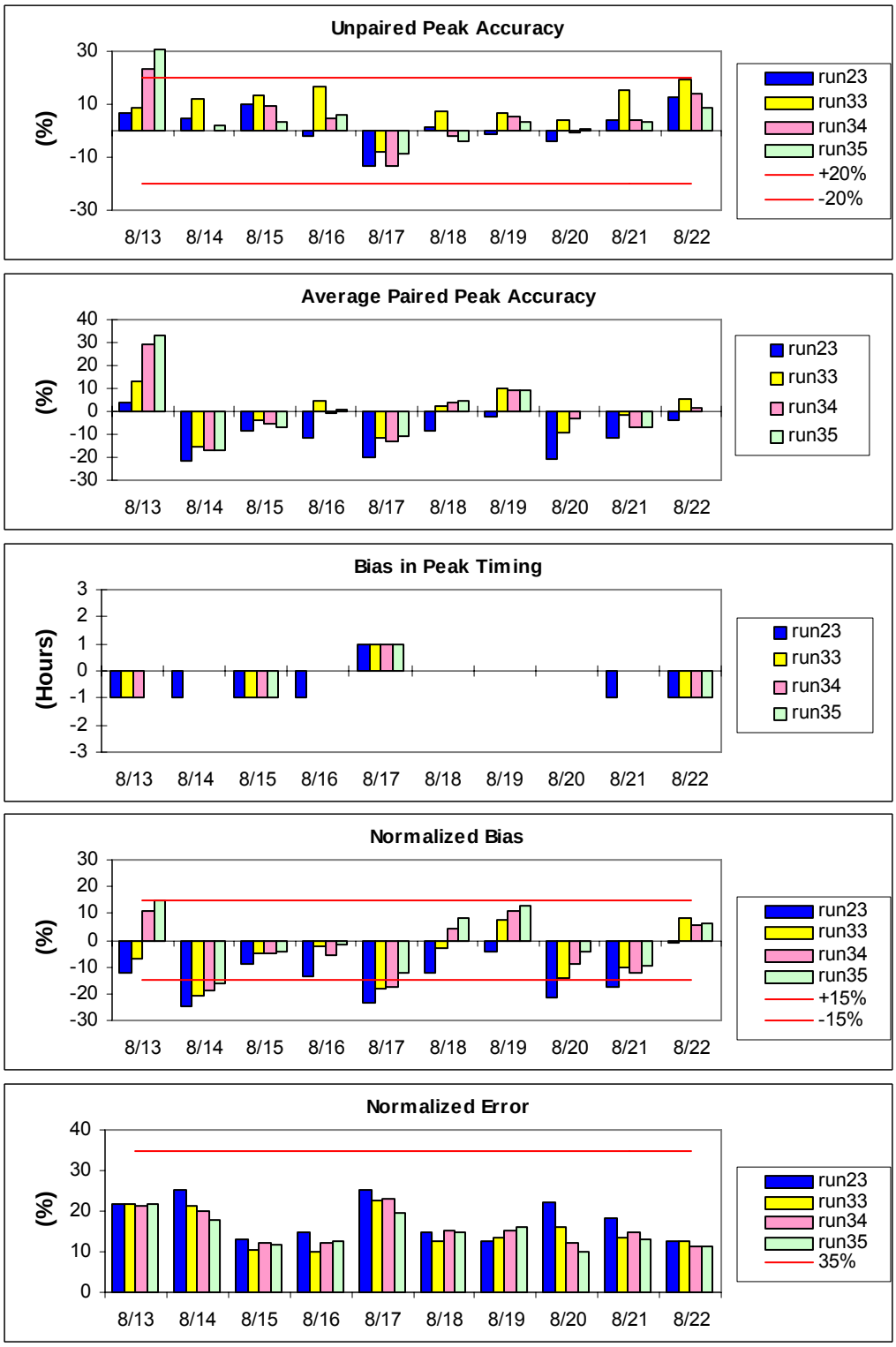


**Figure 8-3.** Daily statistics of the 1999 DFW 8-hour ozone in the 4-km domain for CAMx runs 23, 33, 34 and 35.

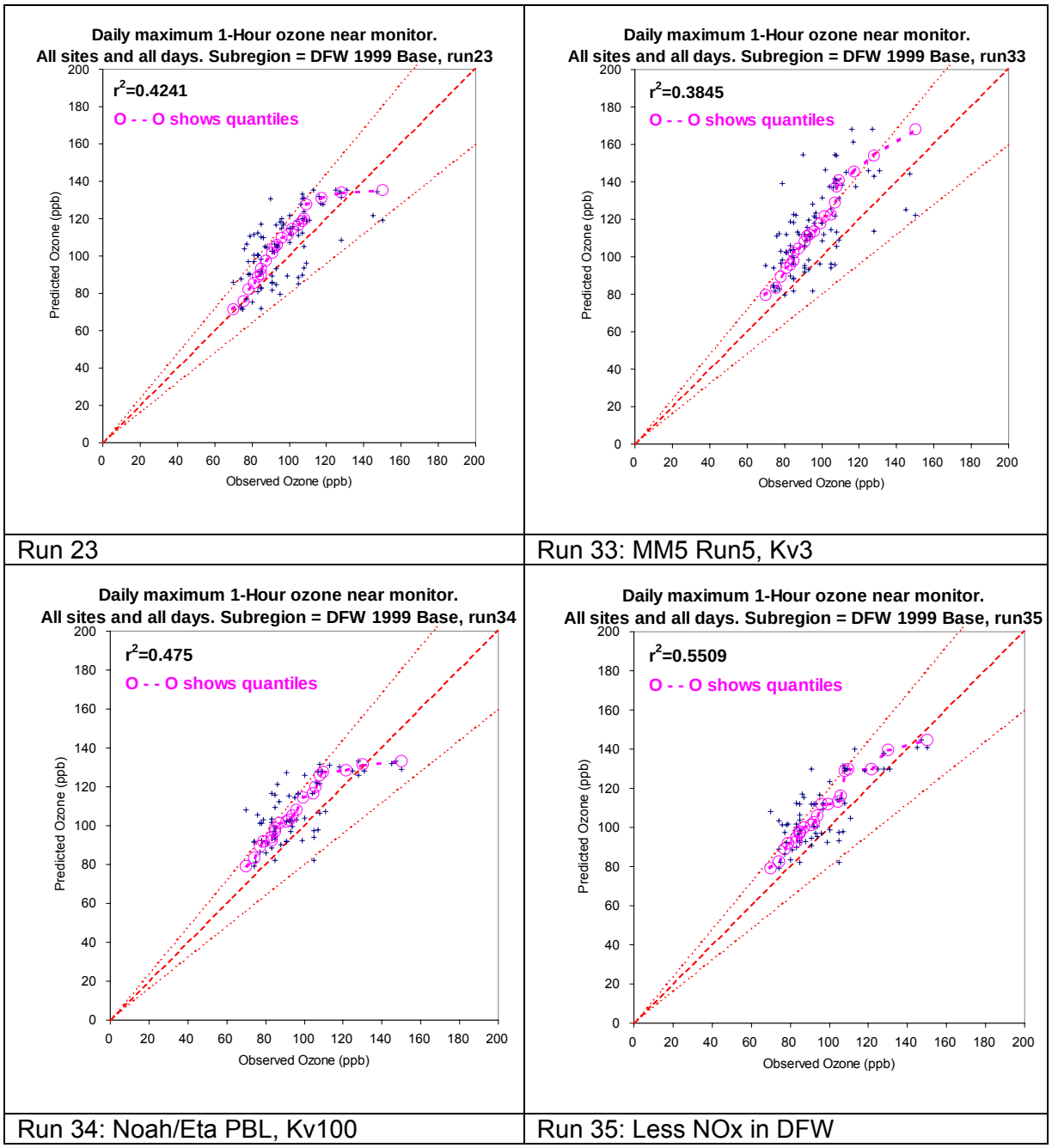


**Figure 8-4.** Scatter and quantile-quantile plots of the largest predicted daily maximum 1-hour ozone near each monitor (within 9x9 cell area) and the observed daily maximum 1-hour ozone for Runs 23, 33, 34 and 35.

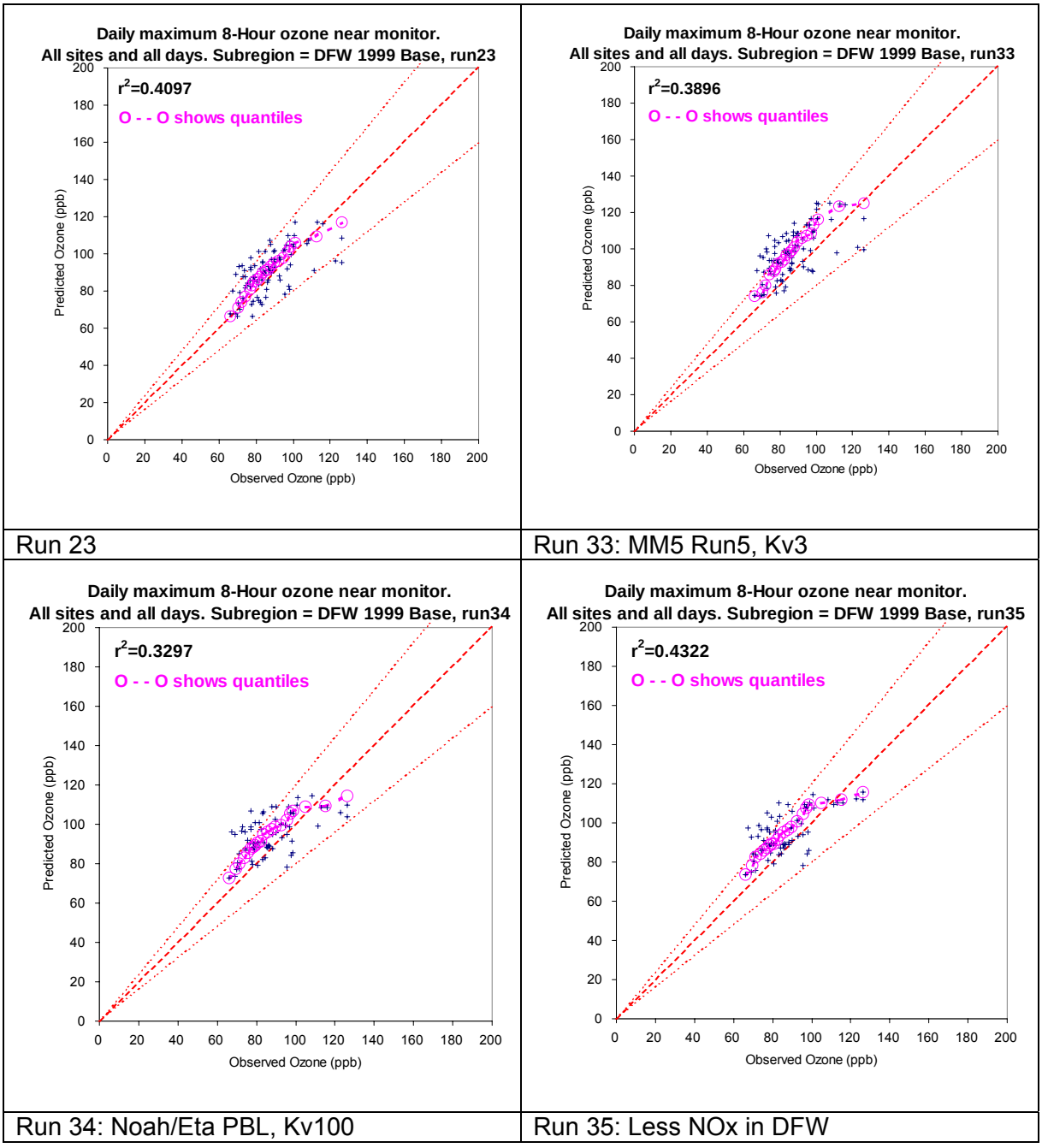


**Figure 8-5**. Scatter and quantile-quantile plots of the largest predicted daily maximum 8-hour ozone near each monitor (within 9x9 cell area) and the observed daily maximum 8-hour ozone for Runs 23, 33, 34 and 35.

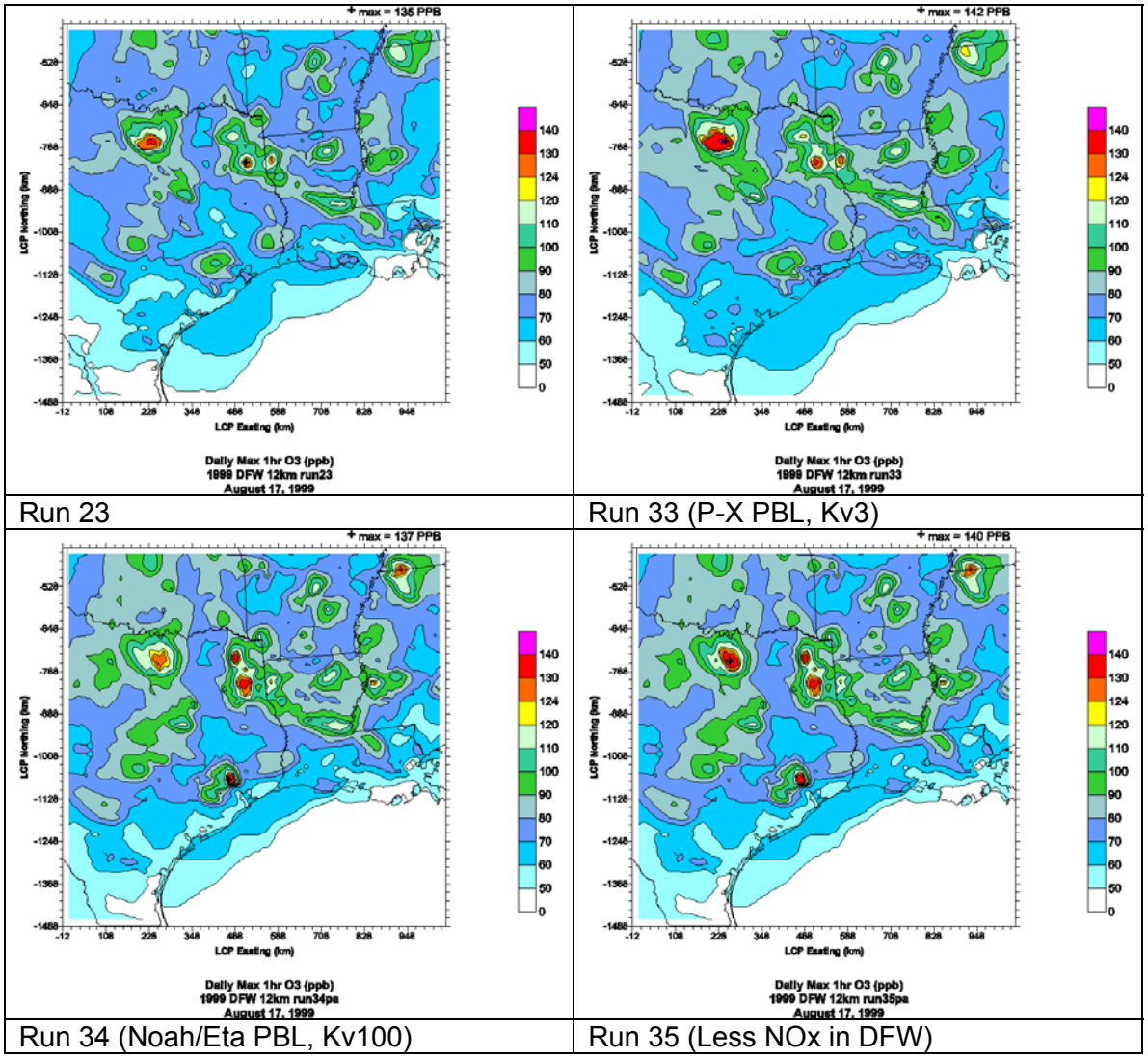


**Figure 8-6**. Spatial plots of the daily maximum 1-hour ozone in the 12-km domain on August 17, 1999 from Runs 23, 33, 34 and 35.

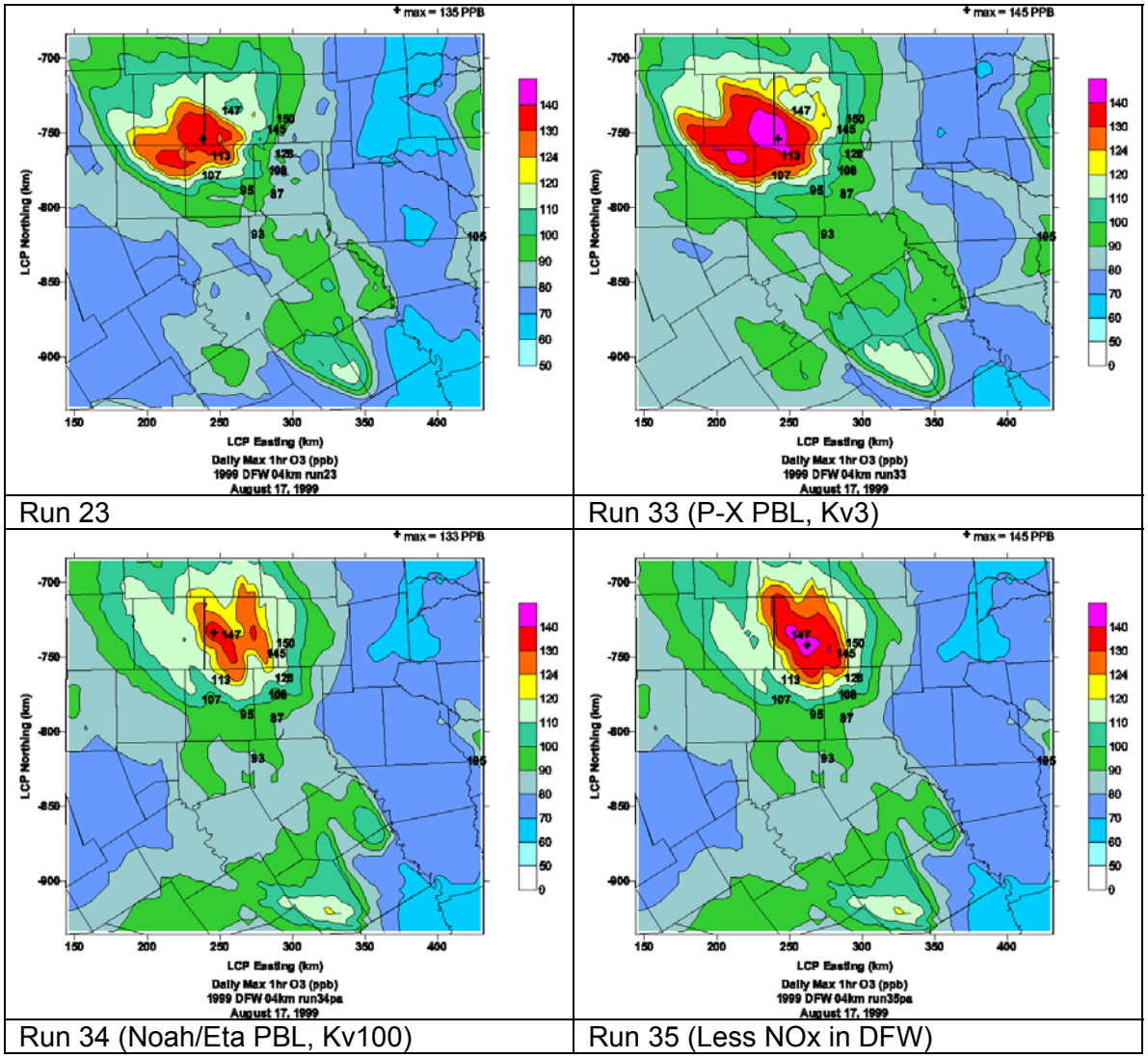


**Figure 8-7**. Spatial plots of the daily maximum 1-hour ozone in the DFW 4-km domain on August 17, 1999 from Runs 23, 33, 34 and 35.

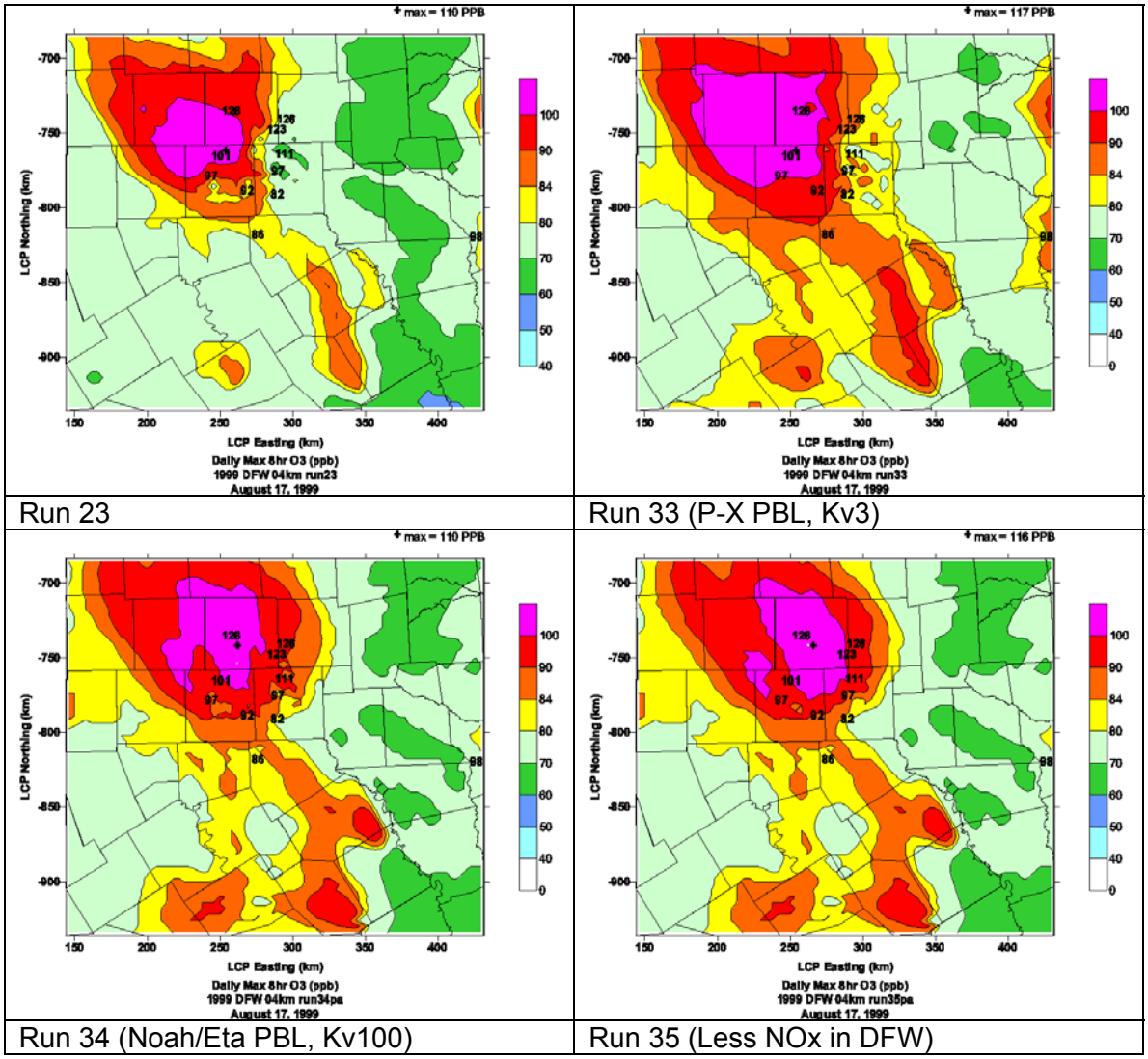


**Figure 8-8**. Spatial plots of the daily maximum 8-hour ozone in the DFW 4-km domain on August 17, 1999 from Runs 23, 33, 34 and 35.

## ANALYSIS OF CPA RESULTS

Representative CPA results are displayed in Figures 8-9 to 8-17 for 13:00 on August 17, 19 and 21 of 1999. Each figure shows 6 different parameters averaged over the PBL depth and a legend key is given in Table 8-3. CPA concepts underlying these figures are:

- Ox Production. This parameter is used as a proxy for ozone production. Ox production is the sum of ozone produced and NO converted to $NO_2$.
- VOC and NOx-limited conditions are distinguished by using the ratio of production of $H_2O_2$ and $HNO_3$ as an indicator, as in the OSAT and APCA ozone source apportionment methods (ENVIRON, 2004a). CPA chooses an indicator cut-point ratio of 0.15 rather than 0.35 (Tonnesen, 2004) and the impact of this choice is shown below.
- The OH chain length represents the number of times, on average, that an OH radical cycles back to OH through radical propagation reactions. Longer OH chain lengths indicate that conditions are right for efficient oxidant chemistry.

**Table 8-3**. Key to CPA figure legends.

| Figure Legend | Meaning |
|---|---|
| PBL avg O3 | Hourly ozone concentration (ppb) averaged over the PBL depth |
| PBL avg OxProd | Hourly Ox production (ppb/hr) averaged over the PBL depth |
| PBL avg POx_VOCsns | Hourly Ox production under VOC-limited conditions averaged over the PBL depth |
| PBL avg POx_NOxsns | Hourly Ox production under NOx-limited conditions averaged over the PBL depth |
| PBL ISOPwOH/(OHw_all_HC) | OH reacting with isoprene as a fraction of OH reacting with all hydrocarbons for the hour shown |
| PBL avg OH_CL | OH chain length for the hour shown |

The PBL average ozone concentration may be larger or smaller than the surface ozone concentration due to vertical gradients in ozone concentration. The PBL average ozone concentration is included in Figures 8-9 to 8-17 to provide an appropriate context for the CPA variables. However, a key difference between the ozone concentration and the CPA variables is that ozone is advected (transported) by CAMx whereas the CPA variables are not advected. The static nature of the CPA variables provides a snapshot picture of the oxidant chemistry at the time of each Figure (8-9 to 8-17).

A time of 13:00 was chosen for Figures 8-9 to 8-17 because this near the time of the maximum rate of ozone production that strongly influences the maximum ozone concentration that occurs later in the day.

### Run 33: P-X PBL with Kv3

The PBL average ozone for Run 33 (top left in Figures 8-9 to 8-11) shows elevated hourly ozone downwind of Dallas, Fort Worth and other high emission areas on each day. The orientations of ozone plumes vary between days according to wind directions. The PBL averaged ozone shows

less tendency toward an "ozone hole" over the Dallas core than the surface ozone (shown previously). This is because "ozone holes" over the Dallas core are caused by intense surface NOx emissions that most strongly affect the surface layer in CAMx and therefore have less impact on PBL average ozone levels.

The hourly Ox production for Run 33 (top right in Figures 8-9 to 8-11) shows hot spots over urban areas and major NOx point sources in rural areas. The same hot spots tend to appear on each day shown but the magnitudes of Ox production vary from day-to-day due to differences in meteorology and/or emissions. The peak Ox production levels exceed 36 ppb/hr through the PBL depth on each day.

The hourly Ox production is classified between VOC- and NOx-limited areas (at the hour shown) in the middle row of Figure 8-9 to 8-11. The areas of most intense Ox production tend to be VOC-limited on all days but there are clear differences in the extent of VOC- and NOx-limited Ox production between days, with August 17$^{th}$ being the most extensively VOC-limited day. The regions that tend to be VOC-limited are the Dallas, Fort Worth and Waco urban areas, and the immediate vicinity of the Big Brown and Limestone EGUs in Freestone and Limestone counties, respectively, whose plumes appear to be heading towards the DFW region on this date.

These CPA analyses are useful for qualitatively understanding areas of VOC- and NOx-limited ozone formation, and are consistent with previous emission sensitivity analyses and ozone source apportionment results, but the CPA results should not be used to make quantitative estimates of the relative benefits of reducing VOC vs. NOx emissions.

The fraction of OH reacting with isoprene (relative to all hydrocarbons) shows the areas where biogenic emissions have high importance: the eastern part and northwest corners of the 4-km grid (Figure 8-9 to 8-11, bottom left). Comparing the bottom left and top panels shows that a high contribution of biogenic isoprene does not necessarily equate to high ozone (Ox) production because NOx from anthropogenic sources also is required for ozone production.

An area of low "OH reacting with isoprene" runs from south to north (Waco to DFW) along IH-35 in Figures 8-9 to 8-11. The relatively low importance of isoprene in these areas is due to differences in land cover (i.e., agricultural and urban areas) and low biogenic emission levels likely contribute to the DFW and Waco urban areas tending to be VOC limited. This suggests that uncertainty in biogenic emissions agricultural and urban areas could influence the sensitivity of ozone to reductions in VOC vs. NOx emissions. Evaluating biogenic emission inventories in these areas where the current biogenic emission inventory has relatively low emission rates should be a higher priority for DFW ozone than forested areas.

The OH chain length analysis shown at bottom right in Figures 8-9 to 8-11 has similar spatial patterns to the Ox production shown at top right.

**Run 34: Noah/Eta PBL**

The CPA analysis of Run 34 has many features in common with Run 33 and so Run 34 is discussed relative to Run 33. The difference in CAMx configuration between Runs 33 and 34 was a change in the meteorological input data from MM5 Run 5 (for Run 33) to MM5 Run 6 (for Run 34).

The PBL average ozone for Run 34 (top left in Figures 8-12 to 8-14) shows differences in spatial distribution from Run 33 reflecting differences between two MM5 meteorological realizations. In contrast, the PBL average Ox production (top right in Figures 8-12 to 8-14) shows more spatial similarity between Runs 33 and 34 because the Ox production plot is an hourly snapshot that is not advected. This confirms that areas of high Ox production are closely related to the emission inventory, specifically areas of high anthropogenic ozone precursor emissions in urban areas and near major sources.

The classification of Run 34 Ox production to VOC- and NOx-limited areas (middle row of Figure 8-12 to 8-14) also has strong similarities with Run 33. The areas of most intense Ox production tend to be VOC-limited, namely the Dallas, Fort Worth and Waco urban areas and the immediate vicinity of the Big Brown and Limestone EGUs. August 17$^{th}$ is the most extensively VOC-limited day for Run 34 as well as Run 33 showing that this day was the most stagnant in MM5 Runs 5 and 6. The Dallas core area appears to be more strongly VOC-limited on August 17$^{th}$ in Run 34 than Run 33 whereas on other days differences are less clear.

The fraction of OH reacting with isoprene and OH chain length (bottom of Figures 8-12 to 8-14) are similar between Runs 33 and 34 and the comments for Run 33, above, apply to Run 34.

**Run 35: Less NOx in DFW**

Runs 35 differed from Run 34 in having lower NOx emissions due to a 30% cut in onroad and offroad mobile source NOx in the 4 core DFW counties. The CPA analysis of Run 35 has features in common with both Runs 34 and 33.

Reducing NOx emissions in the DFW area reduced PBL average ozone downwind of DFW (top left in Figures 8-15 to 8-17) in Run 35 relative to Run 34. A similar difference is apparent in the PBL average Ox production (top right in Figures 8-15 to 8-17), which is lower in Run 35 than Run 34 over the DFW area. Reduction in ozone concentrations extend further downwind than Ox production because ozone concentrations are transported further downwind than the NOx emissions that cause ozone production.

The classification of Run 35 Ox production to VOC- and NOx-limited areas (middle row of Figure 8-15 to 8-17) shows differences from Run 34 in the DFW area where NOx emissions were reduced. The areas of VOC-limited Ox production are smaller in extent in Run 35 than Run 34 showing a shift toward NOx-limited Ox production as NOx is reduced in the DFW urban core. The differences are most pronounced on August 19$^{th}$ and 21$^{st}$ where VOC-limited areas almost completely disappear from the DFW core area in Run 35 at 13:00. Areas with VOC-limited Ox production remain in Run 35 on August 17$^{th}$ because the meteorology is more stagnant on August 17$^{th}$ than the later days, due to the combination of low wind speeds and low mixing heights.

The fraction of OH reacting with isoprene and OH chain length (bottom of Figures 8-13 to 8-17) are similar between Runs 35 and 34 and the comments for Run 33, above, apply to Run 35.

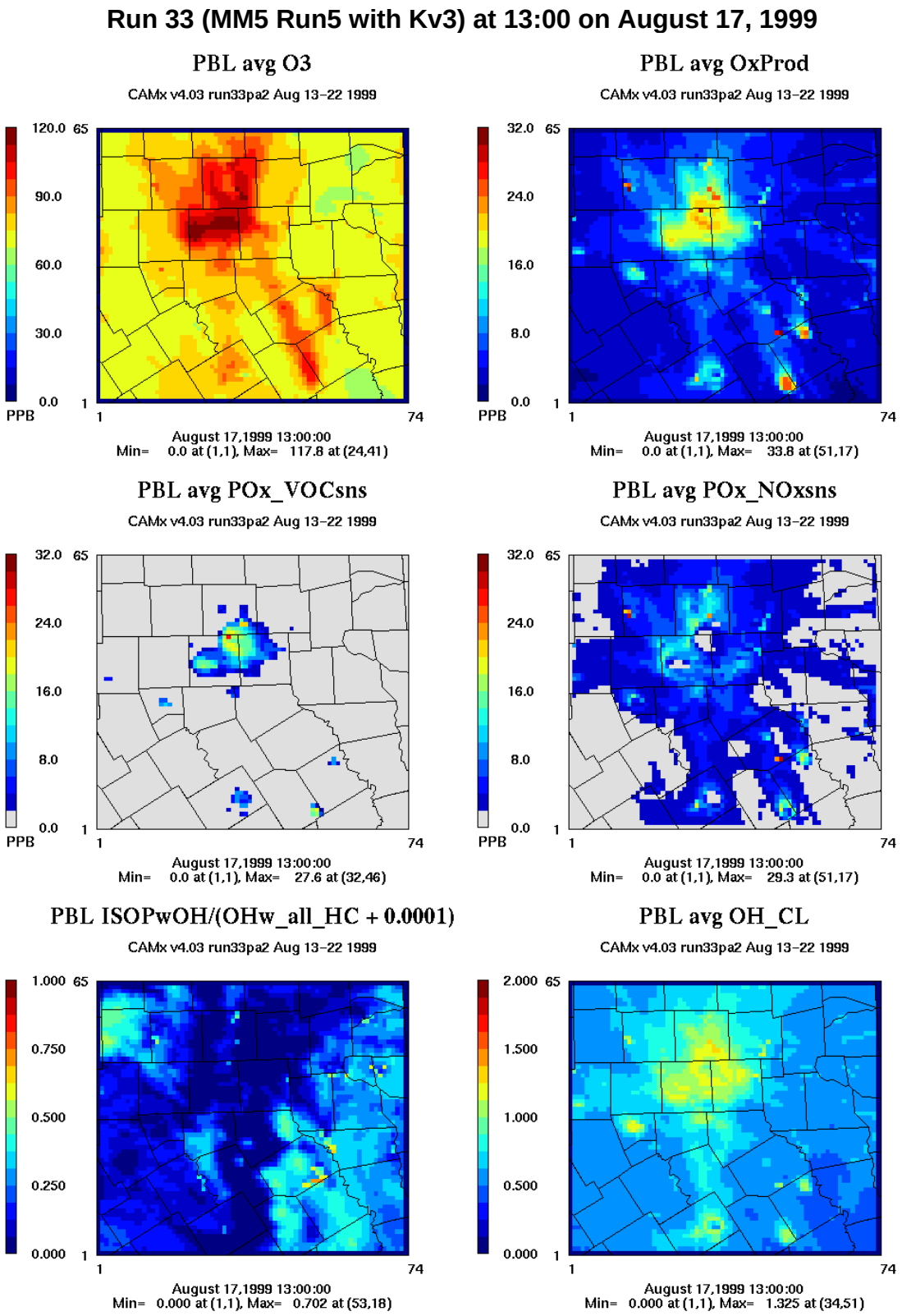


**Figure 8-9**. CAMx chemical process analysis results averaged over the PBL depth for Run 33 at 13:00 on August 17, 1999.

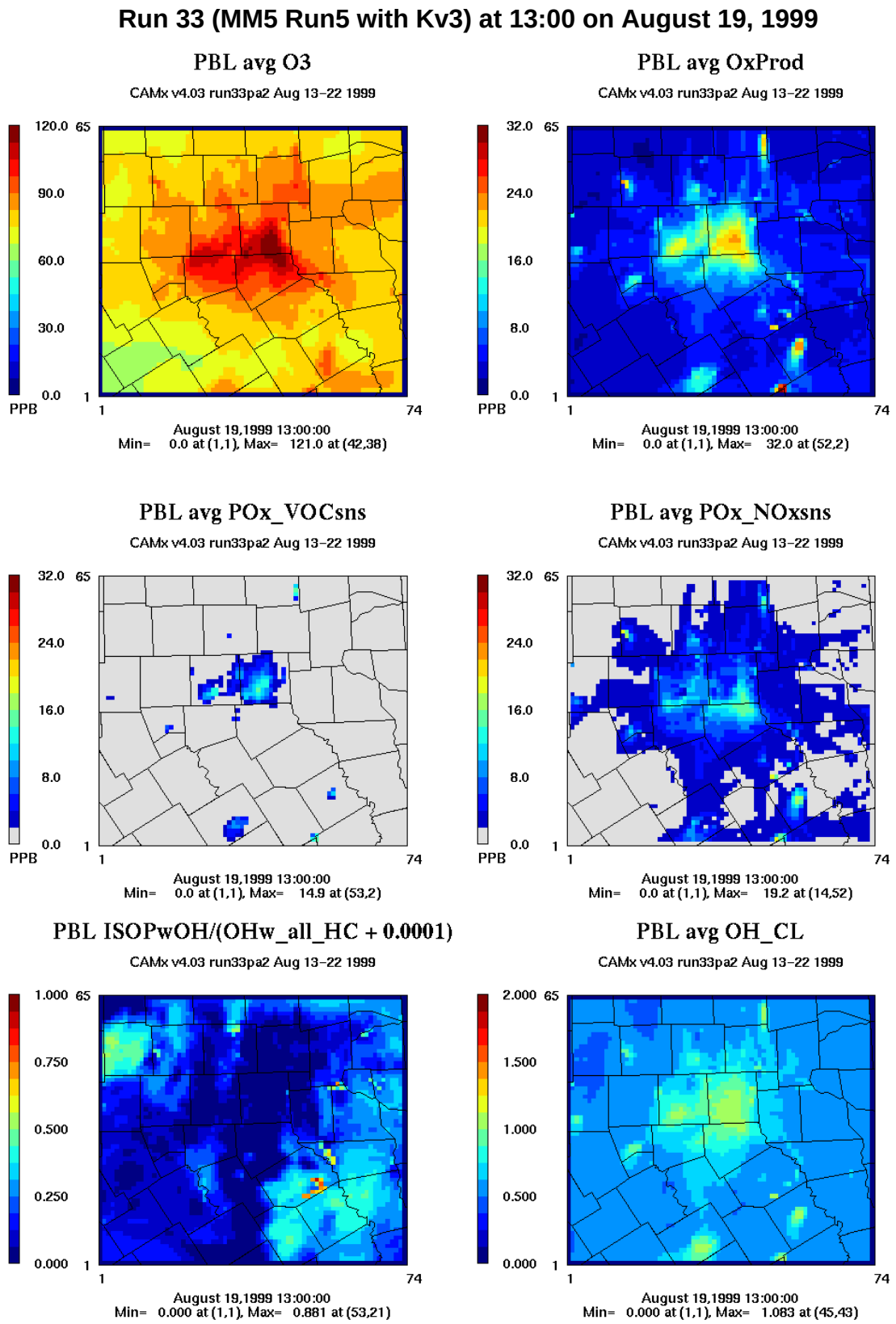


**Figure 8-10**. CAMx chemical process analysis results averaged over the PBL depth for the DFW 4-km grid in Run 33 at 13:00 on August 19, 1999.

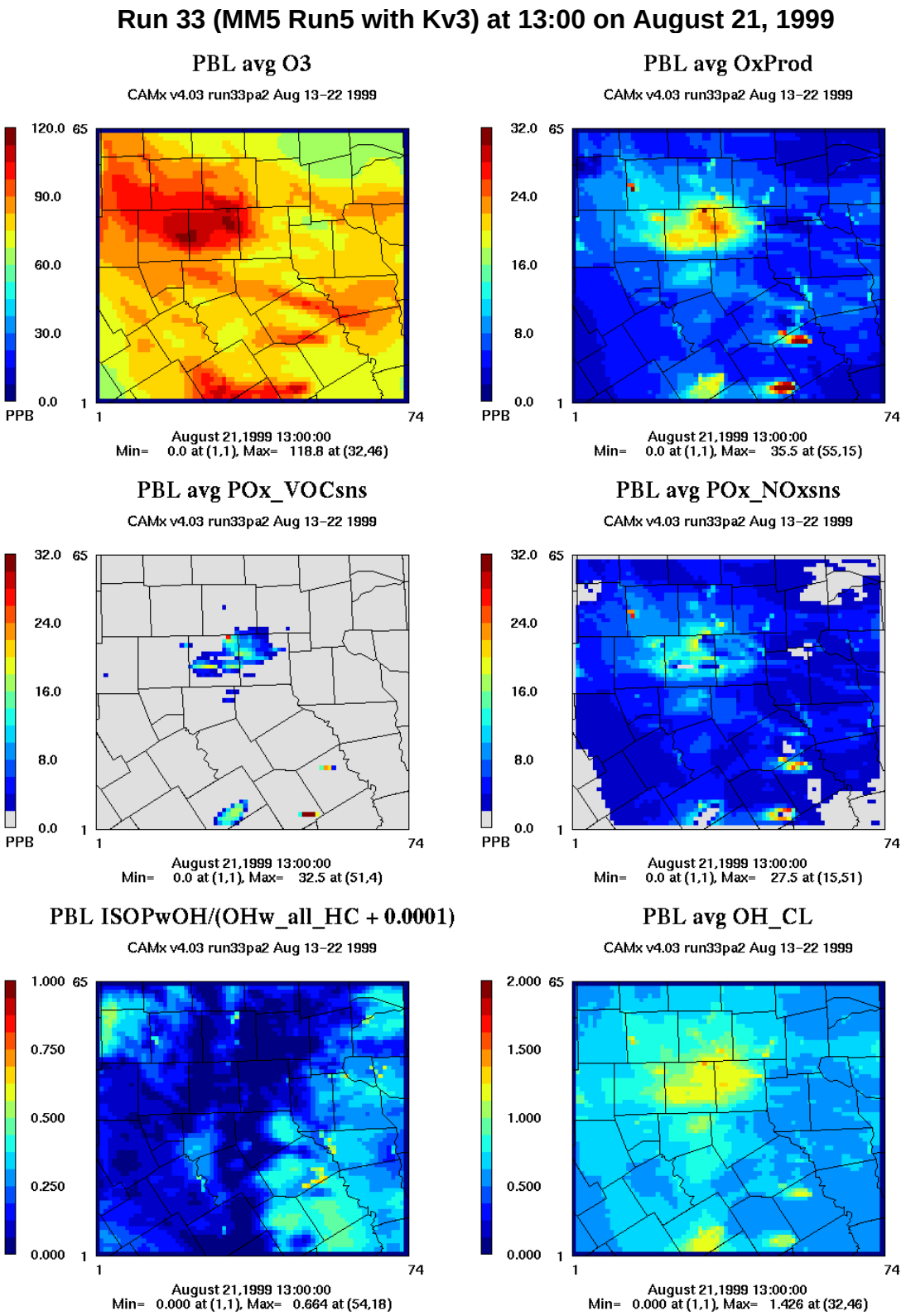


**Figure 8-11**. CAMx chemical process analysis results averaged over the PBL depth for the DFW 4-km grid in Run 33 at 13:00 on August 21, 1999.

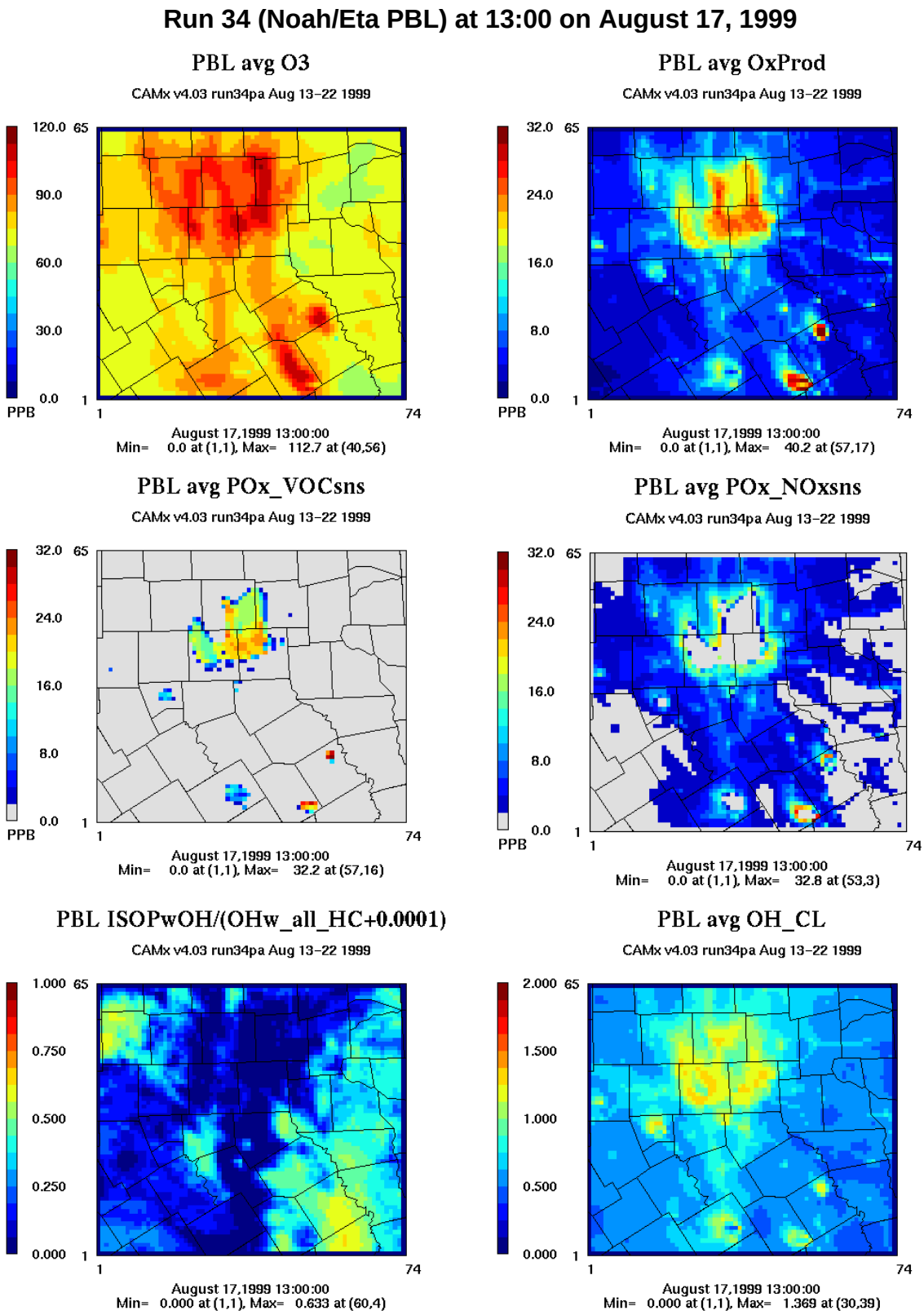


**Figure 8-12**. CAMx chemical process analysis results averaged over the PBL depth for the DFW 4-km grid in Run 34 at 13:00 on August 17, 1999.

## Run 34 (Noah/Eta PBL) at 13:00 on August 19, 1999

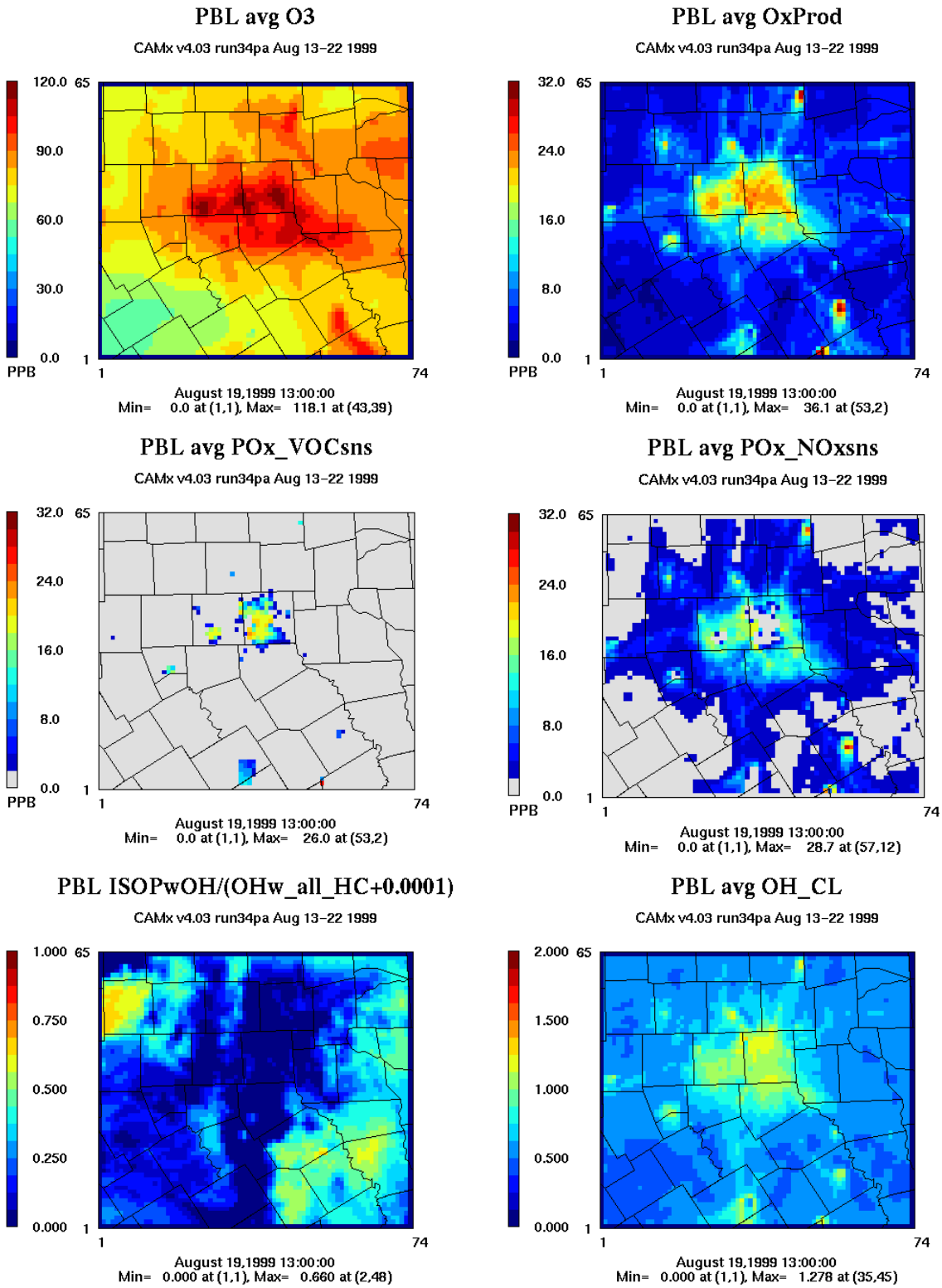


**Figure 8-13**. CAMx chemical process analysis results averaged over the PBL depth for the DFW 4-km grid in Run 34 at 13:00 on August 19, 1999.

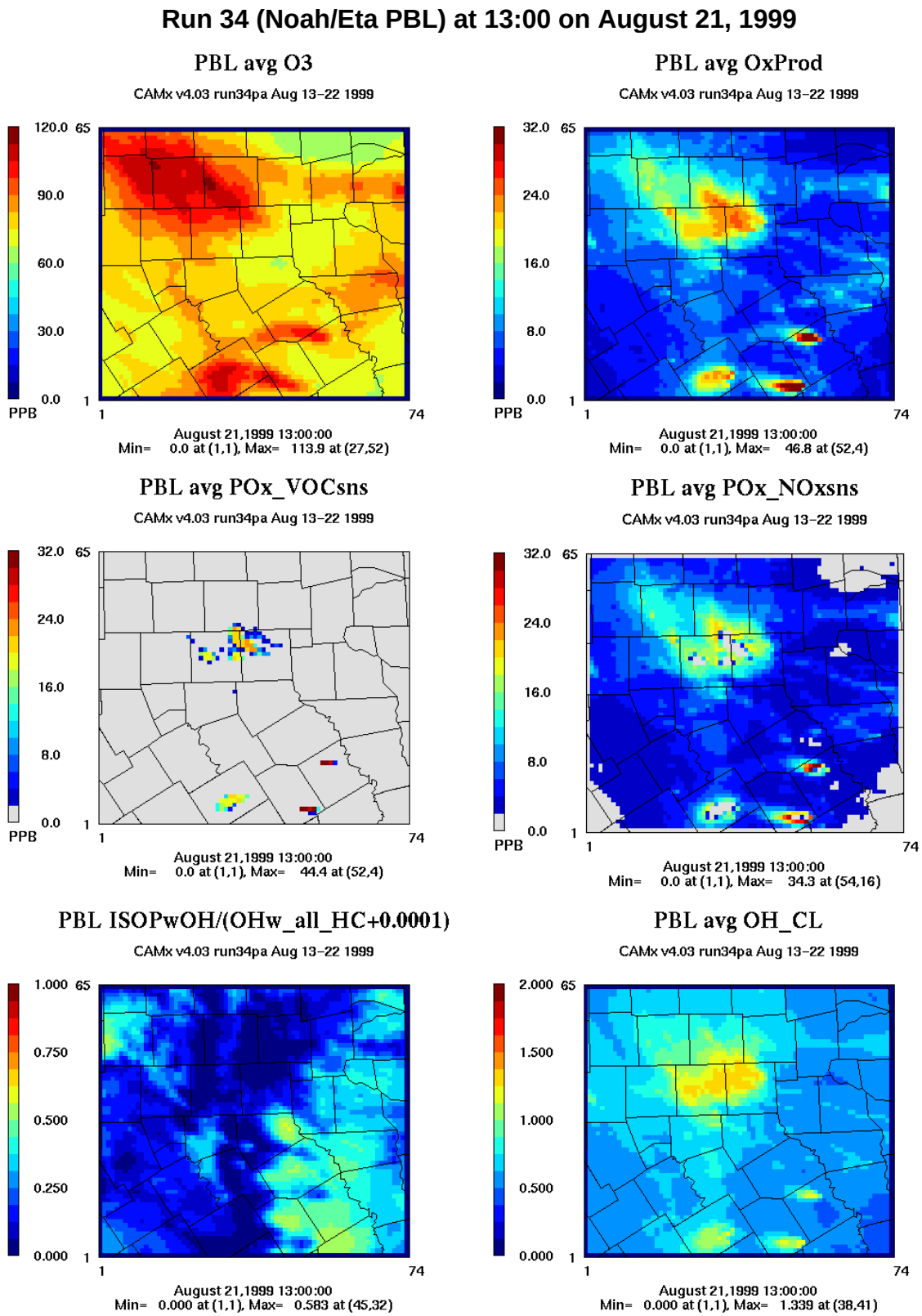


**Figure 8-14**. CAMx chemical process analysis results averaged over the PBL depth for the DFW 4-km grid in Run 34 at 13:00 on August 21, 1999.

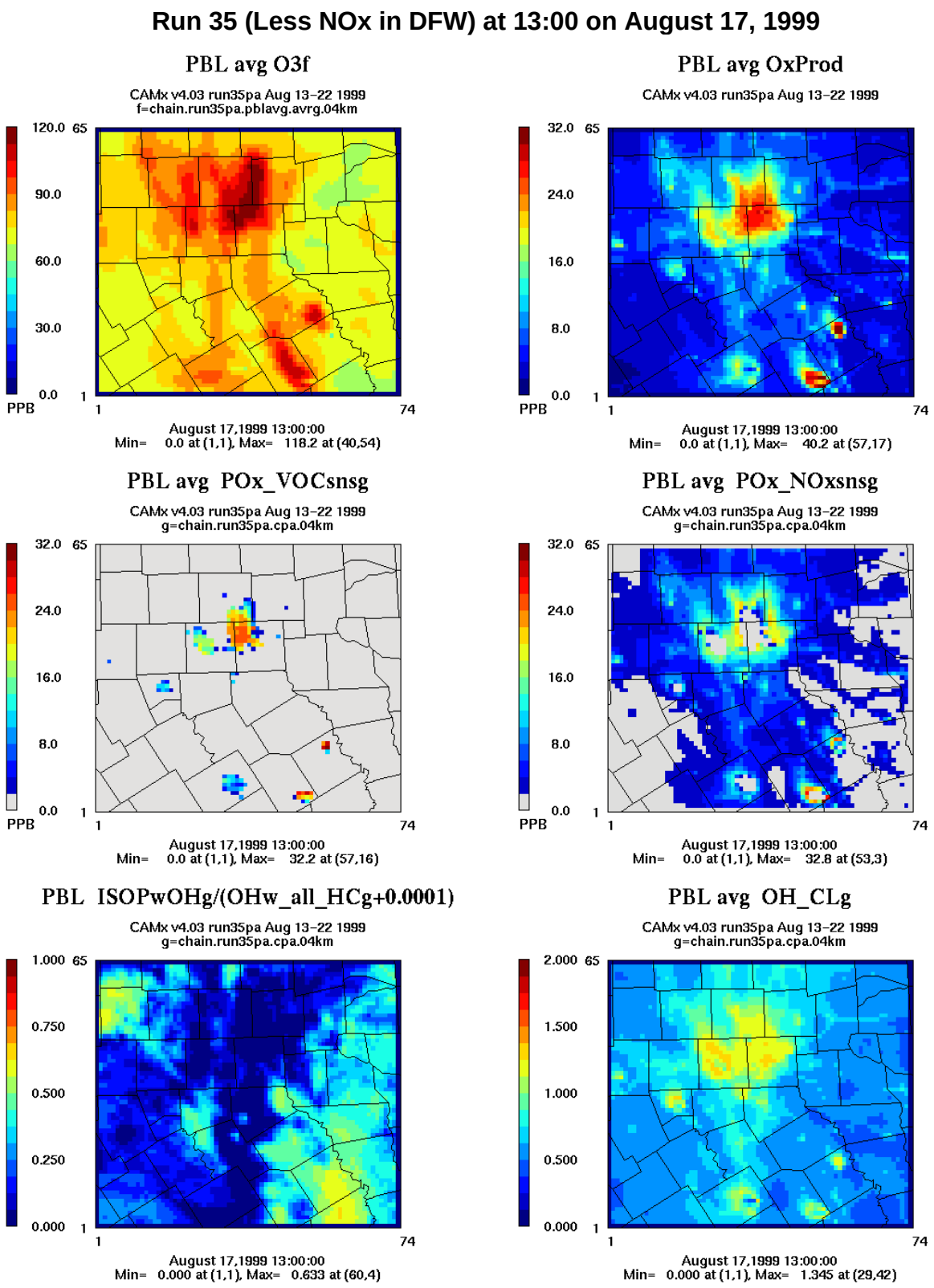


**Figure 8-15**. CAMx chemical process analysis results averaged over the PBL depth for the DFW 4-km grid in Run 35 at 13:00 on August 17, 1999.

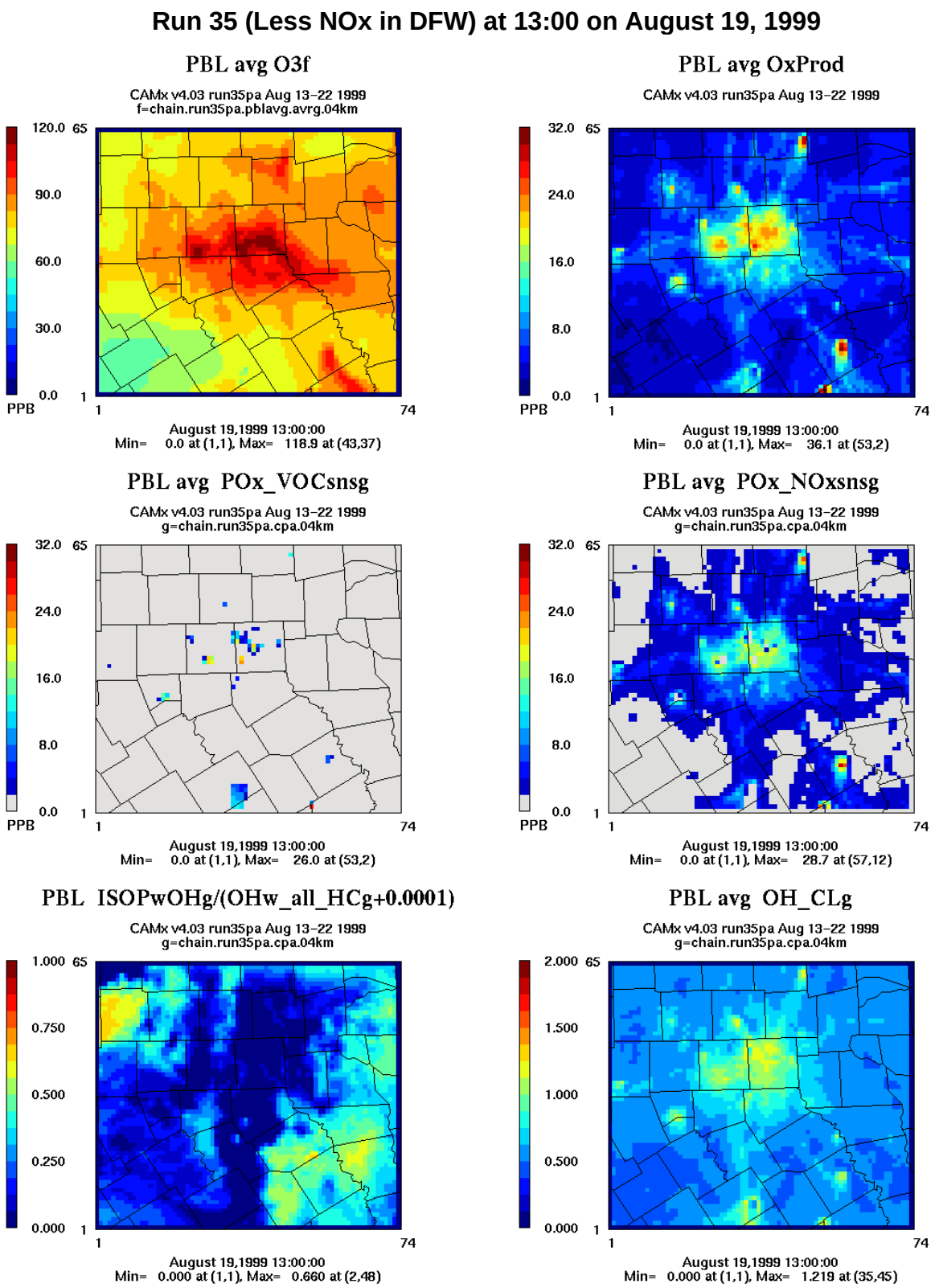


**Figure 8-16**. CAMx chemical process analysis results averaged over the PBL depth for the DFW 4-km grid in Run 35 at 13:00 on August 19, 1999.

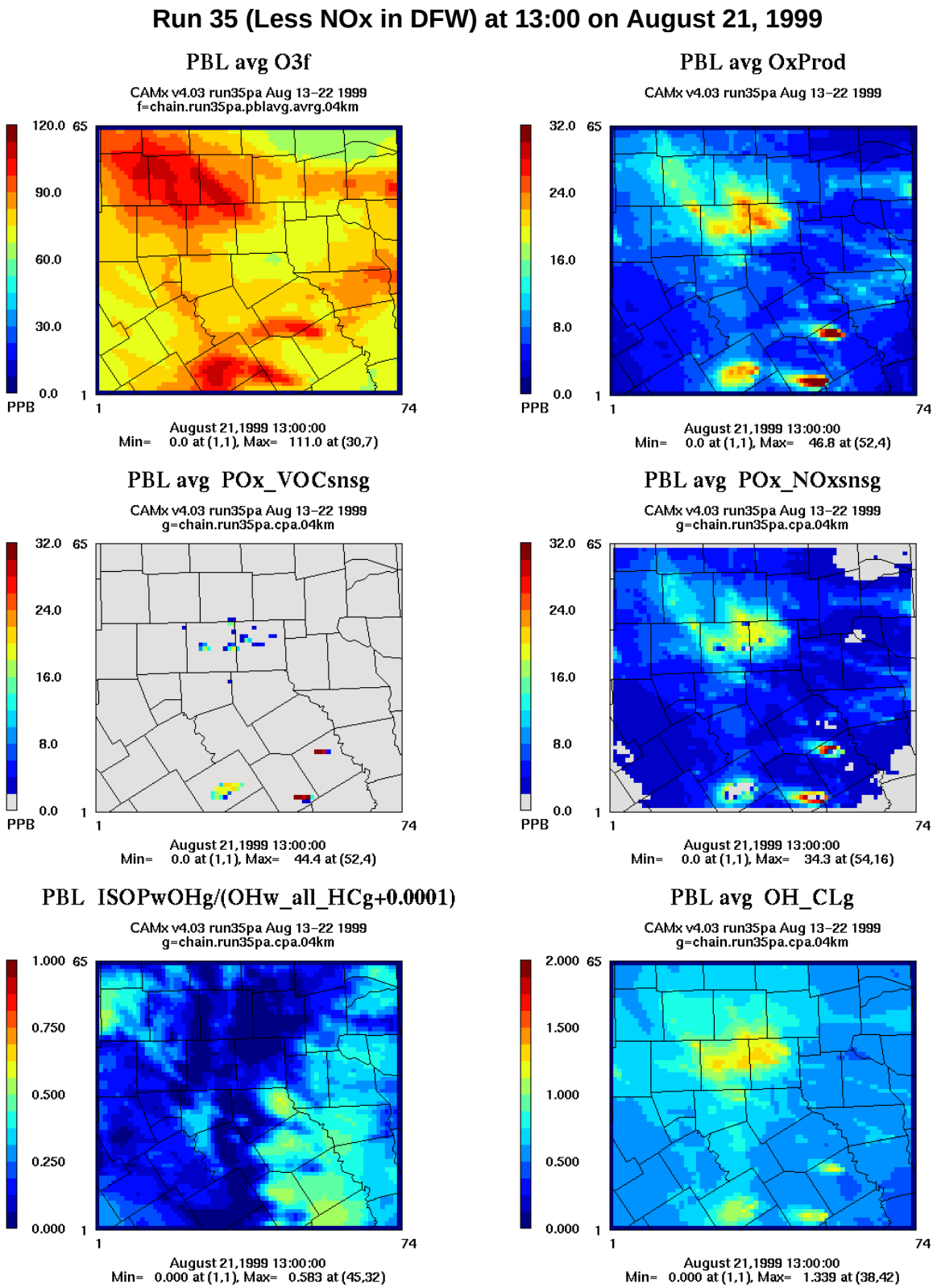


**Figure 8-17**. CAMx chemical process analysis results averaged over the PBL depth for the DFW 4-km grid in Run 35 at 13:00 on August 21, 1999.

## SENSITIVITY TO pH2O2/pHNO3 CUT POINT

The CPA analysis provides useful information on the sensitivity of Ox production to VOC and NOx. However, this CPA analysis relies upon the use of an indicator ratio to distinguish when Ox production is VOC- or NOx-limited (Tonnesen, 2004). The indicator is the ratio of the instantaneous production rates of $H_2O_2$ and $HNO_3$, called pH2O2/pHNO3. Tonnesen (2004) selected a cut point of 0.15 for this indicator in CPA whereas ENVIRON uses a cut point of 0.35 for the same indicator used in OSAT and APCA source apportionment (ENVIRON, 2004a). The sensitivity of the CPA allocation of Ox production to cut point was evaluated as shown in Figures 8-18 and 8-19.

**Run 34 (Noah/Eta PBL, Kv100) at 13:00 on August 17, 1999**

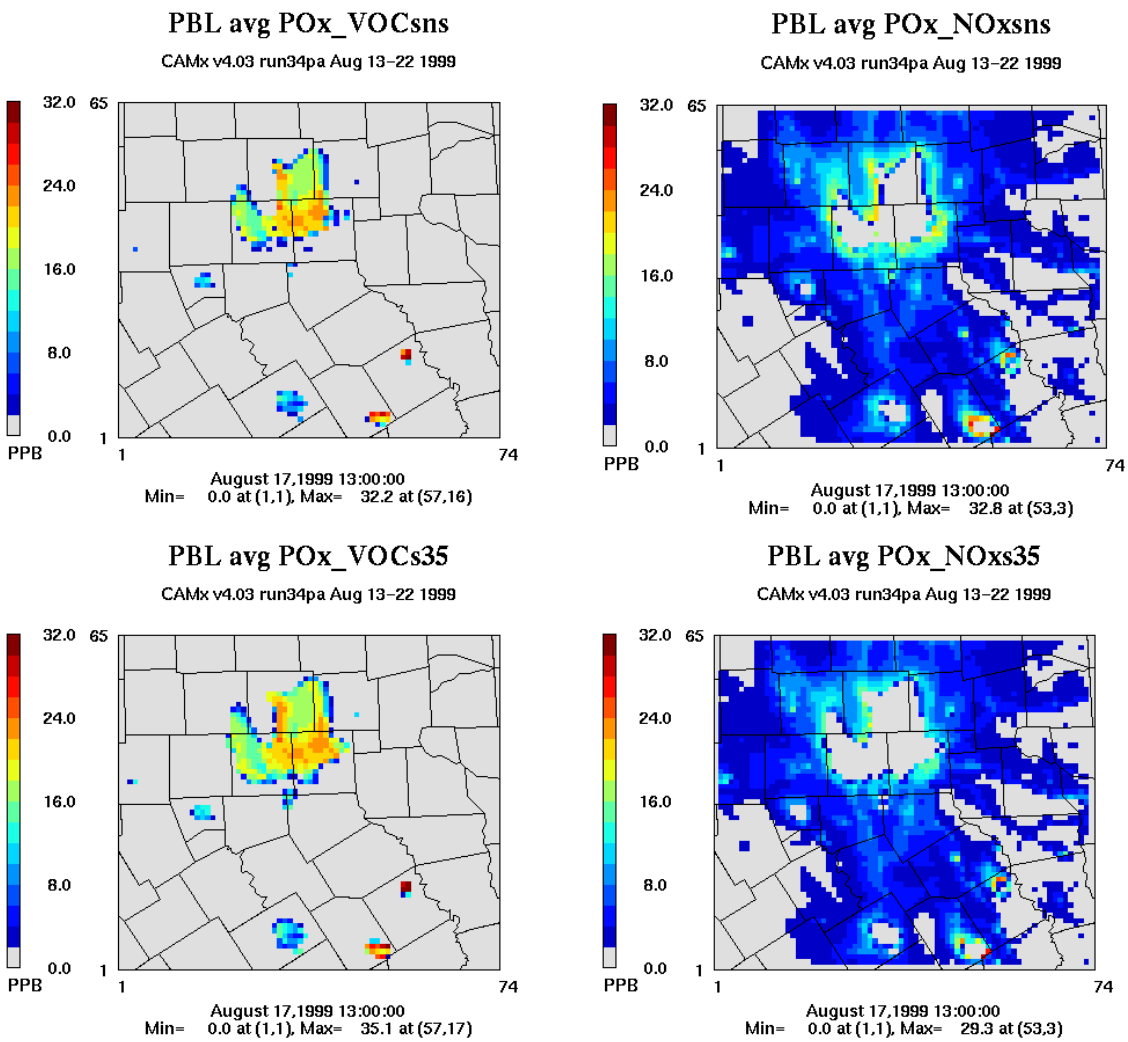


**Figure 8-18.** Comparison of Ox production from VOC-limited (left) and NOx-limited (right) conditions when the pH2O2/pHNO3 cut point set to 0.15 (top) and 0.35 (bottom) for Run 34 on August 17, 1999 at 13:00.

Figure 8-18 compares the Ox production from VOC-limited (left) and NOx-limited conditions when the pH2O2/pHNO3 cut point was set to 0.15 and 0.35 in Run 34 on August 17, 1999 at 13:00. Figure 8-19 shows a similar plot for August 21. The areas and magnitudes of VOC vs. NOx-limited Ox production are changed little by moving the cut-point from 0.35 to 0.15 showing that the pH2O2/pHNO3 indicator ratio has the desirable property of switching abruptly through values in the range 0.15 to 0.35 with no significant difference in the outcome.

**Run 34 (Noah/Eta PBL, Kv100) at 13:00 on August 21, 1999**

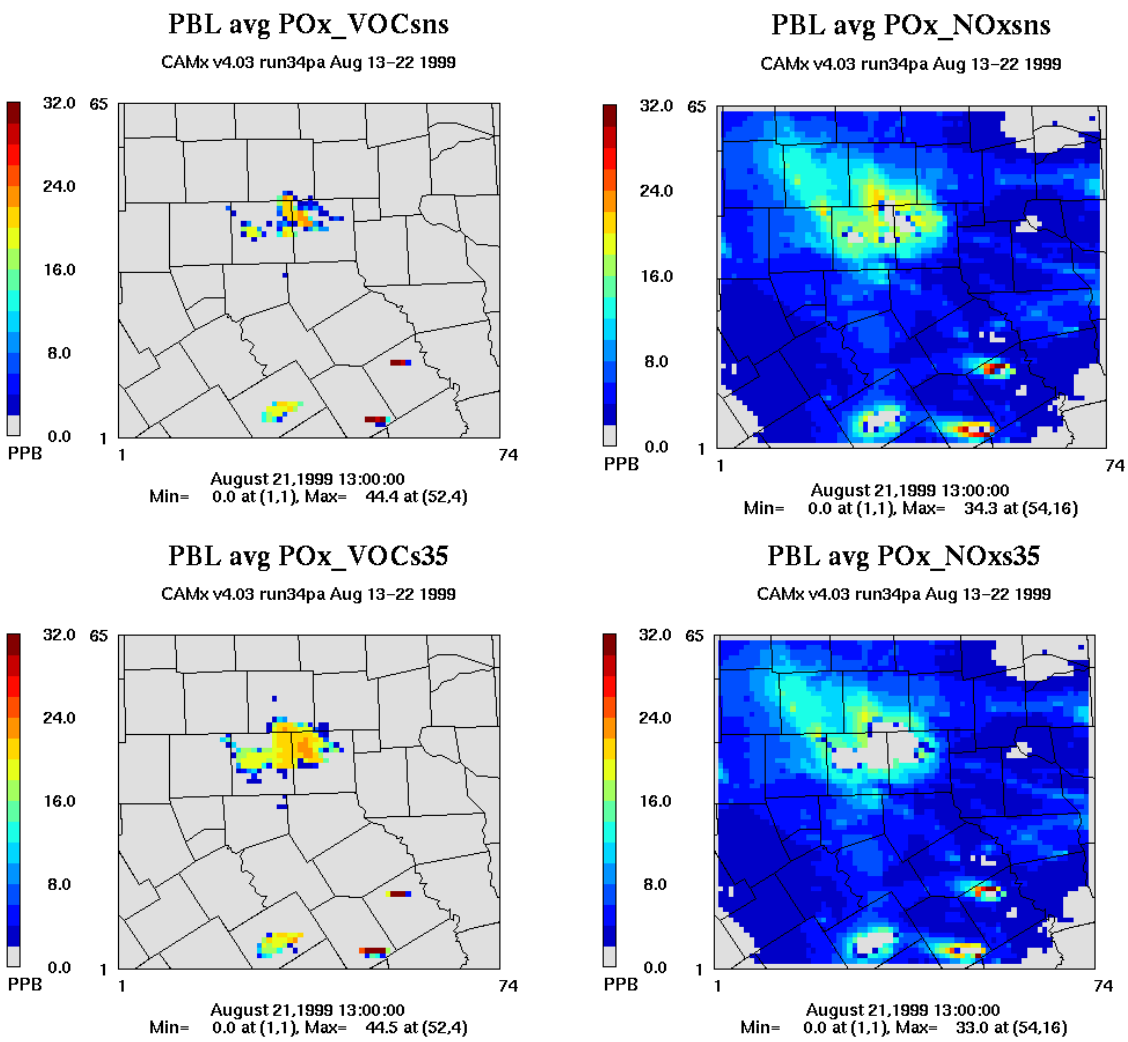


**Figure 8-19.** Comparison of Ox production from VOC-limited (left) and NOx-limited (right) conditions when the pH2O2/pHNO3 cut point set to 0.15 (top) and 0.35 (bottom) for Run 34 on August 21, 1999 at 13:00.

## SUMMARY

The use of different vertical diffusivity profiles led to significant differences in the ozone field, suggesting that more analysis is needed in low-level mixing. Process analysis results showed lower levels of OH reacting with isoprene between Waco and DFW. The low biogenic emissions are likely to assist DFW in being VOC-limited, warranting a closer look at the biogenic emission inventory in this area. The use of the cut point ratio of $H_20_2$ and $HNO_3$ production between 0.15 and 0.35 showed no significant difference in NOx-limited and VOC-limited Ox production.

# 9. CAMx 2010 FUTURE YEAR OZONE MODELING

The Texas Environmental Research Consortium (TERC) sponsored Phase 1 of project H35 to examine the role of ozone transport in creating high 8-hour ozone in eastern Texas, including the DFW region, for a 2010 future year scenario. The transport assessment was updated to consider the additional impacts of:

- Improvements to the DFW SIP modeling database as included in Run 34, discussed in Section 8.
- Expected reductions in 2010 EGU NOx emission levels expected to result from EPA's Clean Air Interstate Rule (CAIR).
- Modeling uncertainties related to meteorology, as represented by the difference between MM5 Runs 6 and 7 discussed in Section 5.
- Modeling uncertainties related to improvements in the APCA source apportionment technique to better represent chemical destruction of ozone as it is transported.

Four source apportionment runs were completed for the August 13 – 22, 1999 Dallas/Fort Worth episode for a 2010 future year. These runs used a modified version of CAMx 4.03, which incorporated NOx recycling reactions in the CB4 mechanism, as described in Section 7. One run incorporated an update to the CAMx APCA source apportionment algorithm.

## MODELING INPUTS

The 2010 base case was based on the 1999 Run 34 configuration described in Section 8. The meteorology was extracted from MM5 Run 6, which used the ETA PBL scheme. Vertical diffusivities in the lowest 100 m were modified to the largest value within each column below 100m, at each hour. The expanded modeling domain was used with 20 vertical layers extending up to14-km above the surface.

The domain was split into 28 source regions for the source apportionment modeling. Figures 9-1 to 9-3 show the division among source regions in the 36-km, 12-km, and 4-km domains, respectively. Regions 1 to 9 represent individual counties in DFW. Region 10 represents the 16-county DFW region, outside of regions 1 to 9. Regions 11 to 15 divide the remainder of Texas into five more source areas. Regions 17 to 25 represent individual states that were found to be significant contributors to 8-hour ozone in one or more NAAs in Texas in 2007, based on the CAIR guidelines applied to the simulations performed in the first phase of this project (Tai et al., 2005). Georgia and Florida were included because they had the potential to be significant if the entire state's emissions were included; in the 2007 simulations the domain extended only into western Georgia and the Florida Panhandle. Regions 26-28 comprise the remainder of the domain.

The initial conditions were categorized as moderate or clean (Mansell, 2003) as shown in Table 9-1. Below 1700 m, initial conditions were considered moderate; aloft, they were set to clean.

Boundary conditions over the northern and western boundaries, and the southern boundary running through Mexico were set to the moderate group below 1700 m, and to clean conditions above. The remaining boundaries were over maritime areas and were set to clean conditions in all layers.

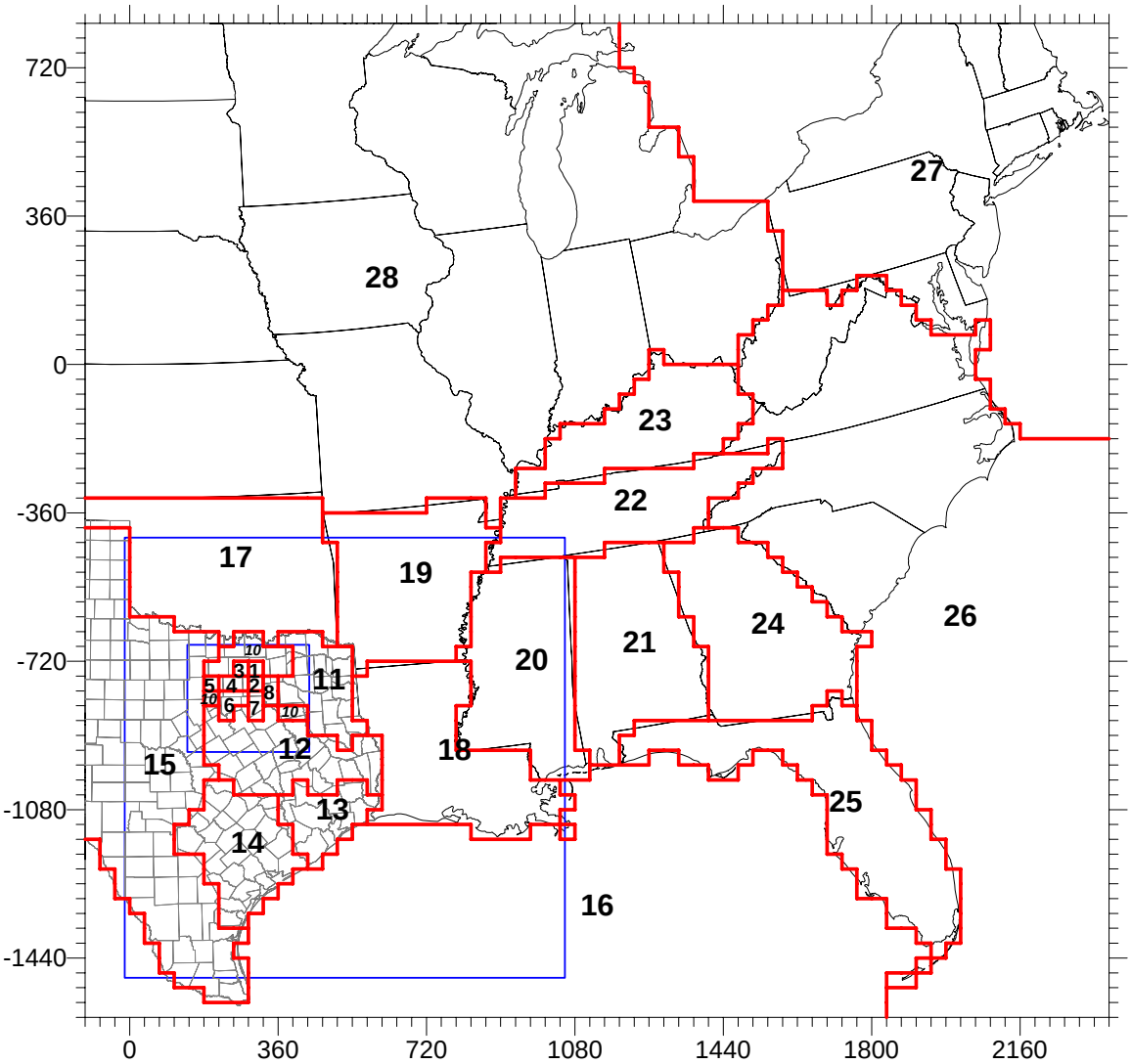


**DFW 2010 Source Regions. 36 km Expanded Domain**

1. Collin Co.
2. Dallas Co.
3. Denton Co.
4. Tarrant Co.
5. Parker Co.
6. Johnson Co.
7. Ellis Co.
8. Kaufman Co.
9. Rockwall Co.
10. DFW 16-County (Regions 1 - 9 plus Cooke, Fannin, Grayson, Henderson, Hood, Hunt, and Wise Counties)
11. Northeast Texas
12. Central Texas
13. Houston
14. South Texas
15. West Texas
16. Gulf of Mexico and Mexico
17. Oklahoma
18. Louisiana
19. Arkansas
20. Mississippi
21. Alabama
22. Tennessee
23. Kentucky
24. Georgia
25. Florida
26. Mid-Atlantic States (SC, NC, VA, WV)
27. Northeast US
28. Northern Plains

**Figure 9-1**. Source area map for source apportionment modeling in the DFW 36-km expanded domain.

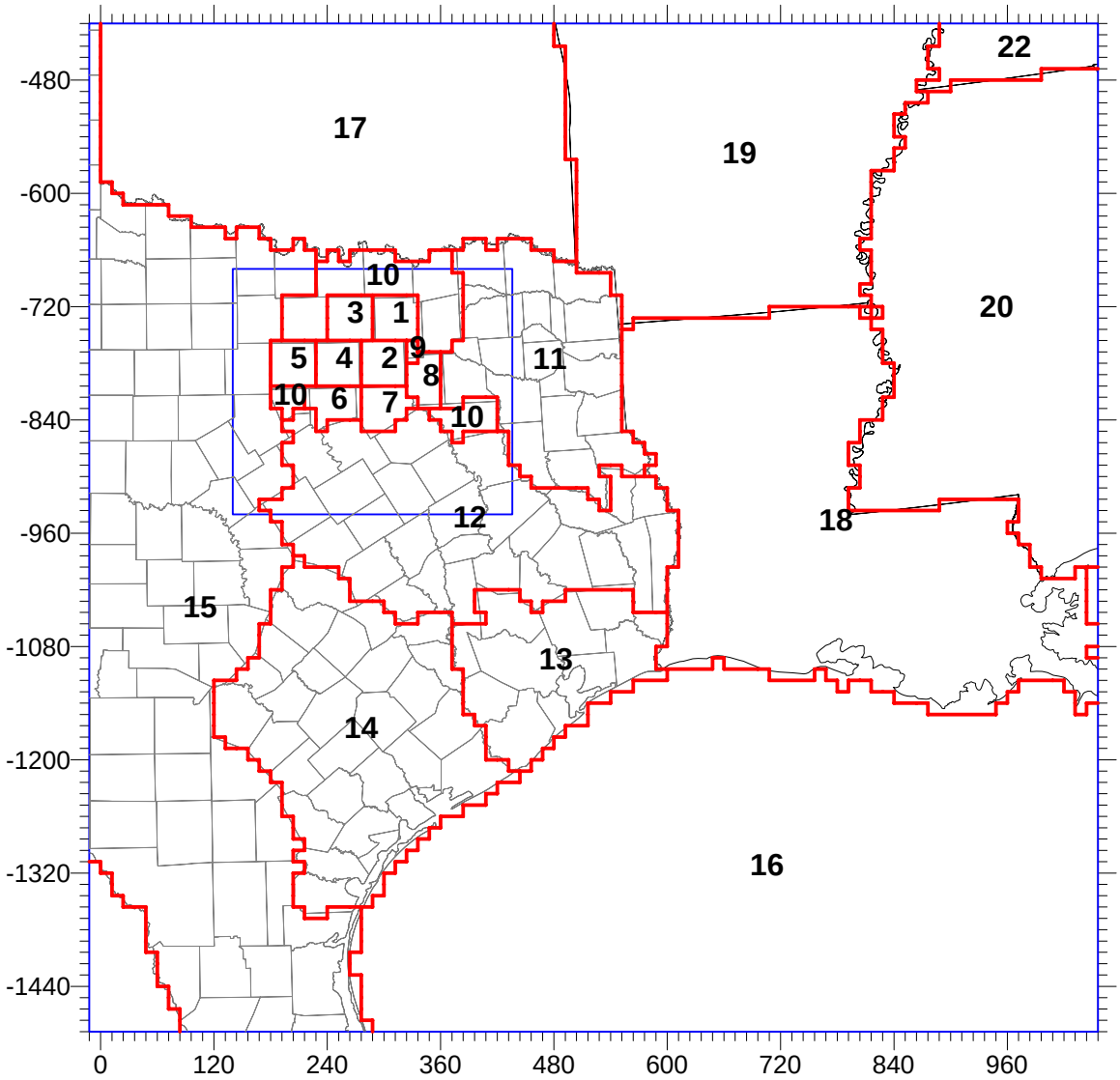


**Figure 9-2**. Source area map for source apportionment modeling in the 12-km domain.

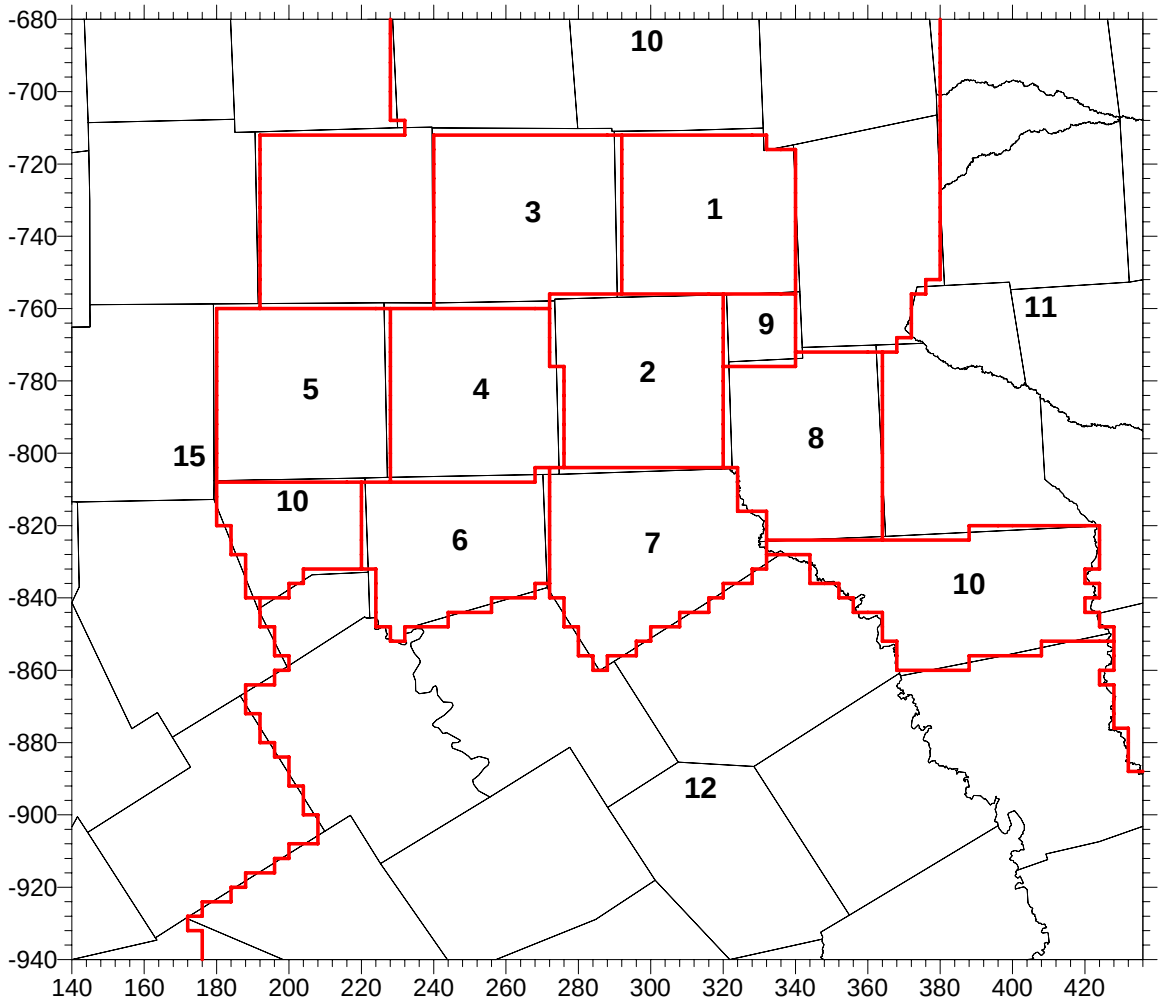


**Figure 9-3**. Source area map for source apportionment modeling in the 4-km domain.

**Table 9-1**. Concentrations [ppb] used to define 2010 initial and boundary conditions.

| Species | Moderate | Clean |
|---|---|---|
| O3 | 40 | 40 |
| CO | 200 | 100 |
| NO | 0.1 | 0.1 |
| NO2 | 1 | 1 |
| HNO3 | 3 | 1 |
| HNO2 | 0.001 | 0.001 |
| ALD2 | 0.555 | 0.05 |
| ETH | 0.51 | 0.15 |
| HCHO | 2.1 | 0.05 |
| OLE | 0.3 | 0.05 |
| PAR | 14.9 | 7.6 |
| TOL | 0.18 | 0.0786 |
| XYL | 0.0975 | 0.0688 |
| ISOP | 0.1 | 0.001 |
| PAN | 0.1 | 0.1 |
| H2O2 | 3 | 1 |
| MEOH | 0.001 | 0.001 |
| ETOH | 0.001 | 0.001 |

## 2010 EMISSIONS

The DFW 2010 future year emissions were available from a previous project for Texas Commission on Environmental Quality (TCEQ), but only for the original DFW domain, which covered (-108, -1584) to (1512, 72) (Mansell et al., 2004). Emissions from states in the expanded region were estimated by scaling existing 2002 future year emissions to 2010 using ratios of the 2010 and 2001 base case annual average emission rates from each state and source group, as found in the proposed CAIR guidelines (EPA, 2004). The final rules adopted were not released in time for this study. Scaling factors for each state outside of the original DFW domain and each source group – area, off-road, mobile, and point sources – are listed in Tables 9-2 to 9-5, respectively. Emissions used for TCEQ in the original DFW domain replaced the overlapping area of emissions in the expanded domain.

Tables 9-6 and 9-7 show weekday emissions from the first date of the simulation -- Friday, August 13, 1999 for the 2010 future year from each of the 28 source regions and 4 emission groups for NOx and VOC, respectively.

**Table 9-2.** CAIR area source emission scaling factors from 2001 to 2010 for each state inside the expanded DFW domain, but outside the original DFW domain.

| State | NOx | VOC | CO | SO2 |
|---|---|---|---|---|
| Connecticut | 0.88 | 0.76 | 0.67 | 0.88 |
| DC | 0.95 | 0.89 | 0.99 | 0.95 |
| Delaware | 0.97 | 0.99 | 0.99 | 0.98 |
| Florida | 1.01 | 0.97 | 0.94 | 1.02 |
| Georgia | 1.03 | 0.98 | 0.98 | 1.01 |
| Iowa | 1.03 | 0.96 | 0.83 | 1.05 |
| Illinois | 0.93 | 0.90 | 0.82 | 0.98 |
| Indiana | 1.04 | 0.95 | 0.89 | 1.08 |
| Kentucky | 1.04 | 0.90 | 0.78 | 1.03 |
| Massachusetts | 0.93 | 0.88 | 0.78 | 0.93 |
| Maryland | 0.96 | 0.94 | 0.98 | 1.10 |
| Maine | 0.89 | 0.79 | 0.67 | 0.87 |
| Michigan | 0.95 | 0.87 | 0.73 | 0.95 |
| Minnesota | 1.03 | 0.96 | 0.77 | 0.96 |
| Missouri | 1.04 | 0.89 | 0.71 | 1.00 |
| North Carolina | 1.03 | 0.96 | 0.93 | 1.02 |
| North Dakota | 1.09 | 1.01 | 0.95 | 1.08 |
| Nebraska | 1.04 | 0.99 | 0.86 | 1.02 |
| New Hampshire | 1.02 | 0.88 | 0.74 | 1.01 |
| New Jersey | 0.94 | 0.89 | 0.89 | 0.92 |
| New York | 0.81 | 0.89 | 0.68 | 0.89 |
| Ohio | 0.99 | 0.92 | 0.76 | 1.01 |
| Pennsylvania | 0.94 | 0.88 | 0.84 | 0.87 |
| Rhode Island | 0.87 | 0.89 | 0.71 | 0.86 |
| South Carolina | 1.05 | 0.97 | 0.92 | 1.06 |
| South Dakota | 1.10 | 1.02 | 0.89 | 1.14 |
| Tennessee | 1.03 | 0.93 | 0.80 | 1.05 |
| Virginia | 1.01 | 0.95 | 0.81 | 1.01 |
| Vermont | 0.86 | 0.91 | 0.69 | 0.96 |
| Wisconsin | 0.97 | 0.91 | 0.81 | 1.03 |
| West Virginia | 0.96 | 0.87 | 0.72 | 0.99 |

**Table 9-3.** CAIR off-road source emission scaling factors from 2001 to 2010 for each state inside the expanded DFW domain, but outside the original DFW domain.

| State | NOx | VOC | CO | SO2 |
|---|---|---|---|---|
| Connecticut | 0.81 | 0.67 | 1.10 | 0.17 |
| DC | 0.91 | 1.05 | 1.16 | 0.29 |
| Delaware | 0.98 | 0.66 | 1.09 | 0.23 |
| Florida | 0.89 | 0.69 | 1.14 | 0.58 |
| Georgia | 0.83 | 0.72 | 1.12 | 0.28 |
| Iowa | 0.83 | 0.73 | 1.07 | 0.08 |
| Illinois | 0.85 | 0.75 | 1.10 | 0.12 |
| Indiana | 0.83 | 0.74 | 1.09 | 0.11 |
| Kentucky | 0.91 | 0.78 | 1.08 | 0.10 |
| Massachusetts | 0.83 | 0.70 | 1.09 | 0.15 |
| Maryland | 0.90 | 0.73 | 1.14 | 0.68 |
| Maine | 0.82 | 0.82 | 1.08 | 0.19 |
| Michigan | 0.84 | 0.76 | 1.07 | 0.19 |
| Minnesota | 0.86 | 0.79 | 1.06 | 0.14 |
| Missouri | 0.88 | 0.74 | 1.11 | 0.13 |
| North Carolina | 0.80 | 0.71 | 1.09 | 0.17 |
| North Dakota | 0.85 | 0.77 | 1.04 | 0.07 |
| Nebraska | 0.84 | 0.75 | 1.09 | 0.09 |
| New Hampshire | 0.78 | 0.76 | 1.11 | 0.20 |
| New Jersey | 0.86 | 0.68 | 1.13 | 0.77 |
| New York | 0.85 | 0.72 | 1.13 | 0.20 |
| Ohio | 0.84 | 0.73 | 1.10 | 0.35 |
| Pennsylvania | 0.81 | 0.76 | 1.11 | 0.28 |
| Rhode Island | 0.82 | 0.67 | 1.12 | 0.76 |
| South Carolina | 0.76 | 0.69 | 1.10 | 0.26 |
| South Dakota | 0.84 | 0.76 | 1.04 | 0.07 |
| Tennessee | 0.93 | 0.78 | 1.08 | 0.16 |
| Virginia | 0.93 | 0.72 | 1.12 | 0.46 |
| Vermont | 0.81 | 0.81 | 1.10 | 0.18 |
| Wisconsin | 0.80 | 0.77 | 1.04 | 0.14 |
| West Virginia | 0.74 | 0.85 | 1.14 | 0.68 |

**Table 9-4.** CAIR mobile source emission scaling factors from 2001 to 2010 for each state inside the expanded DFW domain, but outside the original DFW domain.

| State | NOx | VOC | CO | SO2 |
|---|---|---|---|---|
| Connecticut | 0.49 | 0.48 | 0.52 | 0.16 |
| DC | 0.57 | 0.53 | 0.74 | 0.19 |
| Delaware | 0.63 | 0.80 | 1.11 | 0.17 |
| Florida | 0.61 | 0.84 | 1.08 | 0.10 |
| Georgia | 0.53 | 0.63 | 0.70 | 0.10 |
| Iowa | 0.56 | 0.79 | 0.95 | 0.10 |
| Illinois | 0.57 | 0.67 | 0.81 | 0.13 |
| Indiana | 0.58 | 0.77 | 0.94 | 0.10 |
| Kentucky | 0.57 | 0.79 | 0.96 | 0.11 |
| Massachusetts | 0.55 | 0.60 | 0.76 | 0.17 |
| Maryland | 0.53 | 0.61 | 0.75 | 0.16 |
| Maine | 0.57 | 0.73 | 0.98 | 0.09 |
| Michigan | 0.57 | 0.76 | 1.00 | 0.09 |
| Minnesota | 0.54 | 0.67 | 0.87 | 0.10 |
| Missouri | 0.56 | 0.75 | 0.88 | 0.11 |
| North Carolina | 0.58 | 0.84 | 1.04 | 0.10 |
| North Dakota | 0.58 | 0.80 | 0.98 | 0.10 |
| Nebraska | 0.57 | 0.80 | 0.96 | 0.10 |
| New Hampshire | 0.59 | 0.75 | 0.93 | 0.12 |
| New Jersey | 0.51 | 0.51 | 0.62 | 0.17 |
| New York | 0.51 | 0.57 | 0.75 | 0.12 |
| Ohio | 0.57 | 0.71 | 0.86 | 0.10 |
| Pennsylvania | 0.58 | 0.70 | 0.91 | 0.11 |
| Rhode Island | 0.48 | 0.53 | 0.55 | 0.15 |
| South Carolina | 0.57 | 0.89 | 0.95 | 0.09 |
| South Dakota | 0.59 | 0.81 | 1.00 | 0.11 |
| Tennessee | 0.58 | 0.84 | 1.01 | 0.10 |
| Virginia | 0.60 | 0.75 | 0.86 | 0.11 |
| Vermont | 0.61 | 0.69 | 0.85 | 0.11 |
| Wisconsin | 0.57 | 0.68 | 0.90 | 0.11 |
| West Virginia | 0.55 | 0.79 | 0.87 | 0.10 |

**Table 9-5.** CAIR point source (EGU + non-EGU) emission scaling factors from 2001 to 2010 for each state inside the expanded DFW domain, but outside the original DFW domain.

| State | NOx | VOC | CO | SO2 |
|---|---|---|---|---|
| Connecticut | 0.74 | 0.80 | 1.83 | 0.33 |
| DC | 0.74 | 0.95 | 1.08 | 0.67 |
| Delaware | 0.88 | 0.77 | 1.07 | 1.12 |
| Florida | 0.62 | 0.86 | 1.24 | 0.49 |
| Georgia | 0.97 | 0.87 | 1.23 | 1.22 |
| Iowa | 1.05 | 0.66 | 0.90 | 1.13 |
| Illinois | 0.91 | 0.88 | 1.00 | 1.39 |
| Indiana | 0.78 | 0.94 | 1.06 | 0.87 |
| Kentucky | 0.87 | 1.00 | 1.13 | 0.70 |
| Massachusetts | 0.53 | 0.88 | 1.67 | 0.26 |
| Maryland | 0.85 | 0.94 | 1.02 | 0.92 |
| Maine | 1.02 | 0.89 | 1.09 | 0.87 |
| Michigan | 0.94 | 0.88 | 1.08 | 1.08 |
| Minnesota | 1.16 | 0.83 | 1.17 | 0.99 |
| Missouri | 0.95 | 0.96 | 1.06 | 1.16 |
| North Carolina | 0.63 | 0.96 | 1.11 | 0.62 |
| North Dakota | 0.98 | 0.76 | 1.04 | 1.00 |
| Nebraska | 1.16 | 0.98 | 0.97 | 1.36 |
| New Hampshire | 0.72 | 0.94 | 1.32 | 0.27 |
| New Jersey | 0.70 | 0.86 | 0.70 | 0.80 |
| New York | 0.84 | 0.90 | 1.24 | 0.86 |
| Ohio | 0.82 | 0.80 | 1.06 | 1.06 |
| Pennsylvania | 0.97 | 0.75 | 0.93 | 0.91 |
| Rhode Island | 2.34 | 0.66 | 1.35 | 0.94 |
| South Carolina | 0.87 | 0.77 | 1.12 | 1.01 |
| South Dakota | 0.74 | 1.09 | 0.76 | 2.40 |
| Tennessee | 0.73 | 0.89 | 1.09 | 0.86 |
| Virginia | 0.80 | 0.94 | 1.10 | 0.91 |
| Vermont | 0.41 | 0.88 | 0.63 | 0.94 |
| Wisconsin | 1.07 | 0.87 | 1.08 | 1.09 |
| West Virginia | 0.80 | 0.91 | 1.04 | 1.09 |

**Table 9-6.** 2010 weekday NOx emissions for the DFW episode by source apportionment region.

| Region No. | Source Region | 2010 Base Case NOx (tons/day) | | | | |
|---|---|---|---|---|---|---|
| | | Biogenics | Mobile | Points (elevated + low-level) | Other (area + offroad + Canada) | Total Anthro |
| 1 | Collin Co. | 10 | 12 | 3 | 15 | 29 |
| 2 | Dallas Co. | 4 | 65 | 19 | 76 | 159 |
| 3 | Denton Co. | 8 | 15 | 3 | 19 | 37 |
| 4 | Tarrant Co. | 3 | 38 | 12 | 45 | 95 |
| 5 | Parker Co. | 1 | 6 | 2 | 5 | 13 |
| 6 | Johnson Co. | 5 | 5 | 4 | 7 | 16 |
| 7 | Ellis Co. | 15 | 9 | 45 | 9 | 62 |
| 8 | Kaufman Co. | 5 | 6 | 7 | 4 | 17 |
| 9 | Rockwall Co. | 2 | 3 | 0 | 1 | 4 |
| | Outer DFW | 33 | 22 | 57 | 42 | 121 |
| 10 | DFW 16 county | 85 | 179 | 151 | 222 | 552 |
| 11 | NE Texas | 18 | 80 | 219 | 128 | 427 |
| 12 | Central TX | 125 | 65 | 199 | 144 | 408 |
| 13 | Houston | 23 | 139 | 294 | 175 | 607 |
| 14 | South Texas | 249 | 159 | 326 | 213 | 699 |
| 15 | West Texas | 550 | 130 | 188 | 310 | 627 |
| 16 | Gulf of Mexico/Mexico | 92 | 14 | 617 | 381 | 1012 |
| 17 | Oklahoma | 193 | 175 | 686 | 244 | 1105 |
| 18 | Louisiana | 118 | 179 | 1022 | 962 | 2163 |
| 19 | Arkansas | 136 | 119 | 386 | 303 | 808 |
| 20 | Mississippi | 137 | 169 | 562 | 323 | 1054 |
| 21 | Alabama | 79 | 243 | 675 | 343 | 1261 |
| 22 | Tennessee | 122 | 290 | 570 | 460 | 1321 |
| 23 | Kentucky | 139 | 221 | 757 | 462 | 1440 |
| 24 | Georgia | 115 | 416 | 636 | 300 | 1353 |
| 25 | Florida | 58 | 746 | 632 | 459 | 1837 |
| 26 | Mid Atlantic | 303 | 1164 | 1950 | 901 | 4016 |
| 27 | Northeast US | 310 | 2052 | 1833 | 3230 | 7116 |
| 28 | Northern Plains | 4303 | 3064 | 6077 | 4463 | 13604 |
| | Total | 7152 | 9605 | 17780 | 14024 | 41408 |

**Table 9-7.** 2010 weekday VOC emissions for the DFW episode by source apportionment region.

| Region No. | Source Region | 2010 Base Case VOC (tons/day) | | | | |
|---|---|---|---|---|---|---|
| | | Biogenics | Mobile | Points (elevated + low level) | Other (area + offroad + Canada) | Total Anthro |
| 1 | Collin Co. | 25 | 8 | 1 | 19 | 27 |
| 2 | Dallas Co. | 48 | 40 | 12 | 115 | 168 |
| 3 | Denton Co. | 58 | 9 | 2 | 25 | 35 |
| 4 | Tarrant Co. | 56 | 23 | 9 | 80 | 112 |
| 5 | Parker Co. | 109 | 2 | 1 | 13 | 16 |
| 6 | Johnson Co. | 106 | 3 | 0 | 13 | 16 |
| 7 | Ellis Co. | 96 | 3 | 7 | 15 | 25 |
| 8 | Kaufman Co. | 115 | 3 | 2 | 16 | 21 |
| 9 | Rockwall Co. | 3 | 1 | 0 | 5 | 6 |
| | Outer DFW | 919 | 12 | 4 | 88 | 105 |
| 10 | DFW 16 county | 1537 | 103 | 39 | 388 | 530 |
| 11 | NE Texas | 5092 | 35 | 21 | 210 | 266 |
| 12 | Central TX | 6989 | 29 | 27 | 240 | 295 |
| 13 | Houston | 1950 | 74 | 107 | 281 | 462 |
| 14 | South Texas | 2442 | 75 | 24 | 459 | 558 |
| 15 | West Texas | 6976 | 56 | 16 | 638 | 711 |
| 16 | Gulf of Mexico/ Mexico | 815 | 11 | 48 | 339 | 398 |
| 17 | Oklahoma | 7732 | 101 | 167 | 302 | 570 |
| 18 | Louisiana | 10948 | 95 | 236 | 380 | 711 |
| 19 | Arkansas | 14532 | 61 | 131 | 364 | 556 |
| 20 | Mississippi | 16288 | 80 | 162 | 381 | 624 |
| 21 | Alabama | 15159 | 146 | 340 | 421 | 907 |
| 22 | Tennessee | 9011 | 160 | 341 | 668 | 1170 |
| 23 | Kentucky | 3684 | 123 | 221 | 420 | 764 |
| 24 | Georgia | 12506 | 231 | 78 | 630 | 939 |
| 25 | Florida | 11161 | 652 | 71 | 981 | 1703 |
| 26 | Mid Atlantic | 31206 | 951 | 478 | 1660 | 3089 |
| 27 | Northeast US | 15578 | 1243 | 187 | 4736 | 6165 |
| 28 | Northern Plains | 27279 | 2180 | 1282 | 5430 | 8892 |
| | Total | 200886 | 6404 | 3975 | 18929 | 29309 |

## MODELING RESULTS

**Table 9-8**. List of the four source apportionment runs for the 2010 future year.

| Run | PBL Scheme/ Land Surface Model | Emissions | Source Apportionment Technology Method |
|---|---|---|---|
| Run 34 | Eta/Noah | 2010 Base (No CAIR) | APCA |
| Run 36 | Eta/Noah | 2010 CAIR controls | APCA |
| Run 38 | Eta/Noah | 2010 CAIR controls | APCA2 |
| Run 37 | Pleim-Xiu with Grell convection | 2010 CAIR controls | APCA |

### CAMx Run 34 for Future Year 2010

The 2010 future year base case was configured exactly like Run 34 for 1999 except that 2010 future year emissions (without CAIR) were applied. Spatial plots of the highest episode 8-hour ozone from Run 34 for 1999 and for 2010 are shown in Figure 9-4. The top row displays the 1999 episode maxima in the 4-km and 12-km domains. The middle row shows the 2010 maxima for the same domains. The bottom row shows the difference in 8-hour maxima between the two modeling years.

The episode maximum 8-hour ozone was lower in 2010 compared to 1999 in most of Texas, except for some areas inside the DFW 4-county core and in Houston. Little change was simulated in southern Texas. In the 4-km domain, the 1999 simulated peaks between Johnson and Ellis Counties, and over Denton County were 15 ppb and 10 ppb lower, respectively, in 2010. Near the center of the DFW 4-county core, the episode maximum 8-hour ozone was nearly 9 ppb higher in 2010. These results were comparable to the differences between the 1999 Run 17b and associated 2010 future year modeling performed in 2004 (Mansell, 2004), where daily peaks inside a small area of the DFW core were 9 to 13 ppb higher in 2010.

Table 9-9 shows the episode average contribution to 8-hour ozone in 2010 in the DFW 9-county NAA from each of the 28 source regions and 4 emission groups (biogenics, mobile, points, and area plus offroad). Only grid-hours equal to or exceeding 85 ppb were considered. Bar charts displaying these results are shown in Figure 9-5. The first 9 source regions represent the 9 individual counties in the DFW NAA, where Dallas and Tarrant Counties generated the largest local impact. The remaining regions are sorted in descending order by ozone contribution from all anthropogenic sources. The largest anthropogenic contributor outside of DFW was Louisiana, which averaged 2.9 ppb for the 6019 grid-hours exceeding 85 ppb for 8-hour ozone.

Table 9-10 and Figure 9-6 are similar to Table 9-9 and Figure 9-5, respectively, but show contributions to the DFW 4-county core (Collin, Dallas, Denton, and Tarrant Counties). The highest contributions came from three local counties – Dallas, Tarrant, and Ellis Counties. The next highest contributor was Louisiana.

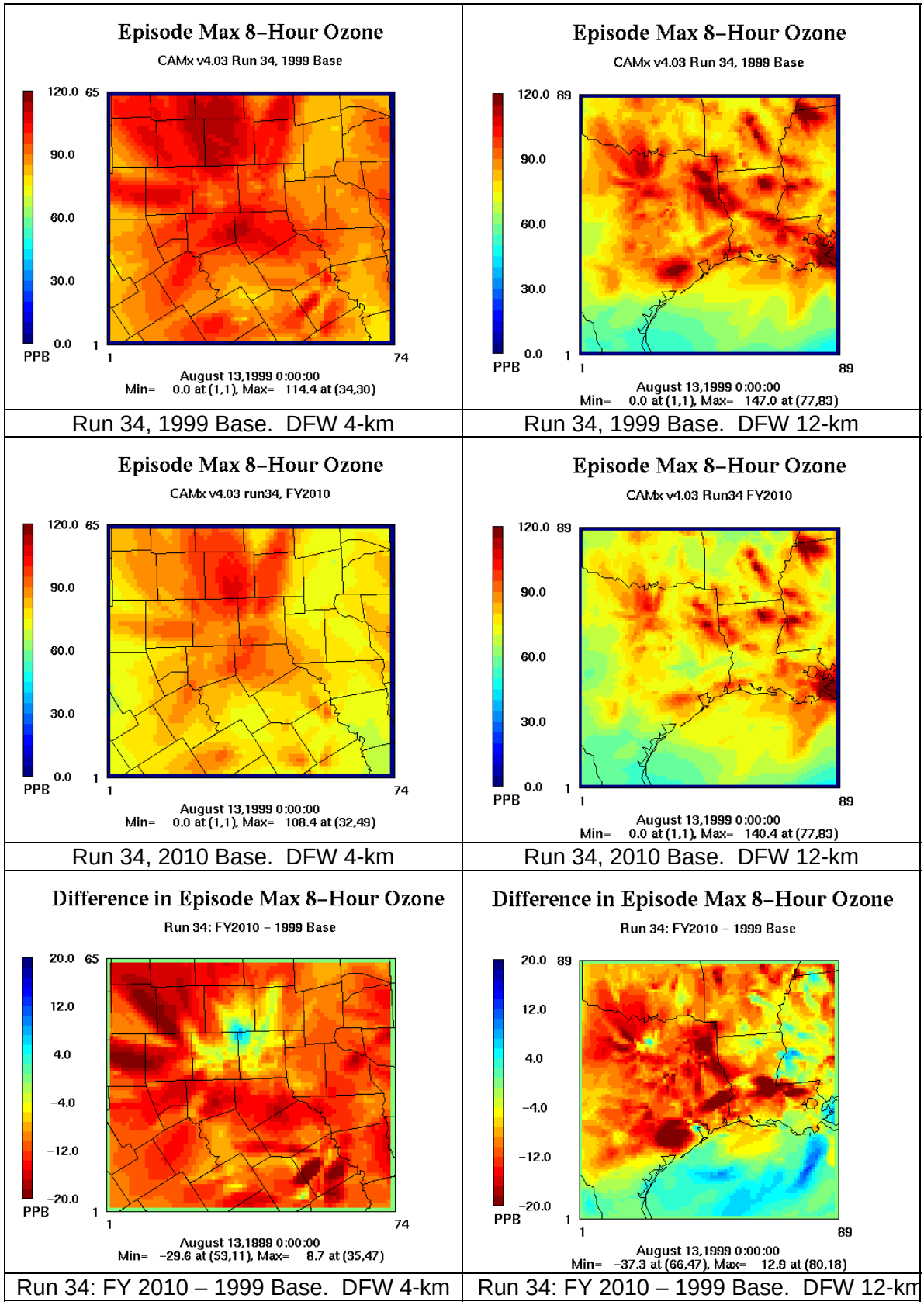


Run 34, 1999 Base. DFW 4-km | Run 34, 1999 Base. DFW 12-km

Run 34, 2010 Base. DFW 4-km | Run 34, 2010 Base. DFW 12-km

Run 34: FY 2010 – 1999 Base. DFW 4-km | Run 34: FY 2010 – 1999 Base. DFW 12-km

**Figure 9-4.** Spatial plots of the episode maximum 8-hour base case ozone for 1999 and 2010 in the DFW 4-km and 12-km domains using the Run 34 configuration.

**Table 9-9**. Episode average contributions from all source regions and emission groups to the Dallas/Fort Worth NAA in CAMx Run 34 for the 2010 future year.

| Episode Average Contributions to 8-hour Ozone (ppb) | | | | | | | | |
|---|---|---|---|---|---|---|---|---|
| Run | run34sa.fy2010 | | | | | | | |
| Receptor | DFW-9 County NAA | | | | | | | |
| #Grid-Hrs | 6019 | | | | | | | |
| BaseO3 >= | 85 | | | | | | | |
| AvgConc | 90.8 | | | | | | | |
| **Source Reg** | **IC** | **BC** | **Biogenic** | **Mobile** | **All Points** | **Area+Offroad** | **Anthro** | **% Anthro** |
| Dallas Co. | | | 0.24 | 6.35 | 1.58 | 8.69 | 16.61 | 34.45 |
| Tarrant Co. | | | 0.15 | 3.55 | 0.77 | 4.22 | 8.54 | 17.70 |
| Ellis Co. | | | 0.38 | 0.37 | 2.25 | 0.58 | 3.20 | 6.64 |
| Denton Co. | | | 0.20 | 1.16 | 0.16 | 0.96 | 2.29 | 4.74 |
| Collin Co. | | | 0.15 | 0.61 | 0.10 | 0.83 | 1.54 | 3.19 |
| Kaufman Co. | | | 0.16 | 0.21 | 0.29 | 0.15 | 0.65 | 1.34 |
| Johnson Co. | | | 0.13 | 0.16 | 0.09 | 0.26 | 0.51 | 1.05 |
| Rockwall Co. | | | 0.04 | 0.12 | 0.00 | 0.08 | 0.20 | 0.41 |
| Parker Co. | | | 0.02 | 0.07 | 0.04 | 0.06 | 0.17 | 0.35 |
| **DFW 9-County** | | | **1.47** | **12.60** | **5.28** | **15.83** | **33.70** | **69.88** |
| **DFW 16-County** | | | **1.66** | **12.75** | **5.72** | **16.15** | **34.62** | **71.78** |
| Louisiana | | | 0.26 | 0.26 | 1.32 | 1.34 | 2.91 | 6.04 |
| Central TX | | | 1.06 | 0.47 | 1.27 | 0.98 | 2.72 | 5.65 |
| Northern Plains | | | 0.52 | 0.31 | 0.81 | 0.61 | 1.73 | 3.59 |
| NE Texas | | | 0.14 | 0.20 | 0.49 | 0.40 | 1.09 | 2.27 |
| Mississippi | | | 0.13 | 0.11 | 0.47 | 0.34 | 0.92 | 1.91 |
| Houston | | | 0.10 | 0.23 | 0.36 | 0.30 | 0.90 | 1.86 |
| S Texas | | | 0.40 | 0.23 | 0.32 | 0.35 | 0.90 | 1.86 |
| Arkansas | | | 0.11 | 0.08 | 0.34 | 0.25 | 0.66 | 1.38 |
| Oklahoma | | | 0.10 | 0.08 | 0.24 | 0.10 | 0.42 | 0.87 |
| Tennessee | | | 0.04 | 0.04 | 0.19 | 0.17 | 0.40 | 0.82 |
| Mexico + Gulf | | | 0.00 | 0.00 | 0.20 | 0.18 | 0.38 | 0.78 |
| Alabama | | | 0.01 | 0.03 | 0.15 | 0.07 | 0.24 | 0.50 |
| Kentucky | | | 0.03 | 0.02 | 0.08 | 0.08 | 0.18 | 0.38 |
| W Texas | | | 0.06 | 0.02 | 0.04 | 0.05 | 0.11 | 0.23 |
| Florida | | | 0.00 | 0.01 | 0.02 | 0.01 | 0.04 | 0.07 |
| Georgia | | | 0.00 | 0.00 | 0.00 | 0.00 | 0.01 | 0.01 |
| Mid Atlantic | | | 0.00 | 0.00 | 0.00 | 0.00 | 0.00 | 0.00 |
| Northeast US | | | 0.00 | 0.00 | 0.00 | 0.00 | 0.00 | 0.00 |
| IC | 4.82 | | | | | | | |
| BC | | 33.17 | | | | | | |
| **Total** | **4.82** | **33.17** | **4.62** | **14.84** | **12.02** | **21.38** | **48.23** | **100.0** |

Notes:

Anthro is the sum of mobile, all points and area+offroad

% Anthro is 100 x Anthro/Total Anthro

**Table 9-10**. Episode average contributions from all source regions and emission groups to the Dallas/Fort Worth 4-County Core in CAMx Run 34 for the 2010 future year.

Episode Average Contributions to 8-hour Ozone (ppb)
Run run34sa.fy2010
Receptor DFW-4 County Core
#Grid-Hrs 4620
BaseO3 >= 85
AvgConc 91.5

| Source Reg | IC | BC | Biogenic | Mobile | All Points | Area+Offroad | Anthro | % Anthro |
|---|---|---|---|---|---|---|---|---|
| Dallas Co. | | | 0.22 | 6.62 | 1.64 | 9.00 | 17.26 | 35.16 |
| Tarrant Co. | | | 0.14 | 3.49 | 0.73 | 4.14 | 8.36 | 17.03 |
| Ellis Co. | | | 0.34 | 0.37 | 2.34 | 0.59 | 3.30 | 6.72 |
| Denton Co. | | | 0.21 | 1.27 | 0.18 | 1.01 | 2.46 | 5.01 |
| Collin Co. | | | 0.12 | 0.62 | 0.09 | 0.81 | 1.52 | 3.09 |
| Kaufman Co. | | | 0.16 | 0.23 | 0.28 | 0.16 | 0.67 | 1.37 |
| Johnson Co. | | | 0.09 | 0.13 | 0.07 | 0.22 | 0.42 | 0.86 |
| Rockwall Co. | | | 0.03 | 0.12 | 0.00 | 0.07 | 0.19 | 0.38 |
| Parker Co. | | | 0.01 | 0.03 | 0.01 | 0.03 | 0.08 | 0.15 |
| **DFW 9-County** | | | **1.32** | **12.88** | **5.34** | **16.03** | **34.25** | **69.77** |
| **DFW 16-County** | | | **1.44** | **12.98** | **5.70** | **16.26** | **34.95** | **71.19** |
| Louisiana | | | 0.30 | 0.28 | 1.47 | 1.50 | 3.25 | 6.63 |
| Central TX | | | 1.00 | 0.47 | 1.45 | 1.02 | 2.94 | 5.99 |
| Northern Plains | | | 0.49 | 0.31 | 0.85 | 0.59 | 1.74 | 3.55 |
| NE Texas | | | 0.15 | 0.22 | 0.53 | 0.45 | 1.20 | 2.45 |
| Mississippi | | | 0.15 | 0.12 | 0.53 | 0.37 | 1.02 | 2.08 |
| Houston | | | 0.11 | 0.23 | 0.37 | 0.31 | 0.90 | 1.83 |
| Arkansas | | | 0.11 | 0.08 | 0.40 | 0.29 | 0.76 | 1.55 |
| S Texas | | | 0.34 | 0.17 | 0.27 | 0.28 | 0.73 | 1.48 |
| Tennessee | | | 0.04 | 0.04 | 0.22 | 0.20 | 0.47 | 0.95 |
| Mexico + Gulf | | | 0.00 | 0.00 | 0.19 | 0.18 | 0.37 | 0.76 |
| Alabama | | | 0.01 | 0.03 | 0.14 | 0.06 | 0.23 | 0.48 |
| Kentucky | | | 0.03 | 0.02 | 0.09 | 0.09 | 0.21 | 0.43 |
| Oklahoma | | | 0.05 | 0.04 | 0.11 | 0.05 | 0.20 | 0.41 |
| W Texas | | | 0.04 | 0.01 | 0.03 | 0.03 | 0.07 | 0.15 |
| Florida | | | 0.00 | 0.01 | 0.02 | 0.01 | 0.03 | 0.07 |
| Georgia | | | 0.00 | 0.00 | 0.00 | 0.00 | 0.00 | 0.01 |
| Mid Atlantic | | | 0.00 | 0.00 | 0.00 | 0.00 | 0.00 | 0.00 |
| Northeast US | | | 0.00 | 0.00 | 0.00 | 0.00 | 0.00 | 0.00 |
| IC | 4.25 | | | | | | | |
| BC | | 33.89 | | | | | | |
| **Total** | **4.25** | **33.89** | **4.26** | **15.01** | **12.37** | **21.69** | **49.07** | **100.0** |

Notes:

Anthro is the sum of mobile, all points and area+offroad

% Anthro is 100 x Anthro/Total Anthro

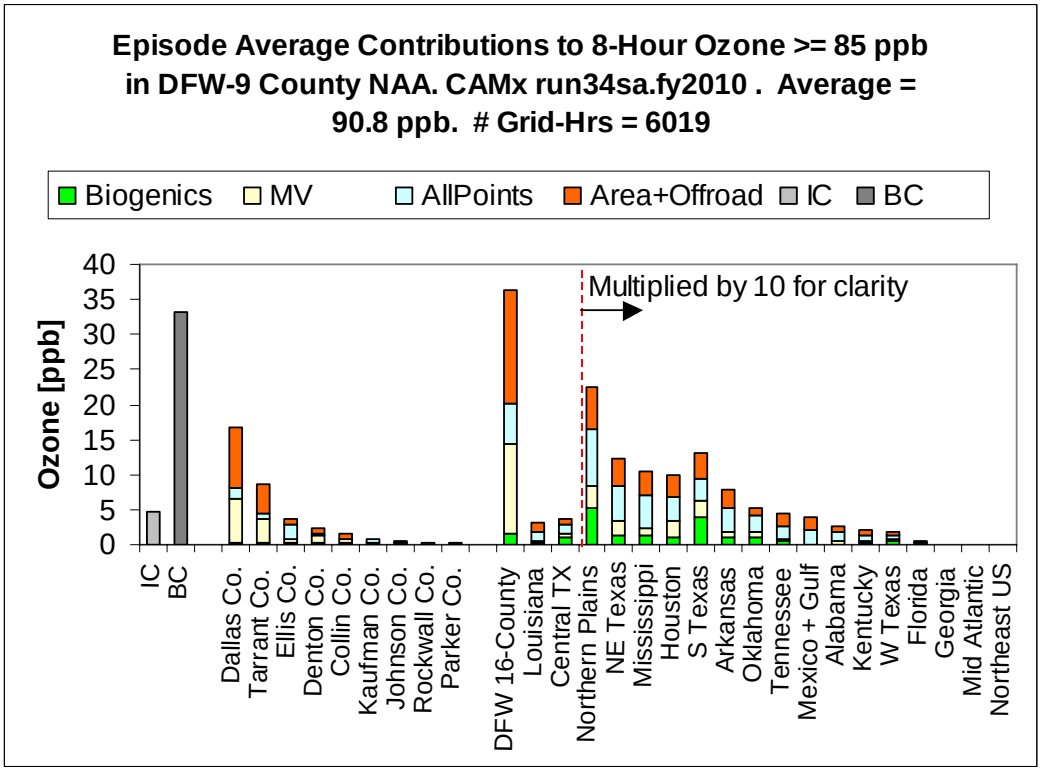


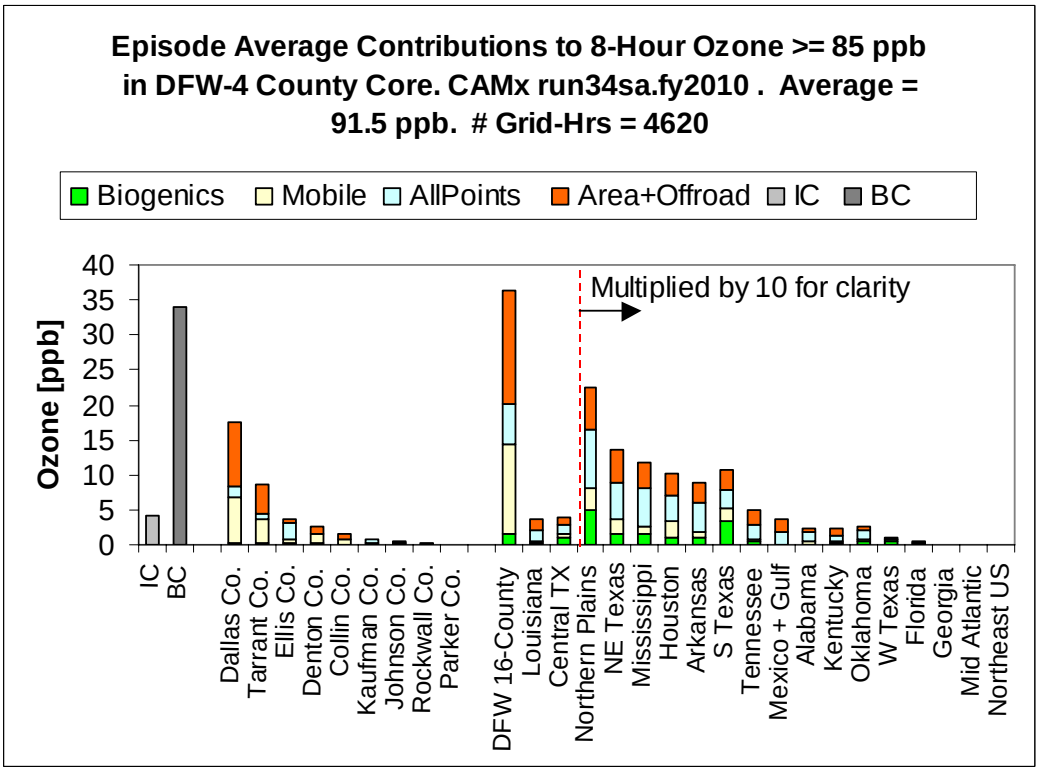


**Figures 9-5 and 9-6.** Bar charts of the episode average contribution to 8-hour ozone from all source regions and emission groups for Dallas/Fort Worth NAA (top) and 4-county core (bottom) using CAMx Run 34 for the 2010 future year.

**CAMx Run 36 for Future Year 2010: CAIR EGU Controls**

Run 36 applied CAIR EGU controls to the 2010 base case (Run 34). Using the ratio of statewide totals of annual average EGU emissions for the 2010 base case and 2010 controls, as found in the proposed CAIR guidelines (EPA, 2004), all EGUs were scaled by state-specific EGU reduction factors. Final guidelines, adopted in March 2005, were not available in time for this study, and may differ from the values used here.

Figure 9-7 plots the NOx EGU reduction factors that were used in this study for each state. Factors are also listed in Table 9-12. Texas' NOx emissions from EGUs were reduced by only 1%. Louisiana's EGU NOx was reduced by 26%. NOx EGU emissions in North and South Dakota were 9% and 50% higher, respectively.

Table 9-11 compares the total point source emissions for each of the 28 source regions on a weekday for the 2010 base case and for the EGU controls. The EGU controls reduced NOx emissions in both Kentucky and Florida by over 300 tons/day. Georgia, Tennessee, Alabama, Mississippi, and Louisiana each reduced EGU NOx by over 100 tons per day. Changes to VOC emissions from EGU controls were small.

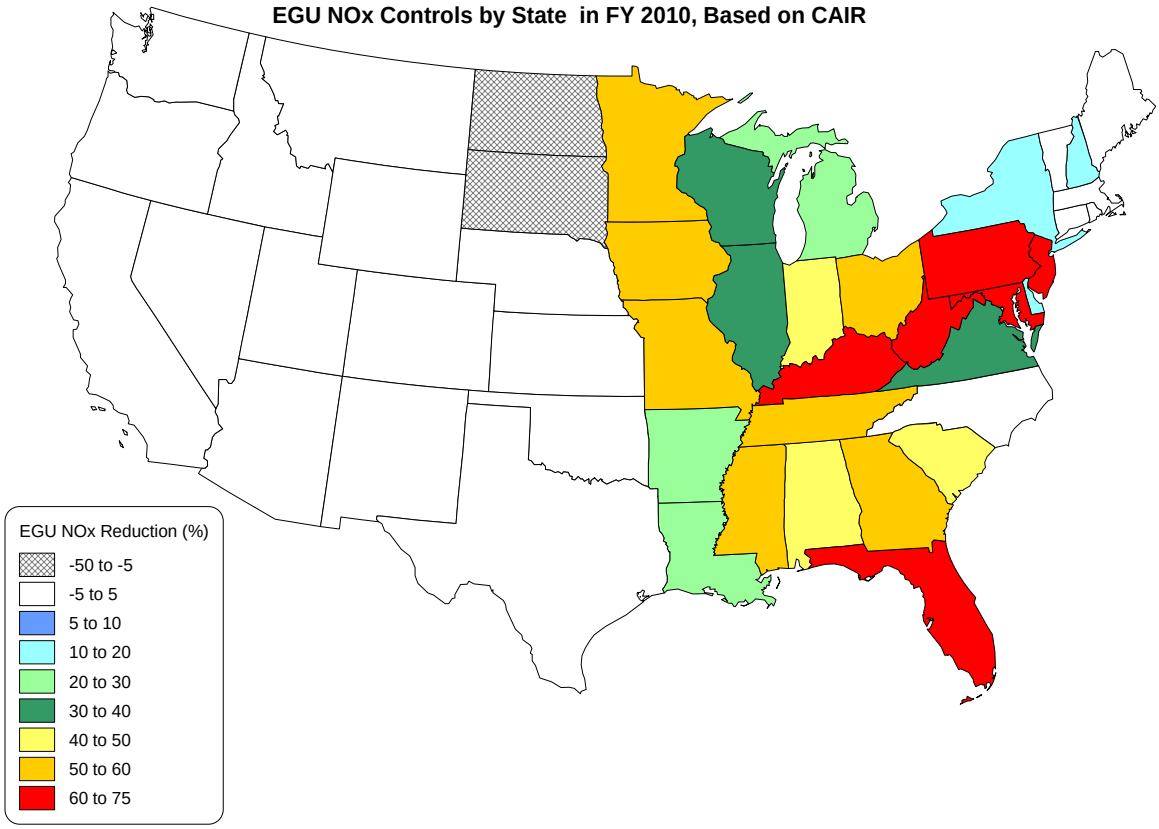


**Figure 9-7**. NOx control factors applied to EGUs for each state in future year 2010.

**Table 9-11**. A comparison of point source emissions between the 2010 base case and 2010 CAIR EGU control case.

| Region No. | Source Region | Point Source NOx Emissions (Elevated + Low-level) | | |
|---|---|---|---|---|
| | | 2010 Base Case (tons/day) | 2010 EGU Controls (tons/day) | Change in EGUs (tons/day) |
| 1 | Collin Co. | 3.0 | 3.0 | 0.0 |
| 2 | Dallas Co. | 18.5 | 18.4 | -0.1 |
| 3 | Denton Co. | 3.2 | 3.2 | 0.0 |
| 4 | Tarrant Co. | 11.9 | 11.9 | -0.1 |
| 5 | Parker Co. | 2.4 | 2.4 | 0.0 |
| 6 | Johnson Co. | 4.4 | 4.4 | 0.0 |
| 7 | Ellis Co. | 44.5 | 44.5 | 0.0 |
| 8 | Kaufman Co. | 6.8 | 6.8 | -0.1 |
| 9 | Rockwall Co. | 0.0 | 0.0 | 0.0 |
| | Outer DFW | 56.5 | 56.1 | -0.4 |
| 10 | DFW 16 county | 151.4 | 150.6 | -0.7 |
| 11 | NE Texas | 218.6 | 216.8 | -1.8 |
| 12 | Central TX | 199.0 | 197.3 | -1.6 |
| 13 | Houston | 293.6 | 293.1 | -0.5 |
| 14 | South Texas | 326.2 | 324.7 | -1.5 |
| 15 | West Texas | 188.0 | 187.1 | -1.0 |
| 16 | Gulf of Mexico/ Mexico | 616.9 | 600.2 | -16.7 |
| 17 | Oklahoma | 686.0 | 689.6 | 3.6 |
| 18 | Louisiana | 1021.8 | 917.7 | -104.1 |
| 19 | Arkansas | 386.0 | 305.3 | -80.8 |
| 20 | Mississippi | 561.9 | 403.5 | -158.4 |
| 21 | Alabama | 674.9 | 513.3 | -161.6 |
| 22 | Tennessee | 570.3 | 382.8 | -187.6 |
| 23 | Kentucky | 756.7 | 430.0 | -326.7 |
| 24 | Georgia | 636.3 | 356.5 | -279.8 |
| 25 | Florida | 631.9 | 309.6 | -322.3 |
| 26 | Mid Atlantic | 1950.1 | 1267.8 | -682.3 |
| 27 | Northeast US | 1833.3 | 1255.6 | -577.7 |
| 28 | Northern Plains | 6077.1 | 4375.2 | -1701.9 |
| | Total | 17779.9 | 13176.7 | -4603.2 |

Figure 9-8 displays spatial maps of the episode maximum 8-hour ozone for the 4-km and 12-km domains on the left and right columns, respectively. The top row shows the 2010 base case (Run 34). The center row shows the episode maxima when EGU controls are applied (Run 36). The bottom row shows the 8-hour ozone reduction from the EGU controls using the difference in episode maxima.

In the 12-km domain, Mississippi showed the largest decrease in episode maximum ozone, dropping up to 15 ppb near the Mississippi River; EGUs in this state were reduced 55%. The DFW NAA showed negligible decrease (-0.3 ppb) in episode maximum 8-hour ozone due to the

CAIR reductions because of the strong influence of local emissions on peak ozone levels in the DFW NAA. The largest change in episode maximum 8-hour ozone inside the 4-km domain was –1.1 ppb east of the DFW NAA. NOx emissions from EGUs in Texas were reduced only 1% by CAIR.

Figures 9-9 and 9-10 display bar charts showing the episode average contributions to the DFW NAA and 4-county core, respectively, from each source region and emissions group. Run 36 is plotted next to Run 34 for 2010 to show the subtle changes from the EGU controls. Both runs used the same set of grid cell hours equal to or exceeding 85 ppb in the Run 34 base case for 2010. The EGU controls reduced the episode average ozone exceeding 85 ppb by 0.3 ppb and 0.4 ppb in the DFW NAA and DFW core, respectively.

Further examination of the average ozone contributions from point sources between Runs 34 for 2010 and Run 36 is shown in Tables 9-12 and 9-13 for the DFW 9-county NAA and 4-county core, respectively. The EGU controls reduced the EGU contribution to episode average ozone exceeding 85 ppb by 0.6 ppb in both the DFW NAA and core areas. The reduction in EGU contribution (0.6 ppb) was greater than the total reduction in ozone (0.3 and 0.4 ppb, above) because ozone contributions from some non-EGU sources increased as EGU emissions were decreased. Greater ozone production from non-EGU sources in response to EGU controls is an aspect of the non-linear relationship between ozone formation and NOx levels.

The states that experienced the largest percentage EGU NOx reductions due to CAIR generally had the largest percent reduction in ozone contribution from all point sources, as can be seen in Figure 9-11. Louisiana, with a 26% NOx reduction in EGUs, reduced its ozone contribution from point sources by 8%. Mississippi, with a 55% NOx EGU reduction, reduced its ozone contribution from point sources by 21% for both DFW receptors.

Table 9-14 compares the peak ozone contribution to any grid-hour equal to or exceeding 85 ppb in the DFW NAA from point sources in each source region between Runs 34 (base case) and Run 36 (EGU controls). The largest point source contribution came from Ellis County at over 12 ppb in both runs. Ellis County was also the largest episode average contributor from point sources. The peak contribution from each source region within Texas did not change significantly between the two runs because the CAIR controls only reduced EGU NOx by 1%.

Outside of Texas, the Northern Plains had the largest base case peak contribution from point sources at 2.9 ppb, due to the size of the source region. When the CAIR controls were applied, Louisiana provided the largest peak contribution at 2.4 ppb. The fractional changes in the peak ozone contribution were similar to the fractional changes in the episode average contributions (Table 9-12), except in Arkansas, where the peak was reduced 11% and the average dropped 21%. In the DFW four-county core receptor, the peak contributions were identical to the nine-county receptor, except from Parker and Johnson Counties, whose peak contributions each dropped over 1 ppb, and from Oklahoma, which was 0.2 ppb lower.

Peak contributions to the DFW NAA from anthropogenic sources in the 2010 base case (Run 34) exceeded 2 ppb – one of the CAIR initial screening criteria for significant contributions -- in Louisiana, Arkansas, Oklahoma, and the Northern Plains; the CAIR controls did not reduce any of these states' contributions below 2 ppb, as shown in Table 15. The largest peak reduction was 0.45 ppb in the Northern Plains. Source regions with insignificant controls, including Texas and Oklahoma, showed slightly higher peak contributions.

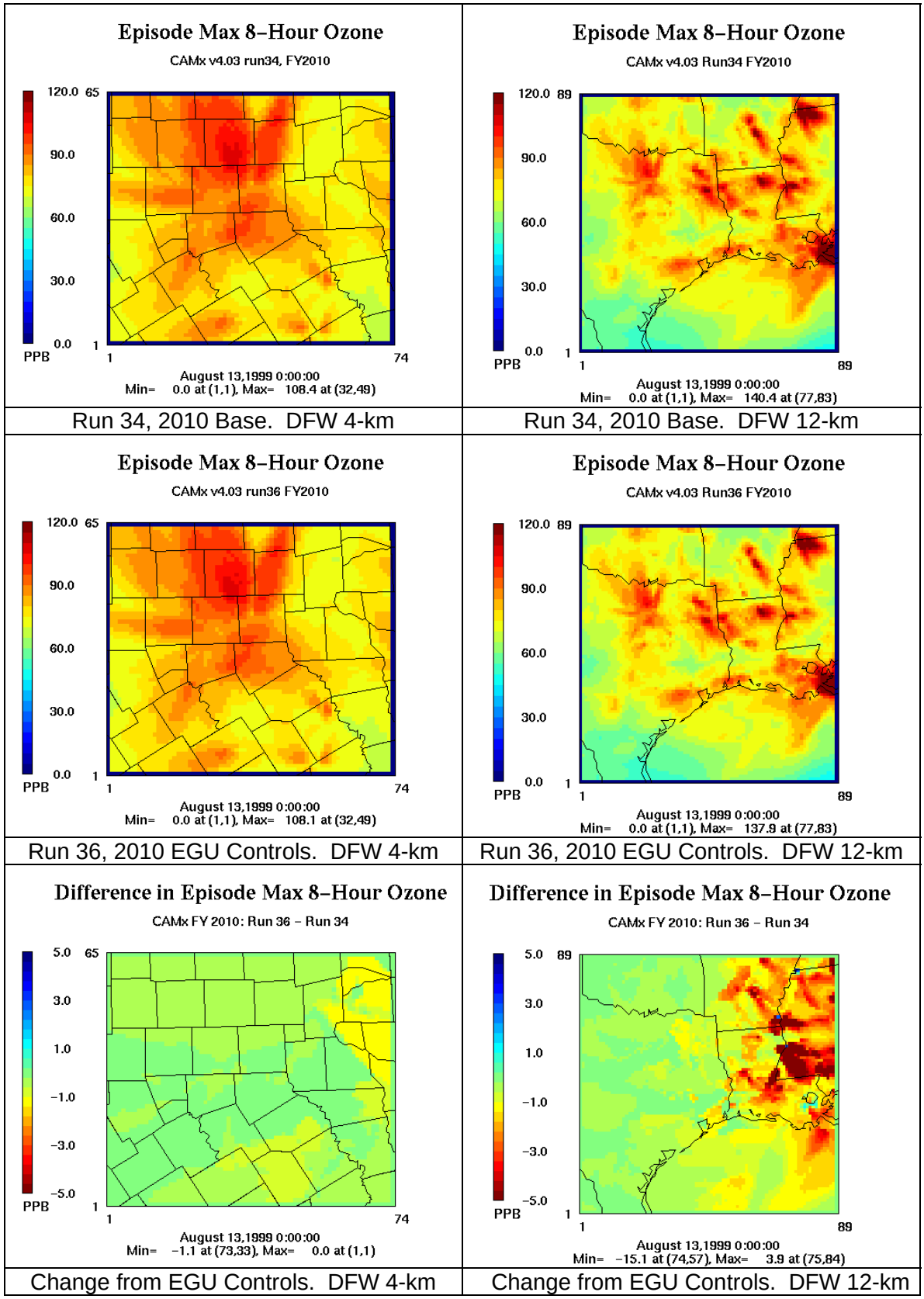


| Run 34, 2010 Base. DFW 4-km | Run 34, 2010 Base. DFW 12-km |
|---|---|
| Run 36, 2010 EGU Controls. DFW 4-km | Run 36, 2010 EGU Controls. DFW 12-km |
| Change from EGU Controls. DFW 4-km | Change from EGU Controls. DFW 12-km |

**Figure 9-8.** Spatial maps of the episode maximum 8-hour ozone in 2010 for the base case (run 34) and for the EGU controls (run 36) in the DFW 4-km and 12-km domains.

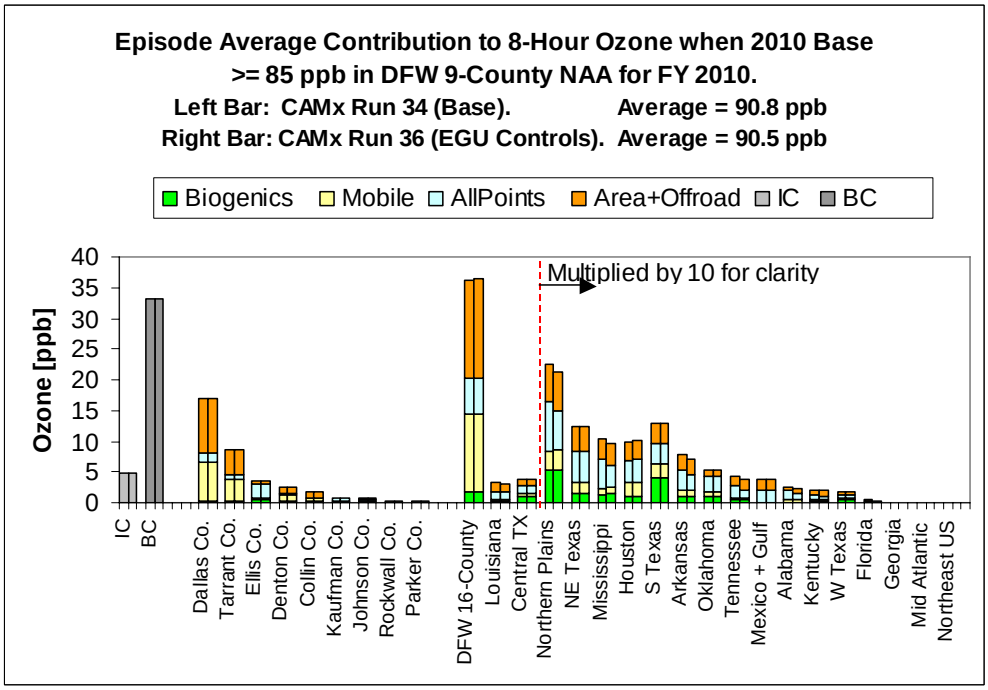


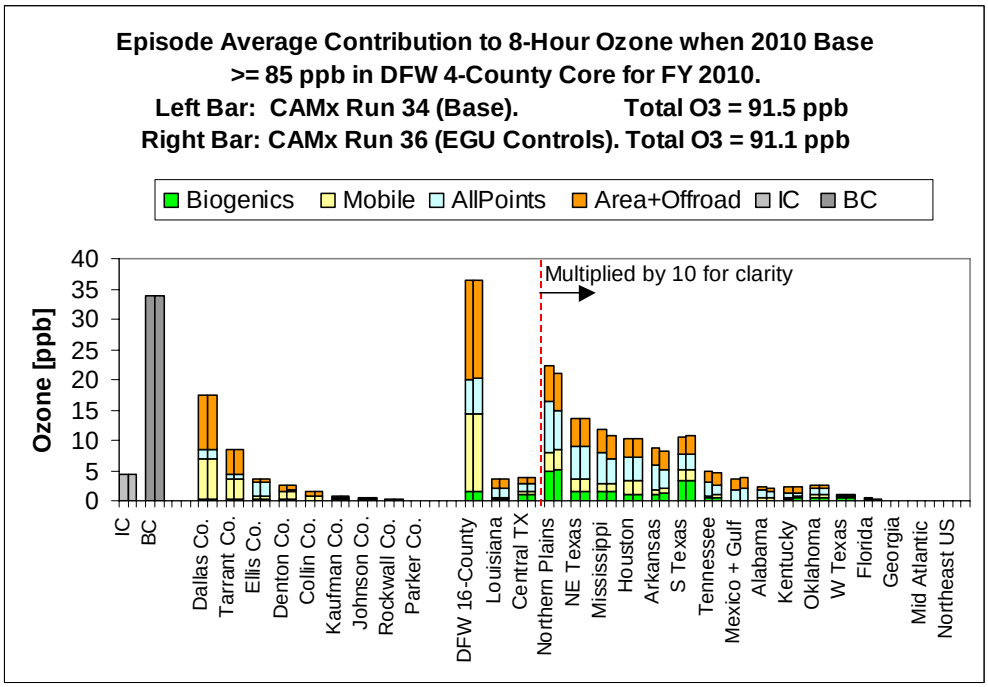


**Figures 9-9 and 9-10.** Episode average 2010 contributions to high 8-hour ozone from each source area and emission group to the DFW NAA (top) and 4-county core (bottom) in CAMx Runs 34 and 36.

**Table 9-12.** A comparison of 2010 episode average ozone contributions (ppb) from point sources with and without EGU controls in relation to each state's change in NOx controls from EGUs in the DFW NAA.

| O3 Contributions From All Point Sources | | | | | |
|---|---|---|---|---|---|
| Receptor | DFW-9 County NAA | | | | |
| #Grid-Hrs | 6019 | | | | |
| BaseO3 >= | 85 | | | | |
| Grid | DFW 04-km | | | | |
| **Run** | **Run 34: 2010 Base** | **Run 36: 2010 with EGU Controls** | **Ppb Change in Ozone** | **% Change in Ozone** | **% Change in Statewide EGU NOx Emissions** |
| Dallas Co. | 1.58 | 1.57 | -0.01 | -1% | -1% |
| Tarrant Co. | 0.77 | 0.77 | 0.00 | 0% | -1% |
| Ellis Co. | 2.25 | 2.26 | 0.01 | 0% | -1% |
| Denton Co. | 0.16 | 0.16 | 0.00 | 0% | -1% |
| Collin Co. | 0.10 | 0.10 | 0.00 | 0% | -1% |
| Kaufman Co. | 0.29 | 0.29 | 0.00 | 0% | -1% |
| Johnson Co. | 0.09 | 0.09 | 0.00 | 0% | -1% |
| Rockwall Co. | 0 | 0 | 0.00 | 0% | -1% |
| Parker Co. | 0.04 | 0.04 | 0.00 | 0% | -1% |
| **DFW 9-County** | **5.28** | **5.28** | **0.00** | **0%** | **-1%** |
| **DFW 16-County** | **5.72** | **5.72** | **0.00** | **0%** | **-1%** |
| Louisiana | 1.32 | 1.21 | -0.11 | -8% | -26% |
| Central TX | 1.27 | 1.27 | 0.00 | 0% | -1% |
| Northern Plains | 0.81 | 0.63 | -0.18 | -22% | -37% |
| NE Texas | 0.49 | 0.49 | 0.00 | 0% | -1% |
| Mississippi | 0.47 | 0.37 | -0.10 | -21% | -55% |
| Houston | 0.36 | 0.37 | 0.01 | 3% | -1% |
| S Texas | 0.32 | 0.32 | 0.00 | 0% | -1% |
| Arkansas | 0.34 | 0.27 | -0.07 | -21% | -27% |
| Oklahoma | 0.24 | 0.24 | 0.00 | 0% | 1% |
| Tennessee | 0.19 | 0.13 | -0.06 | -32% | -51% |
| Mexico + Gulf | 0.20 | 0.20 | 0.00 | 0% | 0% |
| Alabama | 0.15 | 0.12 | -0.03 | -20% | -45% |
| Kentucky | 0.08 | 0.05 | -0.03 | -38% | -61% |
| W Texas | 0.04 | 0.04 | 0.00 | 0% | -1% |
| Florida | 0.02 | 0.01 | -0.01 | -50% | -61% |
| Georgia | 0 | 0 | 0.00 | N/A | -57% |
| Mid Atlantic | 0 | 0 | 0.00 | N/A | |
| Northeast US | 0 | 0 | 0.00 | N/A | |
| **Total** | **12.02** | **11.44** | **-0.58** | **-5%** | |

**Table 9-13**. A comparison of 2010 episode average ozone contributions (ppb) from point sources with and without EGU controls in relation to each state's change in NOx controls from EGUs in the DFW 4-county core.

| | | | | | |
|---|---|---|---|---|---|
| O3 Contributions From All Point Sources | | | | | |
| Receptor | DFW-4 County Core | | | | |
| #Grid-Hrs | 4620 | | | | |
| BaseO3 >= | 85 | | | | |
| Grid | DFW04-km | | | | |
| **Run** | **Run 34: 2010 Base** | **Run 36: 2010 with EGU Controls** | **Ppb Change in Ozone** | **% Change in Ozone** | **% Change in Statewide EGU NOx emissions** |
| Dallas Co. | 1.64 | 1.63 | -0.01 | -1% | -1% |
| Tarrant Co. | 0.73 | 0.73 | 0.00 | 0% | -1% |
| Ellis Co. | 2.34 | 2.35 | 0.01 | 0% | -1% |
| Denton Co. | 0.18 | 0.18 | 0.00 | 0% | -1% |
| Collin Co. | 0.09 | 0.09 | 0.00 | 0% | -1% |
| Kaufman Co. | 0.28 | 0.28 | 0.00 | 0% | -1% |
| Johnson Co. | 0.07 | 0.07 | 0.00 | 0% | -1% |
| Rockwall Co. | 0 | 0 | 0.00 | N/A | -1% |
| Parker Co. | 0.01 | 0.01 | 0.00 | 0% | -1% |
| **DFW 9-County** | **5.34** | **5.34** | **0.00** | **0%** | **-1%** |
| **DFW 16-County** | **5.70** | **5.70** | **0.00** | **0%** | **-1%** |
| Louisiana | 1.47 | 1.35 | -0.12 | -8% | -26% |
| Central TX | 1.45 | 1.45 | 0.00 | 0% | -1% |
| Northern Plains | 0.85 | 0.65 | -0.20 | -24% | -37% |
| NE Texas | 0.53 | 0.53 | 0.00 | 0% | -1% |
| Mississippi | 0.53 | 0.42 | -0.11 | -21% | -55% |
| Houston | 0.37 | 0.37 | 0.00 | 0% | -1% |
| Arkansas | 0.40 | 0.32 | -0.08 | -20% | -27% |
| S Texas | 0.27 | 0.27 | 0.00 | 0% | -1% |
| Tennessee | 0.22 | 0.16 | -0.06 | -27% | -51% |
| Mexico + Gulf | 0.19 | 0.20 | 0.01 | 5% | 0% |
| Alabama | 0.14 | 0.11 | -0.03 | -21% | -45% |
| Kentucky | 0.09 | 0.06 | -0.03 | -33% | -61% |
| Oklahoma | 0.11 | 0.11 | 0.00 | 0% | 1% |
| W Texas | 0.03 | 0.03 | 0.00 | 0% | -1% |
| Florida | 0.02 | 0.01 | -0.01 | -50% | -61% |
| Georgia | 0 | 0 | 0.00 | N/A | |
| Mid Atlantic | 0 | 0 | 0.00 | N/A | |
| Northeast US | 0 | 0 | 0.00 | N/A | |
| **Total** | **12.37** | **11.74** | **-0.63** | **-5%** | |

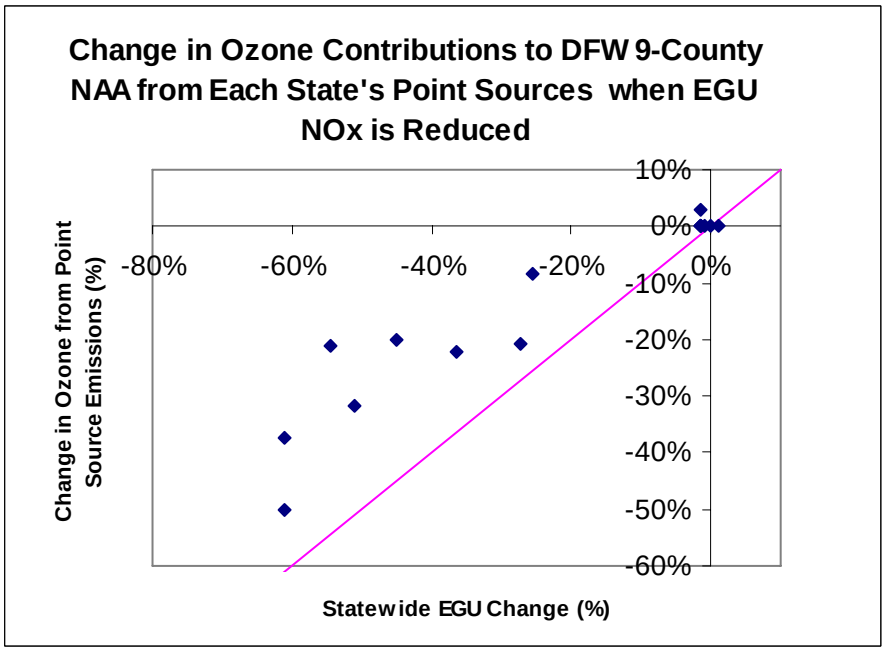


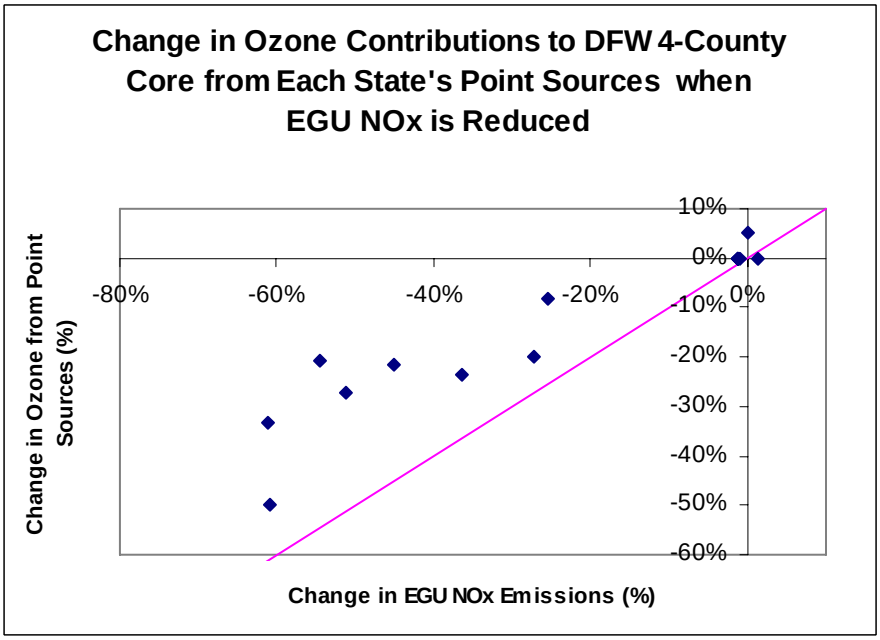


**Figure 9-11.** Change in episode average EGU contributions to high 8-hour ozone against change in emissions, by state, for the DFW NAA and 4-county core area.

**Table 9-14.** A comparison of 2010 peak ozone contributions (ppb) from point sources to the DFW NAA with and without EGU controls

| Max O3 Contributions From All Point Sources | | | | |
|---|---|---|---|---|
| Receptor | DFW-9 County NAA | | | |
| #Grid-Hrs | 6019 | | | |
| BaseO3 >= | 85 | | | |
| Grid | DFW 04-km | | | |
| **Run** | **Run 34: 2010 Base** | **Run 36: 2010 with EGU Controls** | **Ppb Change in Ozone** | **% Change in Ozone** |
| Ellis Co. | 12.22 | 12.29 | 0.07 | 1% |
| Tarrant Co. | 4.14 | 4.13 | -0.01 | 0% |
| Dallas Co. | 3.65 | 3.63 | -0.02 | -1% |
| Denton Co. | 2.24 | 2.23 | -0.01 | 0% |
| Kaufman Co. | 1.95 | 1.95 | 0.00 | 0% |
| Johnson Co. | 1.89 | 1.89 | 0.00 | 0% |
| Collin Co. | 1.71 | 1.71 | 0.00 | 0% |
| Parker Co. | 1.62 | 1.61 | -0.01 | -1% |
| Rockwall Co. | 0.00 | 0.00 | 0.00 | N/A |
| **DFW 9-County** | **13.20** | **13.20** | **0.00** | **0%** |
| **DFW 16-County** | **13.55** | **13.55** | **0.00** | **0%** |
| Central TX | 4.77 | 4.76 | -0.01 | 0% |
| NE Texas | 3.68 | 3.70 | 0.02 | 1% |
| Northern Plains | 2.88 | 2.33 | -0.55 | -19% |
| Louisiana | 2.60 | 2.43 | -0.17 | -7% |
| Arkansas | 2.56 | 2.28 | -0.28 | -11% |
| Oklahoma | 1.89 | 1.90 | 0.01 | 1% |
| S Texas | 1.56 | 1.56 | 0.00 | 0% |
| Mississippi | 1.00 | 0.81 | -0.19 | -19% |
| Houston | 0.93 | 0.94 | 0.01 | 1% |
| Mexico + Gulf | 0.78 | 0.80 | 0.02 | 3% |
| W Texas | 0.55 | 0.55 | 0.00 | 0% |
| Alabama | 0.53 | 0.42 | -0.11 | -21% |
| Tennessee | 0.35 | 0.23 | -0.12 | -34% |
| Kentucky | 0.21 | 0.12 | -0.09 | -43% |
| Florida | 0.07 | 0.04 | -0.03 | -43% |
| Georgia | 0.01 | 0.00 | -0.01 | -100% |
| Mid Atlantic | 0.00 | 0.00 | 0.00 | N/A |
| Northeast US | 0.00 | 0.00 | 0.00 | N/A |

**Table 9-15.** A comparison of 2010 peak ozone contributions (ppb) from anthropogenic sources to the DFW NAA with and without EGU controls

| Max O3 Contributions From Anthropogenic Sources | | | |
|---|---|---|---|
| Receptor | DFW-9 County NAA | | |
| #Grid-Hrs | 6019 | | |
| BaseO3 >= | 85 | | |
| Grid | DFW 04-km | | |
| **Run** | **Run 34: 2010 Base** | **Run 36: 2010 with EGU Controls** | **Ppb Change in Ozone** |
| Dallas Co. | 39.02 | 39.20 | 0.18 |
| Tarrant Co. | 29.54 | 29.63 | 0.09 |
| Ellis Co. | 16.83 | 16.92 | 0.09 |
| Denton Co. | 13.71 | 13.75 | 0.04 |
| Collin Co. | 10.51 | 10.52 | 0.01 |
| Johnson Co. | 5.20 | 5.20 | 0.00 |
| Kaufman Co. | 4.46 | 4.48 | 0.02 |
| Parker Co. | 4.23 | 4.22 | -0.01 |
| Rockwall Co. | 1.75 | 1.76 | 0.01 |
| **DFW 9 county** | **50.45** | **50.66** | **0.21** |
| **DFW 16 county** | **50.52** | **50.72** | **0.20** |
| Northern Plains | 8.10 | 7.65 | -0.45 |
| Central TX | 7.83 | 7.86 | 0.03 |
| NE Texas | 6.82 | 6.87 | 0.05 |
| Louisiana | 5.65 | 5.53 | -0.12 |
| Arkansas | 5.18 | 4.90 | -0.28 |
| S Texas | 3.99 | 3.99 | 0.00 |
| Oklahoma | 3.42 | 3.44 | 0.02 |
| Houston | 2.95 | 2.97 | 0.02 |
| Mississippi | 1.92 | 1.75 | -0.17 |
| Mexico + Gulf | 1.48 | 1.51 | 0.03 |
| W Texas | 1.35 | 1.35 | 0.00 |
| Tennessee | 0.89 | 0.85 | -0.04 |
| Alabama | 0.85 | 0.75 | -0.10 |
| Kentucky | 0.43 | 0.37 | -0.06 |
| Florida | 0.12 | 0.10 | -0.02 |
| Georgia | 0.02 | 0.01 | -0.01 |
| Northeast US | 0.01 | 0.01 | 0.00 |
| Mid Atlantic | 0.00 | 0.00 | 0.00 |

**CAMx Run 38 for 2010: APCA vs. APCA2**

Run 38 for the 2010 future year is identical to Run 36 except for the method of source apportionment. Both runs applied EGU controls and included additional NOx recycling reactions in the chemical mechanism (CB4xi). In the APCA technique (Anthropogenic Precursor Culpability Assessment), which was used for source apportionment in Runs 34 and Run 36, ozone contributions from each source region and emission group were tracked based on net changes in ozone due to chemistry. Net changes in ozone are always a trade-off between ozone production and destruction reactions. In APCA2, which was the method used in Run 38, ozone contributions are modified to separately reflect processes that increase and decrease ozone.

Tables 9-16 and 9-17 show episode average contributions from all source regions and emission groups in Run 38 to high 8-hour ozone in the DFW NAA and 4-county core, respectively. These tables also show the difference between Run 36 (APCA) and Run 38 (APCA2) for each source region and emission group over the same set of grid-hours exceeding 85 ppb. Average contributions changing at least 0.10 ppb are colored red for increases and blue for decreases.

The APCA2 method increased average ozone contributions from all source regions compared to APCA, except for the Northern Plains, initial conditions (ICs) and boundary conditions (BCs) that decreased. The contribution increases and decreases with APCA2 must cancel because the total ozone is the same with APCA2 and APCA. The contribution of BCs decreased by 5.5 ppb (16 %) using APCA2. The DFW 16-county source region showed the largest increase when using APCA2; contributions to the DFW NAA and core counties were 2.9 ppb and 2.7 ppb higher, respectively, with the bulk coming from Dallas and Tarrant Counties. Outside of the DFW region, ozone contributions from central Texas increased the most, followed by Louisiana. Bar charts comparing the contributions between APCA and APCA2 for the DFW 9-county NAA and 4-county core are shown in Figures 9-12 and 9-13, respectively.

APCA2 tends to decrease contributions from far distant sources (e.g., Northern Plains and boundary conditions) because APCA2 better accounts for chemical destruction of these ozone contributions over multi-day transport times. Contributions from local and nearby sources tend to increase because they are not strongly influenced by chemical decay. The contributions of sources at an upwind distance of about two States (e.g., Tennessee and Alabama) were about equal between APCA and APCA2.

Table 9-18 shows the episode peak anthropogenic contribution from each source region to 8-hour ozone in the DFW NAA between Runs 36 and 38. APCA2 had a higher peak than APCA in every source region except Tennessee, similar to the episode average contributions.

**Table 9-16.** Episode average contributions (ppb) from all source regions and emission groups to the DFW 9-county NAA in CAMx Run 38 (APCA2) for 2010, and difference in contributions between APCA2 and APCA.

Episode Average Contributions to 8-hour Ozone
Run run38sa.fy2010 (APCA2)
Receptor DFW-9 County
#Grid-Hrs 6019
Avg Conc 90.4

| | Episode Average from APCA2 | | | | | | Difference: Run 38 - Run 36 (APCA2 - APCA) | | | | | |
|---|---|---|---|---|---|---|---|---|---|---|---|---|
| Source Reg | IC/BC | Biogenic | Mobile | All Points | Area/Offroad | Anthro | IC/BC | Biogenic | Mobile | All Points | Area/Offroad | Anthro |
| Dallas Co. | | 0.30 | 6.62 | 1.66 | 9.45 | 17.72 | | 0.06 | 0.24 | 0.09 | 0.73 | 1.05 |
| Tarrant Co. | | 0.18 | 3.79 | 0.84 | 4.66 | 9.29 | | 0.03 | 0.23 | 0.07 | 0.43 | 0.73 |
| Ellis Co. | | 0.57 | 0.42 | 2.32 | 0.65 | 3.39 | | 0.19 | 0.05 | 0.06 | 0.07 | 0.17 |
| Denton Co. | | 0.30 | 1.29 | 0.19 | 1.10 | 2.58 | | 0.10 | 0.12 | 0.03 | 0.13 | 0.28 |
| Collin Co. | | 0.26 | 0.69 | 0.11 | 0.95 | 1.75 | | 0.11 | 0.07 | 0.01 | 0.12 | 0.20 |
| Kaufman Co. | | 0.21 | 0.26 | 0.32 | 0.18 | 0.76 | | 0.05 | 0.05 | 0.03 | 0.03 | 0.11 |
| Johnson Co. | | 0.17 | 0.18 | 0.10 | 0.29 | 0.57 | | 0.04 | 0.02 | 0.01 | 0.03 | 0.06 |
| Rockwall Co. | | 0.06 | 0.14 | 0.00 | 0.09 | 0.23 | | 0.02 | 0.02 | 0.00 | 0.01 | 0.03 |
| Parker Co. | | 0.01 | 0.08 | 0.05 | 0.08 | 0.20 | | -0.01 | 0.01 | 0.01 | 0.02 | 0.03 |
| **DFW 9-County** | | **2.06** | **13.47** | **5.59** | **17.45** | **36.49** | | **0.59** | **0.81** | **0.31** | **1.57** | **2.66** |
| **DFW 16-County** | | **2.31** | **13.66** | **6.11** | **17.84** | **37.60** | | **0.65** | **0.85** | **0.39** | **1.63** | **2.87** |
| Louisiana | | 0.27 | 0.33 | 1.43 | 1.57 | 3.32 | | 0.00 | 0.07 | 0.22 | 0.21 | 0.49 |
| Central TX | | 1.22 | 0.70 | 1.63 | 1.37 | 3.70 | | 0.16 | 0.23 | 0.36 | 0.38 | 0.97 |
| Northern Plains | | 0.46 | 0.33 | 0.62 | 0.63 | 1.58 | | -0.08 | 0.01 | -0.01 | 0.00 | 0.00 |
| NE Texas | | 0.11 | 0.30 | 0.64 | 0.55 | 1.48 | | -0.03 | 0.10 | 0.15 | 0.15 | 0.39 |
| Houston | | 0.08 | 0.30 | 0.44 | 0.39 | 1.12 | | -0.02 | 0.07 | 0.07 | 0.08 | 0.21 |
| S Texas | | 0.47 | 0.30 | 0.42 | 0.45 | 1.17 | | 0.07 | 0.07 | 0.10 | 0.10 | 0.27 |
| Mississippi | | 0.14 | 0.14 | 0.40 | 0.38 | 0.91 | | 0.00 | 0.03 | 0.03 | 0.04 | 0.08 |
| Arkansas | | 0.11 | 0.10 | 0.34 | 0.33 | 0.78 | | 0.00 | 0.02 | 0.07 | 0.07 | 0.17 |
| Oklahoma | | 0.10 | 0.12 | 0.33 | 0.14 | 0.59 | | 0.00 | 0.04 | 0.09 | 0.04 | 0.17 |
| Mexico + Gulf | | 0.00 | 0.00 | 0.39 | 0.40 | 0.79 | | 0.00 | 0.00 | 0.19 | 0.22 | 0.41 |
| Tennessee | | 0.04 | 0.04 | 0.13 | 0.17 | 0.34 | | 0.00 | 0.00 | 0.00 | 0.00 | -0.01 |
| Alabama | | 0.01 | 0.03 | 0.12 | 0.07 | 0.23 | | 0.00 | 0.00 | 0.00 | 0.00 | 0.02 |
| Kentucky | | 0.03 | 0.02 | 0.05 | 0.09 | 0.17 | | 0.00 | 0.00 | 0.00 | 0.00 | 0.01 |
| W Texas | | 0.06 | 0.03 | 0.06 | 0.07 | 0.16 | | 0.00 | 0.01 | 0.02 | 0.02 | 0.05 |
| Florida | | 0.00 | 0.01 | 0.02 | 0.02 | 0.05 | | 0.00 | 0.00 | 0.01 | 0.01 | 0.02 |
| Georgia | | 0.00 | 0.00 | 0.00 | 0.00 | 0.01 | | 0.00 | 0.00 | 0.00 | 0.00 | 0.01 |
| Mid Atlantic | | 0.00 | 0.00 | 0.00 | 0.00 | 0.00 | | 0.00 | 0.00 | 0.00 | 0.00 | 0.00 |
| Northeast US | | 0.00 | 0.00 | 0.00 | 0.00 | 0.00 | | 0.00 | 0.00 | 0.00 | 0.00 | 0.00 |
| IC | 3.40 | | | | | | -1.42 | | | | | |
| BC | 27.64 | | | | | | -5.51 | | | | | |
| **Total** | **31.04** | **5.41** | **16.41** | **13.13** | **24.47** | **54.00** | **-6.93** | **0.75** | **1.50** | **1.69** | **2.95** | **6.13** |

Notes:

Anthro is the sum of mobile, all points and area+offroad

Differences >0.10 are colored red, less than -0.10 are blue

**Table 9-17.** Episode average contributions (ppb) from all source regions and emission groups to the DFW 4-County Core in CAMx Run 38 (APCA2) for 2010; and difference in contributions between APCA2 and APCA.

Episode Average Contributions to 8-hour Ozone
Run run38sa.fy2010 (APCA2)
Receptor DFW-4 County Core
#Grid-Hrs 4620
AvgConc 91.1

| | Episode Average from APCA2 | | | | | | Difference: Run 38 - Run 36 (APCA2 - APCA) | | | | | |
|---|---|---|---|---|---|---|---|---|---|---|---|---|
| **Source Region** | **IC/BC** | **Biogenic** | **Mobile** | **All Points** | **Area/Offroad** | **Anthro** | **IC/BC** | **Biogenic** | **Mobile** | **All Points** | **Area/Offroad** | **Anthro** |
| Dallas Co. | | 0.29 | 6.86 | 1.70 | 9.75 | 18.31 | | 0.07 | 0.21 | 0.07 | 0.72 | 0.99 |
| Tarrant Co. | | 0.17 | 3.73 | 0.79 | 4.57 | 9.08 | | 0.03 | 0.23 | 0.06 | 0.41 | 0.69 |
| Ellis Co. | | 0.50 | 0.40 | 2.38 | 0.64 | 3.43 | | 0.16 | 0.02 | 0.03 | 0.05 | 0.11 |
| Denton Co. | | 0.31 | 1.43 | 0.20 | 1.17 | 2.80 | | 0.10 | 0.15 | 0.02 | 0.15 | 0.33 |
| Collin Co. | | 0.22 | 0.69 | 0.10 | 0.93 | 1.72 | | 0.10 | 0.07 | 0.01 | 0.11 | 0.20 |
| Kaufman Co. | | 0.21 | 0.28 | 0.31 | 0.19 | 0.78 | | 0.05 | 0.05 | 0.03 | 0.03 | 0.11 |
| Johnson Co. | | 0.13 | 0.14 | 0.08 | 0.24 | 0.46 | | 0.04 | 0.01 | 0.01 | 0.01 | 0.04 |
| Rockwall Co. | | 0.05 | 0.13 | 0.00 | 0.08 | 0.22 | | 0.02 | 0.01 | 0.00 | 0.01 | 0.03 |
| Parker Co. | | 0.01 | 0.03 | 0.02 | 0.04 | 0.09 | | 0.00 | 0.00 | 0.01 | 0.01 | 0.01 |
| **DFW 9-County** | | **1.89** | **13.69** | **5.58** | **17.61** | **36.89** | | **0.57** | **0.75** | **0.24** | **1.50** | **2.51** |
| **DFW 16-County** | | **2.04** | **13.82** | **5.99** | **17.90** | **37.72** | | **0.60** | **0.78** | **0.29** | **1.55** | **2.65** |
| Louisiana | | 0.32 | 0.37 | 1.62 | 1.79 | 3.77 | | 0.01 | 0.08 | 0.27 | 0.27 | 0.62 |
| Central TX | | 1.13 | 0.73 | 1.86 | 1.44 | 4.02 | | 0.13 | 0.25 | 0.41 | 0.41 | 1.07 |
| Northern Plains | | 0.44 | 0.32 | 0.63 | 0.59 | 1.54 | | -0.08 | 0.00 | -0.02 | -0.02 | -0.04 |
| NE Texas | | 0.11 | 0.32 | 0.69 | 0.61 | 1.63 | | -0.04 | 0.10 | 0.16 | 0.16 | 0.43 |
| Mississippi | | 0.17 | 0.16 | 0.45 | 0.43 | 1.03 | | 0.01 | 0.04 | 0.03 | 0.05 | 0.10 |
| Houston | | 0.09 | 0.30 | 0.44 | 0.40 | 1.14 | | -0.02 | 0.07 | 0.07 | 0.09 | 0.23 |
| S Texas | | 0.42 | 0.23 | 0.38 | 0.38 | 0.99 | | 0.08 | 0.06 | 0.11 | 0.09 | 0.26 |
| Arkansas | | 0.12 | 0.10 | 0.40 | 0.37 | 0.88 | | 0.00 | 0.02 | 0.08 | 0.08 | 0.19 |
| Tennessee | | 0.04 | 0.05 | 0.16 | 0.21 | 0.41 | | -0.01 | 0.00 | 0.00 | 0.00 | 0.00 |
| Mexico + Gulf | | 0.00 | 0.00 | 0.40 | 0.40 | 0.79 | | 0.00 | 0.00 | 0.20 | 0.22 | 0.41 |
| Alabama | | 0.01 | 0.03 | 0.12 | 0.07 | 0.22 | | 0.00 | 0.00 | 0.01 | 0.01 | 0.01 |
| Oklahoma | | 0.05 | 0.06 | 0.16 | 0.07 | 0.30 | | 0.00 | 0.02 | 0.05 | 0.02 | 0.10 |
| Kentucky | | 0.04 | 0.03 | 0.06 | 0.11 | 0.20 | | 0.00 | 0.00 | 0.00 | 0.00 | 0.01 |
| W Texas | | 0.04 | 0.02 | 0.04 | 0.04 | 0.10 | | 0.00 | 0.01 | 0.01 | 0.01 | 0.03 |
| Florida | | 0.00 | 0.01 | 0.02 | 0.02 | 0.05 | | 0.00 | 0.00 | 0.01 | 0.01 | 0.02 |
| Georgia | | 0.00 | 0.00 | 0.00 | 0.00 | 0.01 | | 0.00 | 0.00 | 0.00 | 0.00 | 0.01 |
| Mid Atlantic | | 0.00 | 0.00 | 0.00 | 0.00 | 0.00 | | 0.00 | 0.00 | 0.00 | 0.00 | 0.00 |
| Northeast US | | 0.00 | 0.00 | 0.00 | 0.00 | 0.00 | | 0.00 | 0.00 | 0.00 | 0.00 | 0.00 |
| IC | 2.92 | | | | | | -1.33 | | | | | |
| BC | 28.37 | | | | | | -5.50 | | | | | |
| Total | 31.29 | 5.02 | 16.55 | 13.42 | 24.83 | 54.80 | -6.83 | 0.68 | 1.43 | 1.68 | 2.95 | 6.10 |

Notes:

Anthro is the sum of mobile, all points and area+offroad

Differences >0.10 are colored red, less than -0.10 are blue

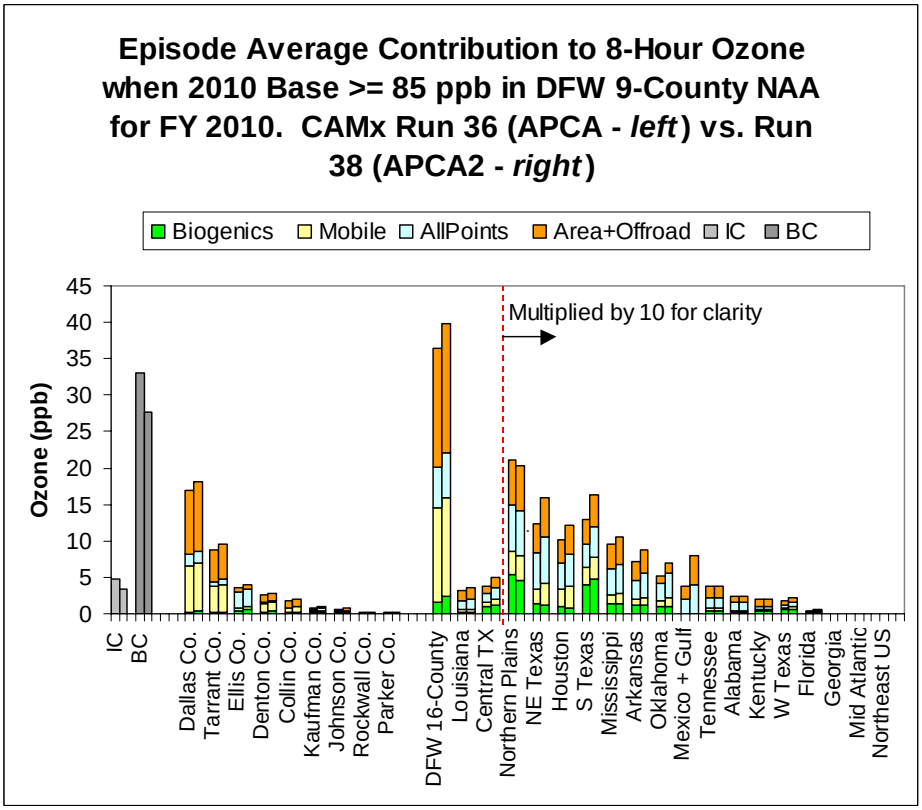


**Figure 9-12.** Episode average 2010 contributions to high 8-hour ozone in the DFW NAA for Run 36 (APCA) and Run 38 (APCA2).

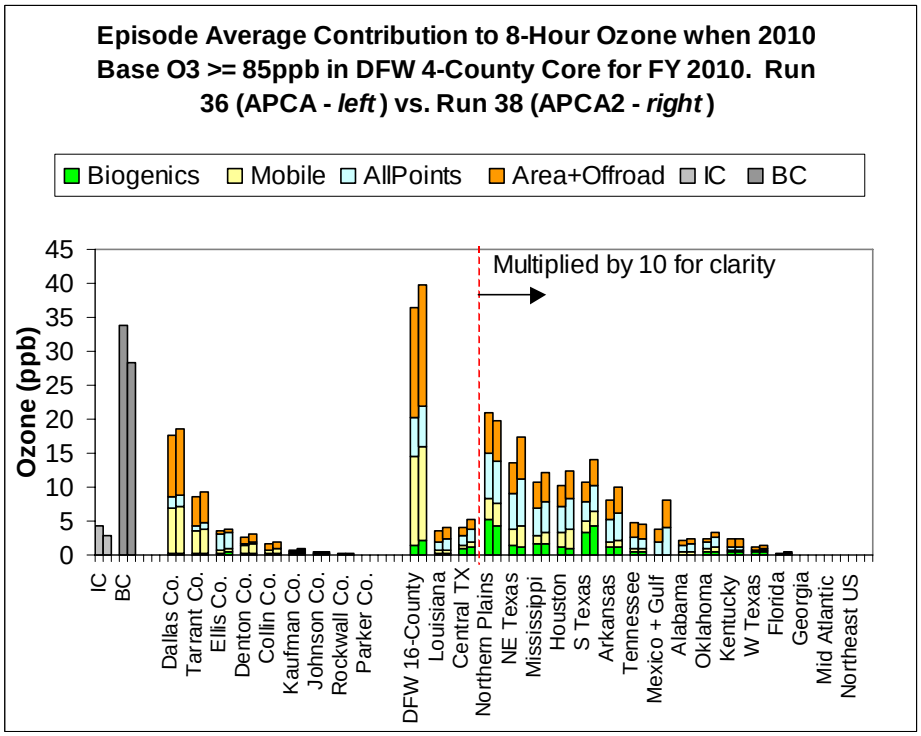


**Figure 9-13.** Episode average 2010 contributions to high 8-hour ozone in the DFW 4-county core for Run 36 (APCA) and Run 38 (APCA2).

**Table 9-18.** A comparison of APCA and APCA2 2010 peak 8-hour ozone contributions (ppb) from anthropogenic sources to the DFW NAA.

| Max O3 Contributions From Anthropogenic Sources | | | |
|---|---|---|---|
| Receptor | DFW-9 County NAA | | |
| BaseO3 >= | 85 | | |
| Grid | DFW 04-km | | |
| **Source Region** | **Run 36: APCA** | **Run 38: APCA2** | **APCA2 - APCA** |
| Dallas Co. | 39.20 | 40.34 | 1.14 |
| Tarrant Co. | 29.63 | 31.62 | 1.99 |
| Ellis Co. | 16.92 | 18.38 | 1.46 |
| Denton Co. | 13.75 | 15.68 | 1.93 |
| Collin Co. | 10.52 | 11.25 | 0.73 |
| Johnson Co. | 5.20 | 5.65 | 0.45 |
| Kaufman Co. | 4.48 | 5.27 | 0.79 |
| Parker Co. | 4.22 | 4.97 | 0.75 |
| Rockwall Co. | 1.76 | 2.03 | 0.27 |
| **DFW 9-county** | **50.66** | **52.21** | **1.55** |
| **DFW 16-county** | **50.72** | **52.31** | **1.59** |
| Central TX | 7.86 | 9.18 | 1.32 |
| Northern Plains | 7.65 | 9.17 | 1.52 |
| NE Texas | 6.87 | 7.88 | 1.01 |
| Louisiana | 5.53 | 7.46 | 1.93 |
| Arkansas | 4.90 | 6.32 | 1.42 |
| S Texas | 3.99 | 5.18 | 1.19 |
| Oklahoma | 3.44 | 5.23 | 1.79 |
| Houston | 2.97 | 3.72 | 0.75 |
| Mississippi | 1.75 | 2.10 | 0.35 |
| Mexico + Gulf | 1.51 | 3.28 | 1.77 |
| W Texas | 1.35 | 1.69 | 0.34 |
| Tennessee | 0.85 | 0.78 | -0.07 |
| Alabama | 0.75 | 0.78 | 0.03 |
| Kentucky | 0.37 | 0.40 | 0.03 |
| Florida | 0.10 | 0.16 | 0.06 |
| Georgia | 0.01 | 0.02 | 0.01 |
| Northeast US | 0.01 | 0.01 | 0.00 |
| Mid Atlantic | 0.00 | 0.00 | 0.00 |

Note: Differences >0.10 are colored red, less than -0.10 are blue.

**CAMx Run 37 for 2010: Meteorology Sensitivity Run**

The fourth source apportionment run evaluates ozone contributions to the Dallas/Fort Worth area using a different set of meteorology inputs. Run 37 inputs were extracted from MM5 Run 7, which used the Pleim-Xiu PBL and Grell convective scheme, which had been used in CAMx Run 25 for 1999 as discussed in Section 5. NOx recycling reactions and CAIR EGU controls were included in this run. Run 37 was compared to Run 36 which used meteorology from MM5 Run 6.

Spatial plots of the episode maximum 8-hour ozone are provided in Figure 9-14. The left column shows the 4-km domain and the right column shows the 12-km domain. Plots of Run 37 are shown in the center row. Plots of the maxima from Run 36 are in the top row for comparison. The bottom row shows the difference in episode maxima when using the different meteorology.

Run 37 simulated a slightly higher peak that was more eastward in Denton County compared to Run 36. Run 37 also predicted peak 8-hour ozone up to 19 ppb lower over Dallas County. In the 12 km domain, Run 37 simulated nearly 30 ppb more ozone near Houston than Run 36. Ozone model performance near Houston was not evaluated to determine which meteorological fields performed better there since this task focused on DFW.

The episode average source apportionments using the standard APCA technique are shown in Tables 9-19 and 9-20 for the DFW NAA and 4-county core, respectively. Since the different meteorology leads to 8-hour ozone exceeding 85 ppb at different times and hours, the episode averages for Run 37 were calculated for all grid hours when 8-hour ozone was equal to or greater than 85 ppb from Run 37. Run 37 had 3544 grid-hours exceeding 85 ppb in the DFW NAA (Table 9-19) whereas Run 36 had 6019.

Run 37 had 41% and 42% fewer grid hours equal to or exceeding 85 ppb than Run 36 in the DFW NAA and 4-county core, respectively. The total average ozone above 85 ppb also was lower in Run 37 compared to Run 36. Tables 9-19 and 9-20 show the difference in episode average contributions between Runs 36 and 37 for each source region and emission group. Average contributions changing at least 0.10 ppb are colored red for increases and blue for decreases.

Local sources and source regions north and east of DFW contributed more to both DFW receptor areas in Run 37 compared to Run 36. These source regions include the 16-county DFW region, northeast Texas, Arkansas, and Oklahoma. Contributions from source regions south of DFW – central Texas, southern Texas, and Mexico/Gulf of Mexico – contributed less in Run 37. The Houston source region was an exception amid areas to the south of DFW, contributing more in Run 37 than in Run 36, because Run 37 produced more ozone in the Houston area (Figure 9-14).

Run 37 was less reliant on boundary contributions, which averaged 2 ppb lower than Run 36. This was partially offset by higher initial conditions and higher contributions from anthropogenic sources. Bar charts of episode average contributions from all source regions and emission groups from Runs 36 and 37 are displayed in Figures 9-15 and 9-16 for the DFW NAA and four county core area.

Peak anthropogenic contributions from each source region to the DFW NAA from Runs 36 and 37 are listed in Table 9-21. No distinctive pattern was detected because the peak contribution from each source region between the two runs could occur at different times. Excluding differences within individual counties in the DFW NAA, the largest difference in peak anthropogenic contributions came from Houston, where Run 37 was 2 ppb larger than Run 36. Again, this was most likely due to the higher levels of ozone simulated near Houston in Run 37. Oklahoma, south Texas, and Louisiana also showed higher anthropogenic peaks in Run 37; northeast Texas and central Texas were lower.

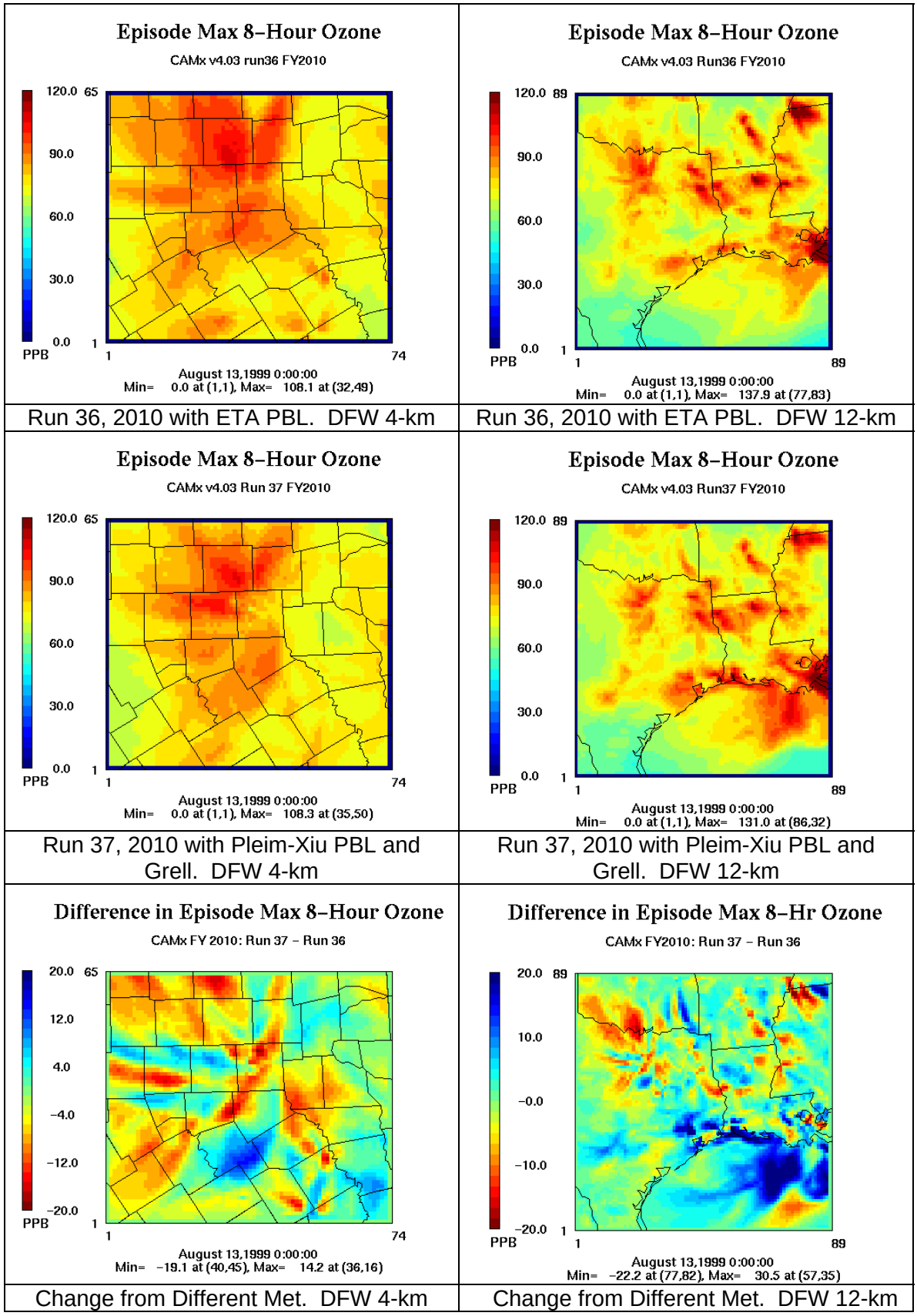


| Run 36, 2010 with ETA PBL. DFW 4-km | Run 36, 2010 with ETA PBL. DFW 12-km |
|---|---|
| Run 37, 2010 with Pleim-Xiu PBL and Grell. DFW 4-km | Run 37, 2010 with Pleim-Xiu PBL and Grell. DFW 12-km |
| Change from Different Met. DFW 4-km | Change from Different Met. DFW 12-km |

**Figure 9-14.** Spatial maps of the episode maximum 8-hour ozone in 2010 for CAMx Runs 36 and 37 using different meteorological inputs: DFW 4-km (left) and 12-km (right) domain

**Table 9-19**. Episode average contributions (ppb) from all source regions and emission groups to the DFW NAA in CAMx Run 37 for 2010, and the difference in contributions between Runs 36 and 37 for 2010.

Episode Average Contributions to 8-hour Ozone
Run run37sa.fy2010.a0
Receptor DFW-9 County NAA
#Grid-Hrs 3544
AvgConc 89.9

| | Episode Average from Run 37 for 2010 | | | | | | Difference: Run 37 - Run 36 | | | | | |
|---|---|---|---|---|---|---|---|---|---|---|---|---|
| **Source Reg** | **IC/BC** | **Biogenic** | **Mobile** | **All Points** | **Area + Offroad** | **Anthro** | **IC/BC** | **Biogenic** | **Mobile** | **All Points** | **Area + Offroad** | **Anthro** |
| Dallas Co. | | 0.26 | 6.41 | 1.74 | 9.05 | 17.20 | | 0.02 | 0.03 | 0.17 | 0.33 | 0.53 |
| Tarrant Co. | | 0.16 | 3.89 | 0.85 | 4.64 | 9.37 | | 0.01 | 0.33 | 0.08 | 0.41 | 0.81 |
| Ellis Co. | | 0.31 | 0.30 | 2.10 | 0.47 | 2.88 | | -0.07 | -0.07 | -0.16 | -0.11 | -0.34 |
| Denton Co. | | 0.19 | 1.17 | 0.15 | 0.98 | 2.29 | | -0.01 | 0.00 | -0.01 | 0.01 | -0.01 |
| Collin Co. | | 0.14 | 0.61 | 0.09 | 0.82 | 1.53 | | -0.01 | -0.01 | -0.01 | -0.01 | -0.02 |
| Kaufman Co. | | 0.18 | 0.25 | 0.36 | 0.18 | 0.80 | | 0.02 | 0.04 | 0.07 | 0.03 | 0.15 |
| Johnson Co. | | 0.10 | 0.15 | 0.08 | 0.26 | 0.49 | | -0.03 | -0.01 | -0.01 | 0.00 | -0.02 |
| Rockwall Co. | | 0.05 | 0.14 | 0.00 | 0.09 | 0.24 | | 0.01 | 0.02 | 0.00 | 0.01 | 0.04 |
| Parker Co. | | 0.01 | 0.07 | 0.04 | 0.06 | 0.17 | | -0.01 | 0.00 | 0.00 | 0.00 | 0.00 |
| **DFW 9-County** | | **1.40** | **12.99** | **5.41** | **16.55** | **34.97** | | **-0.07** | **0.33** | **0.13** | **0.67** | **1.14** |
| **DFW 16-County** | | **1.56** | **13.12** | **5.68** | **16.83** | **35.64** | | **-0.10** | **0.31** | **-0.04** | **0.62** | **0.91** |
| Louisiana | | 0.26 | 0.27 | 1.19 | 1.36 | 2.81 | | -0.01 | 0.01 | -0.02 | 0.00 | -0.02 |
| Central TX | | 0.74 | 0.36 | 0.90 | 0.71 | 1.97 | | -0.32 | -0.11 | -0.37 | -0.28 | -0.76 |
| Northern Plains | | 0.52 | 0.29 | 0.59 | 0.58 | 1.46 | | -0.02 | -0.03 | -0.04 | -0.05 | -0.12 |
| NE Texas | | 0.18 | 0.37 | 0.83 | 0.65 | 1.85 | | 0.04 | 0.17 | 0.34 | 0.25 | 0.76 |
| Houston | | 0.14 | 0.34 | 0.42 | 0.41 | 1.17 | | 0.04 | 0.11 | 0.05 | 0.10 | 0.26 |
| S Texas | | 0.27 | 0.18 | 0.20 | 0.25 | 0.63 | | -0.13 | -0.05 | -0.12 | -0.10 | -0.27 |
| Mississippi | | 0.14 | 0.12 | 0.35 | 0.34 | 0.81 | | 0.00 | 0.01 | -0.02 | 0.00 | -0.02 |
| Arkansas | | 0.15 | 0.13 | 0.45 | 0.40 | 0.98 | | 0.04 | 0.05 | 0.18 | 0.14 | 0.37 |
| Oklahoma | | 0.10 | 0.10 | 0.35 | 0.13 | 0.58 | | 0.00 | 0.02 | 0.11 | 0.03 | 0.16 |
| Mexico + Gulf | | 0.00 | 0.00 | 0.11 | 0.11 | 0.22 | | 0.00 | 0.00 | -0.09 | -0.07 | -0.16 |
| Tennessee | | 0.04 | 0.04 | 0.13 | 0.18 | 0.34 | | 0.00 | 0.00 | 0.00 | 0.01 | -0.01 |
| Alabama | | 0.01 | 0.02 | 0.07 | 0.04 | 0.12 | | 0.00 | -0.01 | -0.05 | -0.03 | -0.09 |
| Kentucky | | 0.02 | 0.01 | 0.03 | 0.05 | 0.09 | | -0.01 | -0.01 | -0.02 | -0.04 | -0.07 |
| W Texas | | 0.06 | 0.01 | 0.03 | 0.04 | 0.08 | | 0.00 | -0.01 | -0.01 | -0.01 | -0.03 |
| Florida | | 0.00 | 0.01 | 0.01 | 0.01 | 0.03 | | 0.00 | 0.00 | 0.00 | 0.00 | 0.00 |
| Georgia | | 0.00 | 0.00 | 0.00 | 0.00 | 0.01 | | 0.00 | 0.00 | 0.00 | 0.00 | 0.01 |
| Mid Atlantic | | 0.00 | 0.00 | 0.00 | 0.00 | 0.00 | | 0.00 | 0.00 | 0.00 | 0.00 | 0.00 |
| Northeast US | | 0.00 | 0.00 | 0.00 | 0.00 | 0.00 | | 0.00 | 0.00 | 0.00 | 0.00 | 0.00 |
| IC | 5.66 | | | | | | 0.84 | | | | | |
| BC | 31.21 | | | | | | -1.94 | | | | | |
| **Total** | **36.87** | **4.19** | **15.37** | **11.34** | **22.09** | **48.79** | **-1.10** | **-0.47** | **0.46** | **-0.10** | **0.57** | **0.92** |

Notes:

Anthro is the sum of mobile, all points and area+offroad

Differences >0.10 are colored red, less than -0.10 are blue

**Table 9-20.** Episode average contributions (ppb) from all source regions and emission groups to the DFW 4-county core in CAMx Run 37 for 2010, and the difference in contributions between Runs 36 and 37 for 2010.

Episode Average Contributions to 8-hour Ozone
Run run37sa.fy2010.a0
Receptor DFW-4 County Core
#Grid-Hrs 2690
AvgConc 90.4

| | Episode Average from Run 37 for 2010 | | | | | | Difference: Run 37 - Run 36 | | | | | |
|---|---|---|---|---|---|---|---|---|---|---|---|---|
| **Source Reg** | **IC/BC** | **Biogenic** | **Mobile** | **All Points** | **Area+Offroad** | **Anthro** | **IC/BC** | **Biogenic** | **Mobile** | **All Points** | **Area+Offroad** | **Anthro** |
| Dallas Co. | | 0.23 | 6.59 | 1.77 | 9.24 | 17.60 | | 0.01 | -0.06 | 0.14 | 0.21 | 0.28 |
| Tarrant Co. | | 0.14 | 3.87 | 0.76 | 4.56 | 9.20 | | 0.00 | 0.37 | 0.03 | 0.40 | 0.81 |
| Ellis Co. | | 0.22 | 0.25 | 1.98 | 0.41 | 2.64 | | -0.12 | -0.13 | -0.37 | -0.18 | -0.68 |
| Denton Co. | | 0.20 | 1.29 | 0.16 | 1.04 | 2.49 | | -0.01 | 0.01 | -0.02 | 0.02 | 0.02 |
| Collin Co. | | 0.14 | 0.65 | 0.10 | 0.87 | 1.62 | | 0.02 | 0.03 | 0.01 | 0.05 | 0.10 |
| Kaufman Co. | | 0.20 | 0.29 | 0.39 | 0.21 | 0.89 | | 0.04 | 0.06 | 0.11 | 0.05 | 0.22 |
| Johnson Co. | | 0.07 | 0.12 | 0.08 | 0.22 | 0.41 | | -0.02 | -0.01 | 0.01 | -0.01 | -0.01 |
| Rockwall Co. | | 0.05 | 0.16 | 0.00 | 0.10 | 0.26 | | 0.02 | 0.04 | 0.00 | 0.03 | 0.07 |
| Parker Co. | | 0.00 | 0.02 | 0.01 | 0.02 | 0.05 | | -0.01 | -0.01 | 0.00 | -0.01 | -0.03 |
| **DFW 9-County** | | **1.25** | **13.24** | **5.25** | **16.67** | **35.16** | | **-0.07** | **0.30** | **-0.09** | **0.56** | **0.78** |
| **DFW 16-County** | | **1.34** | **13.32** | **5.45** | **16.84** | **35.59** | | **-0.10** | **0.28** | **-0.25** | **0.49** | **0.52** |
| Louisiana | | 0.31 | 0.31 | 1.37 | 1.57 | 3.25 | | 0.00 | 0.02 | 0.02 | 0.05 | 0.10 |
| Central TX | | 0.71 | 0.39 | 0.98 | 0.73 | 2.09 | | -0.29 | -0.09 | -0.47 | -0.30 | -0.86 |
| Northern Plains | | 0.51 | 0.29 | 0.62 | 0.58 | 1.49 | | -0.01 | -0.03 | -0.03 | -0.03 | -0.09 |
| NE Texas | | 0.18 | 0.38 | 0.86 | 0.70 | 1.93 | | 0.03 | 0.16 | 0.33 | 0.25 | 0.73 |
| Mississippi | | 0.17 | 0.14 | 0.42 | 0.40 | 0.96 | | 0.01 | 0.02 | 0.00 | 0.02 | 0.03 |
| Houston | | 0.17 | 0.42 | 0.50 | 0.50 | 1.42 | | 0.06 | 0.19 | 0.13 | 0.19 | 0.51 |
| S Texas | | 0.20 | 0.10 | 0.13 | 0.16 | 0.38 | | -0.14 | -0.07 | -0.14 | -0.13 | -0.35 |
| Arkansas | | 0.16 | 0.12 | 0.46 | 0.41 | 0.99 | | 0.04 | 0.04 | 0.14 | 0.12 | 0.30 |
| Tennessee | | 0.05 | 0.04 | 0.15 | 0.22 | 0.41 | | 0.00 | -0.01 | -0.01 | 0.01 | 0.00 |
| Mexico + Gulf | | 0.00 | 0.00 | 0.12 | 0.11 | 0.23 | | 0.00 | 0.00 | -0.08 | -0.07 | -0.15 |
| Alabama | | 0.01 | 0.02 | 0.07 | 0.04 | 0.13 | | 0.00 | -0.01 | -0.04 | -0.02 | -0.08 |
| Oklahoma | | 0.05 | 0.05 | 0.19 | 0.07 | 0.31 | | 0.00 | 0.01 | 0.08 | 0.02 | 0.11 |
| Kentucky | | 0.03 | 0.02 | 0.04 | 0.06 | 0.12 | | -0.01 | -0.01 | -0.02 | -0.05 | -0.07 |
| W Texas | | 0.02 | 0.00 | 0.01 | 0.01 | 0.02 | | -0.02 | -0.01 | -0.02 | -0.02 | -0.05 |
| Florida | | 0.00 | 0.01 | 0.01 | 0.01 | 0.03 | | 0.00 | 0.00 | 0.00 | 0.00 | 0.00 |
| Georgia | | 0.00 | 0.00 | 0.00 | 0.00 | 0.01 | | 0.00 | 0.00 | 0.00 | 0.00 | 0.01 |
| Mid Atlantic | | 0.00 | 0.00 | 0.00 | 0.00 | 0.00 | | 0.00 | 0.00 | 0.00 | 0.00 | 0.00 |
| Northeast US | | 0.00 | 0.00 | 0.00 | 0.00 | 0.00 | | 0.00 | 0.00 | 0.00 | 0.00 | 0.00 |
| IC | 4.82 | | | | | | 0.57 | | | | | |
| BC | 32.38 | | | | | | -1.49 | | | | | |
| **Total** | **37.2** | **3.91** | **15.61** | **11.38** | **22.41** | **49.36** | **-0.92** | **-0.43** | **0.49** | **-0.36** | **0.53** | **0.66** |

Notes:

Anthro is the sum of mobile, all points and area+offroad

Differences >0.10 are colored red, less than -0.10 are blue

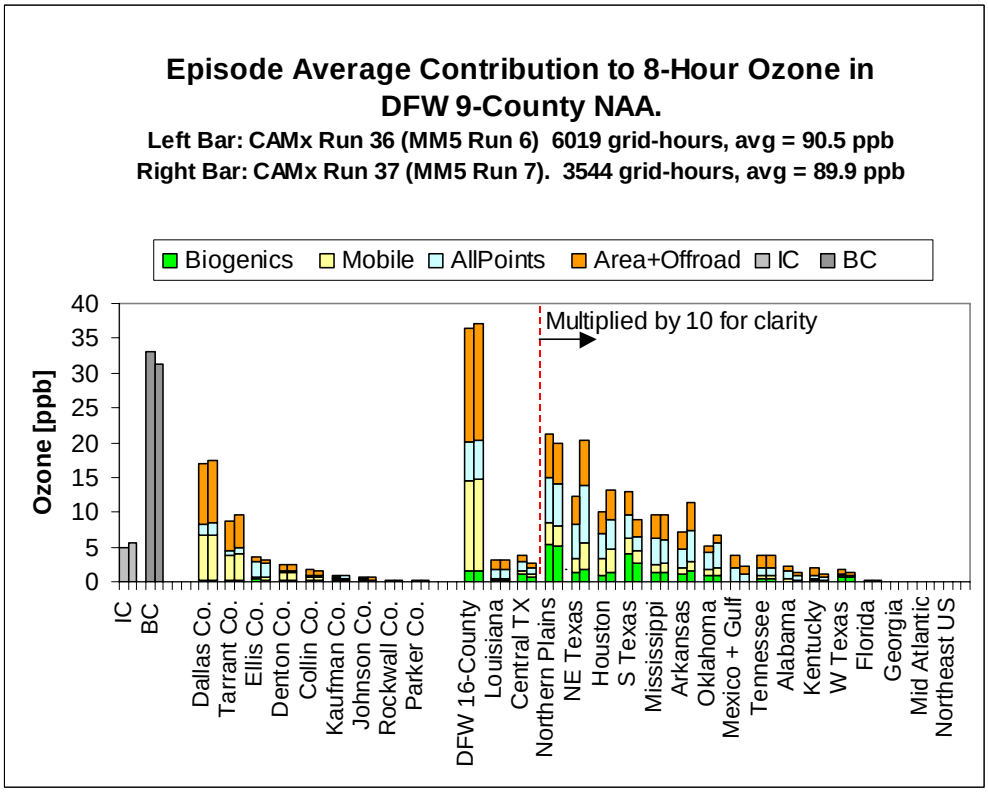


**Figures 9-15.** Episode average 2010 contributions (ppb) to high 8-hour ozone in the DFW NAA with CAMx Runs 36 and 37 using different meteorological inputs.

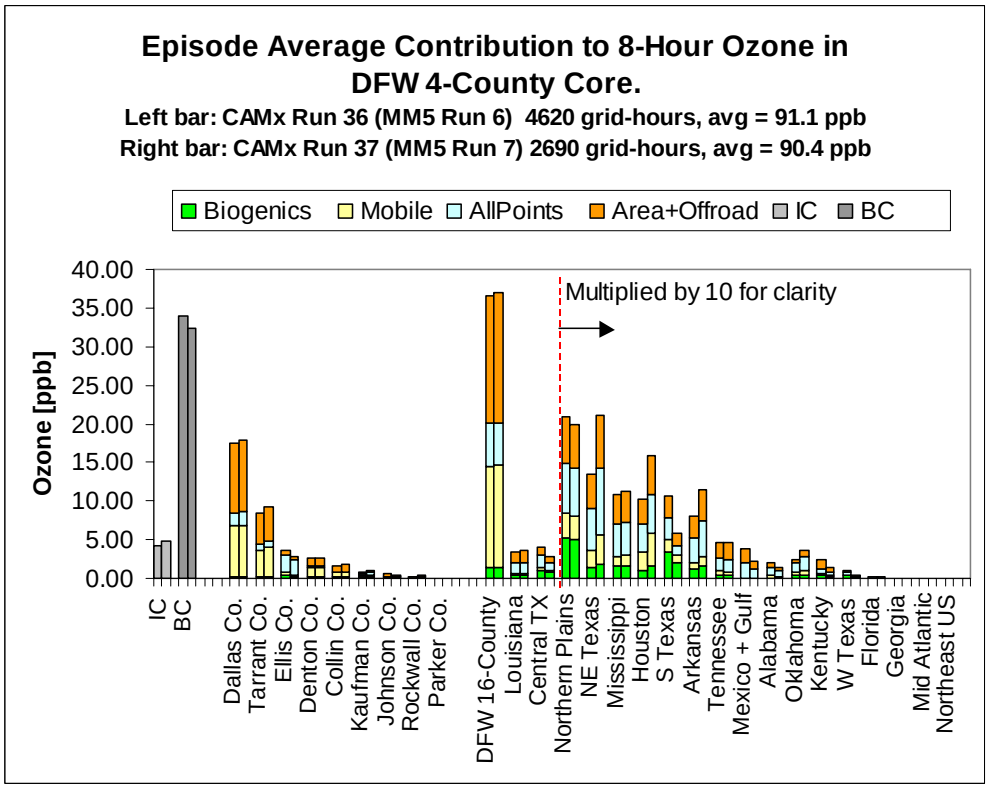


**Figures 9-16.** Episode average 2010 contributions (ppb) to high 8-hour ozone in the DFW 4-county core with CAMx Runs 36 and 37 using different meteorological inputs.

**Table 9-21.** A comparison of peak anthropogenic contributions (ppb) to 8-hour ozone between CAMx Run 36 and Run 37 in the DFW 9-county NAA.

| Max O3 Contributions From Anthropogenic Sources | | | |
|---|---|---|---|
| Receptor | DFW-9 County NAA | | |
| BaseO3 >= | 85 | | |
| Grid | DFW 04-km | | |
| **Source Region** | **Run 36 (ETA PBL with CAIR Controls)** | **Run 37(PX PBL with Grell, CAIR Controls** | **ppb Change in Ozone** |
| Dallas Co. | 39.20 | 35.67 | -3.53 |
| Tarrant Co. | 29.63 | 31.03 | 1.40 |
| Ellis Co. | 16.92 | 13.13 | -3.79 |
| Denton Co. | 13.75 | 12.15 | -1.60 |
| Collin Co. | 10.52 | 9.47 | -1.05 |
| Johnson Co. | 5.20 | 6.25 | 1.05 |
| Kaufman Co. | 4.48 | 4.99 | 0.51 |
| Parker Co. | 4.22 | 5.87 | 1.65 |
| Rockwall Co. | 1.76 | 1.92 | 0.16 |
| **DFW 9-county** | **50.66** | **50.02** | **-0.64** |
| **DFW 16-county** | **50.72** | **50.48** | **-0.24** |
| Central TX | 7.86 | 6.80 | -1.06 |
| Northern Plains | 7.65 | 6.10 | -1.55 |
| NE Texas | 6.87 | 5.35 | -1.52 |
| Louisiana | 5.53 | 6.75 | 1.22 |
| Arkansas | 4.90 | 4.42 | -0.48 |
| S Texas | 3.99 | 4.57 | 0.58 |
| Oklahoma | 3.44 | 5.10 | 1.66 |
| Houston | 2.97 | 5.14 | 2.17 |
| Mississippi | 1.75 | 1.81 | 0.06 |
| Mexico + Gulf | 1.51 | 1.10 | -0.41 |
| W Texas | 1.35 | 1.33 | -0.02 |
| Tennessee | 0.85 | 0.69 | -0.16 |
| Alabama | 0.75 | 0.52 | -0.23 |
| Kentucky | 0.37 | 0.26 | -0.11 |
| Florida | 0.10 | 0.13 | 0.03 |
| Georgia | 0.01 | 0.03 | 0.02 |
| Northeast US | 0.01 | 0.00 | -0.01 |
| Mid Atlantic | 0.00 | 0.00 | 0.00 |

Note: Differences >0.10 are colored red, less than -0.10 are blue

# 10. SUMMARY AND CONCLUSIONS

Phase 2 of Project H35 improved ozone model performance for the August 13-22, 1999 DFW SIP episode and investigated how updated modeling assumptions impacted ozone transport assessments. There were three components to the work:

- Ten (10) CAMx sensitivity runs were completed to investigate how changes in modeling inputs and assumptions affect ozone model performance. Two MM5 runs were completed to support the CAMx sensitivity analysis. A revised 1999 base case (Run 34) was developed from the sensitivity tests.
- Process analysis was used to investigate the revised 1999 base case and two related model scenarios.
- APCA ozone source apportionment was used to investigate the impact of several modeling assumptions on ozone transport for 2010 future year scenarios.

## IMPROVING MODEL PERFORMANCE

This project started from the CAMx base case developed for the Dallas/Fort Worth (DFW) August 13-22, 1999 episode referred to as "Run 17b" (Emery et al., 2004). Ten modifications were applied separately to understand how model performance for 1-hour and 8-hour ozone might be improved. Sensitivity tests included changes in the domain extent, meteorology, emissions, and chemistry. All runs used version 4.03 of CAMx and started from model inputs for the August 13-22, 1999 episode described by Emery et al. (2004).

### Domain Modifications

Two of the modifications we examined involved expanding the modeling domain. One expanded the horizontal domain eastward into the Atlantic Ocean and northward into parts of Canada. Model performance did improve somewhat. The second change extended the model top from 4-km to 14-km; this run showed minor improvements in ozone performance. When both assumptions were applied, model performance improved a little more. These changes were judged to be improvements because they improved model performance and reduced dependence on boundary condition (BC) assumptions. As a result, all remaining sensitivity tests used the expanded horizontal domain with higher model top.

Further expansion of the modeling domain could be accomplished by modeling the entire continental US as, for example, is done by the regional planning organizations (RPOs) engaged in particulate matter (PM) and visibility modeling. Modeling the national RPO domain would require preparing emissions and meteorology for all 48 conterminous US states plus parts of Mexico, Canada and Cuba. Boundary conditions for the national RPO grid could be obtained from a global tropospheric chemistry model. The potential benefits of further extending the DFW modeling domain to cover the entire US are unclear.

Expanding the modeling domain increased computer run times and memory requirements. The increased resource requirements are not a burden for standard CAMx runs but have more

significance for ozone source apportionment analyses that require greater computational resources than standard runs.

**Alternative Meteorology**

Ozone sensitivity to different CAMx meteorological input data was examined. The meteorology used in Run 17b was from an MM5 simulation that used the Pleim-Xiu PBL and land-surface model (MM5 Run 5). Vertical diffusivities (Kv) were calculated using an O'Brien profile methodology. One meteorological modification implemented a vertical diffusivity field calculated using an approach implemented in EPA's CMAQ model. This run generally lowered daytime ozone peaks and elevated nighttime ozone due to stronger and deeper mixing.

Another meteorological modification (MM5 Run 7) used the Grell cumulus scheme in MM5 rather than the Kain-Fritsch scheme. CAMx ozone performance showed little statistical improvement, but the spatial distribution of the daily maximum ozone in the DFW area on August 17$^{th}$, when the highest 1-hour ozone was observed in the episode, correctly increased the peak 1-hour ozone and shifted the peak closer to the higher observed ozone.

When CAMx was supplied modified meteorology (MM5 Run 6) using the Noah/Eta PBL and LSM schemes rather than the Pleim-Xiu schemes, model performance was generally improved, although the time series of the 1-hour ozone showed some erratic patterns that resulted in mixed changes in performance. Overall, MM5 Run 6 was judged to give superior meteorological and air quality model performance.

**Emission Modifications**

Changes to the emissions were also investigated as sensitivity tests. Ozone model performance in the DFW 4-km domain improved when the mobile source NOx emissions were reduced by 30% in the four DFW core counties. This result is due to intense surface NOx emissions in the DFW core area inhibiting ozone formation immediately downwind of the core where high ozone levels are observed. The peak ozone on August 17$^{th}$ increased and shifted eastward closer to the observed peak location. Increasing biogenic emissions by 30% domain-wide produced higher daytime ozone but did not systematically improve model performance. A smaller increase in biogenic emissions, or an increase targeted in the DFW are, might improve DFW ozone performance. Doubling VOC emissions from non-EGU point sources had little impact on ozone levels and model performance.

The results of the sensitivity test showing improved ozone model performance with lower NOx emissions in the DFW core do not justify changing the emission inventory. Note that ozone model performance in DFW also is sensitive to changes in meteorology and chemistry. Further evaluation of the DFW NOx emission inventory would be useful to reduce uncertainty.

**Chemistry Mechanisms**

Two chemical mechanism changes were evaluated. One was a revised version of the CB4 mechanism called CB2002, and the second was an extension of the CB4 mechanism by adding

17 inorganic chemistry reactions called CB4xi. The most important extra inorganic reactions in CB4xi are several "NOx recycling" reactions. CB2002 reduced ozone levels relative to the standard CB4 and degraded model performance. When the NOx recycling reactions were added to CB4, ozone concentrations were increased regionally by a few ppb both in the daytime and at night.

### Conclusions from the Sensitivity Tests

The ten sensitivity tests, summarized above, showed that reducing NOx in the DFW core counties, adding more biogenic emissions, and implementing the NOx recycling reactions in CB4 consistently produced higher ozone. These runs generally improved the normalized bias and average paired peak accuracy, but hurt the unpaired peak accuracy. The use of the CMAQ-based vertical diffusivity profiles and the CB2002 chemical mechanism lowered ozone. All other tests either led to mixed results or very little change.

The eastward shift in the peak predicted daily maximum 1-hour ozone to sites that observed the highest ozone on August 17 bears additional analysis. The two assumptions that brought the greatest eastward migration are the use of the Grell convective scheme in MM5 and the reducing NOx emissions in the core DFW counties.

## REVISED BASE CASE: RUN34

Based on the sensitivity testing and model performance evaluation, a revised base case was developed for the DFW August 13-22, 1999 SIP episode referred to as Run 34. Changes in Run 34 from the previous Run 17b base case are:

- Expanded modeling domain extending to the Atlantic Ocean and Canada
- Higher model top at about 14-km
- Meteorology from MM5 "Run 6" using the Noah/Eta PBL scheme
- Enhanced near surface mixing from the "Kv100" adjustment
- Extended inorganic chemistry (CB4xi) with "NOx recycling" reactions.

Run 34 shows improved ozone model performance compared to Run 17b. A tendency toward ozone under-prediction (negative bias) was improved by the updated meteorology "MM5 Run 6" and the chemistry updates (NOx recycling). The "Kv100" vertical mixing adjustment improved ozone predictions in areas with intense surface NO emissions in the DFW core area. Expanding the modeling domain, both vertically and horizontally, reduced the impact of boundary condition assumptions at some cost of increased computer resources to model a larger domain.

## CHEMICAL PROCESS ANALYSIS

Chemical Process Analysis (CPA) was used to investigate several aspects of atmospheric chemistry that are important to understanding DFW model performance and control strategy development:

- Determining geographic areas of high ozone productivity.
- Classifying geographic areas as being "VOC-limited" or "NOx-limited" with respect to ozone formation chemistry.
- Investigating the efficiency of ozone formation chemistry as measured by the "OH chain length."
- Determining the contribution of biogenic (isoprene) emissions to VOC reactivity and ozone production.

CPA was applied for three model scenarios:

Run 34 – The revised base case, discussed above.
Run 33 – Similar to Run 34 but using meteorology from MM5 Run 5 and a "Kv3" vertical mixing adjustment tested by the TCEQ.
Run 35 – Similar to Run 34, but with 30% less mobile source NOx in the four core DFW counties.

Model performance was evaluated prior to using CPA. Model performance for Run 34 was found to be superior to Run 33. Model performance for Run 35 showed some improvements over Run 34 but the differences were smaller than when the 30% NOx reduction was evaluated as part of the 10 sensitivity tests discussed above. To reiterate the statements made above, the results of the sensitivity test showing improved ozone model performance with lower NOx emissions in the DFW core do not justify changing the emission inventory. Further evaluation of the DFW NOx emission inventory would be useful to reduce uncertainty.

The CPA analysis for the DFW 4-km grid showed many common features across days and scenarios (Runs 33 to 35).

- Ozone production showed hot spots over urban areas and major NOx point sources in rural areas consistently across days.
- The areas of most intense Ox production tend to be VOC-limited on all days but there are differences in the extent of VOC and NOx-limited areas between days
- August 17$^{th}$ is the most extensively VOC-limited day during the episode (Figure 10-1).
- Other days examined were less strongly VOC-limited than August 17$^{th}$.
- When mobile source NOx emissions were reduced by 30% in the DFW core the VOC-limited area almost completely disappeared on the days other than August 17$^{th}$.
- The regions that tend to be VOC-limited are the Dallas, Fort Worth and Waco urban areas and the immediate vicinity of the Big Brown and Limestone EGUs in Freestone and Limestone counties.
- The fraction of OH reacting with isoprene (relative to all hydrocarbons) revealed areas where biogenic emissions have high importance: the eastern part and northwest corners of the 4-km grid.
- A high fraction of OH reacting with isoprene of biogenic isoprene does not necessarily correspond to high ozone production because NOx (predominantly from anthropogenic sources) also is required for ozone production to occur.
- An area of low fraction of OH reacting with isoprene runs from south to north (Waco to DFW) near IH-35. The relatively low importance of isoprene in these areas is due to differences in land cover (i.e., agricultural and urban areas) leading to low biogenic emission levels. This land cover difference likely contributes to the DFW urban area tending to be VOC-limited.

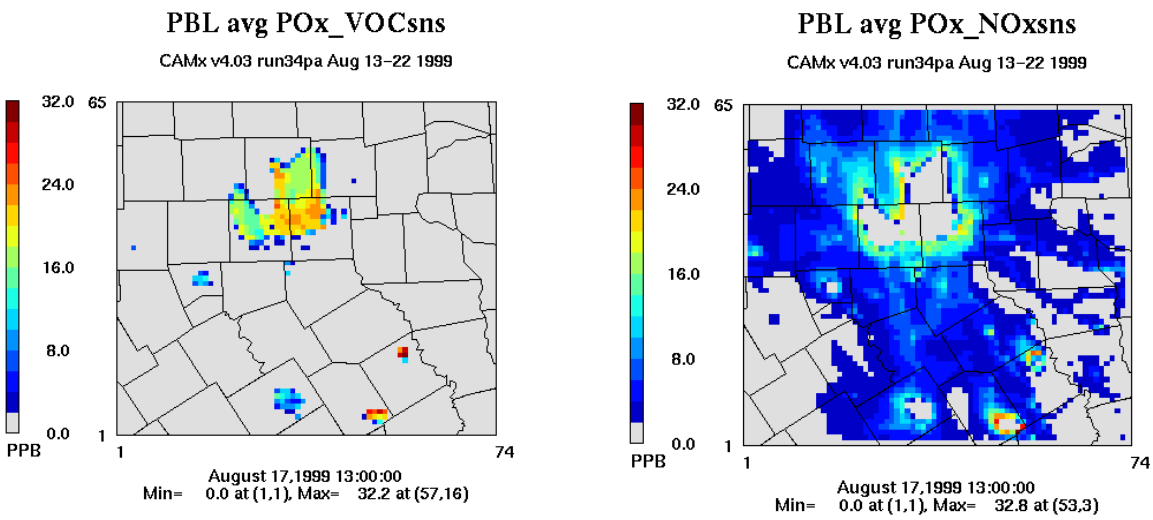


**Figure 10-1**. Assignment of oxidant production as VOC-limited (left) and NOx-limited (right) in the boundary layer for the DFW 4-km grid in Run 34 at 13:00 on August 17, 1999.

The CPA analyses are useful for qualitatively understanding areas of VOC- and NOx-limited ozone formation. The CPA results are consistent with previous emission sensitivity analyses and ozone source apportionment results in showing that the DFW core areas can be VOC-limited but surrounding areas are NOx-limited. The CPA results should not be used to make quantitative estimates of the relative benefits of reducing VOC vs. NOx emissions.

## UPDATED TRANSPORT ASSESSMENT

The Texas Environmental Research Consortium (TERC) sponsored Phase 1 of project H35 to examine the role of ozone transport in creating high 8-hour ozone in eastern Texas, including the DFW region, for a 2010 future year scenario. The transport assessment was updated to consider the additional impacts of:

- Improvements to the DFW SIP modeling database as included in Run 34, discussed above.
- Expected reductions in 2010 EGU NOx emission levels expected to result from EPA's Clean Air Interstate Rule (CAIR).
- Modeling uncertainties related to meteorology, as represented by the difference between MM5 Runs 6 and 7 discussed above.
- Modeling uncertainties related to improvements in the APCA source apportionment technique to better represent chemical destruction of ozone as it is transported.

The impacts of the CAIR rule on projected 2010 emissions and ozone are summarized below.

## IMPACT OF CAIR ON 2010 EMISSIONS

The impacts of EPA's Clean Air Interstate Rule (CAIR) on EGU emissions were modeled based on information provided in the CAIR Technical Support Documents (EPA, 2004). All EGUs in

the expanded DFW modeling domain were scaled by state-specific reduction factors calculated from the ratio of statewide, annual average EGU emissions for the 2010 base case and 2010 CAIR control case. Figure 10-2 shows the NOx EGU reduction factors that were derived for each state. Texas' NOx emissions from EGUs were to be reduced by 1%. Louisiana's EGU NOx was reduced by 26 %. The EGU controls reduced NOx emissions in both Kentucky and Florida by over 300 tons/day. Georgia, Tennessee, Alabama, Mississippi, and Louisiana all reduced NOx emissions by over 100 tons per day.

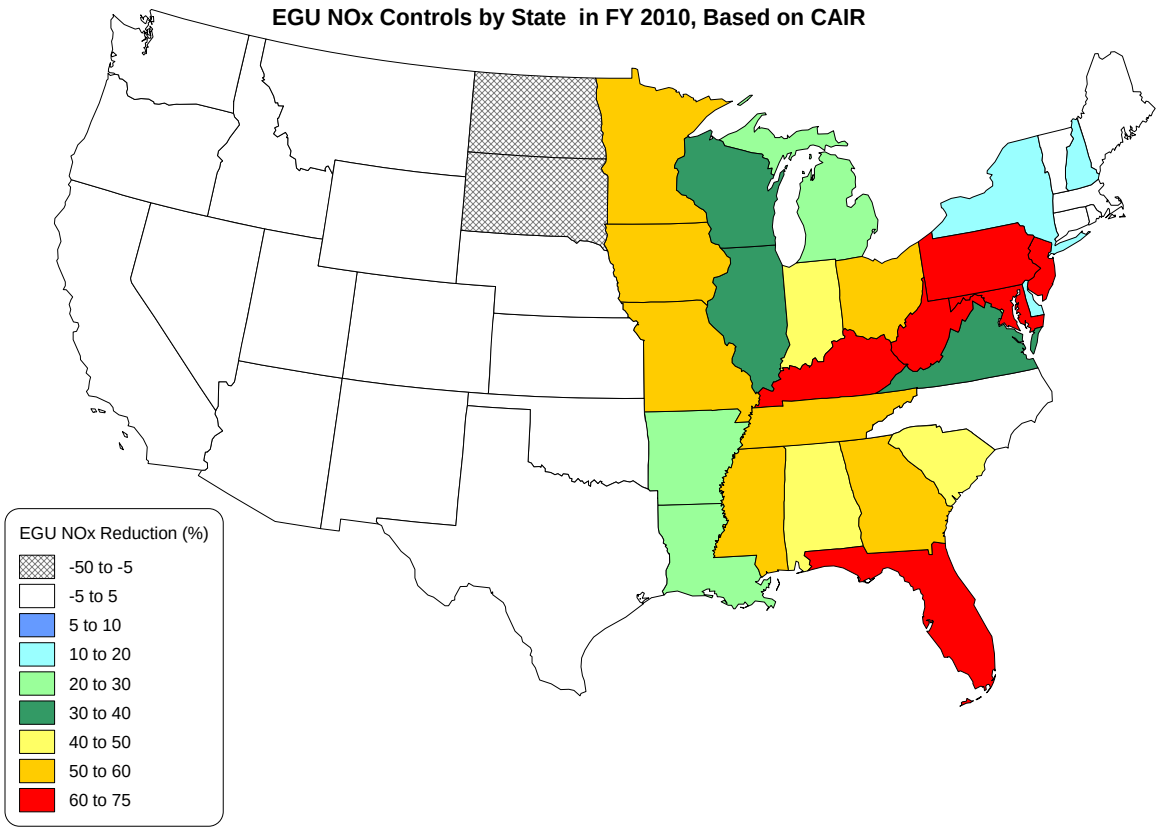


**Figure 10-2**. Percentage NOx reductions due to CAIR applied to EGUs for each State in future year 2010.

## IMPACT OF CAIR ON 2010 OZONE LEVELS

The impacts of CAIR EGU NOx reductions on 2010 episode maximum 8-hour ozone for the 12-km and DFW 4-km grids are shown in Figure 10-3. In the 12-km domain, Mississippi showed the largest decrease in episode maximum 8-hour ozone, dropping up to 15 ppb near the Mississippi River; EGUs in this state were reduced 55 %. The DFW NAA showed negligible decrease in episode maximum 8-hour ozone due to the CAIR reductions because of the strong impact of local emissions on peak ozone levels in the DFW NAA. The largest decrease in episode maximum 8-hour ozone inside the 4-km domain was 1.1 ppb to the east of the DFW NAA.

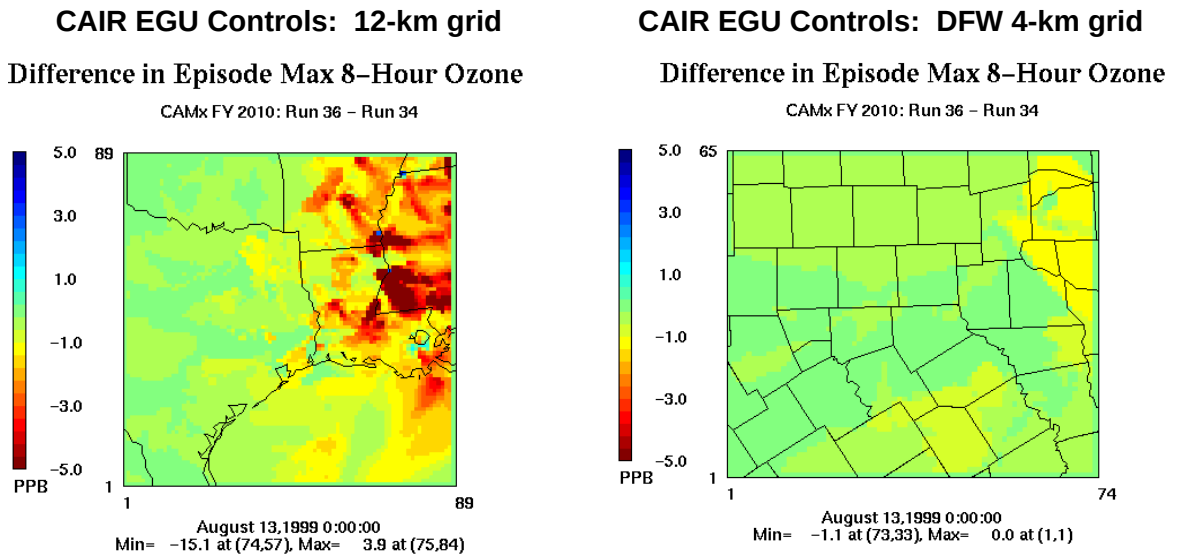


**Figure 10-3**. The impacts of CAIR EGU NOx reductions on 2010 episode maximum 8-hour ozone for the 12-km and DFW 4-km grids.

## IMPACT OF CAIR ON OZONE TRANSPORT

We evaluated the impact of the CAIR emission reductions on DFW ozone transport assessments. Figure 10-4 is a bar chart showing episode average contributions to high 8-hour ozone in the DFW 9-county NAA by source region and emissions group. Side-by-side bars show the subtle changes due to the CAIR EGU controls: The right bar of each pair is with EGU controls. The CAIR controls reduced episode average high ozone in the DFW NAA by 0.3 ppb. The episode peak ozone was also lowered 0.3 ppb over DFW from the CAIR controls.

The states that experienced the largest percentage EGU NOx reductions due to CAIR generally had the largest percent reduction in ozone contribution from all point sources, as shown in Figure 10-5. Louisiana, with a 26 % NOx reduction in EGUs, reduced its ozone contribution from point sources by 8 %. The relative reductions in point source ozone contributions were smaller than the relative reductions in EGU emissions because: (1) EGUs are a sub-set of point sources, and (2) ozone production from some non-EGU sources increased as EGU NOx was decreased. Greater ozone production from non-EGU sources in response to EGU controls is an aspect of the non-linear relationship between ozone formation and NOx levels.

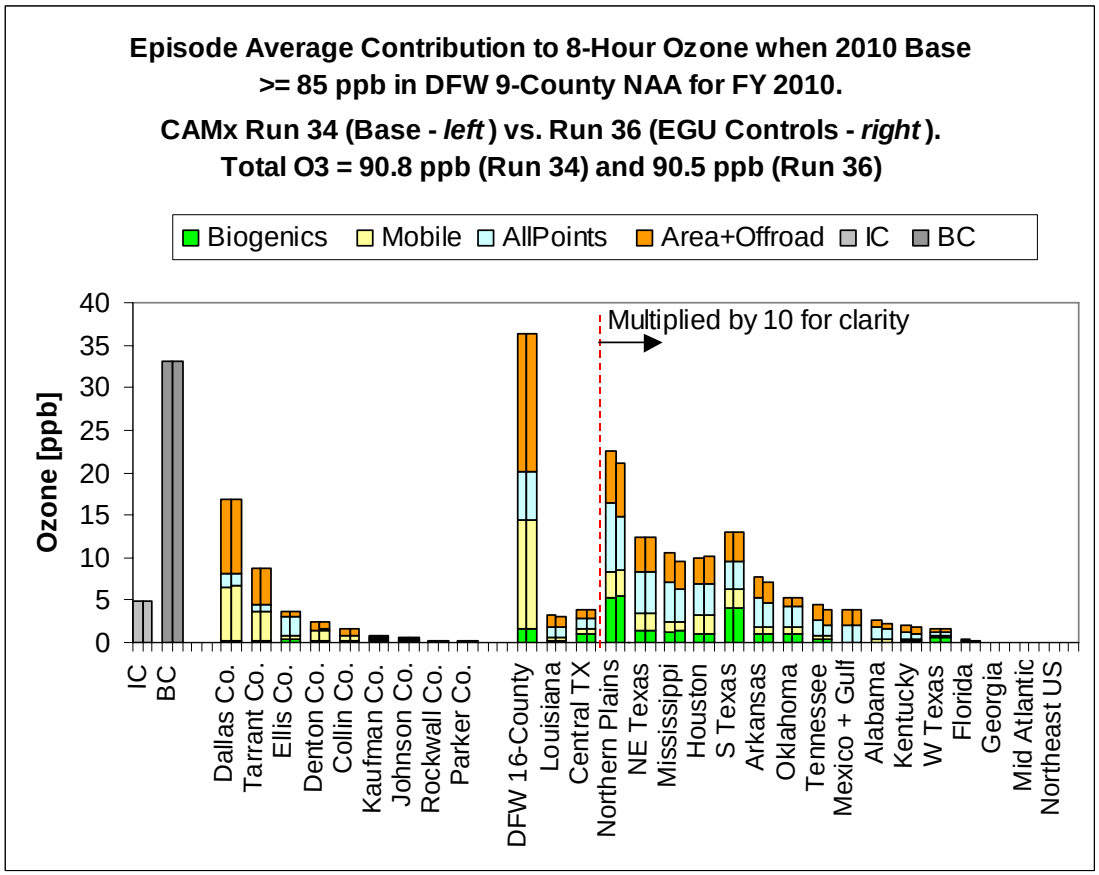


**Figure 10-4**. Episode average 2010 contributions (ppb) to high 8-hour ozone in the DFW 9-county NAA by source region and emissions group with and without CAIR controls.

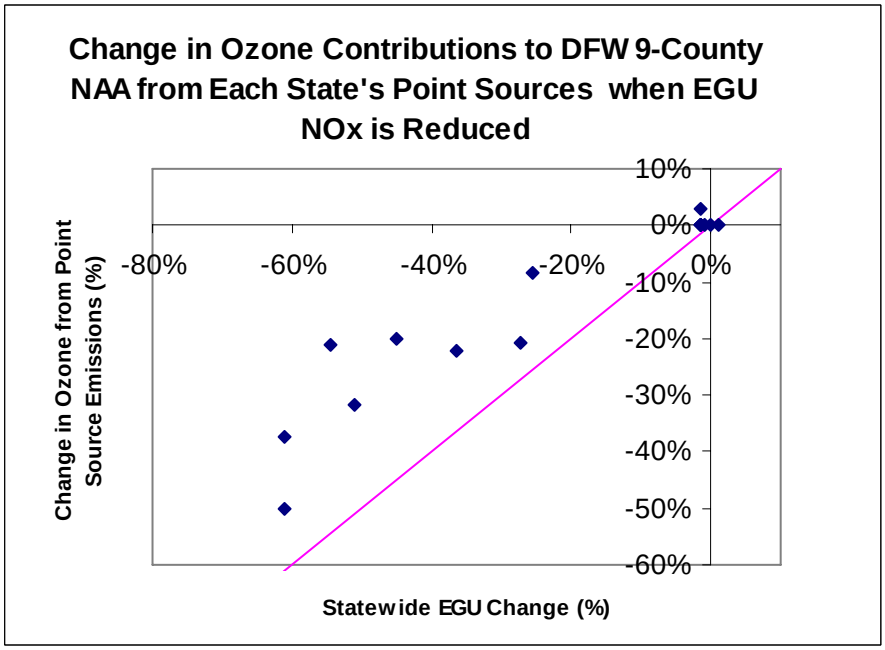


**Figure 10-5**. Change in episode average EGU contributions to high 8-hour ozone in DFW against change in emissions, by State.

## IMPACT OF ALTERNATE METEOROLOGY

We evaluated the sensitivity of DFW ozone transport assessments to using alternate meteorological data from the MM5 model. Figure 10-6 shows episode average contributions to high 8-hour ozone in the DFW 9-county NAA by source region and emissions group. Side-by-side bars compare the ozone contributions with different meteorological data: The left bars are with MM5 "Run 6" as used in the current CAMx base case with CAIR reductions (Run 36); The right bars are with MM5 "Run 7" using an alternate convection scheme called Grell.

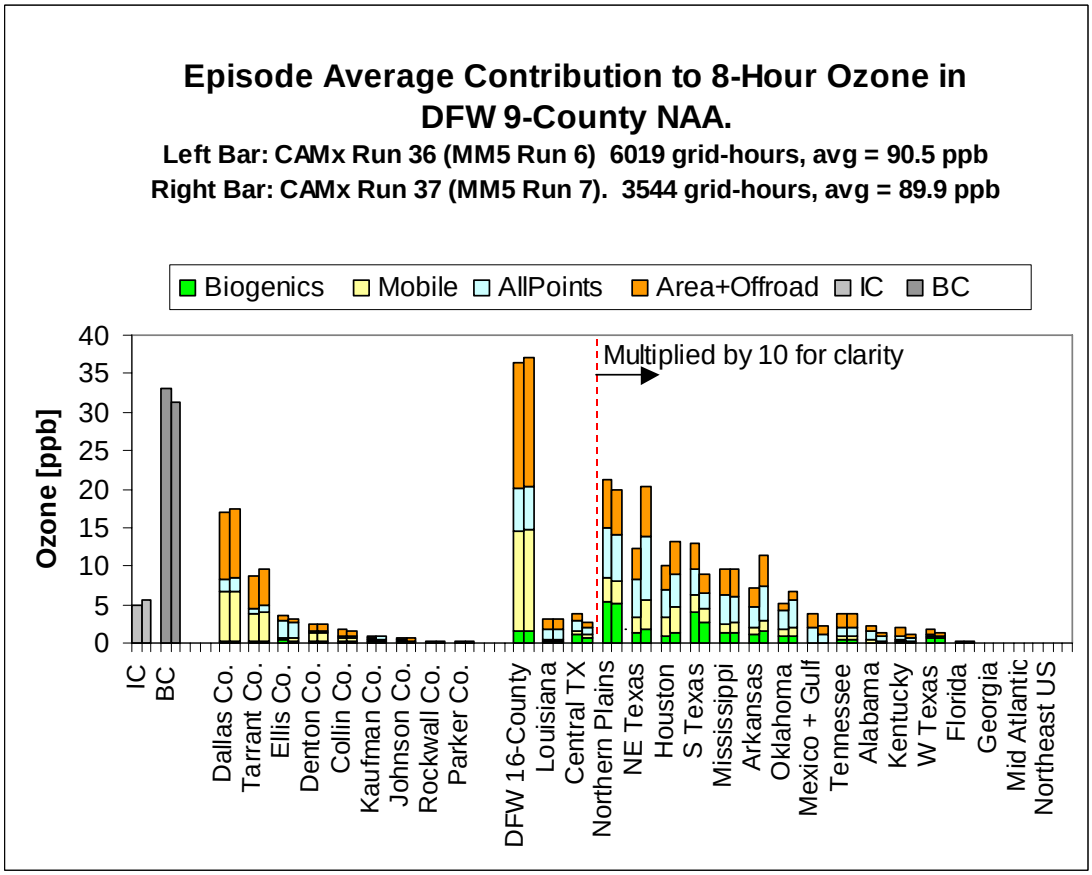


**Figure 10-6**. Episode average 2010 contributions (ppb) to high 8-hour ozone in the DFW 9-county NAA by source region and emissions group with two different meteorological inputs.

Local sources and source regions north and east of DFW contributed more to DFW high ozone when the Grell convection scheme was used in MM5. These source regions include the 16-county DFW region, northeast Texas, Louisiana, Arkansas, and Oklahoma. Contributions from source regions south of DFW – central Texas, southern Texas, and Mexico/Gulf of Mexico – contributed less with Grell, but Houston was an exception in contributing more with Grell. Houston is an exception because the Grell scheme increased ozone production in the Houston area by as much as 30 ppb, causing greater ozone transport from Houston to Dallas. Model performance should be evaluated for the Houston region to determine which MM5 run is better suited in this area. Contributions from States more distant than Oklahoma, Louisiana, Arkansas changed by less than 0.1 ppb. When using Grell, there was less reliance on boundary

contributions, which were reduced by 2 ppb, as anthropogenic contributions and initial conditions were higher.

## IMPACT OF UPDATED SOURCE APPORTIONMENT METHOD: APCA2

We evaluated the sensitivity of DFW ozone transport assessments to updates in the CAMx source apportionment methodology. In the APCA method (Anthropogenic Precursor Culpability Assessment), used for previous the source apportionment analysis, ozone contributions are tracked based net changes in ozone due to chemistry. In the APCA2 method, ozone contributions are modified to separately reflect chemical processes that increase ozone and processes that decrease ozone. Figure 10-7 shows episode average contributions to high 8-hour ozone in the DFW 9-county NAA by source region and emissions group. Side-by-side bars compare the ozone contributions with APCA (left bars) and APCA2 (right bars).

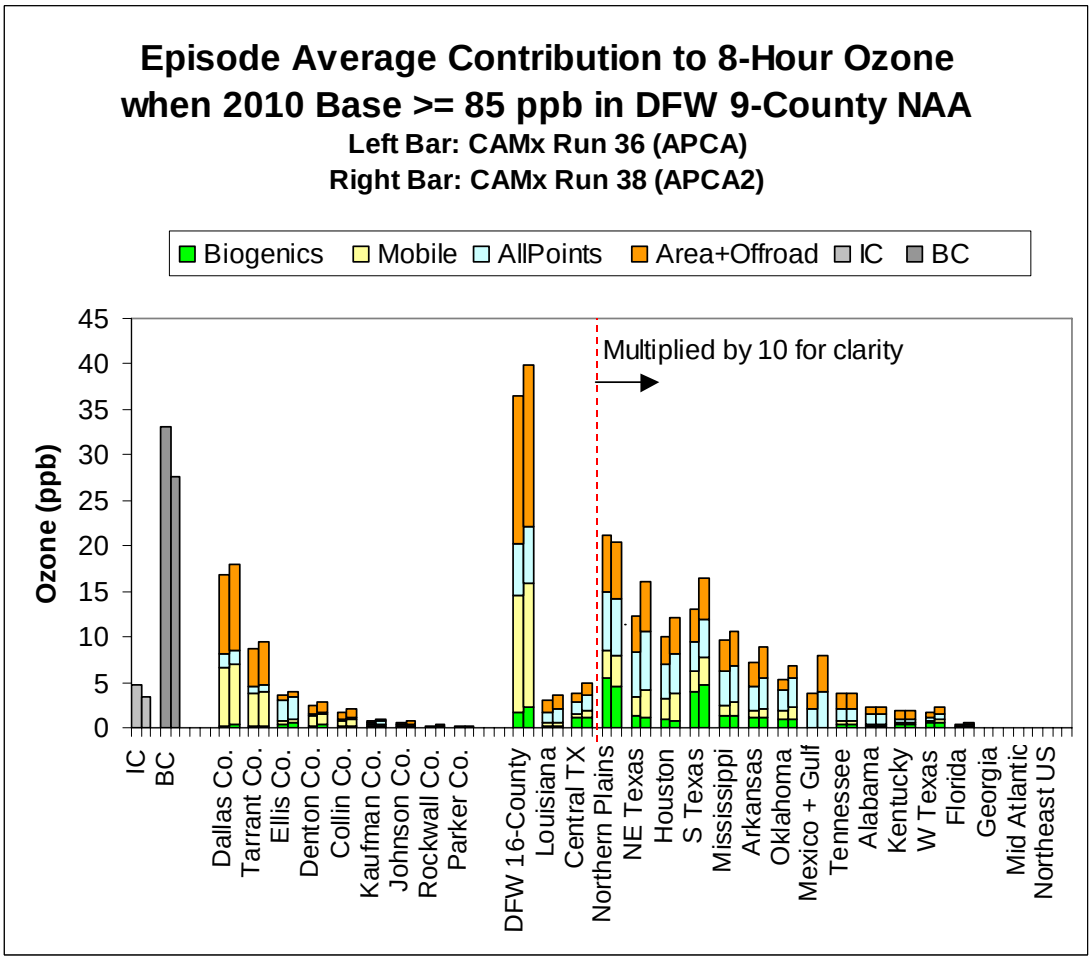


**Figure 10-7**. Episode average 2010 contributions (ppb) to high 8-hour ozone in the DFW 9-county NAA by source region and emissions group with two different APCA methods.

Comparing APCA and APCA2 showed that the updated methodology allocates less ozone to distant sources, more ozone to local sources, and about the same ozone to sources at intermediate

distances. Ozone contributions from far distant sources, such as boundary conditions (BCs) and the Northern Plains, decrease with APCA2 because they are subject to chemical destruction during multi-day transport. The contribution of BCs decreased by 5.5 ppb (16 %) using APCA2. The contribution of DFW area sources was increased by 3.5 ppb (8%), the contribution of Central Texas sources was increased by 0.97 ppb (26%), the contribution of Northeast Texas sources was increased by 0.36 ppb (22%) and the contribution of Louisiana sources was increased by 0.49 ppb (14%) with APCA2. The contributions of sources at an upwind distance of about two States were about equal between APCA and APCA2.

U.S. Environmental Protection Agency, Process Modeling Research Branch, Office of Research and Development, Research Triangle Park, NC. December.

Jeffries, H. E., and Tonnesen, G. S. 1994. Comparison of two photochemical reaction mechanisms using a mass balance and process analysis. Atmospheric Environment 28:2991-3003.

Mansell, G., G. Yarwood, M. Jimenez, T. Dihn and Y. Jia. 2003. "Development of Base Case Photochemical Modeling to Address 1-Hour and 8-Hour Ozone Attainment in the Dallas/Fort Worth Area." Prepared for the Texas Commission on Environmental Quality. August.

Mansell, G., G. Yarwood, S. Lau, J. Russell, E. Tai. 2004. "2010 Future Year Ozone Modeling for the Dallas/Fort Worth Area." Prepared for the Texas Commission on Environmental Quality. August.

Novelli, P.C., P.M. Lang, K.A. Masarie, D.F. Hurst, R. Myers, and J.W. Elkins. 1999. Molecular hydrogen in the troposphere: global distribution and budget. *J. Geophys. Res*. 104, 30,427-30,444.

Stoeckenius T.E. and G. Yarwood. 2004. "Dallas-Ft. Worth Transport Project." Report on TERC project H27 prepared for the Houston Advanced Research Center, The Woodlands, Texas. April.

Tai E., S. Kemball-Cooke and G. Yarwood. "Transport Contributions from Out-of-State Sources to East Texas Ozone." Report on TERC project H35 phase 1, prepared for the Houston Advanced Research Center, The Woodlands, Texas. February 7.

UT/ENVIRON. 2002. "Conceptual Model of Ozone Formation in the Dallas/Fort Worth Ozone Non-Attainment Area." Prepared for Texas Commission on Environmental Quality. 16 October.

Yarwood. G., G.Z. Whitten and S. Rao. 2005. "Updates to the Carbon Bond 4 Photochemical Mechanism." Prepared for Lake Michigan Air Directors Consortium. March.

Zaveri, R.A. and L. K Peters. 1999. A new lumped structure photochemical mechanism for large-scale applications. *J. Geophys. Res*., 104, 30,387-30,415.

# 11. REFERENCES

Carter, W.P.L. 2000. "Programs and Files Implementing the SAPRC-99 Mechanism and its Associated Emissions Processing Procedures for Models-3 and Other Regional Models." Available from http://pah.cert.ucr.edu/~carter/SAPRC99/s99files.htm.

Dudhia, J. 1993. "A Non-hydrostatic Version of the Penn State/NCAR Mesoscale Model: Validation Tests and Simulation of an Atlantic Cyclone and Cold Front", *Mon. Wea. Rev*., Vol. 121. pp. 1493-1513.

Emery, C., Y. Jia, S. Kemball-Cook, G. Mansell, S. Lau, and G. Yarwood. 2004. "Modeling an August 13-22, 1999 Ozone Episode in the Dallas/Fort Worth Area." Prepared for the Texas Commission on Environmental Quality. 31 August.

ENVIRON. 2005. "Transport Contributions from Out-of-State Sources to East Texas Ozone." HARC Project H35. Prepared for Houston Advanced Research Center. 7 February.

ENVIRON. 2004a. User's Guide, Comprehensive Air Quality Model with Extensions (CAMx), Version 4.00. Prepared by ENVIRON International Corporation, Novato, CA. January 2004. Available at http://www.camx.com.

ENVIRON. 2004b. "2007 Future Year Ozone Modeling for the Dallas/Fort Worth Area." Prepared for the Texas Commission on Environmental Quality by ENVIRON International Corporation, 101 Rowland Way, Novato, CA 94945 and Texas Engineering Experiment Station, 3000 TAMU, College Station, TX 77843. 25 August 2004.

EPA. 2004. "Technical Support Document for the Interstate Air Quality Rule. Air Quality Modeling Analyses." USEPA Office of Air Quality Planning and Standards, Emissions Analysis and Monitoring Division, Research Triangle Park, NC 27711. January.

Gery, M.W., G.Z. Whitten, J.P. Killus, M.C. Dodge. 1989. "A photochemical kinetics mechanism for urban and regional scale computer modeling." *J. Geophys.* Res., 94, 12925-12956.

IUPAC. 2004. R. Atkinson, D.L. Baulch, R.A. Cox, J.N. Crowley, R.F. Hampson, R.G. Hynes, M.E. Jenkin, J.A. Kerr, M.J. Rossi, and J. Troe. "Evaluated kinetic and photochemical data for atmospheric chemistry - IUPAC subcommittee on gas kinetic data evaluation for atmospheric chemistry." Available from http://www.iupac-kinetic.ch.cam.ac.uk/index.html

JPL. 2002. "Chemical Kinetics and Photochemical Data for Use in Atmospheric Studies – Evaluation Number 14," JPL Publication 02-25. Prepared by Jet Propulsion Laboratory, California Institute of Technology, Pasadena, California.

Jeffries, H.J., I. Voicu, and K. Sexton. 2002. "Experimental Tests of Reactivity and Re-Evaluation of the Carbon Bond Four Photochemical Reaction Mechanism." Report to the

# APPENDIX A

## MODEL PERFORMANCE PRODUCTS FOR RUN34

## MODEL PERFORMANCE PRODUCTS FOR RUN34

| Filename | Contents |
|---|---|
| O3max.{1,8}hr.run34pa.DATE.dfw-{04km, 12km}.png | Daily maximum 1hr and 8 hour plots for the 12-km and 4-km grids for Run 34. |
| Time series (1hr, 8hr) run34pa.aug99.xls | 1 hour and 8-hour time series plots |
| epastats.run34pa.fine2.2dayspin.xls | 1 and 8 hour scatter plots and QQ plots |

# APPENDIX B

# APCA TABLES FOR EACH RUN ON EACH DAY

## APCA TABLES FOR EACH RUN ON EACH DAY

| Filename | Contents |
|---|---|
| DFW.(4,9)cnty.avg.run(34-38)fy2010.dfw04km.ALL.8hr.85ppb.xls | APCA tables for the 4-county DFW core and 9-county DFW NAA receptor areas from 4 CAMx runs for the 2010 future year: Run 34, Run 36, Run 37, and Run 38 |